Stony Brook University

The piRNA pathway in the somatic stem cells of a regeneration-competent flatworm, *Macrostomum lignano*

A Dissertation Presented

by

Xin Zhou

to

The Graduate School

in Partial Fulfillment of the

Requirements

for the Degree of

Doctor of Philosophy

in

Molecular and Cellular Biology

(Cellular and Developmental Biology)

Stony Brook University

December 2015

Stony Brook University

The Graduate School

Xin Zhou

We, the dissertation committee for the above candidate for the

Doctor of Philosophy degree, hereby recommend

acceptance of this dissertation.

Gregory J. Hannon, Ph.D.
Senior Group Leader
Cancer Research UK Cambridge Institute
University of Cambridge

Kevin Czaplinski, Ph.D.
Associate Professor
Department of Biochemistry and Cell Biology
Stony Brook University

Jingfang Ju, Ph.D.
Associate Professor
Department of Pathology
Stony Brook University

Christopher M. Hammell, Ph.D.
Assistant Professor
Cold Spring Harbor Laboratory

Marja C.P. Timmermans, Ph.D.
Alexander von Humboldt Professor
University of Tübingen

This dissertation is accepted by the Graduate School.

Charles Taber

Dean of the Graduate School

Abstract of the Dissertation

The piRNA pathway in the somatic stem cells of a regeneration-competent flatworm, *Macrostomum lignano*

by

Xin Zhou

Doctor of Philosophy

in

Molecular and Cellular Biology

(Cellular and Developmental Biology)

Stony Brook University

2015

piRNA pathway and its central components, PIWI proteins, are essential for transposon silencing and some aspects of gene regulation. Although they predominantly function in the animal germline, increasing evidence has pointed to their involvement in somatic cells. Some flatworms possess a unique somatic stem cell system named neoblasts. These totipotent cells are the only dividing cell population thus critical for postembryonic development, adult homeostasis and the remarkable regeneration ability. In the study led by Kaja A. Wasik and me, we identify and characterize piRNAs and PIWI proteins in the emerging regenerative flatworm model, *Macrostomum lignano,* combining targeted gene knockdown and deep sequencing. We find that *M. lignano* has a highly conserved piRNA pathway utilizing at least three PIWI proteins in the germline and somatic stem cells. One of the PIWIs, Macpiwi1, acts as a pivotal player by interacting with the primary piRNAs in a heterogenic secondary piRNA biogenesis. Knockdown of *Macpiwi1* dramatically reduces piRNA levels, derepresses transposons, and severely impacts stem cell maintenance. Knockdown of the piRNA biogenesis factor *Macvasa* causes an even greater reduction in piRNA levels, with a corresponding increase in transposons. Yet, in *Macvasa* knockdown worms, we detect no major impact on stem cell self-renewal. These results may suggest stem cell maintenance functions of PIWI proteins in flatworms that are distinguishable from their impact on transposons and that might function independently of what are considered canonical piRNA populations.

Table of Content

List of Figures

List of Tables

List of Abbreviations

3R-TAS Telomere-associated sequence of third chromosome right arm
AGO Argonaute
Ago2 Argonaute protein 2
Ago3 Argonaute protein 3
Armi Armitage
ATP Adenosine triphosphate
Aub Aubergine
bp base pair
BrdU Bromodeoxyuridine
BSA Bovine serum albumin
Cas9 CRISPR associated protein 9
cDNA complementary DNA
CEGMA Core eukaryotic genes mapping approach
CIP Calf intestinal alkaline phosphatase
CMFM Calcium magnesium-free medium
CRISPR Clustered regularly interspaced short palindromic repeats
DAPI 4',6-diamidino-2-phenylindole
DGCR8 DiGeorge syndrome chromosomal region 8
DIC Differential interference comtrast
DIRS Dictyostelium intermediate repeat sequence
DMEM Dulbecco's Modified Eagle's Medium
Dox Doxycycline
dsRNA double-stranded RNA
DTT Dithiothreitol
ECL Enhanced chemiluminescence
EDTA Ethylenediaminetetraacetic acid
EdU 5-ethyl2-deoxyuridine
EGTA Ethylene glycol tetraacetic acid
endo-siRNA endogenous small interfering RNA
ER Endoplasmic reticulum
ES cell Embryonic stem cell
FACS Fluorescence-activated cell sorting
FBS Fetal Bovine Serum
FISH Fluorescent *in situ* hybridization
EST Expressed sequence tag
FKBP6 FK506 Binding Protein 6
FPLC Fast protein liquid chromatography
GFP Green fluorescence protein
GSC Germline stem cell
H3K9me3 Histone 3 lysine 9 trimethylation
HEK293 Human embryonic kidney 293 cell
HEPES 4-(2-hydroxyethyl)-1-piperazineethanesulfonic acid
HP1a Heterochromatin protein 1a
HRP Horseradish peroxidase
Hsp83 Heat shock protein 83
HSP90 Heat shock protein 90
IGV Integrative genomics viewer
IP Immunoprecipitation
IPTG Isopropyl β-D-1-thiogalactopyranoside
IRES Internal ribosome entry site
KD Knockdown
KI Knockin
KO Knockout
LINE Long interspersed nuclear element
lncRNA long noncoding RNA
LOQS Loquacious
LTR Long terminal repeat
Macpiwi *M. lignano* Piwi-like protein
Macvasa *M. lignano* Vasa protein
MAD Median absolute deviation
Mael Maelstrom
MBP Maltose-binding protein

MEF Mouse embryonic fibroblast
miRNA microRNA
MILI Mouse Piwi-like protein 2
MIWI Mouse Piwi-like protein 1
MIWI2 Mouse Piwi-like protein 4
MOI Multiplicity of infection
mRNA messenger RNA
MSCV Murine stem cell virus
ORF Open reading frame
PAGE Polyacrylamide gel electrophoresis
PAZ PIWI-ARGONAUTE-ZWILLE
PBS Phosphate-buffered saline
PCR Polymerase chain reaction
PEV Position-effect variegation
PGC Premordial germ cell
PGK Phosphoglycerate kinase promoter
PLE Penelope-like element
piRNA PIWI-interacting RNA
PIWI P element-induced wimpy testes
PLD Phospholipase D
PMSF Phenylmethanesulfonylfluoride
PNK Polynucleotide kinase
Pol II RNA polymerase II
Pri-miRNA Primary microRNA
PPM Part per million
PRMT5 Protein Arginine Methyltransferase 5
PVDF Polyvinylidene fluoride
RACE Rapid amplification of cDNA end
RDC Rhino-Deadlock-Cutoff
RISC RNA-induced silencing complex
RNAi RNA interference
RPKM Read per kilo base pair per million
RPM Read per million
rpsL Ribosomal protein S12
rRNA Ribosomal RNA
RsAgo *R. sphaeroides* Argonaute
RT Reverse transcriptase
rtTA Reverse tetracycline-controlled transactivator
SDS Sodium dodecyl sulfate
SINE Short interspersed nuclear element
siRNA small interfering RNA
shRNA short hairpin RNA
Shu Shutdown
SMEDWI *S. mediterranea* Piwi-like protein
SRA Sequence read archive
TALEN Transcription activator-like effector nuclease
TARBP2 TAR (HIV-1) RNA binding protein 2
TBS Tris-buffered saline
Tdrd Tudor domain containing protein
Tdrkh Tudor And KH Domain Containing protein
TE Transposable element
TEM Transmission electron microscopy
TIR Terminal inverted repeat
Tj Traffic Jam
Tris Trisaminomethane
tRNA Transfer RNA
TthAgo *T. thermophilus* Argonaute
UTR Untranslated region
Vas Vasa
WT Wild type
Zuc Zucchini

Acknowledgment

Finally, I have seen the light from the end of the tunnel! It has not been easy to get to this point. But I am glad that this day has come eventually. A Ph.D. is a lonely business. But it does not lack great company and support all the way. Here I would like to express my gratitude to all the amazing people without whom I would never make it this far.

First of all, I would like to thank my family. It was not an easy decision for them back then when I chose to study abroad thousands of miles away from home. But they understood and supported me any way all these years. They are the ones who have always been there for me whatever I do and whoever I want to become. Second, I need to say thank you to everyone who contributed to the work in this thesis. I have a million thanks to Kaja Wasik, who offered me the *M. lignano* piRNA project when I was stuck with everything else I have tried, for helping me with everything she could from the bench side to manuscript writing. The *M. lignano* work was a truly pleasant and exciting collaboration that I would remember forever. I want to say thank you to the two great computational biologists, Osama El Demerdash and James Gurtowski, for all the computational support. Giorgia Battistoni optimized several protocols at the early stage of this work and without her efforts my work would have taken much longer. Ilaria Falciatori assisted cell sorting and gave helpful feedback during the manuscript preparation. Peter Ladurner generously shared his expertise in *M. lignano* with us. Julia Wunderer from Ladurner Lab performed *in situ* hybridization for us and provided hundreds of great images when we needed them urgently for the manuscript. Mike Schatz who supervised the genome assembly led by Kaja Wasik and James Gurtowski has been a great mentor. Without him, the genome assembly would not have been possible and this piRNA project would not have existed. Besides those who directly contributed to my thesis, I would also like to say thank you to some of the awesome Hannon Lab folks. We have spent so much time in McClintock building and the bar together days and nights where I would call home. And the folks working there make me feel like we are a big family, with all the support and caring I received from many of them. Vasily Vagin, the brilliant former postdoc who used to sit back to back with me in the lab, has been a great friend, mentor and drinking buddy. He is the one I turn to when I need someone either to brainstorm or to have a glass of Weihenstephan. He will always try to spare some time when I need it. Thanks to Sihem Cheloufi for guiding me into the world of RNAi when I first arrived at Hannon Lab. Our miR-451 work has built the foundation of my understanding of RNAi. Thanks to Simon Knott for the work we have done together on improving shRNAs, and also for being such a funny character. Thanks to those who maintain the infrastructure of the lab, such as Sabrina Boettcher, Nancy Bolanos and Emily Lee. They have done often invisible but tremendous work for the entire Hannon Lab. I would like to thank my friend Christof Fellmann, for all the discussion about shRNAs, late night cooking after long days of work and critical reading of my manuscript. I wish him a great life and career in California. I am grateful to my committee, Kevin Czaplinski, Jingfang Ju, Marja Timmermans and Chris Hammell for steering me towards the right direction. At last but not least, I thank my Ph.D. advisor

Greg Hannon for making everything possible. When I desperately needed a lab to conduct my thesis research, he brought me into the Hannon Lab family and showed me how science should be done. He is one of the sharpest and brightest scientists and mentors one could have the opportunity to interact with. I feel extremely lucky to be able to pursue my scientific career in such an interactive, exciting and vivid environment that never lacks intellectual challenges and rewards each day. Please excuse me if I miss anyone but you know I will not forget. In the end, I wish everyone a great life and a successful career. It is my pleasure to have met you and hopefully we will meet again!

Curriculum Vitae

Xin Zhou was from the city of Tianjin, China. After finishing secondary education at Nankai High School in Tianjin in 2004, she attended University of Science of Technology of China and received Bachelor of Science in life sciences in 2008. In the same year, she joined the Molecular and Cellular Biology graduate program at Stony Brook University for Ph.D. study. In 2010, she joined the laboratory of Dr. Gregory J. Hannon at Cold Spring Harbor Laboratory, focusing on RNA interference. Her work during Ph.D. training has been described in this dissertation below.

List of Publications

Zhou X*, Battistoni G, Gortowski J, El Demerdash O., Falciatori I, Wunderer J, Ladurner P, Schatz MC, Hannon GJ, Wasik KA*. 2015. Dual functions of Macpiwi1 in transposon silencing and stem cell maintenance in the flatworm model *Macrostomum lignano*. *RNA*, 2015 Aug 31. Epub ahead of print.

Wasik KA*, Gortowski J*, **Zhou X**, Ramos OM, Delas Vives MJ, El Demerdash O, Battistoni G, Falciatori I, Vizoso DB, Ladurner P, Schärer L, Hannon GJ, Schatz MC. 2015. The genome and transcriptome of the regeneration-competent flatworm, *Macrostomum lignano*. *Proceedings of the National Acadamy of Sciences*, in press.

Knott S*, Maceli A*, Erard N*, Chang K, Marran K, **Zhou X**, Gordon A, El Demerdash O, Wagenblast E, Fellmann C, Hannon GJ. 2014. A computational algorithm to predict shRNA potency. *Molecular Cell* 56(6):796-807.

Cai C, Rajaram M, **Zhou X**, Liu Q, Marchica J, Li J, Powers RS. 2012. Activation of multiple cancer pathways and tumor maintenance function of the 3q amplified oncogene FNDC3B. *Cell Cycle 11*(9), 1773-1781.

Chapter 1
Introduction

1.1 Transposable elements (TEs) – a double-edged sword

Barbara McClintock first discovered the phenomenon of “jumping genomic elements” in maize, where the color patterns were altered by unstable mutations moving around the genome (McClintock 1951). Her findings raised suspicion in the scientific community at first, due to the common concept that genes were fixed in the genome. However, soon after similar elements were discovered in organisms ranging from bacteria to mammals (Biemont 2010), the significance of TEs started to surface.

1.1.1 Classification of TEs

Based on the presence or absence of RNA intermediates, transposable elements are usually divided into two classes: the class I transposable elements (retrotransposons) and the class II transposable elements (DNA transposons) (Wicker et al. 2007) (Figure 1.1). Retrotransposons utilize a “copy-and-paste” mechanism via RNA intermediates. The genomic template is first transcribed into RNA intermediate and then reversely transcribed into DNA by a reverse transcriptase (RT). Based on different mechanistic features, the class I transposons can be further divided into five orders: long terminal repeat (LTR), Dictyostelium intermediate repeat sequence (DIRS), Penelope-like element (PLE), long interspersed nuclear element (LINE) and short interspersed nuclear element (SINE). The class II transposable elements are divided into two subclasses, based on the number of DNA strands that are cut during transposition. The terminal inverted repeat (TIR) subclass uses a ‘cut-and-paste’ mechanism involving a transposase. The transposition usually generates target site duplication. The other subclass contains TEs that replicate template DNA using ‘copy-and-paste’ mechanisms, such as helitron and maverick. Helitron utilizes a rolling circle replication to replicate template. Only one DNA strand is cut and no target site duplication is generated. The mechanism of maverick remains unclear. The relative amount of class I and class II elements varies greatly across species, ranging from 100% class I elements in yeast *S. cerevisiae* to 100% class II elements in protozoan *T.vaginalis* (Feschotte and Pritham 2007). In human and mouse, the majority (>90%) of TEs are class I elements.

Classification		Structure	TSD	Code	Occurrence
Order	Superfamily				
Class I (retrotransposons)					
LTR	*Copia*	GAG AP INT RT RH	4–6	RLC	P, M, F, O
	Gypsy	GAG AP RT RH INT	4–6	RLG	P, M, F, O
	Bel–Pao	GAG AP RT RH INT	4–6	RLB	M
	Retrovirus	GAG AP RT RH INT ENV	4–6	RLR	M
	ERV	GAG AP RT RH INT ENV	4–6	RLE	M
DIRS	*DIRS*	GAG AP RT RH YR	0	RYD	P, M, F, O
	Ngaro	GAG AP RT RH YR	0	RYN	M, F
	VIPER	GAG AP RT RH YR	0	RYV	O
PLE	*Penelope*	RT EN	Variable	RPP	P, M, F, O
LINE	*R2*	RT EN	Variable	RIR	M
	RTE	APE RT	Variable	RIT	M
	Jockey	ORF1 APE RT	Variable	RIJ	M
	L1	ORF1 APE RT	Variable	RIL	P, M, F, O
	I	ORF1 APE RT RH	Variable	RII	P, M, F
SINE	*tRNA*		Variable	RST	P, M, F
	7SL		Variable	RSL	P, M, F
	5S		Variable	RSS	M, O
Class II (DNA transposons) - Subclass 1					
TIR	*Tc1–Mariner*	Tase*	TA	DTT	P, M, F, O
	hAT	Tase*	8	DTA	P, M, F, O
	Mutator	Tase*	9–11	DTM	P, M, F, O
	Merlin	Tase*	8–9	DTE	M, O
	Transib	Tase*	5	DTR	M, F
	P	Tase	8	DTP	P, M
	PiggyBac	Tase	TTAA	DTB	M, O
	PIF–Harbinger	Tase* ORF2	3	DTH	P, M, F, O
	CACTA	Tase ORF2	2–3	DTC	P, M, F
Crypton	*Crypton*	YR	0	DYC	F
Class II (DNA transposons) - Subclass 2					
Helitron	*Helitron*	RPA Y2 HEL	0	DHH	P, M, F
Maverick	*Maverick*	C-INT ATP CYP POL B	6	DMM	M, F, O

Structural features

Long terminal repeats; Terminal inverted repeats; Coding region; Non-coding region; Diagnostic feature in non-coding region; Region that can contain one or more additional ORFs

Protein coding domains

AP, Aspartic proteinase; APE, Apurinic endonuclease; ATP, Packaging ATPase; C-INT, C-integrase; CYP, Cysteine protease; EN, Endonuclease; ENV, Envelope protein; GAG, Capsid protein; HEL, Helicase; INT, Integrase; ORF, Open reading frame of unknown function; POL B, DNA polymerase B; RH, RNase H; RPA, Replication protein A (found only in plants); RT, Reverse transcriptase; Tase, Transposase (* with DDE motif); YR, Tyrosine recombinase; Y2, YR with YY motif

Species groups

P, Plants; M, Metazoans; F, Fungi; O, Others

Figure 1.1 Classification of transposable elements (TEs). DIRS, Dictyostelium intermediate repeat sequence; LINE, long interspersed nuclear element; LTR, long terminal repeat; PLE, Penelope-like elements; SINE, short interspersed nuclear element; TIR, terminal inverted repeat. Adapted from (Wicker et al. 2007).

1.1.2 Interactions between TEs and the host genome

Regarding the relationship between TEs and the host genome, McClintock (McClintock 1951) and Britten & Davidson (Britten and Davidson 1969) proposed that TEs serve as controlling elements in gene regulation. In contrast, some simply perceived TEs as “junk DNA” (Ohno 1972), as most of these TEs and interspersed repeats did not seem to have functions. Moreover, owing to the ability of transposition, they were considered “selfish DNA” or “genomic parasites” (Doolittle and Sapienza 1980; Orgel and Crick 1980), suggesting that their existence was only due to their selfish nature. However, as the knowledge of TEs grew, the views have been driven towards a common ground – TEs may have both beneficial and deleterious effects on the genome (Kidwell and Lisch 2001), just like most other genetic elements. On one hand, due to their ability to replicate within the genome, they provide a big repertoire of genetic regulatory elements that co-evolve with the host genome. On the other hand, the host genome has developed mechanisms to put TEs under control in order to prevent harmful transposition.

It is imaginable that uncontrolled TE transposition might introduce insertional mutations thus disrupt normal biological functions. Active TEs have been recorded to cause a series of human diseases, such as hemophilia (Kazazian et al. 1988) and neurofibromatosis (Wallace et al. 1991). However, in many aspects, TE insertions in fact help shape the host genome. TEs, a natural source of regulatory elements, are largely attributable to transcript diversity. And this is one of the contributors to the high complexity human genome achieves using relatively small number of genes. TE insertions can alter gene expression at both transcriptional and post-transcriptional levels (Figure 1.2). TEs can provide alternative splice sites and polyadenylation signals to the inserted transcripts. Take the human *ATRN* gene as an example (Tang et al. 2000). An L1 element has been inserted into one intron. As a result, some transcripts are spliced and polyadenylated within the L1 element, while other transcripts are spliced around the element with five additional exons. They two isoforms produce different forms of Attractin with distinct localizations and functions. Some TEs can also provide alternative promoters to the host gene. The classic example for this scenario is the ectopic mouse *Agouti* gene expression driven by the additional promoter from an upstream retrotransposon IAP (Morgan et al. 1999). This expression gives rise to the yellow fur color of agouti mouse. At post-transcriptional level, some TEs generate small RNAs that can silence the target transcripts. For instance, in *Drosophila* TE-derived small RNAs target Nanos mRNA and destabilize it by promoting deadenylation (Rouget et al. 2010). On a larger scale, TEs can provide a means to regulate a gene network involved in specific pathways, by providing regulatory elements or binding sites. For example, the activation of ERV LTRs in embryonic stem cells initiates the switch required for differentiation through epigenetic mechanism (Rowe et al. 2010; Macfarlan et al. 2011; Macfarlan et al. 2012). Furthermore, the host genome is able to domesticate the enzymatic activities carried out by TEs and adopt novel functions. The best known case is the V(D)J recombination in immune cells (Jones and Gellert 2004). Rag1, an enzyme derived from transposase (Kapitonov and Jurka 2005), initiates this process, together with Rag2. The RNA-dependent DNA polymerase, telomerase, is also thought to phylogenetically and functionally relate to non-LTR reverse transcriptase (Eickbush 1997), suggesting its origin from domesticated retrotransposons. In some species

lacking telomerase such as *D. melanogaster*, retrotransposon takes the part in chromosome end maintenance (Pardue and DeBaryshe 2003).

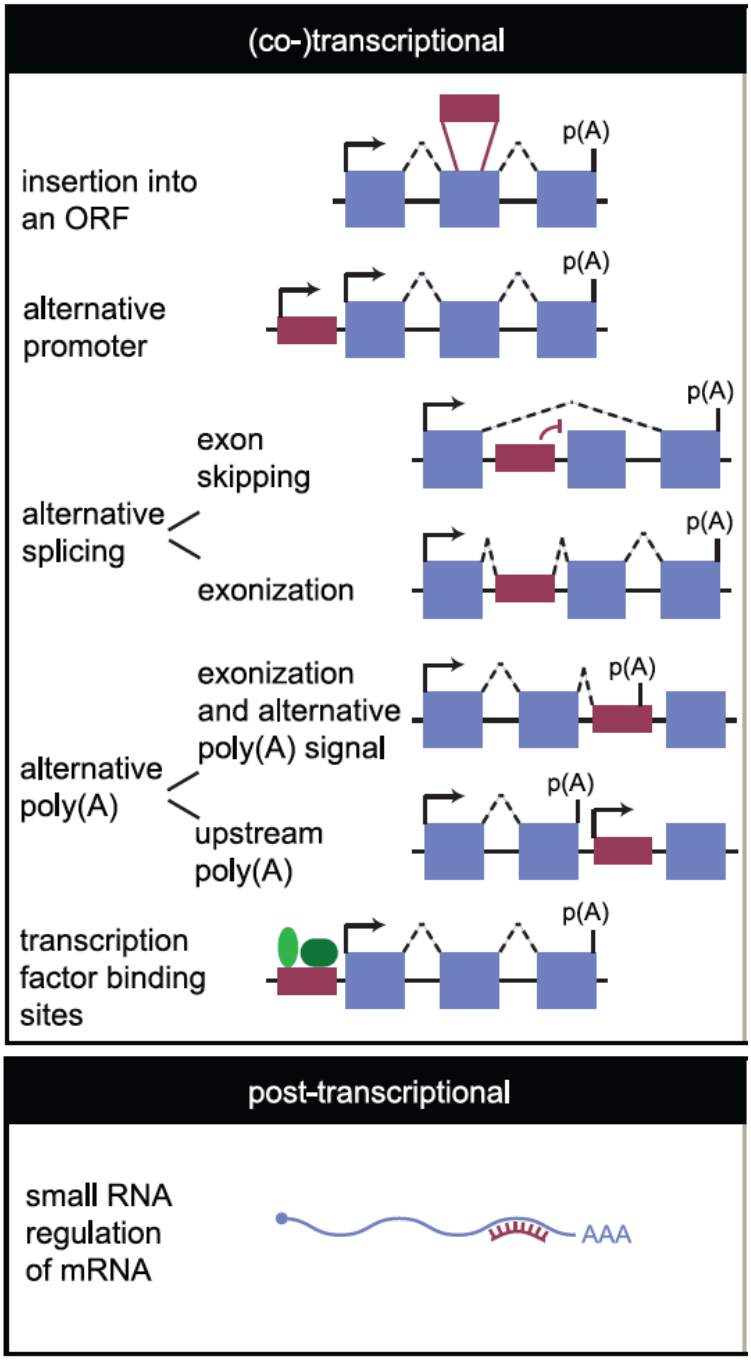

Figure 1.2 Mechanisms by which TEs alter gene expression. These mechanisms can act at either transcriptional or post-transcriptional level. The transcriptional alterations include: insertion of a TE into an open reading frame (ORF); providing alternative tissue- or stage-specific promoter; providing alternative splicing by exon skipping or introducing a new exon; providing alternative polyadenylation site; creating new tissue- or stage-specific transcription factor binding sites. At post-transcriptional level, small RNAs derived from TEs can regulate the expression from target transcripts. Adapted from (Cowley and Oakey 2013).

While maintaining the ability to transpose, TEs are under surveillance to avoid deleterious effects by both TE-driven and host genome-driven mechanisms. Within TEs, the spatiotemporal self-regulation is accomplished by several means, such as the dependence on host regulatory factors, alternative splicing and alternative polyadenylation sites. So TEs are only activated in specific tissues at specific time. For example, *Drosophila* P element is alternatively spliced in somatic tissue and germline in order to restrict the active form in the germline only (Siebel and Rio 1990).

During the evolution with TEs, the host genome has developed several defense mechanisms to suppress harmful TE activities. These mechanisms function primarily through epigenetic regulation, such as DNA and histone methylation. In eukaryotic genomes, TEs are usually methylated and associated with heterochromatins (Lippman et al. 2004). In animal germline, there exists a small RNA-guided immune system against TEs to protect the genomic integrity. This system generally involves Argonaute family proteins and their associated small RNAs (endo-siRNAs, piRNAs et al) (Watanabe et al. 2006). Small RNAs can guide proteins to target site in order to either modify the epigenetic states of TE DNA/chromatins or directly cleave the TE transcripts (Khurana and Theurkauf 2010). Defects in these pathways usually lead to uncontrolled TE activities, DNA damage and functional abnormality (Klattenhoff et al. 2007). In metazoans the small RNA-guided defense system includes the piRNA pathway and endogenous siRNA pathway. The next section will be mainly focused on the prime defender against TEs - the piRNA pathway.

1.2 piRNA pathway: immunity for genomic stability and beyond

1.2.1 Argonaute family proteins – effector of RNAi

Small RNAs play essential roles in gene regulation in metazoans. They interact with and guide Argonaute family proteins to target RNA transcripts by sequence complementarity and fulfill the silencing functions. The small RNA-bound Argonaute protein makes up the central component of the silencing complex. An Argonaute is characteristic for the presence of PAZ (PIWI-ARGONAUTE-ZWILLE) domain and PIWI (P element-induced wimpy testes) domain (Cerutti et al. 2000). The PAZ domain accommodates the 3' end of small RNAs by bending it into a pocket (Lingel et al. 2003; Song et al. 2003), while MID domain binds the 5' end of small RNAs with a strong preference for U and A nucleotides (Frank et al. 2010). The PIWI domain has an RNase H-like structure and is responsible for the cleavage of target RNA transcripts (Song et al. 2004). Only some Argonaute family proteins possess endonuclease activity. And the catalytic activity relies on a catalytic triad DDX with X being H or D (Rivas et al. 2005). The cleavage site is between 10^{th} and 11^{th} nucleotide from the 5' end of the guide (Wang et al. 2009). Catalytically inactive Argonaute proteins silence the targets through other transcriptional and post-transcriptional mechanisms, such histone modification and translation repression (Hock and Meister 2008).

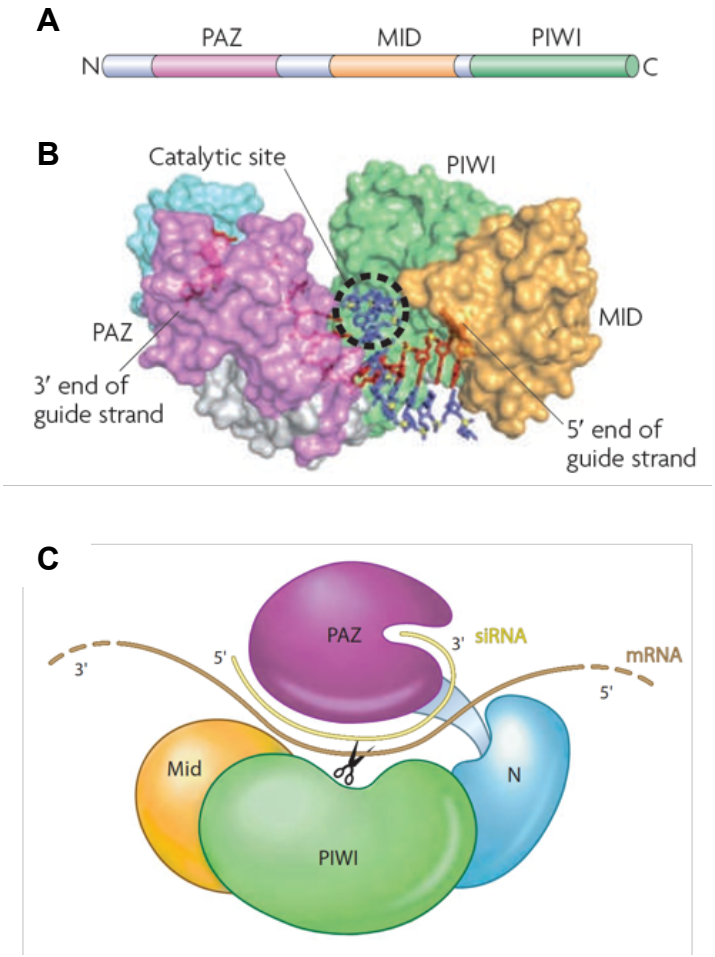

Figure 1.3 Structure of Argonaute proteins. (A) Domains of an Argonaute family protein. N: N-terminus; C: C-terminus; PAZ: PAZ (PIWI-ARGONAUTE-ZWILLE) domain; MID: MID (middle) domain; PIWI: PIWI domain. (B) The structure of a guide RNA-bound Argonaute protein. (C) A schematic presentation of small RNA-guided target cleavage. The small RNA (endo-siRNA in this example) guides Argonaute to the target mRNA by base pairing and the PIWI domain cleaves the target strand. Adapted from (Kim et al. 2009) and (Liu and Paroo 2010).

1.2.2 Classification of small RNAs

Based on different biogenesis mechanisms, there are three major classes of small RNAs in metazoans – microRNAs (miRNAs), endogenous small interfering RNAs (endo-siRNAs) and PIWI-interacting RNAs (piRNAs). Argonaute family proteins can be divided into two subclades – AGO clade and PIWI clade (Carmell et al. 2002; Hock and Meister 2008). miRNAs and endo-siRNAs interact with AGO clade proteins, while piRNAs are associated with PIWI clade. In addition to the distinct biogenesis processes, each small RNA pathway also carries out different biological functions.

1.2.2.1 miRNA pathway

First discovered in *C. elegans* (Lee et al. 1993), canonical miRNAs are small non-coding RNAs 19-23nt long, and characteristic of the RNase III Dicer and Drosha-

dependent biogenesis (Figure 1.4). Canonical miRNAs are originated from the stem-loop structures of pol II (RNA polymerase II) – transcribed primary transcripts (Lee et al. 2004a). In the nucleus, primary piRNA is first cleaved by RNase III Drosha (Lee et al. 2003) at the junction between the stem and single-stranded flanking regions to produce the miRNA precursor. The stem-loop-like precursor is then exported to cytoplasm by Exportin-5 (Yi et al. 2003). Another RNase III, Dicer, subsequently processes the precursor to remove the loop and to generate a dsRNA duplex with 2nt 5' overhangs (Bernstein et al. 2001). This duplex is then loaded into Argonaute (Ago) to form RISC (RNA induced silencing complex) (Hutvagner and Zamore 2002; Mourelatos et al. 2002) following the removal of the passenger strand. The mature Ago-associated miRNA has monophosphate at the 5' end and hydroxyl group at the 3' end as a result of RNase III processing (Elbashir et al. 2001).

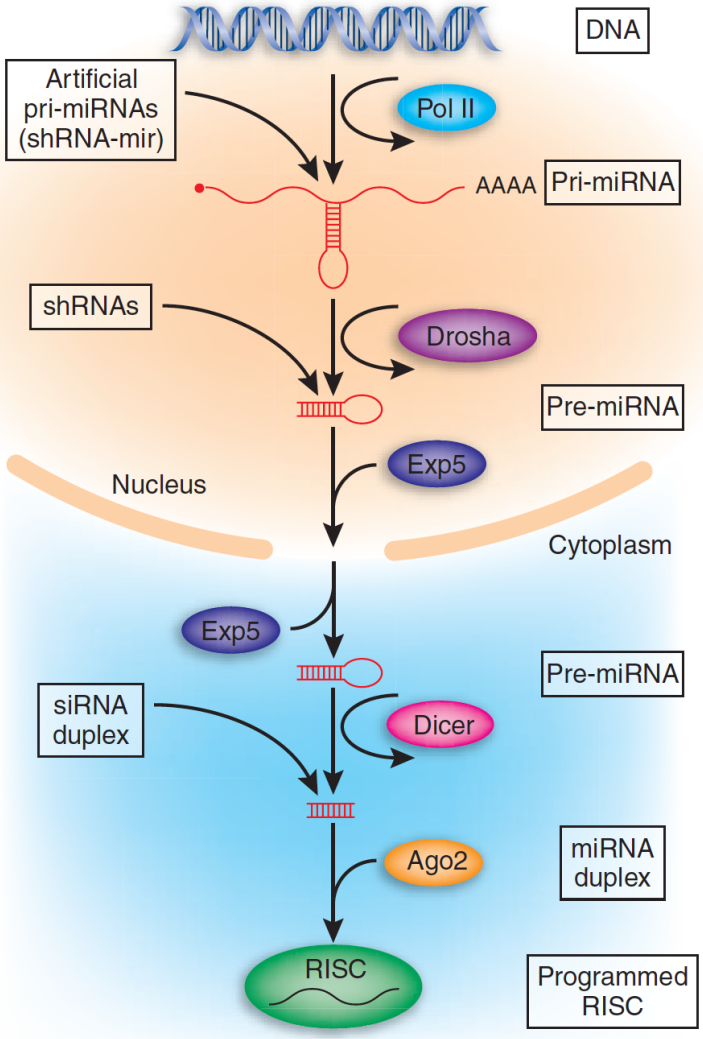

Figure 1.4 Biogenesis of canonical miRNA pathway. This pathway can be reprogrammed for gene silencing. Artificial RNAi can enter the pathway as siRNA duplex, precursor shRNAs or primary miR-like shRNAs. Adapted from (Cullen 2005).

miRNAs play pivotal roles in post-transcriptional gene regulation. The miRNA-guided RISC recognizes target mRNA transcripts and silences gene expression through several different approaches, such as target cleavage, translation suppression and promotion of RNA degradation (Filipowicz et al. 2008). The interaction between miRNAs and targets relies on Watson-Crick base paring. The 2-7nt seed region is critical for target recognition (Lewis et al. 2003; Brennecke et al. 2005; Krek et al. 2005; Lewis et al. 2005). While extensive complementarity induces target cleavage (Yekta et al. 2004), miRNAs are believed to mainly function through approaches other than direct target destruction. However, it is feasible to hijack this endogenous pathway to silence a gene of interest by target cleavage from several entry points (figure 1.4).

1.2.2.2 Endo-siRNA pathway

Endogenous siRNAs are generated from long dsRNA precursors (Figure 1.5). These precursors can come from divergent transcription (*cis*-dsRNAs), complementary transcripts from different sources (*trans*-dsRNAs) or a self-complementary long hairpin structure (Ghildiyal et al. 2008; Okamura et al. 2008a; Okamura et al. 2008b; Watanabe et al. 2008). The precursor dsRNAs are cleaved by Dicer and loaded into Ago proteins (Liu et al. 2003; Lee et al. 2004b; Pham et al. 2004; Czech et al. 2008). The size of siRNAs in flies and mammals is about 21nt long. Besides endogenous sources, this pathway can also utilize exogenous dsRNAs such as viral RNAs and artificially introduced dsRNAs (Ratcliff et al. 1997; Montgomery and Fire 1998; Hammond et al. 2000). The machinery is slightly different across metazoan species. In flies, endo-siRNA pathway depends on Dicer 2 rather than Dicer 1(Lee et al. 2004b; Czech et al. 2008; Okamura et al. 2008a). Interestingly, different Dicer cofactors, LOQS and R2D2 respectively, are preferred by different subset of siRNAs (Liu et al. 2003; Czech et al. 2008). Both endogenous and exogenous siRNAs are loaded into Ago2 (Kawamura et al. 2008). In contrast to mammalian siRNAs, the 3' end of mature Drosophila siRNAs is methylated by methylase Hen1 and thus has a 2'-o-methyl modification (Horwich et al. 2007).

TEs, enriched for repeats, RNA viruses and other exogenous dsRNAs, provide ideal dsRNA substrates for siRNA formation. Therefore, endo-siRNAs can serve as a defense against genomic instability caused by these endogenous and exogenous mobile elements. In *Drosophila*, mutations in Ago2 or Dicer 2 result in TE activation (Chung et al. 2008; Czech et al. 2008; Ghildiyal et al. 2008; Xie et al. 2013) and higher susceptibility to viral infection (Zambon et al. 2006). Apart from the role as a defense system, endo-siRNAs are involved in the regulation of endogenous gene expression. The *cis*-siRNAs have been shown to silence protein coding genes in *trans* in flies (Czech et al. 2008; Ghildiyal et al. 2008; Kawamura et al. 2008; Okamura et al. 2008a; Okamura et al. 2008b; Lau et al. 2009). The *trans*-siRNAs, in many cases derived from gene/pseudogene pairs, suppress the expression of cognate genes. Loss of Ago2 and Dicer leads to upregulation of target genes (Watanabe et al. 2006; Babiarz et al. 2008; Tam et al. 2008).

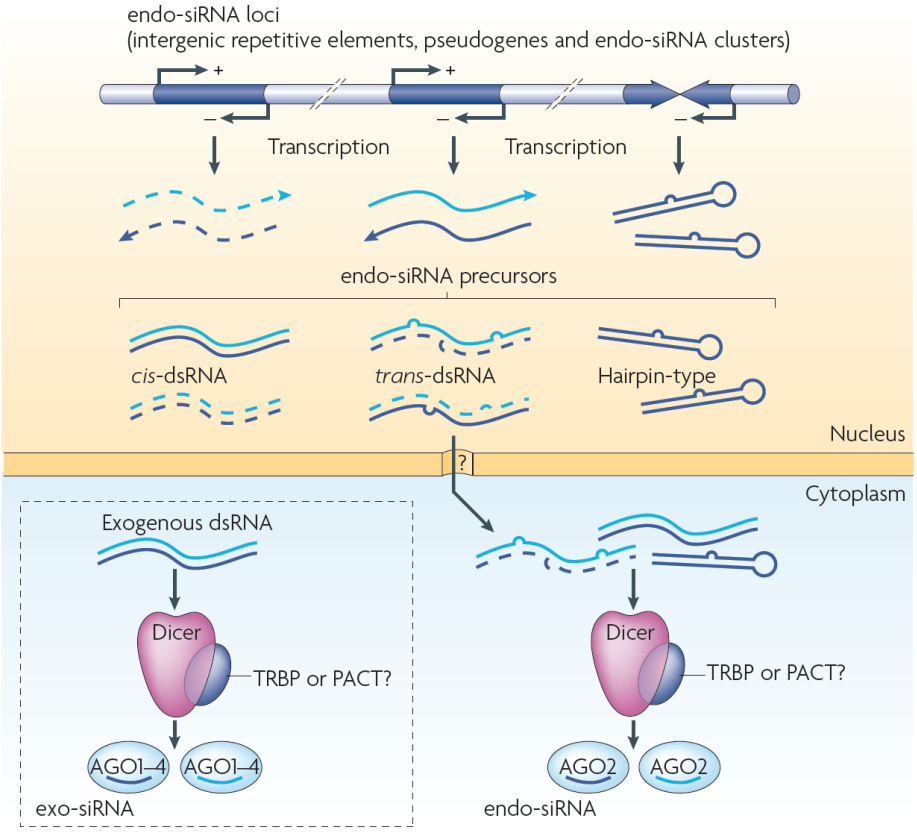

Figure 1.5 Biogenesis of endogenous siRNAs. Adapted from (Kim et al. 2009).

1.2.2.3 piRNA pathway

piRNAs are typically 24-32 nt small RNAs that interact with PIWI proteins and predominantly present in the animal germline. The biogenesis and functions of piRNAs are distinct and complex compared to miRNA and endo-siRNA pathways. piRNAs are the major players in transposon silencing and serve as a defense system against mobile genetic elements during animal germline development and maintenance. However, emerging evidence has painted a far more elaborate picture of piRNA and PIWI functions beyond the well-known transposon regulation.

1.2.3 Biogenesis of piRNAs

piRNA precursor transcripts are transcribed from large (10-100kb) genomic loci named piRNA clusters (Brennecke et al. 2007). These long transcripts are then processed into many different mature piRNAs in the cytoplasmic compartment of the piRNA machinery. Several proteins in the nucleus and cytoplasmic nuage facilitate the transport of piRNA precursors. In *D. melanogaster*, a homologue of heterochromatin protein 1, Rhino, was shown to co-localize with a DEAD box RNA helicase UAP56 on the nuclear side of the nuclear pores. This Rhino-UAP56 nuclear complex is often flanked by another DEAD box RNA helicase, Vasa, in the cytoplasmic nuage (Zhang et al. 2012). These proteins are proposed to facilitate the transfer of piRNA precursor from the nucleus to the cytoplasmic piRNA machinery. An interesting question about piRNA

transcription is how are piRNA precursor transcripts distinguished from other transcripts? In *D. melanogaster,* Rhino might be the key to the answer. A protein complex containing Rhino, Deadlock and Cutoff (RDC) are anchored to H3K9me3 chromatin and defines the boundary of dual-strand piRNA clusters (Mohn et al. 2014). Rhino also anchors UAP56 and a Rai1/DXO-related protein Cuff to stall splicing of piRNA transcripts to ensure the downstream processing of piRNA (Zhang et al. 2014).

The biogenesis of piRNAs is largely distinct from those of other small RNA pathways (Figure 1.6). In the cytoplasm, piRNA precursors are cleaved to form the 5' ends. It remains unclear which enzyme mediates this process. However, increasing evidence has posited Zucchini (Zuc) as the strongest candidate. Zuc is predicted to be a phospholipase resembling the bacterial PLD endonuclease Nuc (Voigt et al. 2012). Protein structures, in vitro assays and genetic analysis further support its ability to cleave single-stranded DNA and RNA (Ipsaro et al. 2012; Nishimasu et al. 2012). Indeed, animal with Zuc deficiency has loss of piRNA production and delocalized piRNA components. The Zuc-mediated primary piRNA biogenesis is a phased process with an interval of ~26nt in *D. melanogaster* (Figure 1.7) (Han et al. 2015a; Mohn et al. 2015). Each cleavage generates the 3' end of previous piRNA and the 5' end of subsequent piRNA. The Zuc-mediated primary piRNAs are then loaded into PIWI proteins with the assistance of chaperon protein complex. The best-known component is heat shock protein 90 (HSP90) homologues (Izumi et al. 2013). In *D. melanogaster,* the HSP90 homologue, Hsp83, interacts with an immunophilin chaperon protein, Shutdown (Shu), and facilitates the loading of piRNA into Piwi or Aubergine (Aub) (Olivieri et al. 2012; Preall et al. 2012). piRNA-loaded Aub but not Piwi then enters the ping-pong amplification loop for secondary piRNA biogenesis. Aub cleaves the transcripts containing complementary target sites and the 3' cleavage product with a new 5' end is loaded into another PIWI protein, Ago3, with the help of Shu and Hsp83. The Ago3-bound piRNA is trimmed from 3' end by unknown exonucleases and methylated by Hen1 at 2' hydroxyl group (Horwich et al. 2007; Saito et al. 2007). Ago3 finds and cleaves the antisense transcript with the guidance of its piRNA. The 3' cleavage product is then loaded into Aub with help of Shu and Hsp83 (Olivieri et al. 2012), and undergoes 3' end trimming and methylation again. Similar biogenesis mechanisms exist in different metazoan species, such as human, mouse and zebra fish. The secondary piRNA pathway can significantly amplify the piRNA production. It was widely believed that the primary and secondary piRNA biogenesis were separate until two recent studies revealed the interplay between them (Han et al. 2015a; Mohn et al. 2015). During secondary ping-pong cycle, cleavage by Ago3 or Aub creates a long 3' intermediate RNA, which is loaded into the corresponding ping-pong partner and becomes the substrate for Zuc cleavage. This initial cut triggers Zuc-mediated phased primary piRNA biogenesis and seeds the spread of piRNAs along the long RNA substrate (Figure 1.6 and 1.7). piRNA biogenesis is a highly coordinated process involving many components. Functional studies have recently revealed factors involved in the secondary biogenesis. These factors include several tudor domain containing proteins (Tudor (Nishida et al. 2009), Spindle-E (Lim and Kai 2007; Shoji et al. 2009; Vagin et al. 2009), Qin (Pan et al. 2005; Zhang et al. 2011; Anand and Kai 2012; Wasik et al. 2015), Krimp (Nagao et al. 2011; Sato et al. 2013), Vret (Handler et al. 2011; Zamparini et al.

2011), Tej (Patil and Kai 2010; Yabuta et al. 2011), Yb (Haase et al. 2010; Olivieri et al. 2010; Saito et al. 2010; Qi et al. 2011; Pandey et al. 2013), Papi (Chen et al. 2009; Vagin et al. 2009; Liu et al. 2011; Saxe et al. 2013)et. al), DEAD box RNA helicase Vasa (Vas) (Lim and Kai 2007; Kuramochi-Miyagawa et al. 2010; Xiol et al. 2014), HMG box protein Maelstrom (Mael) (Findley et al. 2003; Soper et al. 2008; Sato et al. 2011), RNA helicase Armitage (Armi) (Frost et al. 2010; Saito et al. 2010; Zheng et al. 2010; Qi et al. 2011)and GPAT family protein Minotaur (Vagin et al. 2013). Their localization indicates that ping-pong amplification takes place in nuage. Some of the factors, such Armi and Mael, participate in both primary and secondary piRNA biogenesis. The precise roles of these factors are yet to be defined.

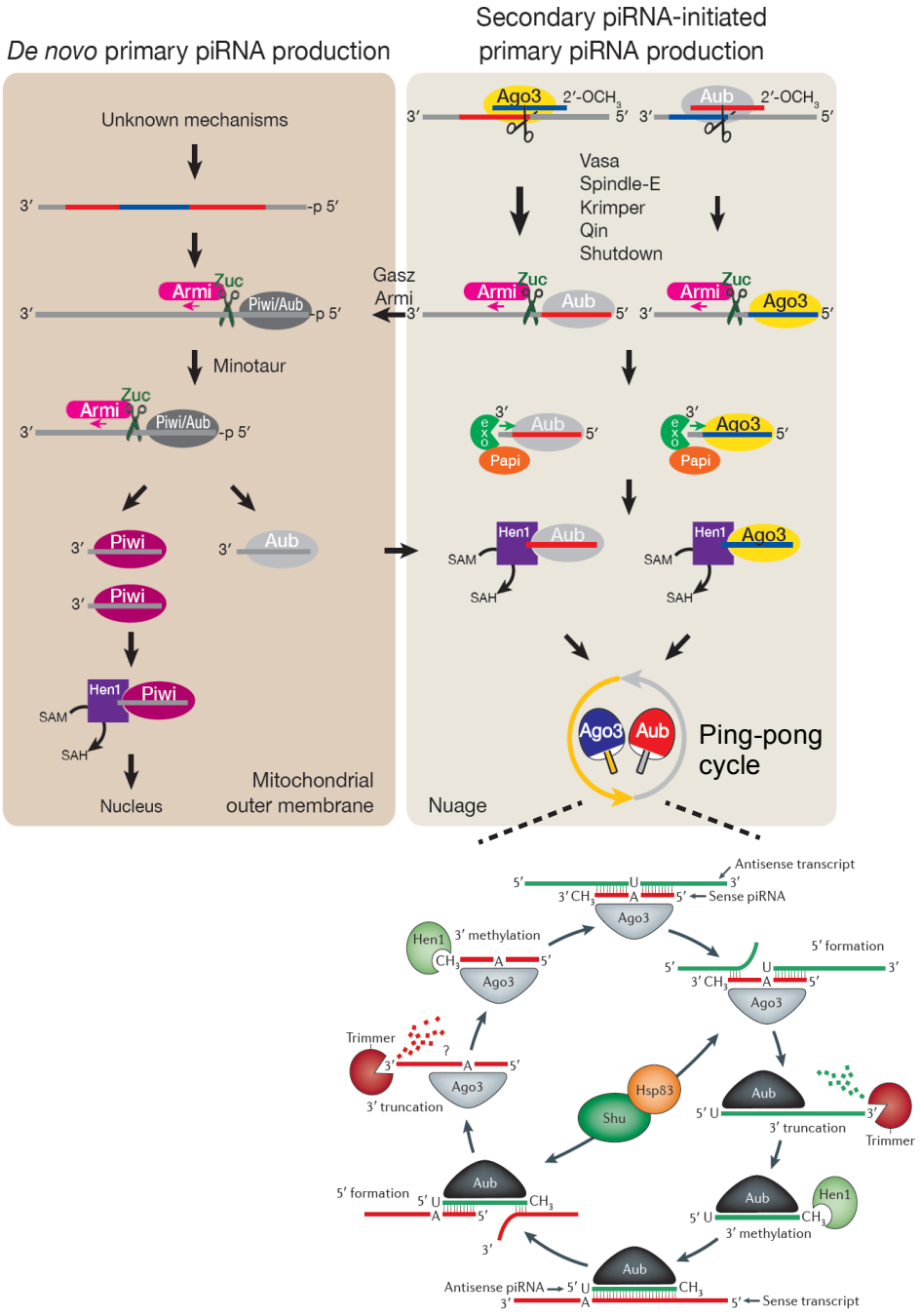

Figure 1.6 The latest piRNA biogenesis model in *D. melanogaster*. In the Zucchini-dependent *de novo* piRNA biogenesis, Zuc, with the assistance of other factors such as Armi and Minotaur, cleaves the target every ~26nt. The cleavage products are subsequently loaded into Piwi and Aub. The piRNA-loaded Aub then enters ping-pong cycle to initiate the heterogenic secondary amplification with Ago3. In parallel, the cleavage of Ago3 and Aub on the long RNA generates a 3' RNA intermediate with a 5'-monophosphate. This intermediate is loaded into the corresponding ping-pong partner and serves as the substrate for Zuc cleavage. Following the initial Zuc cut, the 3' cleavage product becomes the substrate for the *de novo* primary piRNA biogenesis mediated by Zuc. Adapted from (Han et al. 2015a) and (Luteijn and Ketting 2013).

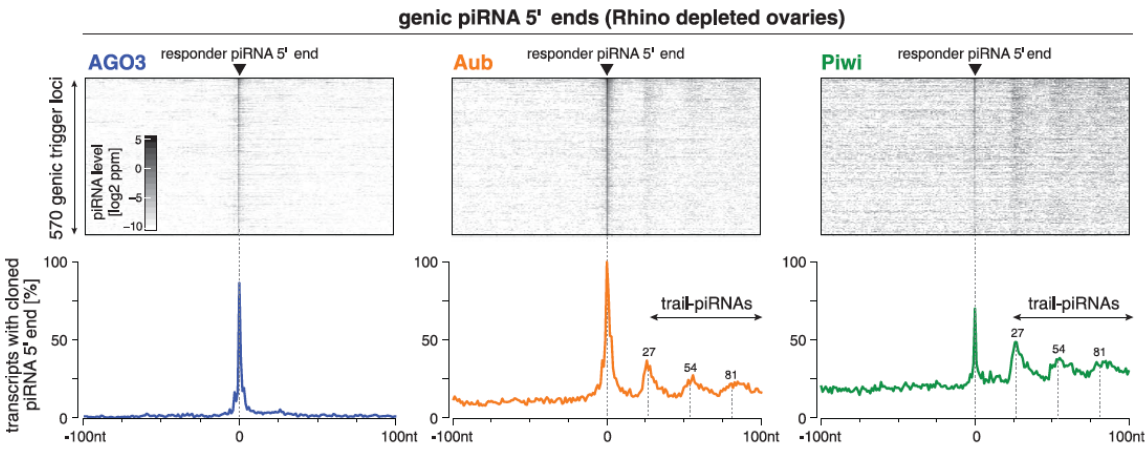

Figure 1.7 Phased piRNA formation mediated by Zucchini in D. *melanogaster*. In Rhino depleted ovaries, where piRNA production starts abruptly, Aub- and Piwi-bound piRNAs, but not Ago3-bound piRNAs, display phased 5' end pattern as a result of *de novo* primary piRNA formation mediated by Zucchini. Adapted from (Mohn et al. 2015).

1.2.4 piRNA-mediated gene regulation in metazoans

1.2.4.1 Gene regulation mechanisms by piRNAs

PIWI and piRNAs silence gene expression at both transcriptional and post-transcriptional levels. At transcriptional level, piRNAs and PIWI can recruit epigenetic modification machinery to supress gene expression. At post-transcription level, PIWI and piRNAs are suggested to act through multiple mechanisms, such as direct target cleavage, RNA degradation and translation repression.

1.2.4.1.1 Post-transcriptional controls

The best-known post-transcriptional silencing is the direct cleavage of target mRNAs. The biogenesis of piRNAs can be regarded as both formation of piRNAs and destruction of targets. Apart from this approach, several lines of evidence have pointed out the potential roles of PIWI in translational control. First, PIWI-piRNA complex is closely related to the translation and mRNA turnover machineries. Mouse MIWI is associated with mRNAs in polysomes and ribonucleoprotein (RNP) fractions (Grivna et al. 2006). MIWI and MILI interact with factors involved in mRNA 5' cap binding (Grivna et al. 2006; Unhavaithaya et al. 2009). Second, PIWI seems to control mRNA turnover through 3' UTR-generated piRNAs. For example, in *Piwi* mutant, protein level of Traffic Jam (Tj), whose 3' UTR generates abundant piRNAs, is upregulated (Saito et al. 2009). In fly embryos, Aub and Ago3 mutations abolish the deadenylation and decay of *nanos* mRNA (Rouget et al. 2010). Aub has been shown to interact with mRNA deadenylase and *nanos* mRNA, guided by piRNAs from 3' UTR of *nanos*. Considered as a whole, PIWI proteins might play underestimated roles in post-transcriptional control other than epigenetic regulation.

1.2.4.1.2 Epigenetic regulation by PIWI and piRNAs

PIWI and piRNAs are involved in epigenetic regulation by histone modification and DNA methylation. In *D. melanogaster,* Piwi and Aub physically interact with heterochromatin protein 1a (HP1a) and this interaction is required for heterochromatin formation (Pal-Bhadra et al. 2004; Brower-Toland et al. 2007). Lack of Piwi/Aub-HP1a interaction leads to loss of heterochromatin and deficiency of position-effect variegation (PEV), in which the expression of a euchromatic gene is silenced, when placed in proximity to a heterochromatic region. Introduction of repeated transgene can induce artificial PEV by recruiting heterochromatin-forming machinery. Mutations in *Piwi* or *Aub* derepress the repeated transgene by inhibiting heterochromatin formation. Besides inhibitory roles, in some cases, PIWI also acts as an epigenetic activator. *Drosophila* Piwi has been shown to regulate epigenetic status of the telomere-associated sequence of third chromosome right arm (3R-TAS) (Yin and Lin 2007). In wild type, this region is semi-euchromatic whereas in *Piwi* mutant it is heterochromatic. The presence of a piRNA, 3R-TAS1, suggests that Piwi might recruit chromatin-modifying machinery to maintain the euchromatic state of this region. In addition, PIWI proteins can also mediate DNA methylation. In mouse, loss of MIWI2 and MILI results in loss of DNA methylation in the transposon-encoding regions and corresponding TE derepression (Aravin et al. 2007; Kuramochi-Miyagawa et al. 2008). The precise mechanism of PIWI-mediated DNA methylation remains elusive.

1.2.4.2 Targets of piRNA/PIWI-mediated gene silencing

1.2.4.2.1 Regulation of transposable elements (TEs) by the piRNA pathway

The best-understood function of piRNAs is TE silencing in animal germline. piRNAs act as the major defense system against genomic instability caused by TE activities. And in the germline, this protection is of particular importance, as the germ cells will pass the genetic information to the next generation. In animal species studied by far, a considerable proportion of piRNAs aligns to TEs, suggesting their involvement in TE regulation. Indeed, disruption of piRNA biogenesis usually leads to TE upregulation. In *D. melanogaster,* disruption of the biggest piRNA cluster *flamenco* induces increase of TE activity (Sarot et al. 2004; Malone et al. 2009), demonstrating the role of piRNA clusters as key regulators of TE expression. In mouse, MILI and MIWI2 are required for the epigenetic silencing of TEs. In the absence of MILI or MIWI2, DNA methylation of TEs is disabled and TE depression occurs (Aravin et al. 2007; Kuramochi-Miyagawa et al. 2008). Deletion of piRNA clusters likewise results in increased TE activity (Xu et al. 2008). Moreover, protection of piRNAs is maternally inheritable in flies (Brennecke et al. 2008). Maternal piRNAs can provide protection against TEs for a whole generation. Whithout them, the progeny suffer from high TE activity, suggesting their function through epigenetic modification. Additionally, these maternal piRNAs might prime the initial piRNA production in the progeny. This maternal protection might be of particular importance because in fly embryos a large number of genes are quiescent.

1.2.4.2.2 Potential roles in mRNA and lncRNA regulation by piRNAs

Transposable elements are only one of the sources and targets of piRNAs. However, little is understood beyond that. In the recent efforts aiming to clarify the additional piRNA functions, several studies have discovered the link between piRNAs and the regulation of non-TE RNAs, such as mRNAs and lncRNAs. In mammalian male germline (mouse, human and common marmoset), pseudogenes are shown to produce antisense-oriented piRNAs that could potentially target cognate genes (Hirano et al. 2014; Pantano et al. 2015; Watanabe et al. 2015). In mouse late spermatocytes, a protein-coding gene *stambp* is regulated by anti-sense oriented piRNAs derived from its pseudogene *stambp-ps1.* Loss of *stambp-ps1* significant decreases the corresponding piRNA level and elevates the expression of *stambp* at post-transcription level. In fact, a considerable number of mRNAs and lncRNAs are suppressed in a piRNA-dependent manner, among which many contain TE-derived sequences in the 3' UTR. Defects in piRNA pathway or loss of piRNA target sites result in increased expression of target RNAs. And this piRNA-induced silencing is at least in part dependent on target cleavage.

1.2.4.3 Biological significance of piRNA pathway in metazoan germline development

PIWI proteins are essential for the germline development and maintenance in metazoans. Their functions are highly conserved across species. Take the well-studied *D. melanogaster* as an example. PIWI proteins direct the germ cell specification during early embryogenesis. Piwi and Aub localize in a specified structure required for germ cell formation, named polar granule (Harris and Macdonald 2001; Megosh et al. 2006). Polar granule is found in the germ plasm at the posterior pole of the embryo. PIWI interacts directly with polar granule components such as Vasa and Oskar. When Oskar is ectopically expressed, PIWI ectopic localization is observed. In the absence of maternal PIWI, embryos suffer from severe decrease of germ cell formation. Overdose of PIWI conversely induces a higher proportion of primordial germ cell (PGC) formation. Aub is also required for germ cell formation in flies. *Aub* null female flies laid few eggs with no germ cells. PIWI proteins are also essential for the maintenance of germline stem cells (GSCs), which was first described in *D. melanogaster.* PIWI was first discovered in a screen for factors involved in asymmetric germ cell division (Lin and Spradling 1997). Flies without PIWI suffer from underdevelopment of ovaries and testes due to the poor maintenance of GSCs (Cox et al. 1998; Cox et al. 2000). In fly gonads, PIWI is expressed in both germline and somatic cells. It has been shown that the PIWI expression in somatic niche cells is essential for GSC maintenance, whereas PIWI in GSCs promotes cell division of GSCs (Chen and McKearin 2005; Smulders-Srinivasan et al. 2010).

1.2.4.4 PIWI-piRNA functions in soma

Although PIWI proteins are predominantly expressed in metazoan germline, increasing evidence has demonstrated their involvement in somatic cells, ranging from pluripotent stem cells to highly differentiated tissues.

1.2.4.4.1 Somatic PIWI in *D. melanogaster*

The best-defined PIWI functions in soma are again from studies of *D. melanogaster.* In ovaries, PIWI proteins are expressed in both germline cells and somatic follicle cells. In contrast to the germline, there is only primary piRNA biogenesis mediated by PIWI in follicle cells, in the absence of Aub, Ago3 and secondary piRNAs (Brennecke et al. 2007). Follicle cell piRNAs mainly originate from two loci, *flamenco* and *traffic jam* (Brennecke et al. 2007; Saito et al. 2009). The *flamenco*-derived piRNAs target *Gypsy* family LTR retrotransposons (Sarot et al. 2004), while *traffic jam* provides a piRNA pool from its 3' UTR. These piRNAs from *traffic jam* are indicated to regulate the turnover of *traffic jam* mRNA, which produces PIWI. Outside gonads, PIWI is mainly expressed in the head. In salivary gland, PIWI is localized to the polytene chromosomes along with epigenetic modifiers such as polycomb proteins, indicating its roles in epigenetic regulation (Brower-Toland et al. 2007). In the brain, Aub and Piwi are detected in some specific areas and their depletion leads to upregulation of transposable elements in these regions (Perrat et al. 2013).

1.2.4.4.2 PIWI and piRNA-mediated somatic elimination in ciliates

Ciliates are single-cell organisms with two separate sets of genomes – a somatic macronucleus for vegetative growth and a germline micronucleus responsible for sexual reproduction known as conjugation. Following conjugation, one of the parental micronuclei undergoes elimination of repetitive elements to form the new somatic macronucleus. This process, named somatic elimination, is mediated by PIWI homologues and piRNAs (Mochizuki et al. 2002; Chalker and Yao 2011). The biogenesis of ciliate piRNAs, unlike canonical piRNAs, is derived from double stranded RNAs in Dicer-dependent manner (Mochizuki and Gorovsky 2005). piRNAs then mark either somatic genes for retention or germline genes for elimination to subsequently build a new somatic genome (Taverna et al. 2002; Aronica et al. 2008; Fang et al. 2012).

1.2.4.4.3 PIWI and piRNAs in memory formation

In sea slug *Aplysia californica*, memory formation is regulated by PIWI and piRNAs. The PIWI homologue associated with piRNAs can methylate the CREB2 promoter, an inhibitor of memory formation, thus promote synaptic transmission and memory (Rajasethupathy et al. 2012).

1.2.4.4.4 Potential involvement of PIWI in cancers

Cancer cells adopt stem cell-like properties and express many stem cell related genes. Indeed, various types of cancers have been reported to express ectopic PIWI

proteins (Siddiqi and Matushansky 2012). However, the relation between PIWI and cancer progression remains elusive and debatable. First, it is unclear whether PIWI is a cause or a consequence of cancer progression. Instead of the causal roles, PIWI overexpression might be a response to the genomic instability in cancer cells. For instance, in human epithelial cancers, where LINE-1 transposition is commonly observed (Pattamadilok et al. 2008), PIWI might be overexpressed in response to the hyperactivity of TEs. Second, there is no evidence so far to demonstrate the mechanisms of PIWI in cancers. Despite the ectopic expression of PIWI, neither piRNAs nor functional pathways have been described in cancers. More comprehensive studies are needed to elucidate the potential functions of PIWI in cancers.

1.2.4.4.5 PIWI and piRNAs in somatic stem cell functions in flatworms

As mentioned previously, PIWI and piRNAs are required for germ line stem cell maintenance. In some organisms, PIWI is also found in somatic stem cells. In some flatworms, there exists a unique somatic stem cell system known as neoblasts (Nimeth et al. 2007; Baguna 2012). These cells are believed to be the only dividing cells in the whole organism and responsible for all activities relying on cell division. PIWI homologues have been shown indispensable for the maintenance and functionality of neoblasts. Three PIWI homologues, Smedwi1, 2 and 3, were identified in planarian *Schmidtea mediterranea.* Silencing of Smedwi 2 and 3 leads to failure in regeneration (Reddien et al. 2005; Palakodeti et al. 2008). While cell division remains detectable, neoblasts exhibit abnormal behavior after amputation, indicating deficient differentiation of stem cells. Moreover, piRNA population is present in this organism, suggesting the likely involvement of PIWI through piRNAs (Friedlander et al. 2009). In another flatworm, *Macrostomum lignano*, a PIWI homologue Macpiwi1 is essential for the neoblast maintenance (De Mulder et al. 2009). Depletion of Macpiwi1 abolishes dividing cells and stem cell-dependent activities, such as regeneration, tissue renewal and postembryonic development. However, the mechanism through which PIWI participates in the stem cell functions remains largely unclear.

1.3 *Macrostomum lignano*: emerging flatworm model for stem cell and ageing research

The regeneration ability of flatworms has fascinated researchers for more than a century (Baguna 2012). Thomas Hunt Morgan and others found out that even a small piece of planarian tissue could develop to a whole new worm. It was suspected that some undifferentiated, embryonic-like cells were responsible for this amazing ability. And Harriet Randolph gave them the name ‘neoblast’. After rambling debates in regard to the roles of neoblasts, not until recently have researchers revealed the identity of these cells. Neoblasts are somatic stem cells and the only dividing cell type in regeneration-competent flatworms (Reddien and Sanchez Alvarado 2004; Nimeth et al. 2007). They are undifferentiated totipotent cells responsible for adult tissue homeostasis, postembryonic development and regeneration. In planarian, even a single transplanted neoblast is capable of full body tissue renewal after lethal dose of irradiation, proving the totipotency of neoblasts (Wagner et al. 2011). Regeneration-

competent flatworms, compared to worms without neoblasts, often have remarkably long lifespans, likely due to neoblasts.

1.3.1 Life history and morphology of *M. lignano*

Besides the classic regeneration model flatworm triclads, in recent years, researchers have promoted a newly discovered flatworm, *Macrostomum lignano,* as a new regeneration and ageing model (Ladurner et al. 2005; Mouton et al. 2009b). First isolated on the sandy beach in Northern Italy in 1995, *M. lignano* is a free-living flatworm that belongs to the basal group of Rhabditophora – the largest taxon within Platyhelminthes (simple, bilaterian and unsegmented flatworms). They can be found in the high-tide interstitial sand fauna on sheltered beaches of the Northern Adriatic Sea. They are tolerant to a wide range of temperature and salinity and can be easily maintained in laboratory conditions. In good culture condition, an adult worm can lay one egg per day. The embryonic development lasts for 5 days and a hatchling grows into adulthood in about two weeks (Egger et al. 2006). *M. lignano* has a median lifespan of 205 ±13 days, a 90% mortality of 373 ± 32 days and a maximum lifespan of more than 745 days (Mouton et al. 2009b). The mortality doubling rate is 0.2 ± 0.02 years, comparable to mammalian ageing models (Mouton et al. 2009a). The demographic data and complete survival curve are available for *M. lignano* (Figure 1.8), which is critical for establishing ageing model.

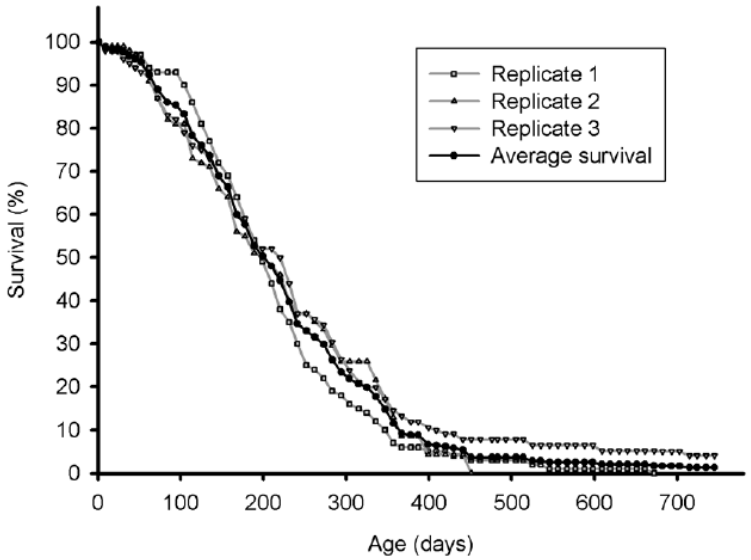

Figure 1.8 Survival curve of *M. lignano*. Adapted from (Mouton et al. 2009a).

M. lignano is a highly transparent hermaphrodite 1-1.5 mm long with a total number of around 25,000 cells (Figure 1.9 A). The epidermal layer is made of multiciliated cells responsible for locomotion. Under the epidermis is the muscle system containing circular diagonal and longitudinal muscle cells. The bilaterally symmetric nervous system contains a brain neuropile, two connected lateral nerve cords and two dorsal and ventral nerve cords (Morris et al. 2007) (Figure 1.9 B). The photoreceptors (eyes) detect light and mediate the negative phototaxis. The mouth and pharynx posterior to the eyes connect to the sac-like gut where food is processed. On each side

of the body, there is one testis and one ovary. Ovaries and developing eggs are located posterior to the testes. Sperm is stored in seminal vesicles and released from the stylet. On the edge of the tail plate there is a dual gland adhesive system that allows worms to attach to the surface quickly.

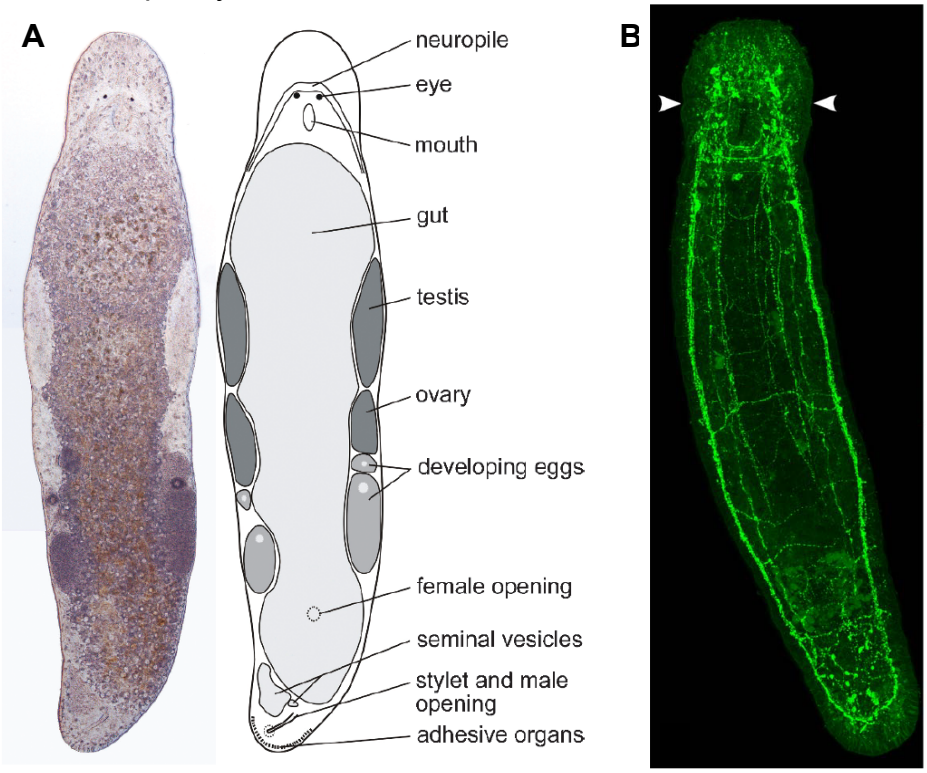

Figure 1.9 Morphology of *M. lignano*. (A) Interference contrast image and schematic drawing of an adult worm. (B) The nervous system of *M. lignano*. GYIRFamidergic cells are stained using anitibodies. Arrows denote the level of eyes. Adapted from (Ladurner et al. 2008) and (Egger et al. 2007).

1.3.2 *M. lignano* genome

M. lignano has eight chromosomes (2n=8) (Egger and Ishida 2005). The haploid genome contains one big chromosome (45.9% of total genome size) and three small ones (Figure 1.10). In contrast to the predominant 2n=6 genome composition of other *Macrostomum* species, the additional chromosomes indicate recent chromosome fission or duplication in *M. lignano*. Moreover, FISH for ribosomal sequences detects frequent duplication occurring across all chromosomes (personal communication with L. Schärer). Indeed, the *M. lignano* genome seems highly repetitive. The attempts to assemble the genome using short sequencing reads yielded very poor results. Our attempt using both short and long sequencing reads significantly improved assembly, yet still failed to assemble the whole chromosomes, suggesting unusually large and frequent repeats present in the genome.

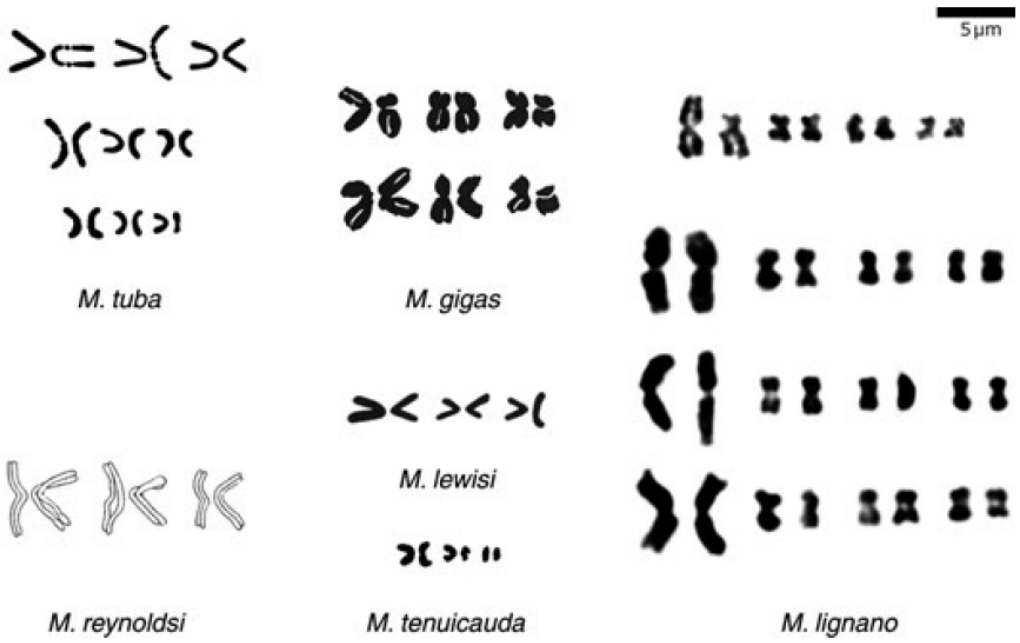

Figure 1.10 Karyotypes of a group of *Macrostomum* species. Replicates are shown for *M. tuba*, *M.gigas* and *M. lignano*. The *M. lignano* replicate on the top was stained with Orcein, while the other three were stained with Giemsa. Adapted from (Egger and Ishida 2005).

1.3.3 Characteristics of neoblasts

1.3.3.1 Distribution of neoblasts

The term 'neoblast' was first adopted by Harriet Randolph to describe the putative undifferentiated cells responsible for regeneration in earthworm and later extended to those in flatworms (Baguna 2012). Only recently have researchers revealed the identity of neoblasts in flatworms (Figure 1.11). Neoblasts, including mesodermal, gastrodermal and gonadal stem cells, are believed to be the only dividing cells in the whole worm. The S-phase and M-phase neoblasts can be visualized using BrdU/EdU incorporation and phosphorylated histone H3 labeling respectively (Bode et al. 2006; Nimeth et al. 2007) (Figure 1.11 B and C). The mesodermal neoblasts are located laterally in the mesodermal parynchyme – the tissue between epidermis and the gut – in proximity to the main lateral nerve cords. Gastrodermal stem cells are localized in the gastrodermis. These cells can also be found around midline (Figure 1.11 A, D and E). The two lines of neoblasts merge at the tail plate. The rostrum anterior to the photoreceptors is devoid of neoblasts (Figure 1.11 B and C). A few dividing cells, likely to be gastrodermal stem cells, are detected in the midline of the body. Overtime, dividing cells migrate from lateral regions to the median axis and rostrum.

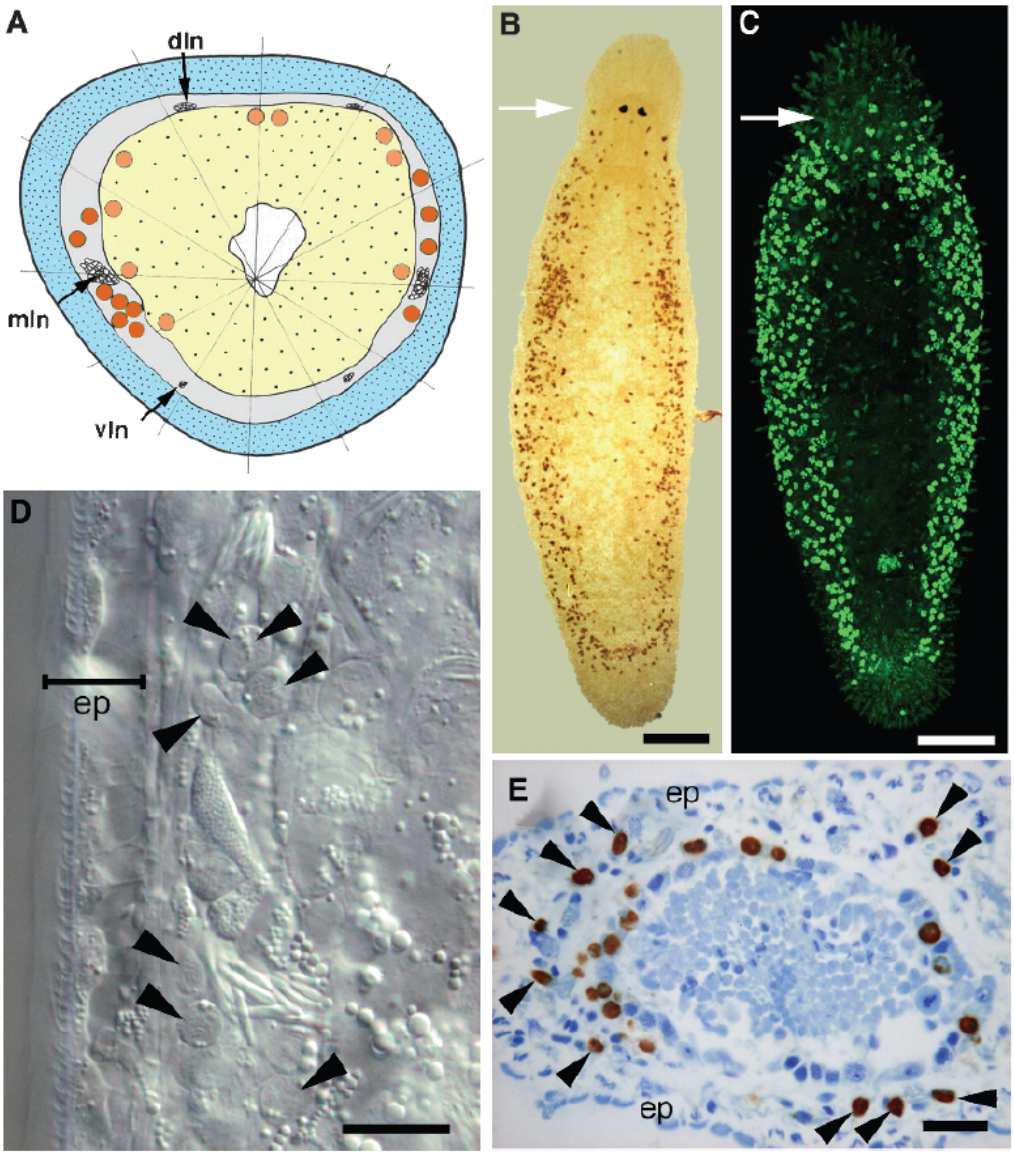

Figure 1.11 Distribution of neoblasts. (A) Schematic presentation of a transversal plane in the worm. Blue: epidermis; grey: mesodermal parynchyme; yellow: gastrodermis; orange: mesodermal neoblasts; light yellow: gastrodermal neoblasts; mln: main lateral nerve cord; vln: ventral nerve cord; dln: dorsal nerve cord. Staining of S-phase (B) cells using BrdU 30min pulse and mitotic cells (C) using anti-phosphorylated H3 antibody. Arrows denote level of eyes. (D) Interference contrast image of a squeeze preparation of a live animal. Arrows point at neoblasts below the epidermis (ep). (E) Lateral sagittal section through the testis after a 30min BrdU labeling. Arrows point at the mesodermal neoblasts below epidermis (ep). The other BrdU-positive cells are spermatogonia and spermatocytes. The center contains differentiating spermatids and spermatozoa, which are not dividing cells. Adapted from (Ladurner et al., 2008).

1.3.3.2 Morphology and dynamics of neoblasts

The ultrastructure of neoblasts can be observed using electron microscopy (Bode et al. 2006) (Figure 1.12). In general, a neoblast is a small cell with a large nucleus,

some free ribosomes, few mitochondria and limited endoplasmic reticulum (ER). Based on the cytoplasmic and nuclear organization, *Macrostomum* neoblasts can be classified into three stages. In stage 1 and 2, there are only some free ribosomes with few mitochondria in the cytoplasm. Heterochromatins are condensed in speckles. In stage 2, the heterochromatin speckles are more connected than stage 1. Rough ER is formed at stage 3 in cytoplasm with large heterochromatin strands in the nucleus. In *M. lignano,* stage 1 neoblasts are only present in hatchlings, whereas adult worms have stage 2 and 3 neoblasts. It remains unclear whether the three stages represent different differentiation stages of a pool of neoblasts or distinct subpopulations with their own cell cycles.

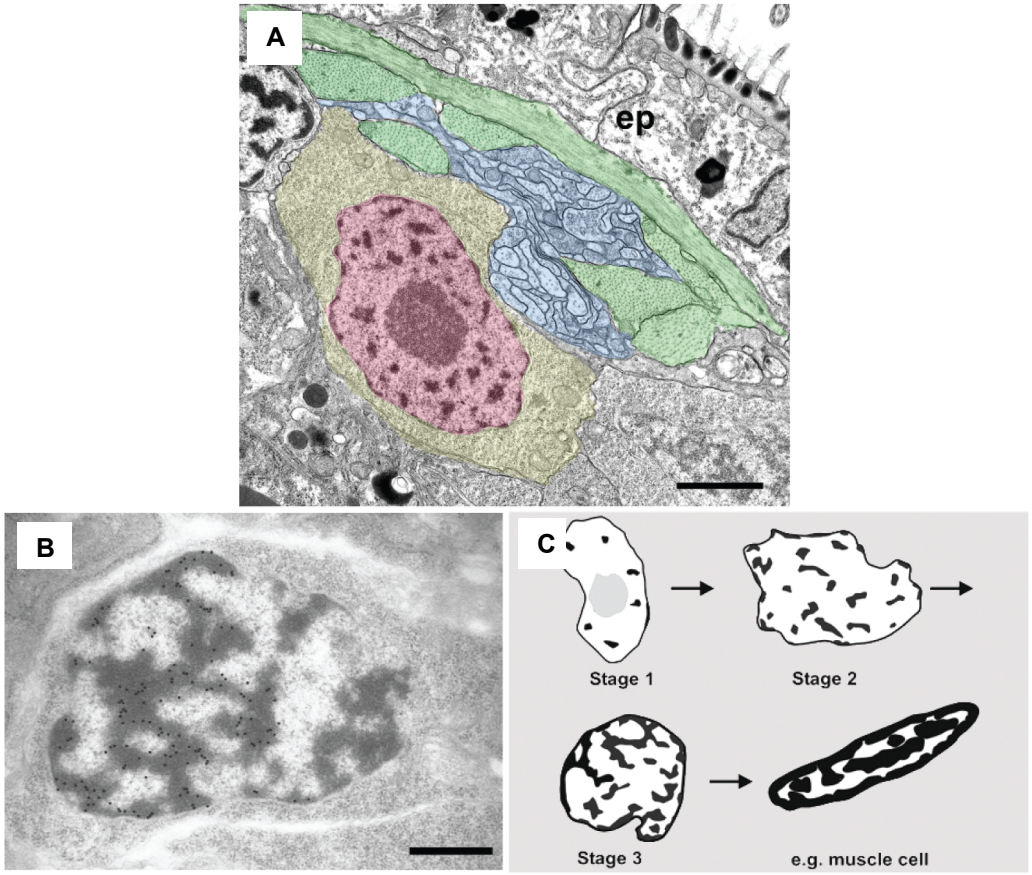

Figure 1.12 Morphology of neoblasts in *M. lignano*. (A) Ultrastructure of a neoblast. The nucleus (red) contains condensed chromatins and is surrounded by thin layer of cytoplasm (yellow). It is in contact with the nerve cord (blue) below the muscle cells (green) and epidermis (ep). (B) Immunogold staining of a BrdU-labeled neoblast. Black dots labels condensed chromatin. (C) Schematic illustration of neoblast nuclei from low to high chromatin complexity. Adapted from (Ladurner et al., 2008).

Based on transmission electron microscopy (TEM) with BrdU labeling, neoblasts can be quantified (Bode et al. 2006). Neoblasts make up about 6.5% of the total cell population. 27% of them are in S-phase. Of all S-phase neoblasts, there are 33% stage 2 cells, 21% stage 3 cells and 46% cells in transition between stage 2 and 3. Non-BrdU-labeled neoblasts exist in adult worm over a 2-week BrdU incorporation, suggesting the presence of neoblasts arrested at G2 phase. Starvation and feeding significantly affect neoblast cell cycle (Nimeth et al. 2004; Nimeth et al. 2007). A 30-day starvation sharply decreases mitosis but mitotic activity is restored rapidly after feeding. The bimodal

increase of mitosis suggests that G2-phase cells first enter mitosis before S-phase cells pass M-phase. Moreover, double labeling for S-phase and M-phase cells also reveals neoblasts with various lengths of cell cycles. BrdU labeling shows that within 14 days about 7,000 cells are renewed in an adult worm.

Gamma radiation has been applied to eliminate neoblasts (De Mulder et al. 2010). Surprisingly, a high dose of 200 Gray or repeated doses of up to 150 Gray over 8 days still failed to completely abolish all neoblasts. About 10% of worms were able to restore cell proliferation after irradiation. This result indicates the presence of a pool of arrested neoblasts or a robust DNA damage mechanism.

1.3.4 Regeneration of *M. lignano*

1.3.4.1 Properties of regeneration

Thanks to the neoblasts, *M. lignano* is capable of regeneration in response to physical disruption such as amputation and incision. However this remarkable regeneration ability has its own limit (Egger et al. 2006) (Figure 1.13). Unlike planarian, *M. lignano* is unable to regenerate every organ. The brain and eyes are not able to regenerate. The rostrum can fully regenerate only when the brain is intact. The pharynx also seems crucial for regeneration. The anterior part after a cut at posterior to pharynx is able to fully regenerate while cut between the eyes and pharynx results in failed regeneration of both halves. Successful regeneration is guaranteed in presence of intact brain and pharynx. Worms cut between testes and ovaries do not undergo reconstruction of testes. Instead, spermatogenesis stops 30h after amputation and resumes about 4 days post-amputation before ovaries are regenerated. The regeneration of tail plate seems independent of the brain. A centerpiece without brain and tail is capable of growing a new tail in spite of the absence of stylet. The regeneration ability is obtained very early on during postembryonic development. Even a 1-day hatchling shows full regeneration ability, suggesting that neoblasts are already functional at early stage of postembryonic development.

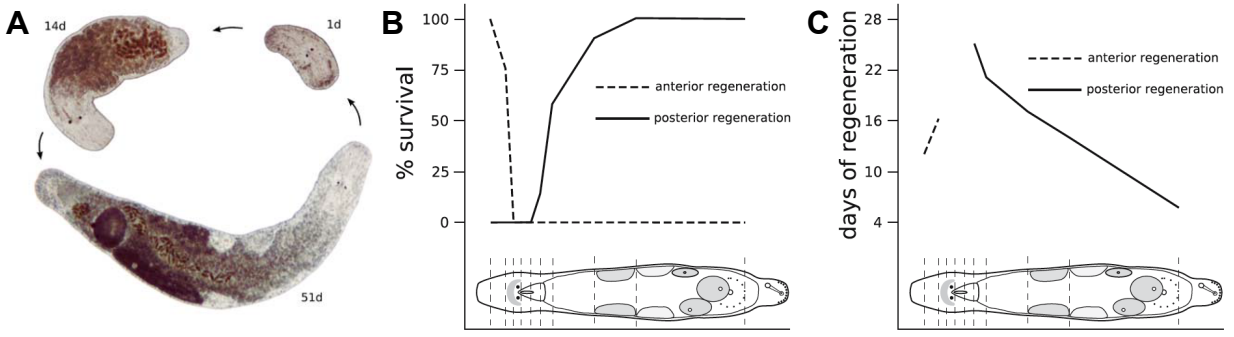

Figure 1.13 Regeneration ability of *M. lignano*. (A) Regeneration cycle of a pharynx-level amputee. Percentage of fully regenerated amputees (B) and days needed for full regeneration at different cutting levels. Adapted from (Egger et al. 2006).

1.3.4.2 Lifespan extension by repeated amputation

In several flatworm species, lifespan extension has been observed during repeated regeneration and starvation. In *M. lignano,* the same effect occurs during repeated amputation (Egger et al. 2006). In one experiment, 20 adult worms were subject to repeated amputation. Half of them survived at least 29 amputations for almost 12 months after the start with no sign of reduced stem cell capacity. In contrast, the maximum lifespan of the untreated worms was merely 42 weeks (less than 10 months). However, repeated regeneration also led to defective and uncontrolled growth. Halfway through the experiment, all worms became eyeless and some developed epidermal grooves on the head and hypertrophic testes. Despite these side effects, worms are rejuvenated by repeated regeneration. The molecular mechanism of the rejuvenation effect remains unknown. It would be of interest to dissect the pathways involved in the maintenance of young state of neoblasts.

1.3.4.3 Neoblast dynamics during regeneration

Neoblast proliferation and differentiation is a common feature shared among flatworm species during regeneration. Following amputation, a distinct structure named blastema is formed at the wound site (Egger et al. 2009a). A blastema is an accumulation of fast dividing neoblasts (Figure 1.14). During tail regeneration, a blastema is formed within 24 hours post-amputation and differentiation from S-phase cells is detected as early as 48 hours post-amputation. Proliferation takes place throughout the regeneration and gradually declines as differentiation progresses. In *M. lignano,* mitotic cells are found within the entire blastema*,* whereas in planarian mitosis occurs mainly on the border between blastema and differentiated cells (Salo and Baguna 1984). During regeneration, tissue formation is observed before BrdU-labeled cells differentiate, which suggests the quick activation of some G0 or G2 arrested neoblasts into mitosis. The formation of blastema involves activation and migration of neoblasts. This event seems to occur only locally or both locally and remotely during regeneration. Following tail amputation, proliferating cells near the wound migrate into blastema, leaving remote proliferating cells unaffected. However, an increase of proliferation takes place in both anterior and posterior regions in the initial stage of rostrum regeneration (Verdoodt et al. 2012). The exact mechanism and signaling directing the neoblast response remain unknown. Many questions are yet to be answered. For example, what signal pathways trigger the activation of neoblast proliferation? What molecules attract neoblasts to the wound site? How is the cell fate determined during regeneration?

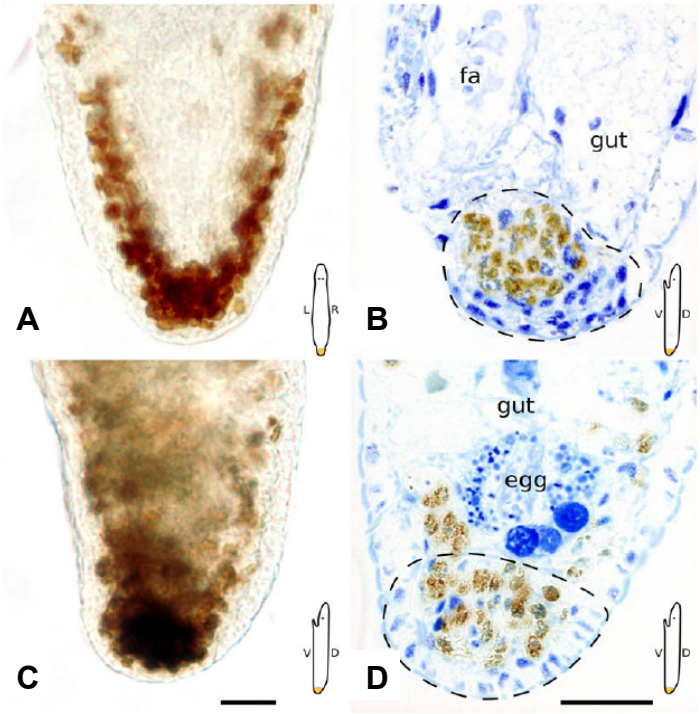

Figure 1.14 Blastema during tail regeneration. Whole mount (A) and section (B) of BrdU pulse labeled blastema at the regenerating tail. Whole mount (C) and section (D) of regenerating tail in BrdU pulse chase experiment. L: left; R: right; V: ventral; D: dorsal; fa: female antrum. Adapted from (Egger et al. 2009a).

1.3.5 Regulation and maintenance of neoblast functions

Pathways regulating stem cell functions are highly conserved across metazoans. The involvement of such pathways remains largely unstudied in this new model organism. Up to date, only two of such pathways – Hippo pathway (Demircan and Berezikov 2013) and PIWI/piRNA pathway (Pfister et al. 2008; De Mulder et al. 2009) – have been shown essential for the normal functions and maintenance of neoblasts. Their functions in *M. lignano* neoblasts are consistent to the known functions in other organisms. Hippo pathway is a key regulator for growth control by regulating the number and differentiation potential of stem cells in animals. In *M. lignano*, depletion of *Hpo* results in higher number of S-phase cells and outgrowth of tissues during homeostasis and regeneration. Silencing of downstream factor *Yap,* which is inhibited by Hippo signaling, causes failure in neoblast maintenance and functions. PIWI/piRNA pathway is essential for animal germline development. A PIWI-like protein, Macpiwi1, was shown to be predominantly present in the dividing cells – somatic neoblasts and gonads – in *M. lignano*. Silencing of Macpiwi1 abolishes S-phase cells and all stem cell-dependent functions, such as tissue renewal, postembryonic development and regeneration. However, the potential involvement of piRNAs and the mechanism of Macpiwi1-mediated stem cell regulation are yet to be addressed.

1.3.6 Molecular tools for mechanistic studies of neoblasts

A number of tools are available or in the process of development for genetic studies in this new model. *M. lignano* is small and transparent, which is ideal for whole mount imaging. So far, whole mount *in situ* hybridization (Pfister et al. 2007; Lengerer et al. 2014) and immunostaining (Pfister et al. 2008) are well established for the identification of gene expression patterns. The small size and transparency also make it much easier for RNAi knockdown. Without injection, efficient RNAi can be achieved using a simple soaking method with dsRNA-containing culture medium (Pfister et al. 2008; De Mulder et al. 2009; Sekii et al. 2009; Kuales et al. 2011). In addition, an expressed sequence tag (EST) library containing 5416 unique sequences was developed as a molecular resource (Morris et al. 2006). Although the aforementioned tools significantly facilitate molecular studies in *M. lignano,* whole genome sequence and gene targeting techniques are yet to be developed to make it a truly powerful model organism. Several groups, including ours, have attempted to achieve such goals, yet faced tremendous challenges. GFP-expressing transgenic lines can be produced using transposase and TALENs (Marie-Orleach et al. 2014). However, the success rate is rather low and most of the GFP-positive worms lose GFP expression over time, suggesting a low efficiency of transgene integration. Alternative methods such as CRISPR/Cas9 are yet to be tested.

The attempts for genome assembly also lead to surprises. Initial genome assembly attempts based on regular Illumina and 454 short sequencing reads yielded to very poor results, indicating the presence of a large amount of repeats in the genome. In order to overcome the ambiguity due to this highly repetitive nature, our group combined Illumina short sequencing reads with PacBio long reads and significantly improved the assembly quality (NC50 = 64kbp) (Wasik et al. submitted). With hope of improved sequencing technology, we hope the whole genome can be assembled at the chromosome level in the near future. The development of comprehensive genetic resources and techniques will significantly accelerate our understanding of the unique natures of neoblasts in this fascinating organism.

Chapter 2
Dual functions of Macpiwi1 in transposon silencing and stem cell maintenance in *Macrostomum lignano*

2.1 Abstract

PIWI proteins and piRNA pathways are essential for transposon silencing and some aspects of gene regulation during animal germline development. In contrast to most animal species, some flatworms also express PIWIs and piRNAs in somatic stem cells where they are required for tissue renewal and regeneration. Here, we identify and characterize piRNAs and PIWI proteins in the emerging model flatworm, *Macrostomum lignano*. We find that *M. lignano* encodes at least three PIWI proteins. One of these, Macpiwi1, acts as a key component of the canonical piRNA pathway in the germline and in somatic stem cells. Knockdown of *Macpiwi1* dramatically reduces piRNA levels, derepresses transposons, and severely impacts stem cell maintenance. Knockdown of the piRNA biogenesis factor *Macvasa* causes an even greater reduction in piRNA levels, with a corresponding increase in transposons. Yet, in *Macvasa* knockdown animals, we detect no major impact on stem cell self-renewal. These results may suggest stem cell maintenance functions of PIWI proteins in flatworms that are distinguishable from their impact on transposons and that might function independently of what are considered canonical piRNA populations.

2.2 Introduction

Argonaute proteins have emerged as essential components of gene regulatory mechanisms. In association with their small RNA partners, the Argonaute family of proteins silences target genes at both transcriptional and post-transcriptional levels. In animals, there are two clades of Argonaute proteins - the Argonaute (AGO) clade and the PIWI clade (Carmell et al. 2002; Hock and Meister 2008). The AGO clade typically

associates with either microRNAs (miRNAs) or endogenous small interfering RNAs (endo-siRNAs). miRNAs play well established roles in the regulation of protein coding mRNAs, while endo-siRNAs are generally involved in transposon silencing (Hock and Meister 2008). PIWI proteins associate with PIWI-interacting RNAs (piRNAs). These are generally 24-35 nucleotides in length and have been shown to protect genomic integrity by suppressing transposable elements (TEs) specifically during animal germline development (Ishizu et al. 2012). piRNAs primarily derive from genomic aggregates of transposon insertions, termed piRNA clusters, and act to guide PIWI proteins to transposon mRNAs by sequence complementarity (Brennecke et al. 2007). PIWI proteins can then silence transposons either post-transcriptionally – by cleaving transposon mRNAs, or transcriptionally – by changing chromatin structure (Luteijn and Ketting 2013). These functions prevent transposon propagation and earned PIWIs their nickname – "*guardians of genome"* (Senti and Brennecke 2010). Altogether, piRNAs and PIWIs are indispensable for germline formation and maintenance, and mutations in piRNA pathway components usually cause sterility (Klattenhoff et al. 2007; Soper et al. 2008; Thomson and Lin 2009).

Although most studies of piRNAs and PIWIs have been focused on transposon silencing in the germline, a number of studies have posited roles for piRNAs in somatic cells. In the California sea hare *Aplysia californica,* piRNAs are thought to participate in memory formation (Rajasethupathy et al. 2012). PIWI expression has also been observed in various types of human cancers, though neither their interactions with piRNAs nor concrete functional roles have been demonstrated in this setting (Suzuki et al. 2012). Notably, PIWIs have also been shown to play a critical role in the regenerative capabilities of flatworm somatic stem cells (neoblasts) (Reddien et al. 2005; Palakodeti et al. 2008; De Mulder et al. 2009). The potential involvement of PIWI proteins in flatworm stem cells is of particular interest since the founding member of the PIWI clade (Piwi in *D. melanogaster*) was described as a factor involved in germline stem cell (GSC) maintenance (Lin and Spradling 1997). In *D. melanogaster* ovaries, the best-studied role of Piwi is transposon silencing, although in *Piwi* knockouts, germline stem cells (GSCs) cease to divide after a few initial divisions, and the germ cell-depleted gonads contain only a few egg chambers/sperm bundles (Cox et al. 1998; Cox et al. 2000). It has remained an open question whether the roles of Piwi in GSC regulation and transposon silencing are interrelated; however, some recent evidence suggests that these two roles are separable (Klenov et al. 2011). Truncation of the nuclear localization signal in Piwi does not affect GSC maintenance, although the same mutation causes derepression of transposable elements (TEs) and sterility, confirming that the Piwi TE silencing function is impaired. These observations suggest that PIWIs may have a conserved role in stem cell regulation, but it remains to be determined whether this role is linked to transposon silencing or piRNA dependent.

Flatworms harbor an unusual population of adult stem cells known as neoblasts (Bode et al. 2006; Baguna 2012). Neoblasts are responsible for the impressive regeneration abilities of these animals – some species can regenerate their entire body after lethal irradiation, with all tissues being derived from a single transplanted neoblast (Wagner et al. 2011). In the planarian, *Schmidtea mediterranea*, at least three PIWI

proteins (SMEDWI1-3) are expressed in neoblasts and the depletion of either SMEDWI2 or SMEDWI3 can impair stem cell function (Reddien et al. 2005; Palakodeti et al. 2008). It is however still largely unclear whether the major role of flatworm PIWIs is to sustain stem cell maintenance, foster differentiation, or perhaps both, depending on the context. It is also unknown whether piRNAs are essential for the action of SMEDWIs as stem cell regulators.

Here, we have focused on the PIWI proteins of an emerging flatworm model - *Macrostomum lignano. M. lignano* has both neoblast populations and regenerative characteristics similar to those of *S. mediterranea* (Reddien and Sanchez Alvarado 2004). The genomic sequence and transcriptome of *M. lignano* have recently been assembled (Wasik et al., submitted), opening the way for its use as new model for studies of not only piRNA pathway but also of stem cell maintenance and differentiation. The one previously described *M. lignano* PIWI protein, Macpiwi1, is present in the germline and in neoblasts. It is required for neoblast maintenance and stem cell-dependent functions, such as regeneration, tissue renewal, and postembryonic development (De Mulder et al. 2009). Here we identify two additional *M.lignano* PIWI proteins, and describe the *M. lignano* piRNA population and its Macpiwi1-associated subpopulation. *M. lignano* piRNAs, like canonical piRNAs, target transposons and undergo the piRNA amplification loop (ping-pong). We find that silencing of *Macpiwi1* leads to reduction of piRNA populations, transposon derepression and loss of stem cell proliferation. The stem cell arrest does not occur if piRNAs are depleted via knockdown of *Macvasa*, which has no impact on stem cell renewal and further differentiation.

2.3 Results

2.3.1 *M. lignano* has conserved small RNA pathway components

Metazoans have highly conserved miRNA and piRNA pathways. The existence of PIWI proteins in *M. lignano* (De Mulder et al. 2009) strongly suggested the presence of small RNA pathways in this organism. In order to address this hypothesis, we searched for well-known and conserved miRNA and piRNA biogenesis factors in the genome and *de novo* transcriptome drafts that we recently assembled. Briefly, we sequenced the genome of *M. lignano* using a combination of ~170x coverage of Illumina short read sequencing (100bp paired-end and mate-pair reads) and ~130x coverage of PacBio long read sequencing (6.5 kbp mean read length) to produce an assembly with a contig N50 of 64 kbp. We also sequenced the mRNA from whole worms and sorted stem cells, and *de novo* assembled the *M. lignano* transcriptome into ~150,000 transcripts. The average assembled transcript length was 516 bp and the N50 of the transcriptome was 649 bp. Nearly all of the transcripts (97%, with > 90% identity) align to our draft genome assembly as well as the majority of core eukaryotic genes (99%) based on CEGMA (Core Eukaryotic Genes Mapping Approach) analysis, suggesting a nearly complete representation of the *M. lignano* genes in our assembly. The genome and transcriptome can be accessed through NCBI: SRP 059553.

The canonical miRNA pathway, in addition to Argonaute proteins, includes RNase III proteins - Drosha and Dicer (Ha and Kim 2014). We were able to identify all of these pathway components as well as other cofactors - DGCR8, TRBP and Exportin-5 (Table 2.1) - in the assembled genome and transcriptome. This has led us to the conclusion that a canonical miRNA pathway is likely to exist in *M. lignano*. Furthermore, Metazoans usually express multiple PIWI proteins as elements of their piRNA pathways. We searched for all potential PIWI proteins in the genome and the *de novo* transcriptome assemblies, and in addition to the previously identified *Macpiwi1* (De Mulder et al. 2009), we identified several candidate genomic loci coding for PIWI-like gene fragments. Only two others, *Macpiwi2* and *Macpiwi3*, however, were found as full-length transcripts. Macpiwi2 had a similar protein sequence (80% identity) to Mapiwi1, whereas Macpiwi3 was only ~30% identical to Macpiwi1. All three Macpiwis had putative PAZ and PIWI domains. The PIWI domains included a catalytic triad (DDH) (Figure 2.1) that has been shown to be required for the cleavage of RNA targets.

piRNA pathway	**miRNA pathway**
PIWI proteins	**AGO proteins**
Macpiwi1	Macago1
Macpiwi2	Macago2
Macpiwi3	
Other factors	**Other factors**
Tdrd1	DROSHA
Tdrkh	DICER1
Tdrd5	DGCR8
Tdrd6	TRBP2
Tdrd7	Exportin-5
Tdrd12	
VASA	
MOV10L1	
Maelstrom	
HEN1	
Hsp90	
Fkbp6	
PRMT5	

Table 2.1 Homologues of piRNA and microRNA pathway components in *M.lignano*. Homologues were identified based on the mRNA sequences from the *de novo* transcriptome assembly. Accession numbers: AM942740 (Macpiwi1), KR132203 (Macpiwi2), KR132204 (Macpiwi3), KR132205 (Tdrkh), KR132206 (Tdrd6), KR132207 (Tdrd9), KR132208 (Tdrd12), AM411989 (Macvasa), AM411990 (Macvasa), KR132209 (MOV10L1), KR132210 (Maelstrom), KR132211 (HEN1), KR132212 (Hsp90), KR132213 (Fkbp6), KR132214 (PRMT5), KR132217 (Macago1), KR132215 (Macago2), KR132216 (Macago2), KR132218 (Drosha), KR132219 (Dicer1), KR132220 (DGCR8), KR132221 (TARBP2), KR132222 (Exportin-5).

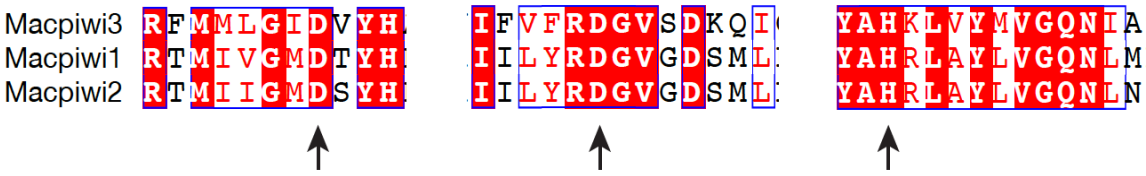

Figure 2.1 Alignment of Macpiwi protein sequences in proximity to the catalytic site. Arrows denote the catalytic triad residues (DDH). Identical (white letters on a red background) or similar (red letters on a white background) residues are labeled.

Phylogenetic analysis showed that Macpiwi proteins are most similar to PIWIs in the planarians and the mollusk *A. californica* (Figure 2.2, Supplementary Figure 1). This is in agreement with the relatively close evolutionary relationship of *Macrostomum* with planarians and mollusks (superphylum Lophotrochozoa) and much more distant relationship with Deuterostomes and Ecdysozoans (Egger et al. 2009b; Egger et al. 2015). piRNA pathways are highly conserved across metazoan species and this conservation seems to extend to flatworms. Despite the relatively far phylogenetic distance, evidence for the majority of well-known fly and mammalian piRNA components (Ku and Lin 2014) could be found in the *M. lignano* genome and transcriptome (Table 2.1). This suggests that a canonical piRNA pathway is likely to be operating in *M. lignano*.

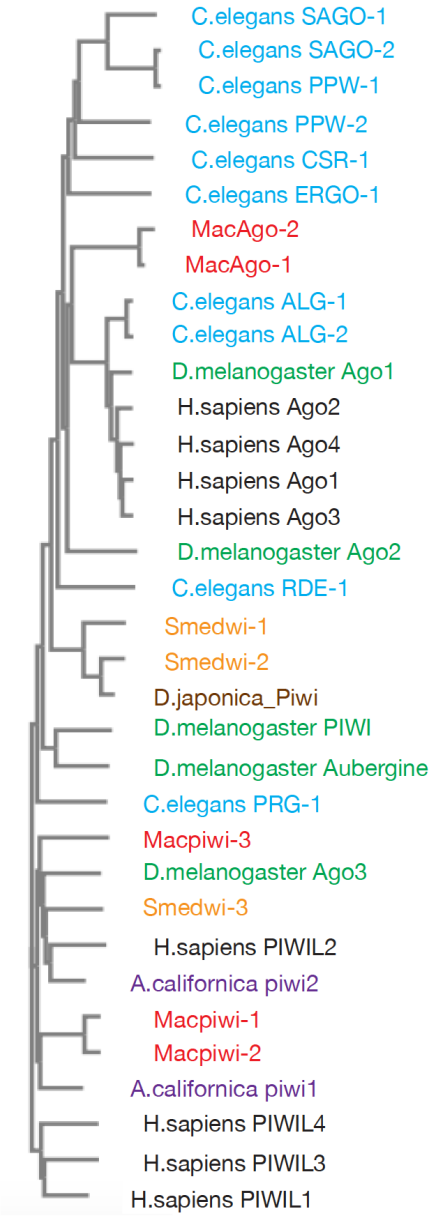

Figure 2.2 A phylogenetic tree depicting the relationship between Ago/PIWI proteins in various metazoans. *M. lignano* (red), *C. elegans* (blue), *S. mediterranea* (orange), *D. melanogaster* (green), *A. californica* (purple), *D. japonica* (brown) and *H. sapiens* (black).

Contribution

Giorgia Battistoni, Kaja A. Wasik and I myself generated the transcriptome data from whole worms and identified potential PIWI proteins. I performed further data analysis.

2.3.2 Abundant miRNA and piRNA populations are present in *M. lignano*

To investigate the content of *M. lignano* small RNA populations, we cloned and sequenced small RNAs from adult worms. Small RNAs in *M. lignano* formed three characteristic populations varying in size, abundance (number of reads), and sequence complexity (number of unique sequences) (Figure 2.3). The population of ~22nt RNAs was very abundant with relatively low complexity while the ~20nt and ~30nt populations had higher sequence complexity but were less abundant.

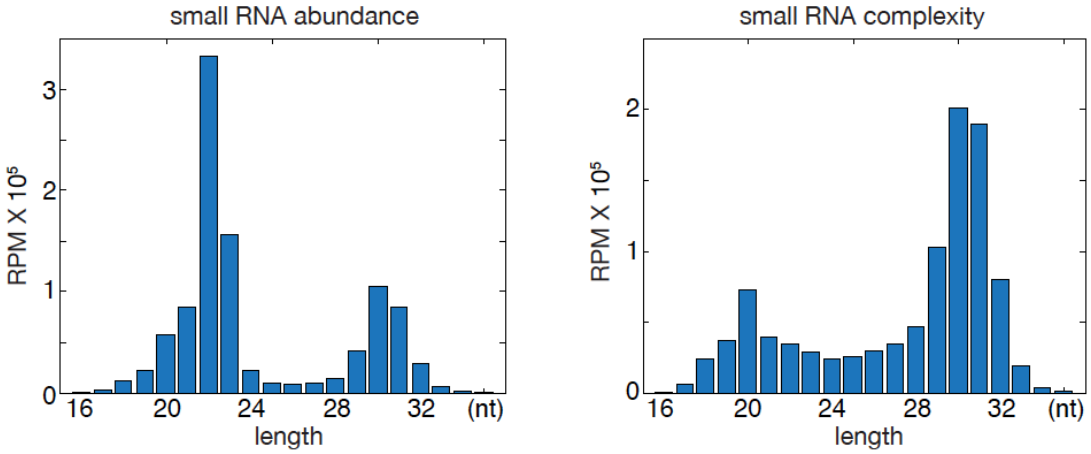

Figure 2.3 Length distribution of total small RNAs from adult *M. lignano* by sequence abundance (left) and complexity (right). Reads per million (RPM) total reads aligned to the genome are plotted.

Based on its size and low complexity, the 22nt small RNA population likely represented canonical miRNAs. Indeed, 631 distinct miRNA sequences were found in *M. lignano* small RNAs with at least 1 read per million (rpm) total reads and 100% sequence identity to their counterparts in miRBase. Only those sequences within typical miRNA size range aligned with sequences in miRBase (Figure 2.4A).

As seen with previously characterized miRNAs, the *M. lignano* miRNA population showed a strong 5' U bias (Figure 2.4C). Since miRNAs are known to derive from stem-loop structures, we used the UNAfold miRNA prediction tool (Markham and Zuker 2008) to identify potential precursor miRNA hairpin structures across the *M. lignano* genome. For 12 out of the 20 most abundant and highly conserved (100% identity to miRBase) miRNAs we identified high-confidence hairpins that likely represent genes from which pri-miRNAs are expressed (Figure 2.4B). A number of conserved miRNAs were found differentially expressed in comparisons between sorted dividing cells (somatic and germline stem cells), and irradiated worms and during regeneration (Figure 2.4D, Supplementary Table 1).

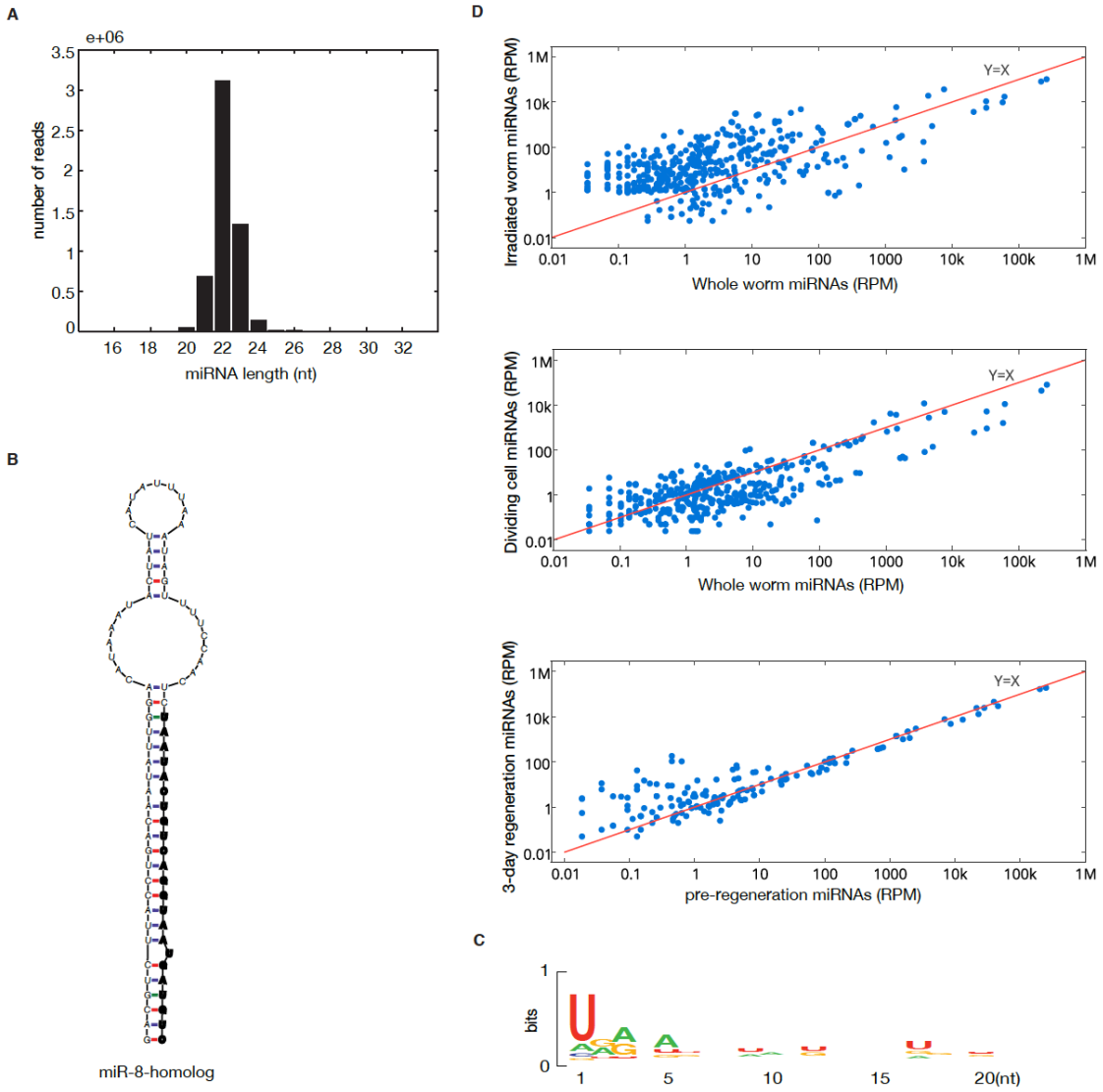

Figure 2.4 Characteristics of *M. lignano* miRNAs. (A) Length distribution of small RNAs that match to miRBase mature miRNAs. (B) Stemloop structure of the miR-8 homologue precursor from the genome draft. The mature miRNA sequence is highlighted in bold. (C) Sequence bias of all small RNAs mapped to miRBase mature miRNAs. (D) Abundance of miRNA in whole worms, irradiated worms, sorted dividing cells, and regenerating worms (0 day or 3 days post anterior amputation). Each dot represents a miRNA.

In metazoans, piRNAs are highly complex 24-32nt small RNAs with a strong U bias at their 5' end. These primarily target transposable elements (TEs) (Brennecke et al. 2007; Senti and Brennecke 2010; Cora et al. 2014). In the planarian, *S. mediterranea*, piRNA populations also share these signature features (Palakodeti et al. 2008). The ~30nt small RNA population *in M. lignano* was within the typical piRNA size range. It also exhibited a strong 5'U bias - another typical piRNA characteristic (Figure 2.5A). Since in other species the principal targets of piRNAs are transposable elements, we mapped all 28-32nt small RNAs to the *M. lignano de novo* transcriptome assembly. Amongst ten transcripts that generated the greatest diversity of piRNAs, four were transposon-related (Table 2.2); the remaining were unannotated or uncharacterized.

The small RNAs that aligned to transposons showed key features of secondary piRNA biogenesis, known as the ping-pong signature (Brennecke et al. 2007), namely a 5' 10nt overlap with piRNAs from the opposite orientation (Figure 2.5B).

piRNAs are usually generated from large genomic loci known as piRNA clusters (10-100kbps) (Brennecke et al. 2007). To investigate whether putative *M. lignano* piRNAs were produced in a similar manner, we identified a set of 436 clusters in the *M. lignano* genome draft. These gave rise to 80.2% of all uniquely mapping piRNAs (Supplementary Table 2). These candidate piRNA clusters have a median length of 9.7kbps, a maximum length of 93.7kbps, and made up 0.63% of the whole genome. Among them, we found both unidirectional and bidirectional clusters (Figure 2.5C). Thus, these piRNA clusters have characteristics similar to those of other species. The *M. lignano* genome is highly repetitive, potentially complicating the identification of piRNA generating loci. We therefore took a second approach, identifying 3228 piRNA-generating transcripts with abundant piRNA production (Supplementary Table 3), reasoning that the extended nature of piRNA-generating transcripts might allow better genome mapping. Of all piRNA-producing transcripts, 1951 aligned within the 436 identified piRNA clusters, while the others were distributed throughout the remainder of the genome and could represent individual transposon copies or fragments. In summary, *M. lignano* piRNAs are in many respects similar to piRNAs that are well characterized in other species.

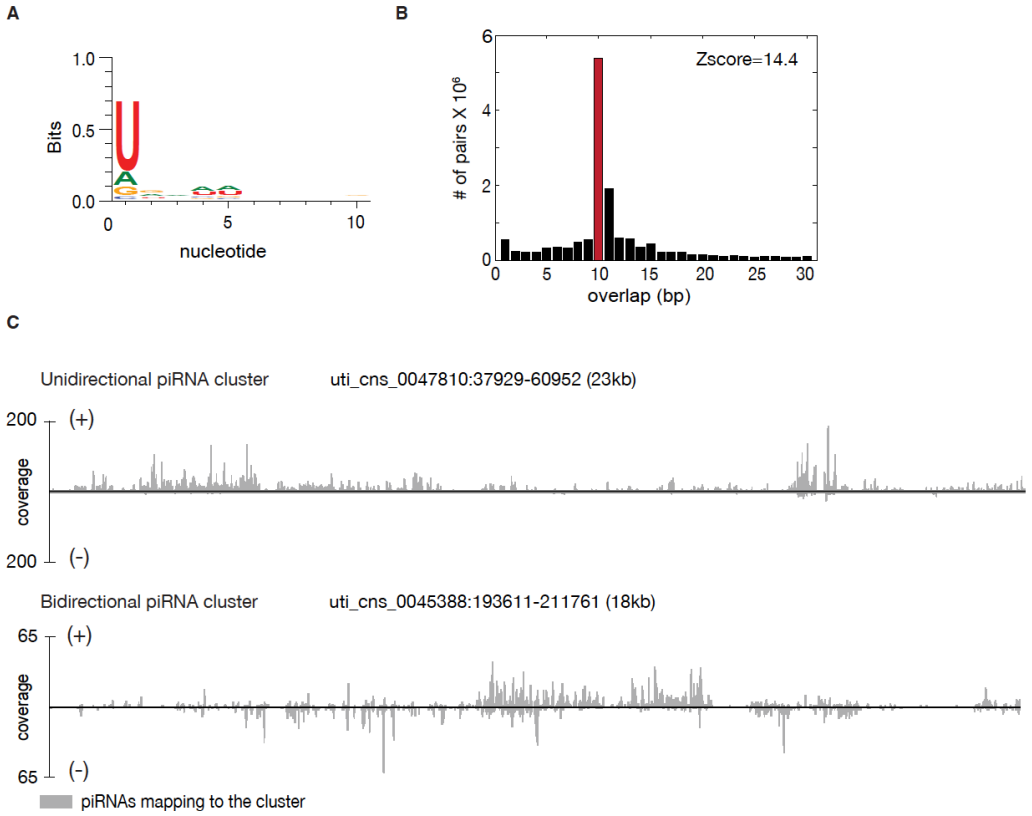

Figure 2.5 Characterization of *M. lignano* piRNAs. (A) Sequence bias of the 28-32 nt long RNA population from whole worms. (B) Distribution of 5' overlap between sense and antisense piRNA strands. Z-score represents the enrichment of 10 bp overlap. (C) Examples of unidirectional and bidirectional

piRNA clusters from the genome draft. The piRNA coverage at each nucleotide position of the clusters is shown in grey.

Transcript ID	Annotation
c114798_g1_i1	Putative uncharacterized protein
c111845_g1_i1	n/a
c130365_g1_i1	Uncharacterized protein
c130428_g2_i1	Retrovirus-related Pol polyprotein from transposon 412
c130415_g1_i1	Retrovirus-related Pol polyprotein from transposon 297
c113560_g2_i2	ATP-dependent DNA helicase PIF1
c130428_g3_i1	Retrovirus-related Pol polyprotein from transposon 297
c130259_g1_i1	Deoxyuridine 5'-triphosphate nucleotidohydrolase, viruses
c130288_g3_i1	Retrovirus-related Pol polyprotein from type-1 retrotransposable element R1
c130058_g1_i3	n/a

Table 2.2 Top 10 piRNA-producing transcripts ranked by sequence complexity.

Contribution

Giorgia Battistoni, Kaja A. Wasik and I generated the small RNA sequencing data from whole worms and characterized the miRNA and piRNA populations. Osama El Demerdash and I identified piRNA clusters from the genome assembly. I identified piRNA-generating transcripts from the transcriptome. Osama El Demerdash and James Gurtowski analyzed the ping-pong signatures mentioned in all the results sections.

2.3.3 The *M. lignano* piRNA pathway uses multiple PIWIs

PIWI proteins are predominantly expressed in the germline (Ku and Lin 2014). In *M. lignano*, however, the expression of Macpiwi1 indicates that PIWI proteins are expressed in multiple cell types, including in the cytoplasm of gonadal cells, developing and mature eggs, as well as dividing somatic neoblasts (De Mulder et al. 2009) (Figure 2.6A and B). *Macpiwi2 in situ* hybridization showed expression in gonads and in eggs at early stages of development (Figure 2.6C). An additional parenchymal staining pattern suggested the presence of *Macpiwi2* also in the neoblasts. Following posterior amputation, *Macpiwi2* expression was increased in the blastema during regeneration.

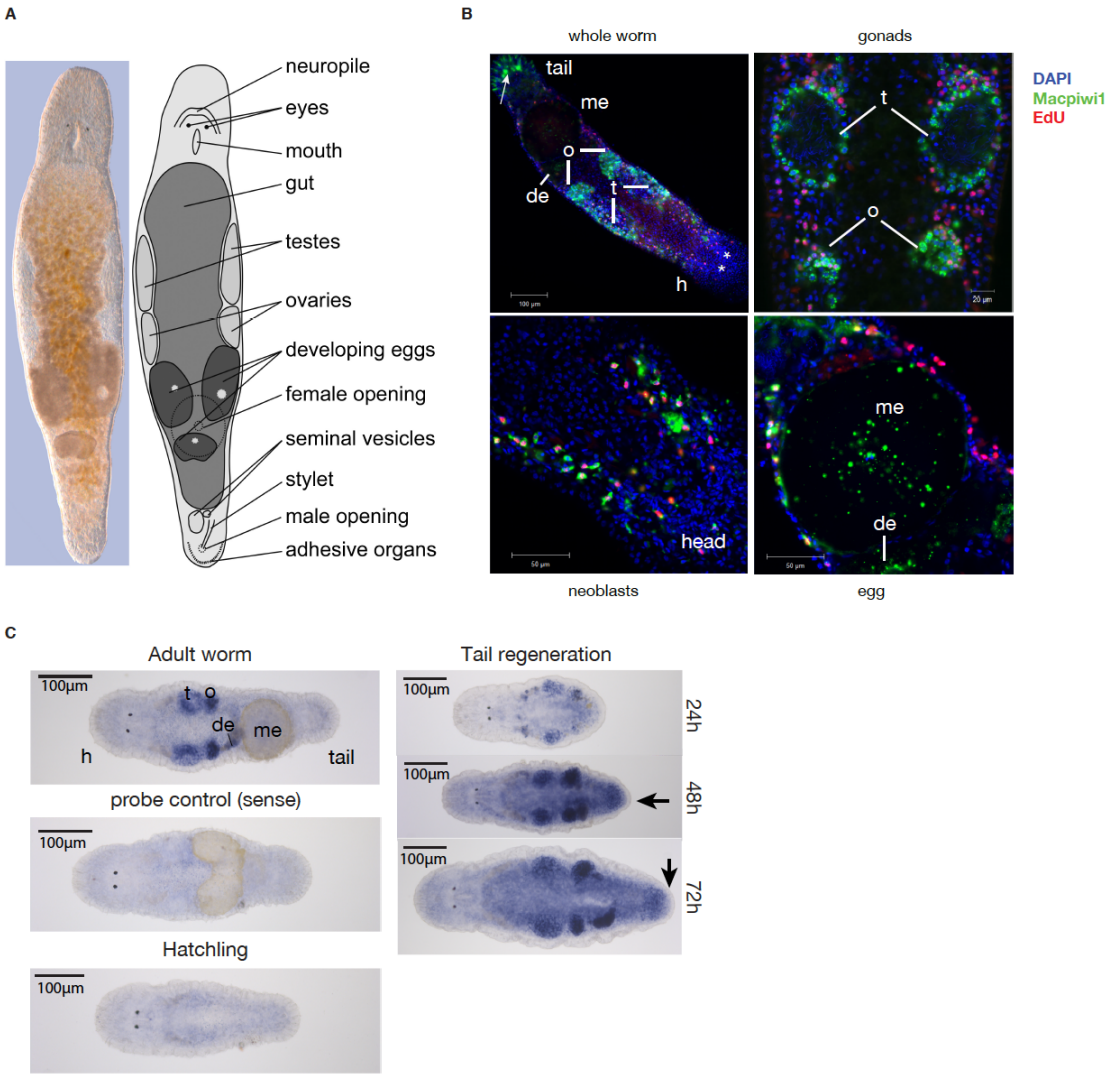

Figure 2.6 Expression patterns of Macpiwi1 and Macpiwi2 in *M. lignano*. (A) Interference contrast image and diagrammatic representation of an adult worm. (B) Immunofluorescence labeling showing localization of Macpiwi1 (green) in adult worms. Dividing cells are labeled with EdU (red). h: head; t: testis; o: ovary; de: developing egg; me: mature egg. Stars denote eyes. Arrow points to nonspecific staining by the secondary antibody. (C) Localization of Macpiwi2 mRNA by whole mount in situ hybridization in adult worms, hatchlings, and during regeneration induced by posterior amputation. Sense riboprobe was used as negative control. Arrows point to blastemas during regeneration. t: testis; o: ovary; de: developing egg; me: mature egg.

Since Macpiwi1 and 2 were enriched in dividing neoblasts, we asked whether piRNAs were also present in these cell types. We isolated two cell populations from adult worms based on their DNA content (2N or 4N), reasoning that the only 4N cells in the organism would be those in G2/M phase (Figure 2.7A). This strategy was based upon the understanding that somatic and germline stem cells are the only abundant, dividing cell types in *M. lignano* (De Mulder et al. 2010). piRNAs were clearly enriched in the 4N dividing cell population (neoblast and germline stem cells); however, a subset of piRNAs present in the 4N cell population was also detectable in the 2N fraction

(Figure 2.7B). This could have represented piRNAs in either germ cells or neoblasts that were in G1/S phase at the time of harvest or non-dividing cell types. To investigate these possibilities, we analyzed the piRNA composition of lethally irradiated worms. Even after a lethal dose of gamma radiation and despite the absence of EdU-positive dividing cells and Macpiwi1 (Figure 2.7C), piRNAs remained detectable in whole worms (Figure 2.7D). Considered as a whole, our data indicate that Macpiwi proteins and piRNAs are likely to exist in cell types other than previously characterized germline and stem cell populations.

Contribution

Giorgia Battistoni, Kaja A. Wasik and I performed Macpiwi1 immunostaining. Julia Wunderer performed Macpiwi2 whole mount *in situ* hybridization. Giorgia Battistoni and Kaja A. Wasik established the S-phase cell sorting method. Battistoni, Kaja A. Wasik and I performed cell sorting, gamma irradiation and small RNA sequencing, and analyzed the sequencing data.

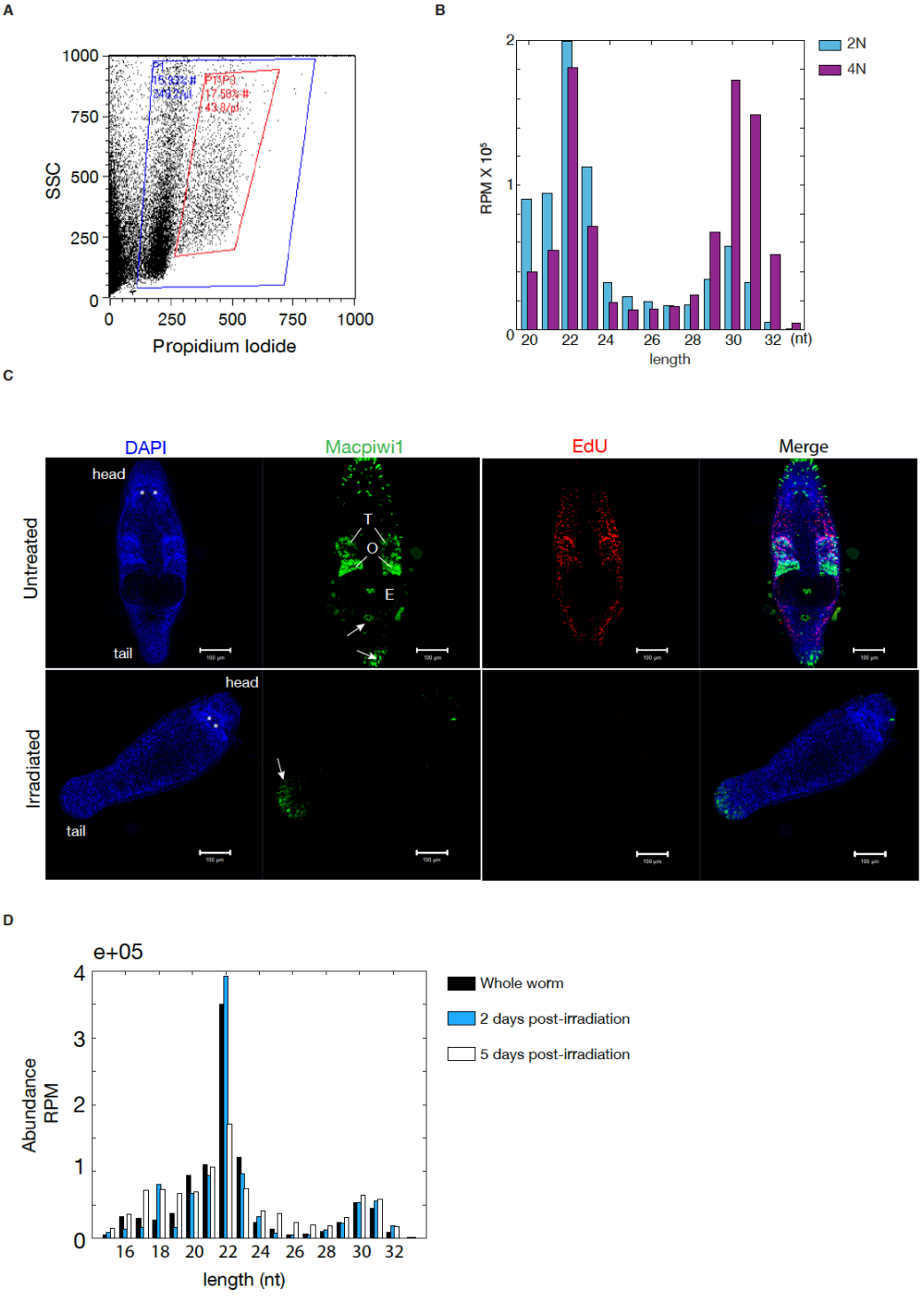

Figure 2.7 piRNAs in sorted dividing cells and irradiated worms. (A) 2N and 4N cell populations from whole worm cells labeled with propidium iodide. Blue quadrangle: total cells; red quadrangle: 4N cells. (B) Length distribution of small RNAs mapping to the genome from 2N and 4N cells. (C) Immunostaining for Macpiwi1 and EdU labeling in untreated and irradiated worms. T: testis; O: ovary. Stars denote eyes. Arrows point to nonspecific staining by the secondary antibody. (D) Length distribution of small RNAs from untreated and irradiated worms 2 days and 5 days post-irradiation.

2.3.4 Macpiwi1 participates in a heterotypic ping-pong cycle

PIWI proteins act in concert with piRNAs. We therefore tried to determine whether specific populations of piRNAs associated with any of the three Macpiwi proteins that were identified. We generated antibodies directed against each protein, but could only detect small RNAs in Macpiwi1 immunoprecipitates (Figure 2.8A and B). Failure to detect associated RNAs with either Macpiwi2 or Macpiwi3 may be simply attributable to the technical qualities of the antibodies.

Of the 3228 piRNA-producing transcripts identified, 3093 contributed to Macpiwi1-associated piRNAs. This suggests that Macpiwi1 interacts with the majority (judged by sequence diversity) of all piRNAs in *M. lignano*. In contrast to piRNAs cloned from the whole worms (total piRNAs) (Figure 2.5B), *Macpiwi1*-associated piRNAs did not display ping-pong signatures (Figure 2.8C) and were predominantly oriented antisense to transposons (Figure 2.8D). In small RNAs from whole worms we did note the presence of sense-oriented piRNAs, which formed ping-pong pairs with antisense piRNAs (Figure 2.8E). These sense-oriented piRNAs were absent from Macpiwi1-associated populations, suggesting their preferential association with another PIWI protein. Uniquely mapping piRNAs are enriched in Macpiwi1 complexes, with 1/3 of piRNAs associated with this protein assignable to discrete genomic locations, in contrast to 1/4 in the total piRNA population (Table 2.3). Considered together, these data suggest that Macpiwi1 binds primary piRNAs to initiate a heterotypic ping-pong cycle with at least one other Macpiwi, which serves as the host for sense piRNAs.

Contribution

Giorgia Battistoni purified and characterized Macpiwi antibodies. Giorgia Battistoni and I performed the Macpiwi1 immunoprecipitation with some optimization by Giorgia Battistoni. I sequenced the small RNAs from IP and analyzed the data.

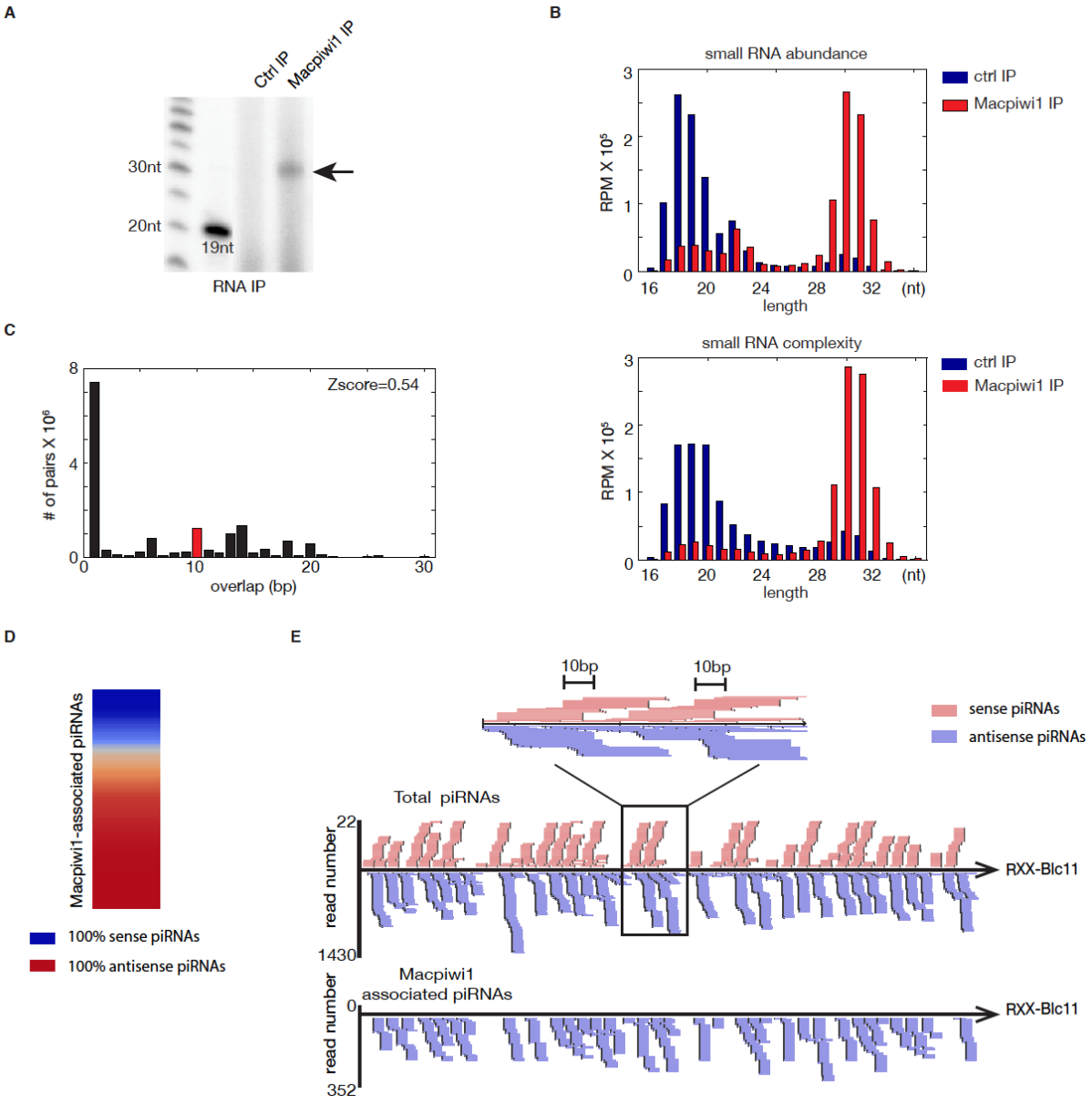

Figure 2.8 Characteristics of Macpiwi1-associated piRNAs. (A) 5' end radiolabeling of Macpiwi1-associated small RNAs pointed to by the arrow. (B)Length distribution of sequence abundance and complexity of Macpiwi1- associated small RNAs. Numbers of uncollapsed and collapsed reads per million total mapping reads (RPM) that aligned to the genome are plotted. (C) Distribution of 5' overlaps between sense and antisense strands of Macpiwi1- associated piRNAs. (D) A heatmap depicting the strand bias of Macpiwi1- associated piRNAs from each transposon consensus sequences. (E) An example of piRNA coverage on a transposon consensus sequence, RXX-Blc11. piRNAs mapping in sense and antisense orientations are labeled in pink and purple respectively. A close-up view shows ping-pong signature characterized by a 10bp overlap between sense and antisense strands.

Total small RNAs

	Whole worm				Macpiwi1 IP			
	Replicate 1		Replicate 2		Replicate 1		Replicate 2	
	Abundance	Complexity	Abundance	Complexity	Abundance	Complexity	Abundance	Complexity
Total reads	14193547	1580600	15092856	1089039	8411889	673929	13727400	509896
All mappers	10207564	1008705	10986209	678302	4814242	350851	7042584	239011
Unique mappers	2939838	335427	3016291	214978	1358671	142882	2056067	102536

piRNAs (28-32nt)

	Whole worm				Macpiwi1 IP			
	Replicate 1		Replicate 2		Replicate 1		Replicate 2	
	Abundance	Complexity	Abundance	Complexity	Abundance	Complexity	Abundance	Complexity
All mappers	3510975	670484	3198136	414195	3180859	266321	4912910	190265
Unique mappers	902418	253361	764398	154113	1023860	119031	1558519	85384
Unique mappers %	25.70	37.79	23.90	37.21	32.19	44.69	31.72	44.88

Table 2.3 Mapping statistics of small RNAs from whole worm and Macpiwi1 IP.

2.3.5 Macpiwi1 and the piRNA pathway mediate transposon silencing

To determine the effects of depleting individual *M. lignano* piRNA pathway components on overall piRNA and mRNA levels, we knocked down *Macpiwi1*, *Macpiwi2,* and *Macvasa* using RNAi (Figure 2.9A). Vasa is a DEAD-box RNA helicase required for germline piRNA biogenesis in flies and mammals (Kuramochi-Miyagawa et al. 2010; Zhang et al. 2012). In *D. melanogaster,* Vasa localizes at the nuclear envelope and is thought to deliver piRNA transcripts to cytoplasmic piRNA machinery (Liang et al. 1994; Zhang et al. 2012). In *M. lignano*, the *vasa* homologue, *Macvasa*, is expressed in two isoforms in the germline and in somatic stem cells (Pfister et al. 2008).

Depletion of *Macpiwi1* or both isoforms of *Macvasa* affected both piRNA levels and mRNA expression. Knockdown of *Macpiwi1* caused a decline in piRNA abundance and the overall complexity of piRNA populations, as compared with a control knockdown (Figure 2.9B). Effects of *Macvasa* knockdown on piRNA levels were even more dramatic – the piRNA population became essentially undetectable in treated worms (Figure 2.9B). The number of ping-pong pairs was drastically decreased in both knockdowns (Figure 2.9C), probably due to overall piRNA depletion. Any remaining ping-pong signature was likely a result of a small amount of residual protein expression. Both *Macpiwi1* and *Macvasa* knockdowns led to a global decrease in piRNA levels from piRNA-producing transcripts determined from analysis of wild-type animals (Figure 2.9D and E).

An examination of the transcriptome profiles indicated transposon derepression in both *Macpiwi1* and *Macvasa* knockdowns (Figure 2.9F), whereas the set of CEGMA protein coding genes was not affected in either knockdown. This confirms that piRNAs

from *M. lignano* preferably target transposable elements and mediate transposon silencing, as has been seen in other species where the piRNA pathway has been studied.

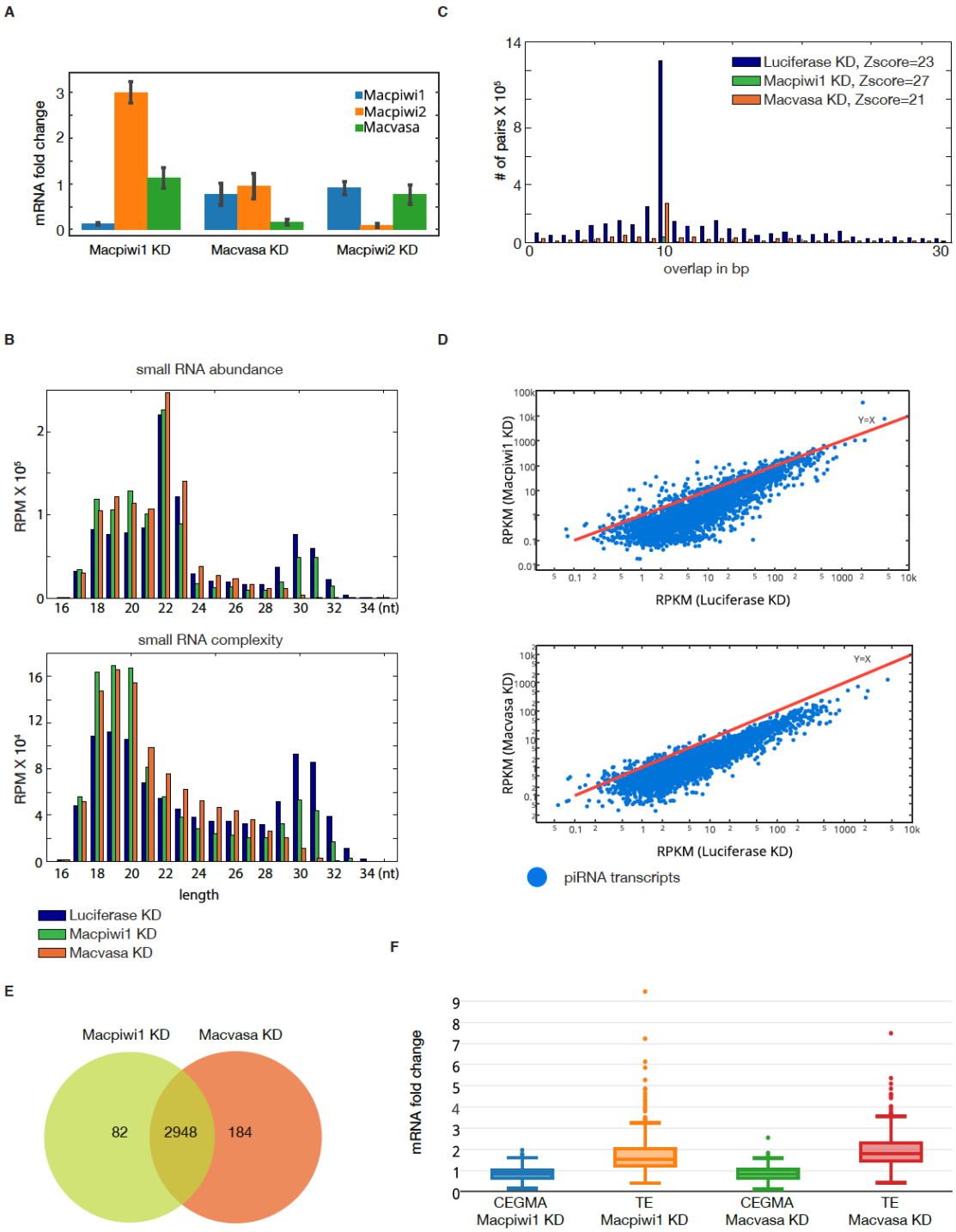

Figure 2.9 *Macpiwi1* and *Macvasa* silencing leads to piRNA downregulation and transposon derepression. (A) Quantitative-PCR showing RNAi knockdown efficiency as compared to *luciferase* dsRNA. (B) Length distribution plotted against sequence abundance and complexity of small RNAs from *luciferase*, *Macpiwi1* and *Macvasa* knockdown (KD) worms. Numbers of uncollapsed and collapsed reads per million total reads (RPM) aligned to the genome are plotted. (C) Distribution of 5' overlaps between

piRNAs from sense and antisense strands in *Macpiwi1*, *Macvasa* and *luciferase* KD. (D) Read counts of piRNAs mapped to individual transposon-related transcripts are plotted for *luciferase* KD and *Macpiwi1* or *Macvasa* KD worms. Each dot represents a transposon consensus sequence. Axes are presented on log10 scale. RPKM: reads per kilo base pair per million. (E) A Venn diagram showing numbers of transcripts with decreased piRNA production and the overlap of those between *Macpiwi1* KD and *Macvasa* KD. (F) mRNA fold change of CEGMA core gene set and transposon consensus sequences in *Macpiwi1* KD and *Macvasa* KD, compared with *luciferase* KD.

In contrast to *Macpiwi1*, *Macpiwi2* knockdown did not result in any detectable morphological change (Figure 2.11A) or substantial change in piRNA levels (Figure 2.10A). However, the piRNA content displayed a shift with more piRNAs produced from a subset of transcripts (Figure 2.11D) and as a consequence TE expression was slightly further repressed (Figure 2.11C). In the absence of *Macpiwi2*, ping-pong intensity was partially decreased (Figure 2.11B). These observations strongly suggested that Macpiwi2 was not the exclusive receiver protein in a Macpiwi1-driven heterotypic ping-pong cycle. These data provoke the notion that Macpiwi2 either binds the same set of piRNAs as Macpiwi1 and can be completely compensated by the presence of the latter protein or that Macpiwi2 binds a population of RNAs that are not obvious in our RNAseq libraries, in line with the ~3-fold upregulation of *Macpiwi1* mRNA following *Macpiwi2* KD.

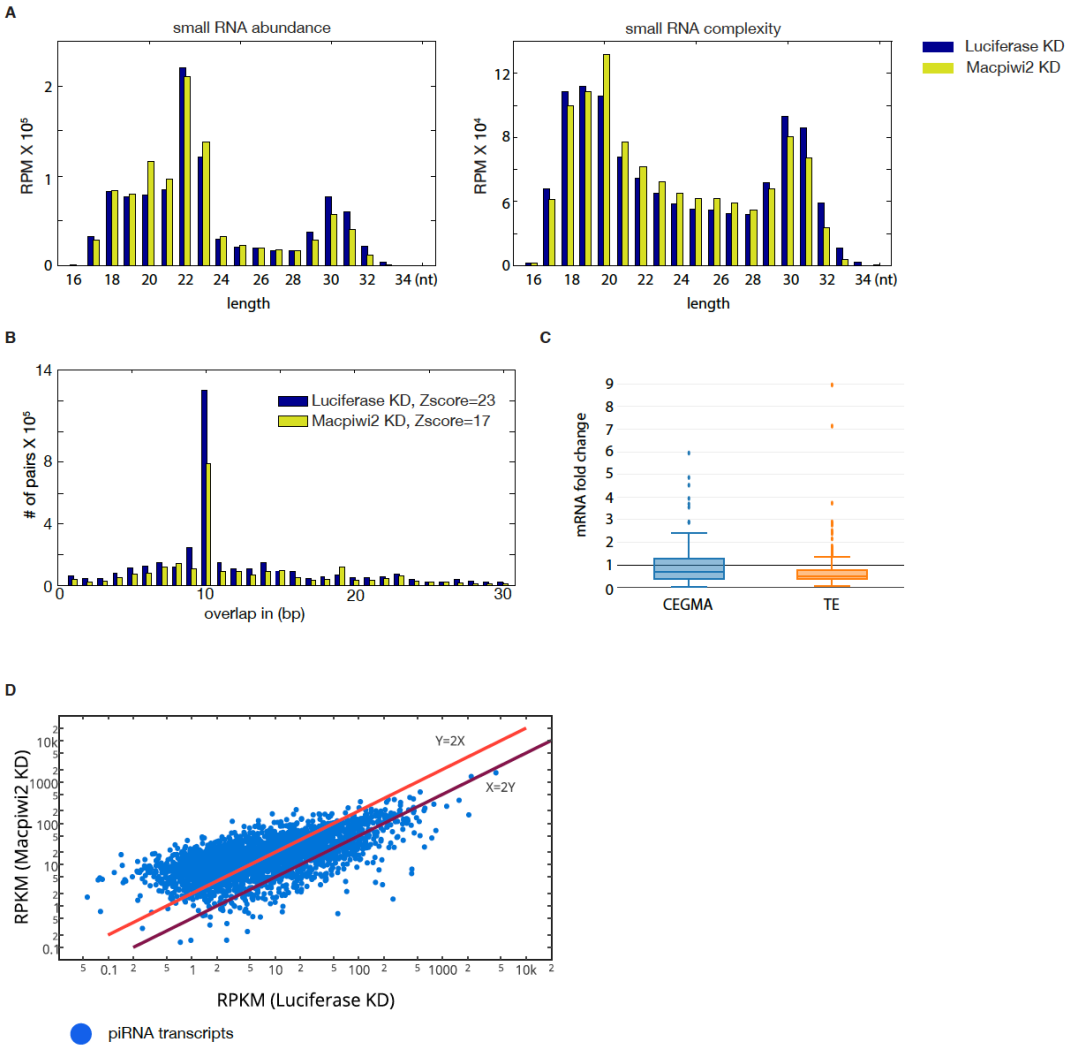

Figure 2.10 Impact of *Macpiwi2* knockdown on piRNA production and transposon silencing. (A) Length distribution of sequence abundance and complexity of small RNAs mapped to genome from *luciferase* and *Macpiwi2* KD. (B) Distribution of 5' overlap between piRNAs from sense and antisense strands in *luciferase* and *Macpiwi2* KD. (C) mRNA fold change of CEGMA core gene set and transposon consensus sequences in *Macpiwi2* KD, compared with *luciferase* KD. (D) Read counts of piRNAs mapped to individual transposon-related transcripts are plotted for *luciferase* KD and *Macpiwi2* KD worms. Each dot represents a transposon consensus sequence. Axes are presented on log10 scale.

Contribution

I performed the RNAi experiments and sequenced small RNAs and transcriptomes. James Gurtowski performed CEGMA. Osama El Demerdash assembled the transposon consensus sequences. I analyzed small RNA and transcriptome data.

2.3.6 Macpiwi1 is essential for stem cell maintenance

In all other species studied so far, loss of the piRNA pathway components leads to transposon derepression and sterility (Klattenhoff et al. 2007; Klattenhoff and Theurkauf 2008). Given their expression patterns, when silencing *Macpiwi1*, *Macvasa* and *Macpiwi2*, we paid particular attention to effects on dividing cell populations. To track changes in the germline and neoblasts, we stained for Macpiwi1 and Macvasa proteins and labeled dividing cells by EdU incorporation. As reported previously (De Mulder et al. 2009), Macpiwi1 is present in both germline and neoblasts, where it is essential for stem cell maintenance and functions in adult homeostasis, regeneration and postembryonic development. In accord with prior studies, silencing of *Macpiwi1* caused defects in adult worms (Figure 2.12A), hatchlings, and regenerating worms (Figure 2.12B). Macpiwi1 protein was undetectable in *Macpiwi1*-depleted adult worms within two weeks of treatment with dsRNA (Figure 2.11B). By three weeks following silencing of *Macpiwi1* in adults, EdU-positive cells were eliminated and gonads degenerated (Figure 2.12A, Figure 2.11A). In hatchlings, *Macpiwi1* knockdown resulted in retarded development and in the failure in gonad formation (Figure 2.12B), and EdU-positive cells were dramatically decreased in 9-day old hatchlings (Figure 2.12B). *Macpiwi1* silencing also resulted in severe defects in regeneration. Three days after anterior amputation, EdU-positive cells accumulated at the blastema, however, stem cells failed to develop into new tissues (Figure 2.12B). Nine days post-amputation, EdU-positive cells were undetectable and regeneration did not progress (Figure 2.12B). Prolonged exposure to *Macpiwi1* RNAi eventually led to mortality in all of the above conditions, most likely due to the lack of stem cells whose activity is required for tissue maintenance.

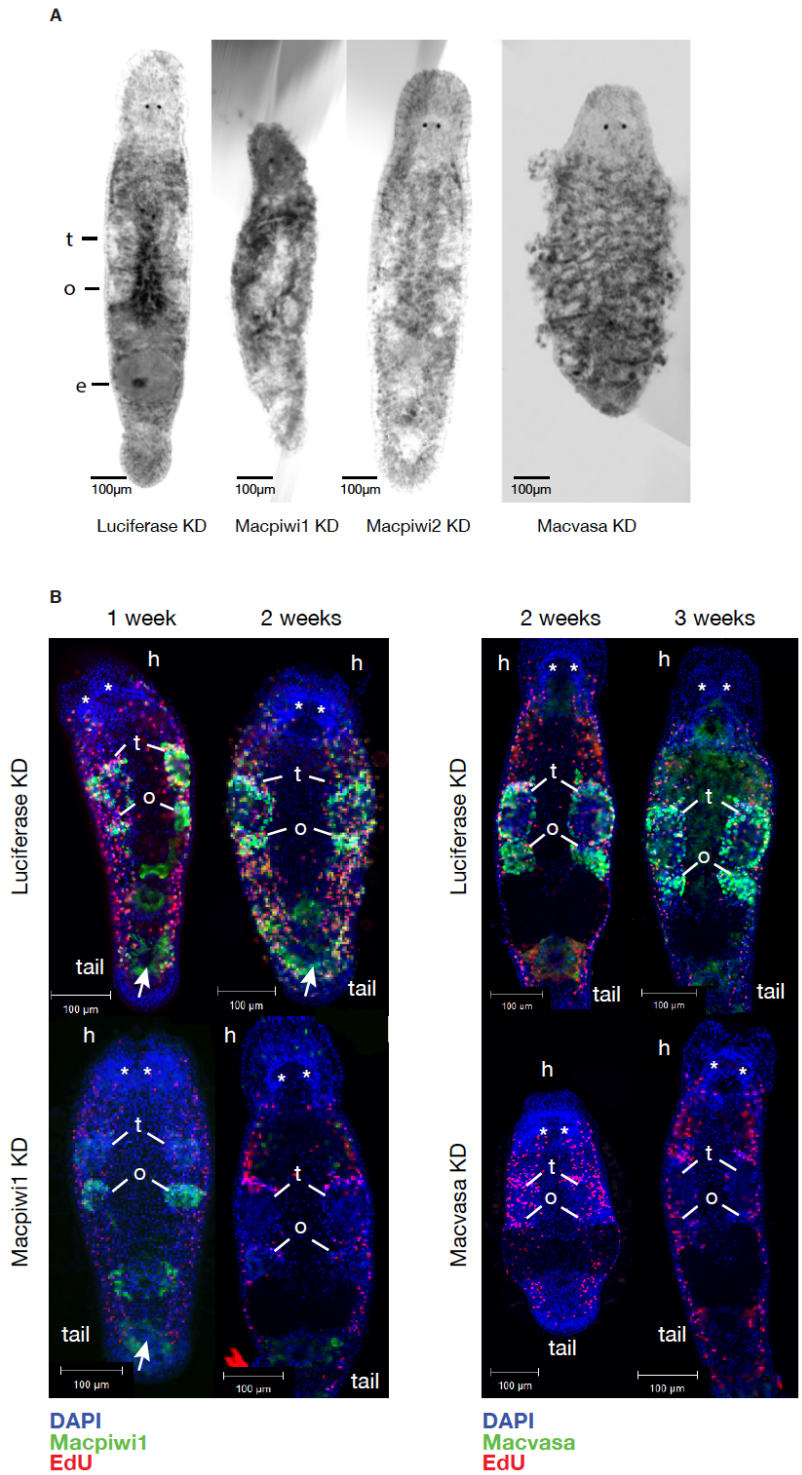

Figure 2.11 Morphology of adult worms and knockdown efficiency following RNAi. (A) Differential interference contrast (DIC) images of adult worms treated with *luciferase* (4 weeks), *Macpiwi1* (3 weeks), *Macpiwi2* (5 weeks) and *Macvasa* (4 weeks) RNAi. t: testis; o: ovary: e: egg. (B) Macpiwi1 and Macvasa immunostaining following *Macpiwi1* and *Macvasa* RNAi respectively. *Luciferase* RNAi serves as a negative control. t: testis; o: ovary: e: egg. Stars denote eyes. Arrows point to nonspecific staining from the secondary antibody.

Macvasa-knockdown worms suffered an even more dramatic piRNA loss and a greater increase in transposon expression than did *Macpiwi1*-knockdown animals (Figure 2.9B and F), yet the phenotypes of these animals were dramatically different. Despite substantive piRNA loss, *Macvasa*-knockdown worms failed to show phenotypes expected for stem cell defects in adults, hatchlings, or regenerating worms within 3 weeks of RNAi treatment (Figure 2.12A and B). This was consistent with one previous study of *Macvasa* knockdown (Pfister et al. 2008). After three weeks of RNAi treatment, we noticed a gradual decrease of Macpiwi1 staining in *Macvasa* knockdown animals (Fig. 6A), indicating either decreased expression, stability, or delocalization of the Macpiwi1 protein. Mortality and morphological changes (Figure 2.11A) occurred in some worms during the fourth week of *Macvasa* RNAi treatment. EdU-positive cells were, however, constantly present in *Macvasa* knockdown worms in all conditions, even after piRNAs underwent a depletion more severe than that in *Macpiwi1* knockdown worms (Figure 2.12A). Differential expression analysis identified sixteen apoptosis-related genes that were increased upon *Mapiwi1* but not *Macvasa* knockdown (Figure 2.12C). The activation of apoptosis might be a strong contributor to stem cell failure in *Macpiwi1*-knockdown worms. Considered as a whole, our data could suggest that Macpiwi1 has functions in stem cell maintenance that are distinct from its roles in transposon repression. *Macvasa* knockdown had profound effects on piRNA populations but did not seem to disrupt the stem cell maintenance function of Macpiwi1. This raises several interesting possibilities. Macpiwi1 could maintain stem cells in a piRNA-independent fashion, and such piRNA-independent activities have been suggested for PIWI proteins in other organisms (Klenov et al. 2011). Alternatively, those small RNAs needed for stem cell maintenance functions may not depend upon Macvasa for their production and could form a piRNA population that is either not readily identified in our sequencing data or be modified in a fashion that makes them less amenable to capture by our cloning protocol.

Contribution

I performed all immunostaining. Kaja A. Wasik's provided help with imaging. I performed differential expression analysis using transcriptome data.

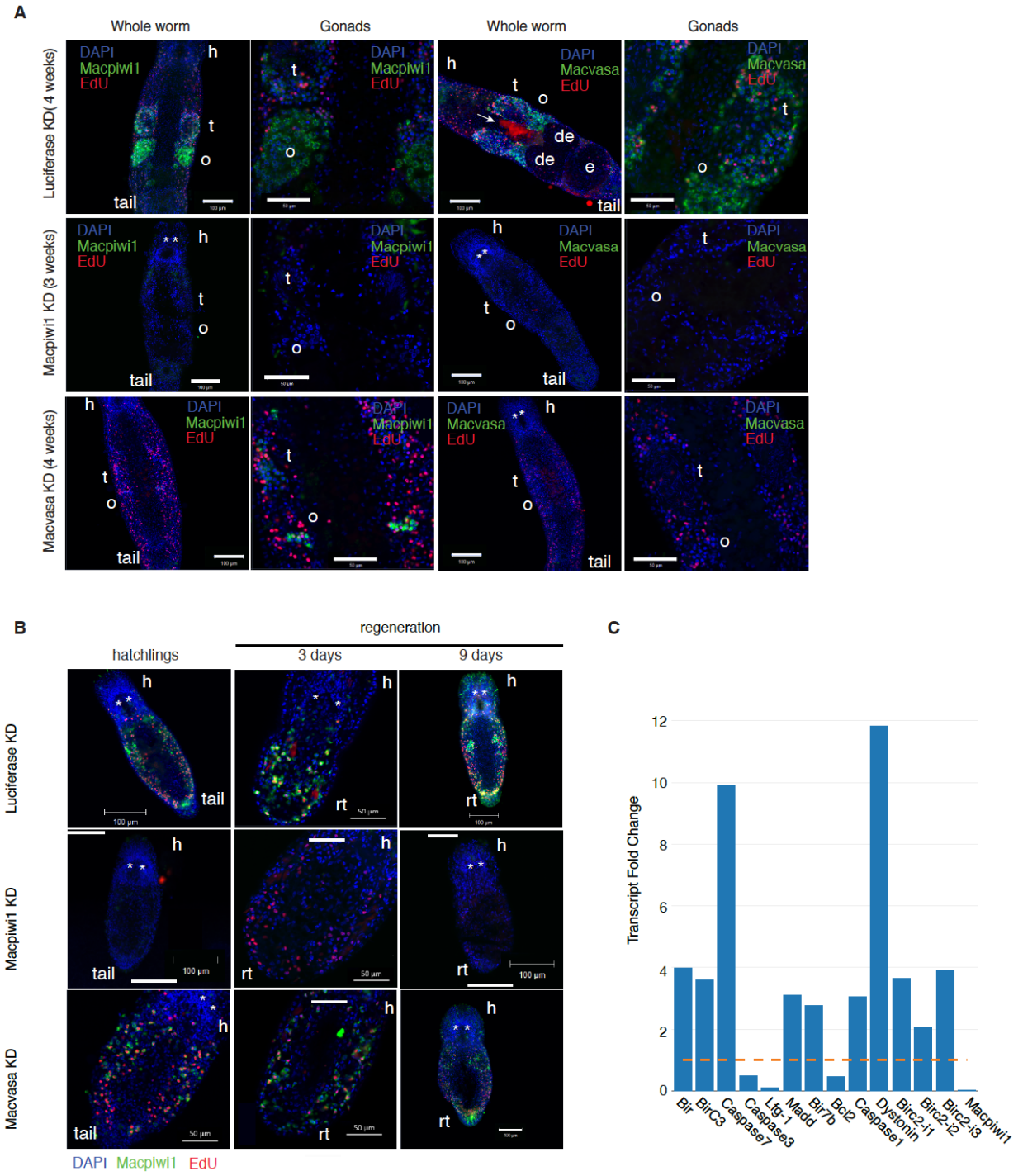

Figure 2.12 Depletion of Macpiwi1 but not Macvasa results in stem cell failure. (A) Macpiwi1 and Macvasa immunostaining after *luciferase* KD (4 weeks), *Macpiwi1* KD (3 weeks), and *Macvasa* KD (4 weeks) in adult worms. EdU-positive cells are shown in red. t: testis; o: ovary; de: developing egg: e: egg; h: head. Stars denote eyes. The arrow denotes nonspecific staining of diatoms in the gut. (B) Macpiwi1 immunostaining in 1-week old hatchlings, regenerating worms 3 days and 9 days post anterior amputation. EdU-positive cells are shown in red. h: head; rt: regenerating tail. Stars denote eyes. (C) Fold change of differentially expressed apoptosis-related transcripts in *Macpiwi1* KD, normalized to *luciferase* RNAi. Yellow dash line: fold change=1. *Macpiwi1* is plotted as a control.

2.4 Experimental methods

2.4.1 Animal culture, regeneration, gamma-irradiation and RNA isolation

M. lignano was kept in petri dishes with nutrient-enriched f/2 medium and fed *ad libitum* with diatoms (*Nitzchia curvilineata*) (Andersen et al. 2005). Climate chamber conditions were set at 20°C, 60% humidity and a 14/10 h day/night cycle. For regeneration, worms were cut at the post-pharyngeal level in order to completely remove gonads. The anterior part was kept under normal conditions with diatoms. Gamma irradiation was performed as previously described (De Mulder et al. 2010). 200-400 worms were resuspended in TRIzol reagent (Life Technologies) for RNA extraction according to manufacturer's instruction.

2.4.2 Cloning of *Macpiwi1* and *Macpiwi2*

The *Macpiwi1* full-length coding sequence was published previously (De Mulder et al. 2009). In order to obtain a full-length mRNA sequence, 5' and 3' RACE were performed using SMARTer RACE cDNA amplification kit (Clontech). Primer sequences used: 5'-CGACACGTCAACATGCAGCATCAGAG-3' (5'RACE) and 5'-GAGGACGTGAATGACGCCAACATCAA-3' (3'RACE). A partial *Macpiwi2* sequence was identified from the *de novo* transcriptome assembly (Wasik et al., submitted). 5' and 3' RACE were performed in order to obtain the full-length transcript sequence. Primers sequences are: 5'-CTCGGTCCTGCATCACGGGCAGCACGTA-3' (5'RACE) and 5'-AAAGTCGCTCCGTGCAGGGTGTGGTGTT-3' (3'RACE). The PCR fragments were cloned using Zero Blunt TOPO PCR cloning kit (Life Technologies) for sequencing.

2.4.3 Reverse transcription and quantitative PCR

Reverse transcription was performed using 2 µg of total RNA, oligo (dT) and SuperScript III reverse transcriptase (Life Technologies) following the manufacturer's instruction. *Macpiwi1*, *Macpiwi2* and *Macvasa* expression levels were measured using Sybr-green PCR on Eppendorf Realplex thermal cycler. Beta-actin was used as a housekeeping gene for normalization. PCR primers used:
Actin forward: 5'-CGTGACCTCACCGACTACCT-3',
Actin reverse: 5'-GGGCAGCTCGTAGCTCTTCT-3',
Macpiwi1 forward: 5'-AGGCCATTGTGGTGAAGAAG-3',
Macpiwi1 reverse: 5'-ACTGCGACACCAGGAAGAAG-3',
Macpiwi2 forward: 5'-GCTGCACCTGATGAATGTTG-3',
Macpiwi2 reverse: 5'-TTCGACGGATCCAGGTAAAG-3',
Macvasa forward: 5'-GCTTCATGGACTCGGTGACT-3',
Macvasa reverse: 5'-GGCCGAGAACATCACAATCT-3'.

2.4.4 Whole mount in situ hybridization of Macpiwi2

Whole mount in situ hybridization was performed as previously described (Pfister et al. 2007) with modifications (Lengerer et al. 2014). The template DNA for DIG-labeled *in situ* probe synthesis was made using Q5 High-Fidelity DNA Polymerase (New

England Biolabs). Color development was carried out at 37 °C for 1 hour and at 4 °C for 80 minutes. Primer binding sites used for template DNA synthesis were:
5'-AGCTTCTGGCTTCGGGTATC-3';
5'-CAGATCGATGTCGTAAGTCTGC-3'.

2.4.5 Immunofluorescence and labeling of S-phase cells

Polyclonal Macpiwi1 antibody was produced by PrimmBiotech by rabbit immunization with the peptide, RPAPPPGLSAQAG (position 44-56 aa). The antibody was purified from serum using synthetic peptides and the sulfolink immobilization kit (Thermo Scientific) according to manufacturer's instructions. Macpiwi1 and Macvasa staining was performed as previously described (Pfister et al. 2008; De Mulder et al. 2009). For double staining of S-phase cells and Macpiwi1 or Macvasa, worms were soaked in 5mM EdU for 30min. EdU-positive cells were labeled using click-iT cell reaction buffer kit (Life Technologies) and Alexa Fluor 594 azide (Life Technologies) according to the manufacturer's instructions, after the secondary antibody reaction. Nuclei were stained with DAPI (5µg/ml) (Sigma Aldrich) at room temperature for 15min. Specimens were mounted with prolong gold antifade reagent (Life Technologies) for imaging. Images were captured using Zeiss LSM 710 confocal microscope.

2.4.6 RNA interference

RNAi knockdown of *Macpiwi1* and *Macvasa* was performed as previously described (Pfister et al. 2008; De Mulder et al. 2009). dsRNA was synthesized using the T7 Ribomax express RNAi system (Promega). Worms were soaked in f/2 medium containing 4 µg/ml of dsRNA probes and 35 µg/ml of antibiotics (Ampicillin and Kanamycin alternately every other day). Medium was changed twice a day. Before amputation, whole worms were presoaked for two weeks. Eggs were soaked as soon as they were laid. Worms were fed on diatoms throughout the entire experiment. Three biological replicates were performed for each knockdown condition. Approximately 300 worms were used for each replicate. Each biological replicate was used for all downstream applications including immunostaining (20 worms each staining), small RNA cloning and mRNA sequencing.

2.4.7 Immunoprecipitation, RNA end labeling and western blot

Approximately 10,000 worms were collected and lysed in worm lysis buffer 2.0 (20mM HEPES, 150mM NaCl, 2mM EDTA, 2mM EGTA, 0.1M PMSF, 0.5% NP-40, 0.5% Triton X-100, 10% glycerol, 1mM DTT, cOmplete mini protease inhibitor cocktail (Roche), 100U/ml RNasin RNase inhibitor (Promega)) using a Dounce homogenizer. Crude lysate was centrifuged at >12,000 ×g at 4 °C for 15min. The supernatant was transferred to a new tube while the pellet was washed with worm lysis buffer 2.0 and centrifuged again. Supernatants from the two centrifugations were combined and the volume was brought up to 0.5 ml using worm lysis buffer 2.0. Polyclonal Macpiwi1 antibody or pre-immune rabbit serum (1:10) was added to cleared lysate and incubated at 4°C overnight under rotation. 50µl of protein A agarose beads (Roche) blocked with

5% BSA was added and incubation was carried on at 4°C for 4 hours. Beads were spun down and washed in NT2 buffer (50mM Tris pH 7.4, 150mM NaCl, 1mM MgCl2, 0.05% NP40, 100U/ml RNasin, 1mM DTT) at 4 °C with a series of increasing salt concentrations (150mM NaCl, 2 x 10min; 300mM NaCl, 2 x 10min; 500mM NaCl, 2 x 10min). After washing, beads were spun down and digested with 2µg/µl of proteinase K in 200ul of proteinase K buffer (200mM Tris-HCl pH 7.5, 25mM EDTA, 300mM NaCl, 2% SDS) at 65°C for 1 hour. RNA was extracted using equal volumes of acidic phenol: chloroform and chloroform sequentially, followed by ethanol precipitation at -20°C overnight.

For end labeling of RNA, 1/10 of the RNA isolated was treated with CIP (New England Biolabs) at 37°C for 30min before labeled using [γ-^{32}P] ATP (Perkin Elmer) and PNK (New England Biolabs) at 37°C for 1 hour. Labeled RNA was visualized on a 12% polyacrylamide gel.

For western blotting of Macpiwi1, protein samples were resuspended in Laemmli buffer, boiled for 5min and run on 10% SDS-PAGE. Proteins were transferred onto a PVDF membrane using a wet transfer method at 35V overnight. Membranes were blocked in 5% fat-free milk at room temperature for 1 hour and incubated with polyclonal Macpiwi1 antibody (1:200) at 4°C overnight. Membranes were washed in TBS-T (3 x 5min) and incubated with HRP-conjugated anti-rabbit IgG secondary antibody (Cell Signaling) at room temperature for 1 hour. After washes in TBS-T (5 x 5min), Amersham ECL prime detection reagent was used for detection.

2.4.8 S-phase cell sorting

At least 10,000 worms were collected and relaxed in F/2-7,14% $MgCl_2$ (1:1) at room temperature for 10min. Relaxed worms were washed in CMFM (88mM NaCl, 1mM KCl, 2.4mM $NaHCO_3$, 7.5mM Tris-HCl (pH 7.6)) on ice (3 x 5min). Worms were trypsinized with 1% Trypsin in CMFM at 37°C for 20min with agitation. An equal volume of maceration solution (glacial acetic acid: glycerol: H_2O 1:1:13, 9% sucrose) was added and incubated at room temperature for 1min. Cells were spun down at 5,000 xg, 4°C for 10min, resuspended in PBS with 5% RNase inhibitor and incubated on ice for 5min. Centrifugation was repeated and cells were resuspended and incubated in 0.5mg/ml lysolecithin (Sigma Aldrich) in PBS with 5% RNase inhibitor at room temperature for 10min. Cells were blocked with 2% BSA on ice for 5min and let recover in 500ul 2% FBS in PBS for 10min at 4°C. Propidium iodide (20µg/ml) (Sigma Aldrich) was added to cell suspension and incubated on ice for 30min. Cells were sorted using an Aria IIU cell sorter (BD biosciences) and directly mixed with TRIzol LS reagent (Life Technologies) for RNA extraction.

2.4.9 Small RNA and mRNA sequencing

Small RNAs with 5' phosphate and 3' hydroxyl group were cloned using a previously published method (Lau et al. 2001). 1-10µg of total RNA was used as input. RNA-seq libraries were generated using Encore Complete RNA-Seq DR Multiplex

System (Nugen) according to manufacturer's instruction. Samples were sequenced on Illumina Hiseq 2000. All sequencing raw data is available in Sequencing Read Archive (SRA) under accession SRP059454.

2.4.10 Small RNA sequencing data analysis

Three biological replicates were generated for each experiment, except for irradiated worms for which two replicates were generated. All sequence alignment against the genome draft, *de novo* transcriptome, or transposon consensus was performed using Bowtie (Langmead 2010), allowing up to two mismatches. Samtools (Li et al. 2009) and BEDTools (Quinlan and Hall 2010) were used for downstream processing, including read count and strand bias calculations from each genomic location. BAM files generated by Bowtie were loaded into the Integrative genomics viewer (IGV) to display read alignments and coverage. To examine ping-pong signature, we used the ping-pong tool from piPipes (Han et al. 2015b) on piRNA sequences. Nucleotide bias of piRNAs and microRNAs was displayed using Weblogo 3.0 (Crooks et al. 2004) command line interface.

The identification of piRNA clusters (Brennecke et al. 2007) and piRNA-producing transcripts (Li et al. 2013) was done according to previously published methods with adjustments. All collapsed and uniquely mapped 28-32nt small RNA reads were aligned to the genome draft or *de novo* transcriptome. For piRNA cluster identification, numbers of reads were counted in 1kb sliding windows with a step size of 968nt. Windows containing at least 10 reads were merged and defined as piRNA clusters. Transcripts with at least 100 RPKM or PPM of mapping reads were qualified as piRNA-producing transcripts.

To generate transposon consensus sequences, we used the TEdenovo pipeline from REPET package (Flutre et al. 2011). Due to the highly repetitive nature of *M. lignano* genome, only RepeatMasker (Smit et al. 2013-1015)-annotated repeats and piRNA clusters were used as input. Low complexity repeats and microsatellites were excluded from the final consensus sequences.

2.4.11 Differential expression analysis of RNA-seq data

For differential expression of genes, paired-end reads were processed using RSEM (Li and Dewey 2011) with *de novo* transcriptome assembly. Differentially expressed genes (FDR <=0.05, fold change <=0.5 or >=2) were identified using EBSeq (Leng et al. 2013). Expression change of transposons was analyzed on transposon consensus sequences according to the strategy described previously (Le Thomas et al. 2013). Reads were aligned to transposon consensus with Bowtie allowing multiple mapping and up to three mismatches. Read count for each transposon was calculated with normalization for length of consensus sequence, number of aligned locations of each read and total number of reads aligned to whole genome. Three biological replicates of each condition were generated for statistical analysis.

2.4.12 Phylogenetic tree and protein alignment

Phylogenetic tree of PIWI proteins was generated using Clustal Omega. Protein sequence alignment is performed using ESPript 3.0.

2.5 Discussion

PIWI proteins are well established as being essential for transposable element silencing in many animal species, including *D. melanogaster, M. musculus* and *H. sapiens* (Juliano et al. 2011). Here, we show that one of *M. lignano* PIWI proteins, Macpiwi1, has essential roles in transposon repression, analogous to those documented in other animals.

PIWI proteins in *M. lignano* appear to diverge from those in other flatworm species (Fig. 1B), despite the relatively close phylogenetic relationship. In a recent study revising the phylogeny of flatworms (Laumer et al. 2015), *M. lignano* was shown to occupy a very basal position among Platyhelminthes, corroborating the commonly believed primacy of *M. lignano* among flatworms. Given the basal position of *M. lignano*, understanding the *M. lignano* piRNA pathway might shed some light on the divergence of piRNA pathways within Platyhelminthes and Metazoans.

Like other metazoans, *M. lignano* has multiple PIWI proteins, Macpiwi1, 2, and 3, and an abundant piRNA population that appears enriched for transposon sequences. Based on our attempts to clarify the hierarchy of Macpiwis, several observations imply that Macpiwi1 is the binding partner for primary piRNAs that subsequently enter the secondary amplification loop in a heterotypic ping-pong cycle. However, it remains unclear which additional Macpiwi protein(s) cooperate with Macpiwi1 in ping-pong amplification. *Macpiwi2* knockdown fails to abolish piRNA production, although there are some groups of differentially expressed piRNAs (Sup. Fig. 4D) and slightly more repressed transposon expression (Sup. Fig. 4C) suggest also participation of other Macpiwis. Nevertheless, the weakened ping-pong signature in *Macpiwi2* knockdown animals (Sup. Fig. 4B) poses it as one possible ping-pong partner for Macpiwi1.

In some settings, PIWI proteins also play essential roles in stem cell maintenance. In *M. lignano*, this is also the case, both for maintenance of the germline and for sustaining populations of totipotent stem cells, the neoblasts. In *M. lignano*, stem cell maintenance functions for Macpiwi1 appear to be separable from its role in transposon repression, based on our analysis of *Macvasa* knockdown worms. Distinctions between transposon repression and stem cell maintenance functions have also been made in other organisms. In *D. melanogaster* (Klenov et al. 2011), *Piwi*-null mutants display activation of transposons and severe disruption of germline stem cell maintenance. A Piwi mutant lacking its nuclear localization signal is capable of sustaining stem cell self-renewal, even though it fails to repress transposons in the bulk of the germline. Additionally, mutation of the nuclease that processes primary piRNA precursors, Zucchini, prevents loading of primary piRNAs into Piwi, but does not interfere with germline stem cell maintenance (Klenov et al. 2011). Here we find that

Macvasa-knockdown worms, which lack the vast majority of piRNAs, are fully capable of stem cell division, regeneration, and postembryonic development, despite transposon activation. Whether this indicates that Macpiwi1 functions in stem cell maintenance without the need to bind any small RNA partner, however, remains to be determined.

2.6 Supplementary information

Supplementary Figure 1 Sequence alignment of PIWI domains from PIWI proteins in various metazoan species. Identical (white letters on a red background) or similar (red letters on a white background) residues are labeled.

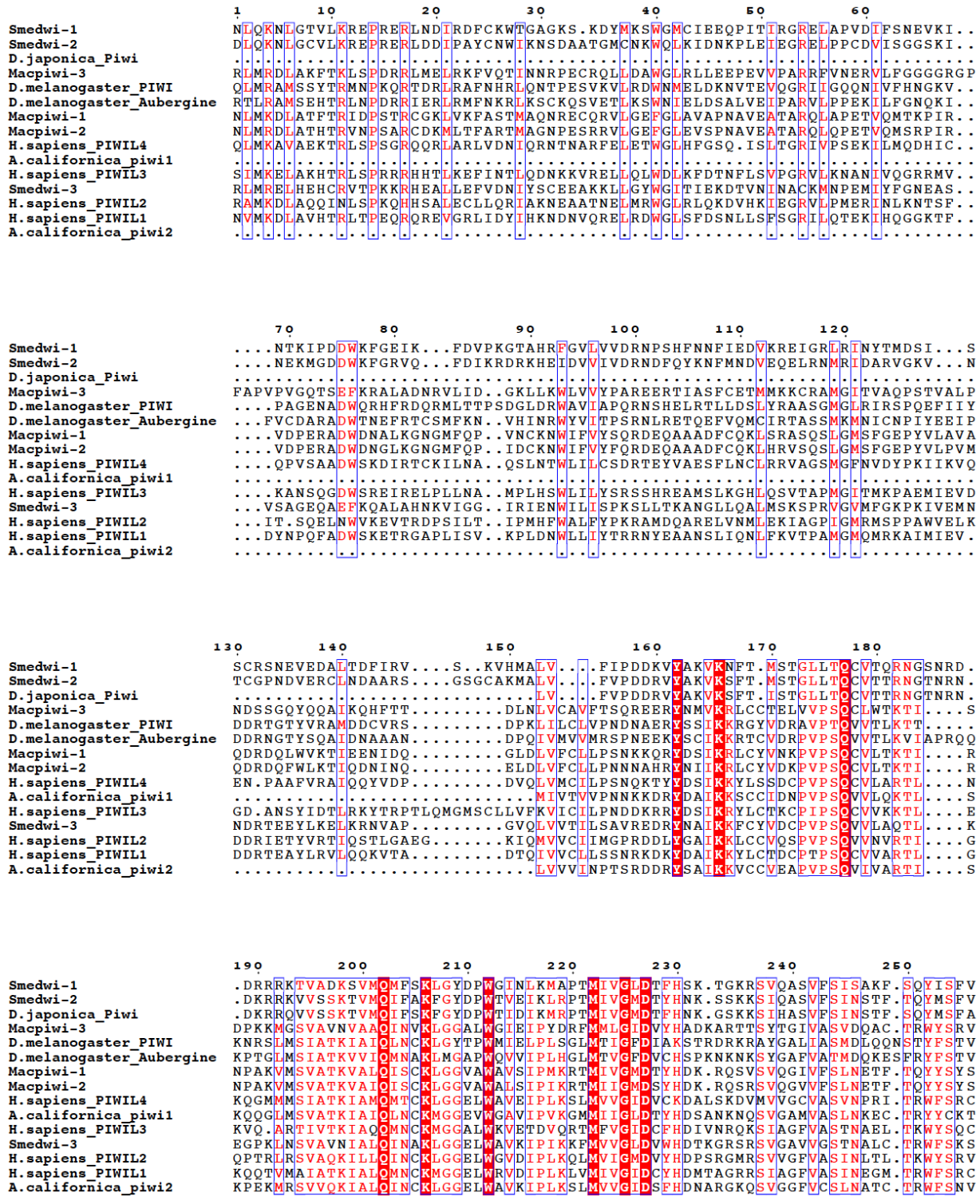

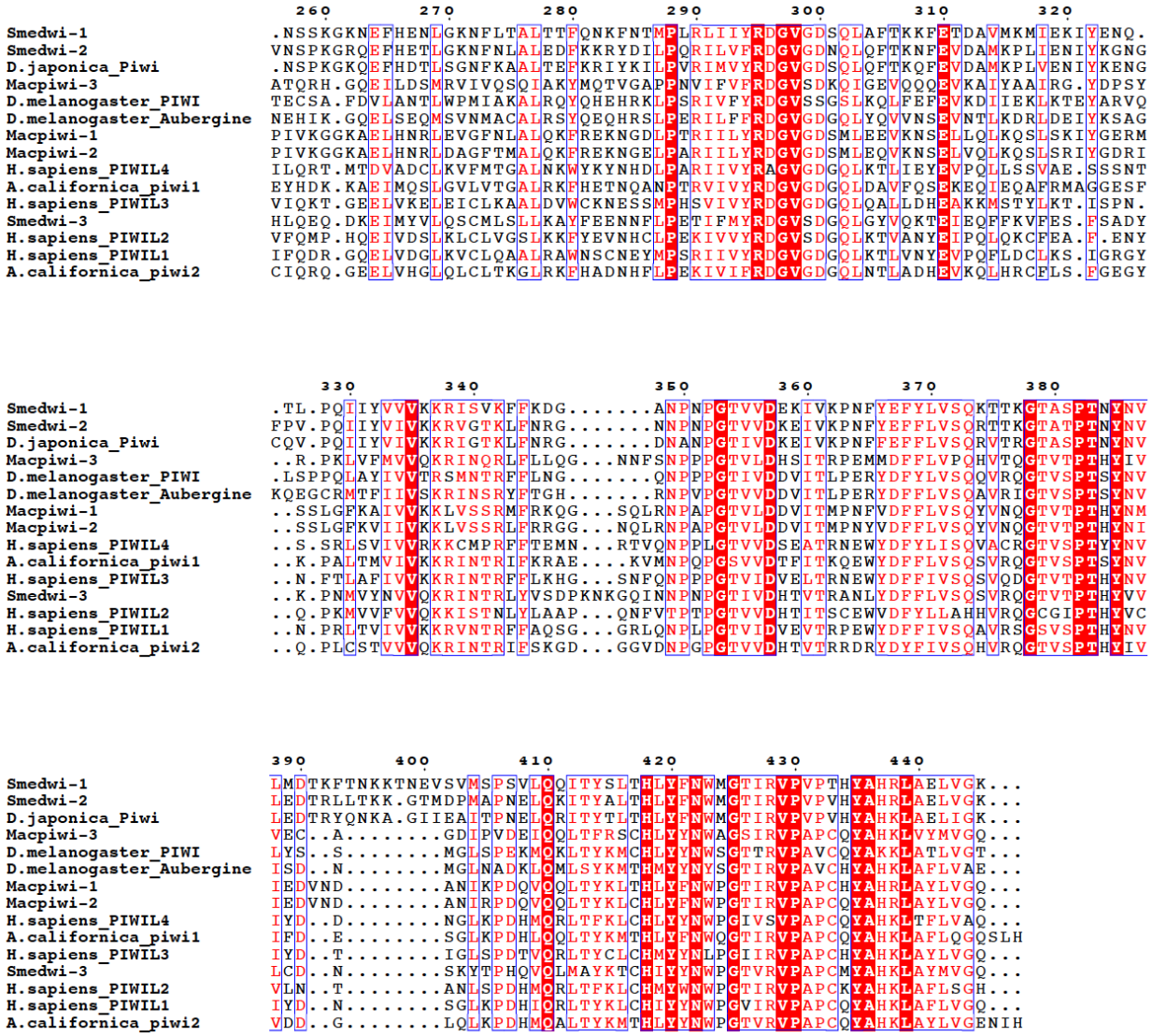

Supplementary Table 1 List of conserved miRNAs and their expression levels in different conditions.

miRNA ID	RPM Whole worm	RPM Dividing cells	RPM Irradiated worm	RPM Regeneration day 0	RPM Regeneration day 3
bantam	13.09	15.84	3.84	0.45	183.04
bantam-3p	3.20	3.97	1.15	0.13	41.90
let-7	22.35	14.51	1184.70	4.41	69.53
let-7-5p	5.96	4.29	331.67	1.10	15.06
let-7a	25.66	18.73	1401.51	4.48	54.61
let-7a-5p	22.39	16.53	1458.40	3.86	45.39
let-7b	6.27	13.57	850.16	7.84	6.03
let-7b-5p	3.68	9.38	630.24	5.95	2.19
let-7c	5.61	6.96	3069.88	0.62	0.00

let-7c-5p	5.79	7.11	3148.94	0.67	0.00
let-7d	1.21	0.07	129.96	0.00	0.00
let-7d-5p	1.62	0.00	183.35	0.00	0.00
let-7e	0.14	0.64	34.43	0.06	0.00
let-7e-5p	0.00	0.59	28.38	0.00	0.00
let-7f	5.10	9.82	1264.81	0.62	0.00
let-7f-5p	4.96	10.36	1322.89	0.67	0.00
let-7g	7.37	2.32	502.36	0.00	0.00
let-7g-5p	10.06	3.26	675.25	0.00	0.00
let-7i	2.89	1.75	113.82	0.00	0.00
let-7i-5p	2.89	1.80	120.29	0.00	0.00
let-7j-5p	1.52	1.11	82.59	0.26	3.04
miR-1	7624.96	4966.03	36891.62	39574.17	45690.75
miR-10	0.48	2.37	7.23	0.90	0.90
miR-100	0.86	3.33	473.32	0.93	0.00
miR-100-5p	0.48	2.20	319.15	0.52	0.00
miR-100a-5p	0.10	0.42	54.05	0.11	0.00
miR-100b	0.03	0.12	17.70	0.04	0.00
miR-101	0.00	1.01	5.42	0.00	0.00
miR-101-3p	0.00	0.39	1.75	0.00	0.00
miR-101a	0.00	0.44	2.96	0.00	0.00
miR-101a-3p	0.00	0.27	1.21	0.00	0.00
miR-101b-3p	0.07	0.15	5.34	0.00	0.00
miR-103	11.23	21.27	430.89	4.26	0.00
miR-103-3p	6.61	12.41	252.99	2.46	0.00
miR-103a	0.65	1.16	24.05	0.22	0.00
miR-103a-3p	1.96	3.48	72.16	0.67	0.00
miR-103b	1.31	2.32	48.10	0.45	0.00
miR-103b-3p	1.31	2.32	48.10	0.45	0.00
miR-10-3p	0.86	0.00	0.41	0.00	1.25
miR-10-5p	0.41	1.46	4.08	0.67	1.35
miR-106a	1.21	0.02	2.68	0.00	0.00
miR-106b	2.48	0.59	5.59	0.00	0.00
miR-106b-3p	0.21	0.72	1.42	0.00	0.00
miR-106b-5p	1.27	0.30	2.82	0.00	0.00
miR-107	1.93	16.38	233.07	4.70	0.00
miR-107-3p	0.59	6.86	93.58	2.02	0.00
miR-107a	0.72	1.92	34.08	0.45	0.00
miR-107a-3p	0.07	0.76	10.79	0.22	0.00
miR-107b	0.07	1.92	12.03	0.45	0.00
miR-10a	1.48	4.07	19.23	2.46	0.25
miR-10a-5p	1.52	5.72	25.92	3.36	0.00
miR-10b	2.41	3.21	89.20	0.00	0.00

miR-10b-5p	2.07	2.69	74.38	0.00	0.00
miR-10c-5p	0.17	0.30	9.67	0.00	0.00
miR-11	1.38	0.79	0.30	0.04	6.08
miR-11-3p	0.90	0.69	0.11	0.02	2.29
miR-1175-3p	3756.69	11758.23	172.07	265.64	313.91
miR-12	26.07	4.49	0.00	0.00	3.74
miR-122	0.00	70.69	0.00	0.00	0.00
miR-122-5p	0.00	56.73	0.00	0.00	0.00
miR-122a-5p	0.00	4.74	0.00	0.00	0.00
miR-12-3p	1.62	0.30	0.00	0.00	0.25
miR-124	57696.64	1577.96	9742.37	22955.44	13009.18
miR-124-3p	32827.73	907.55	5603.88	13125.65	7424.49
miR-124-4-3p	130.32	5.95	47.94	61.12	32.17
miR-1249	0.00	0.00	1.21	0.00	0.00
miR-124a	21249.68	597.24	3692.86	8566.03	4832.52
miR-124a-1-3p	1643.21	44.27	272.55	650.85	370.02
miR-124a-3p	5060.71	138.82	866.02	2014.95	1143.54
miR-124b	1782.00	50.31	321.26	713.65	403.04
miR-124b-3p	129.42	5.97	47.75	61.08	32.07
miR-124c-3p	1643.21	44.27	272.55	650.85	370.02
miR-125	6.82	0.69	155.11	0.00	0.70
miR-125-5p	4.89	0.49	115.77	0.00	0.55
miR-125a	1.17	0.10	30.30	0.00	0.10
miR-125a-5p	2.07	0.15	55.78	0.00	0.15
miR-125b	10.19	1.04	237.21	0.00	1.10
miR-125b-3p	0.48	0.05	11.07	0.00	0.05
miR-125b-5p	5.34	0.54	124.48	0.00	0.60
miR-125c	0.48	0.05	11.04	0.00	0.05
miR-12-5p	5.75	0.91	0.00	0.00	0.75
miR-126	0.34	0.94	39.09	0.00	0.00
miR-126-3p	0.62	1.23	63.72	0.00	0.00
miR-126-5p	0.07	5.95	50.57	0.00	0.00
miR-126a	0.00	0.00	2.16	0.00	0.00
miR-126a-3p	0.14	0.20	14.66	0.00	0.00
miR-126a-5p	0.00	1.33	10.19	0.00	0.00
miR-126b	0.00	0.44	3.40	0.00	0.00
miR-126b-3p	0.00	0.44	3.40	0.00	0.00
miR-126b-5p	0.00	0.44	3.51	0.00	0.00
miR-127	0.41	6.71	3.45	0.00	0.00
miR-127-3p	0.17	3.08	1.42	0.00	0.00
miR-128	2.41	0.42	10.25	0.00	0.00
miR-128-3p	1.65	0.30	7.23	0.00	0.00
miR-128a-3p	0.28	0.05	1.21	0.00	0.00

miR-128b-3p	0.28	0.05	1.21	0.00	0.00
miR-129	0.00	0.00	4.47	0.00	0.00
miR-129-2-3p	0.00	0.00	2.93	0.00	0.00
miR-129-3p	0.00	0.00	3.56	0.00	0.00
miR-129-5p	0.00	0.00	5.70	0.00	0.00
miR-129a	0.00	0.00	1.15	0.00	0.00
miR-129a-3p	0.00	0.00	1.42	0.00	0.00
miR-129a-5p	0.00	0.00	1.75	0.00	0.00
miR-129b	0.00	0.00	1.59	0.00	0.00
miR-129b-3p	0.00	0.00	1.62	0.00	0.00
miR-130	0.28	0.37	9.07	0.02	0.05
miR-1306	0.00	0.00	1.64	0.00	0.00
miR-1306-5p	0.00	0.00	4.38	0.00	0.00
miR-130a	2.69	4.37	69.94	0.22	0.60
miR-130a-3p	1.58	2.94	40.02	0.15	0.40
miR-130b	0.28	0.20	9.31	0.00	0.00
miR-130b-3p	0.83	1.26	23.64	0.06	0.15
miR-130c-3p	0.83	1.11	22.68	0.06	0.15
miR-133	448.39	383.55	69.12	213.74	89.28
miR-133-3p	140.06	107.88	21.12	64.05	28.83
miR-133-5p	16.77	14.71	2.66	8.20	3.34
miR-133a	234.74	201.89	33.67	106.63	45.24
miR-133a-3p	188.90	167.87	24.98	81.56	34.71
miR-133b	97.32	20.23	13.53	37.07	24.64
miR-133b-3p	64.75	13.03	8.99	24.64	16.41
miR-133c	59.30	53.00	5.92	21.64	9.78
miR-133c-3p	29.89	26.50	2.96	10.85	4.89
miR-133d	0.41	1.38	0.16	0.22	0.20
miR-133d-3p	16.77	14.71	2.66	8.20	3.34
miR-13-3p	0.62	0.00	0.08	0.07	2.89
miR-138	0.24	0.00	17.42	0.00	0.00
miR-138-5p	0.28	0.00	18.85	0.00	0.00
miR-138a	0.10	0.00	6.90	0.00	0.00
miR-138b	0.03	0.00	2.52	0.00	0.00
miR-13a	1.96	3.01	1.37	2.20	1.65
miR-13a-3p	1.96	3.01	1.37	2.20	1.65
miR-13b	2.27	0.00	0.30	0.21	10.97
miR-13b-3p	0.62	0.00	0.08	0.06	2.99
miR-1-3p	4427.35	2732.58	19201.51	21413.84	24277.05
miR-14	3.86	6.05	0.14	0.00	3.84
miR-140	0.55	0.15	3.40	0.00	0.00
miR-140-3p	1.03	0.91	12.05	0.00	0.00
miR-140-5p	1.31	0.00	0.44	0.00	0.00

miR-141	0.00	0.59	1.12	0.15	0.40
miR-142	0.90	0.27	1.40	0.00	0.00
miR-142-3p	2.03	0.25	0.77	0.00	0.00
miR-142-5p	0.21	0.42	1.18	0.00	0.00
miR-143	3.07	6.05	389.14	0.32	0.00
miR-143-3p	2.20	4.56	288.33	0.22	0.00
miR-14-3p	1.17	1.53	0.05	0.00	1.00
miR-144	1.45	0.00	0.00	0.00	0.00
miR-144-3p	1.14	0.00	0.00	0.00	0.00
miR-145	1.03	0.49	12.16	0.00	0.00
miR-145-3p	0.00	0.00	3.07	0.00	0.00
miR-145-5p	1.07	0.44	11.89	0.00	0.00
miR-145a-5p	0.10	0.05	1.15	0.00	0.00
miR-146a	0.00	0.25	1.37	0.00	0.00
miR-146a-5p	0.00	0.39	1.97	0.00	0.00
miR-146b-5p	0.00	0.39	1.78	0.00	0.00
miR-148-3p	0.00	6.51	0.00	0.00	0.00
miR-148a	0.00	15.57	0.00	0.00	0.00
miR-148a-3p	0.00	17.96	0.00	0.00	0.00
miR-15	3.10	0.05	9.48	0.00	0.05
miR-151	0.65	0.10	16.11	0.00	0.00
miR-151-5p	5.23	0.39	127.77	0.00	0.00
miR-151a-5p	1.31	0.10	31.94	0.00	0.00
miR-152	0.00	0.44	1.07	0.00	0.00
miR-155-5p	0.00	0.12	1.04	0.00	0.00
miR156b	0.00	0.00	1.48	0.22	0.00
miR156c	0.00	0.00	1.97	0.30	0.00
miR156e	0.03	0.00	1.23	0.19	0.00
miR156f	0.00	0.00	1.48	0.22	0.00
miR156g	0.00	0.00	1.23	0.19	0.00
miR156h	0.00	0.00	1.23	0.19	0.00
miR156i	0.00	0.00	1.48	0.22	0.00
miR159	0.03	1.92	1.89	0.17	0.00
miR159a	0.17	2.76	2.66	0.26	0.00
miR159b	0.14	1.28	1.12	0.15	0.00
miR-15a	19.46	1.48	149.71	0.00	0.00
miR-15a-5p	11.61	0.89	89.80	0.00	0.00
miR-15b	31.41	0.64	97.61	0.00	0.65
miR-15b-3p	0.21	0.00	1.81	0.00	0.00
miR-15b-5p	21.97	0.54	68.05	0.00	0.55
miR-15c	0.14	0.10	1.10	0.00	0.10
miR-15c-5p	0.21	0.15	1.64	0.00	0.15
miR-1-5p	276.10	163.08	1052.06	1253.27	1383.74

miR-16	99.01	3.38	753.16	0.90	0.00
miR-16-5p	52.31	1.73	361.64	0.45	0.00
miR168	0.00	0.76	1.56	0.15	0.40
miR168a	0.00	0.67	1.18	0.11	0.30
miR-16a	1.38	0.00	16.44	0.22	0.00
miR-16a-5p	9.88	0.47	76.35	0.28	0.00
miR-16b	2.34	0.47	49.61	0.34	0.00
miR-16b-5p	1.65	0.10	21.01	0.28	0.00
miR-16c-5p	8.61	0.27	58.76	0.06	0.00
miR-17	1.41	0.02	5.37	0.00	0.00
miR-17-3p	0.03	0.00	1.59	0.00	0.00
miR-17-5p	31.44	0.64	71.14	0.00	0.00
miR-17a-5p	1.31	0.02	4.03	0.00	0.00
miR-18	11.12	0.00	27.75	0.00	0.00
miR-181a	0.00	3.04	34.02	0.17	0.90
miR-181a-3p	0.00	0.00	1.92	0.00	0.00
miR-181a-5p	0.00	8.44	110.48	0.43	2.49
miR-181b	0.00	1.14	22.49	0.00	0.00
miR-181b-5p	0.00	0.94	21.48	0.00	0.00
miR-181c	0.55	0.20	3.31	0.00	0.00
miR-181c-5p	0.45	0.22	3.10	0.00	0.00
miR-181d	0.00	0.00	1.23	0.00	0.00
miR-181e	0.00	0.07	2.00	0.00	0.00
miR-183	0.00	2.52	2.19	0.00	0.00
miR-183-5p	0.00	1.48	1.15	0.00	0.00
miR-1839	0.00	0.00	2.05	0.00	0.00
miR-1839-5p	0.00	0.00	2.68	0.00	0.00
miR-184	17.56	11.62	50.79	0.63	105.69
miR-184-3p	11.71	10.76	25.15	0.45	106.88
miR-184a	0.96	1.09	1.48	0.04	11.27
miR-185	0.24	0.17	6.00	0.39	0.00
miR-185-5p	0.21	0.15	4.93	0.34	0.00
miR-186	0.55	0.99	2.41	0.00	0.00
miR-186-5p	0.62	0.99	1.89	0.00	0.00
miR-188	0.00	0.00	4.60	0.00	0.00
miR-188-5p	0.00	0.00	1.56	0.00	0.00
miR-18a	11.16	0.00	27.89	0.00	0.00
miR-18a-5p	18.08	0.00	56.21	0.00	0.00
miR-18b	0.34	0.00	1.37	0.00	0.00
miR-18b-5p	1.17	0.00	2.93	0.00	0.00
miR-19	1.34	0.20	0.27	0.00	0.00
miR-190a	0.00	0.07	1.81	0.00	0.00
miR-190a-5p	0.00	0.10	1.92	0.00	0.00

miR-190b	0.14	0.00	1.40	0.00	0.00
miR-191	12.91	0.89	120.78	0.30	0.00
miR-191-5p	20.18	1.55	187.08	0.41	0.00
miR-191a	2.00	0.22	18.93	0.04	0.00
miR-191a-5p	2.00	0.22	18.93	0.04	0.00
miR-192	0.62	7.65	0.19	0.00	0.00
miR-192-5p	0.48	5.28	0.00	0.00	0.00
miR-193a-5p	1.21	0.00	0.19	0.00	0.00
miR-193b-3p	0.41	0.05	2.03	0.00	0.00
miR-194	1.10	1.23	1.31	0.00	0.00
miR-195	2.48	0.00	22.93	0.00	0.00
miR-195-5p	0.96	0.00	9.67	0.00	0.00
miR-195a-5p	0.14	0.00	2.03	0.00	0.00
miR-196	0.00	0.00	2.74	0.00	0.35
miR-196a	0.00	0.00	5.67	0.00	0.65
miR-196a-5p	0.00	0.02	5.20	0.00	0.50
miR-199	0.28	0.44	14.19	0.00	0.00
miR-199-3p	0.14	0.81	22.90	0.00	0.00
miR-199-5p	0.45	0.00	4.11	0.00	0.00
miR-199a	0.86	0.20	12.30	0.00	0.00
miR-199a-3p	0.65	4.10	108.46	0.00	0.00
miR-199a-5p	1.62	0.00	13.89	0.00	0.00
miR-199b	0.07	0.44	11.70	0.00	0.00
miR-199b-3p	0.24	1.51	40.57	0.00	0.00
miR-199c-3p	0.07	0.42	11.94	0.00	0.00
miR-19a	5.58	0.44	1.97	0.00	0.00
miR-19a-3p	3.31	0.30	1.15	0.00	0.00
miR-19b	25.93	3.95	5.31	0.00	0.00
miR-19b-3p	17.46	2.57	3.56	0.00	0.00
miR-1a	427.80	305.80	2478.36	2504.79	2974.56
miR-1a-3p	1468.13	889.89	5984.37	6912.20	7719.75
miR-1b	351.79	234.34	1765.33	1879.12	2176.96
miR-1b-3p	276.37	163.13	1052.66	1253.46	1383.74
miR-1b-5p	350.76	234.09	1763.55	1878.71	2176.91
miR-1c	273.24	161.92	1047.90	1248.68	1381.25
miR-1c-3p	282.19	164.24	1056.28	1257.60	1385.14
miR-1c-5p	282.19	164.24	1056.28	1257.60	1385.14
miR-2	0.69	0.00	0.00	0.00	1.15
miR-20	7.44	0.81	182.72	0.00	0.00
miR-200	4.48	0.57	1.59	3.53	1.65
miR-200-3p	4.13	0.52	1.21	3.53	1.55
miR-200a	0.00	0.91	34.57	0.00	0.00
miR-200a-3p	0.00	0.94	35.37	0.00	0.00

miR-200b	4.58	0.72	5.20	3.53	1.65
miR-200b-3p	0.03	0.30	7.15	0.00	0.00
miR-200b-5p	4.48	0.57	1.26	3.53	1.65
miR-201-5p	0.07	0.00	4.66	0.00	0.00
miR-202	0.07	0.05	9.64	0.00	0.00
miR-202-3p	0.00	0.00	28.44	0.00	0.00
miR-202-5p	0.21	0.15	22.49	0.00	0.00
miR-203	0.14	0.76	1.56	0.15	0.00
miR-204	0.00	0.37	14.44	0.00	0.00
miR-204-5p	0.00	0.25	9.59	0.00	0.00
miR-204a	0.00	0.05	1.92	0.00	0.00
miR-205	29.24	31.71	18.14	10.88	10.37
miR-205-5p	5.65	6.02	3.51	2.09	2.00
miR-205a	5.65	6.12	3.51	2.09	2.00
miR-205a-5p	2.82	3.31	1.75	1.05	1.00
miR-205b-5p	1.41	1.53	0.88	0.52	0.50
miR-206	4.13	0.42	8.22	7.62	6.98
miR-206-3p	1.45	0.15	2.88	2.67	2.44
miR-20a	9.26	0.99	218.39	0.00	0.00
miR-20a-5p	26.14	2.74	565.20	0.00	0.00
miR-21	7.75	93.94	76.87	1.64	1.10
miR-210	0.14	0.15	0.96	0.95	2.89
miR-210-3p	0.00	0.15	0.96	1.08	1.10
miR-21-3p	0.10	0.35	1.07	0.00	0.00
miR-21-5p	8.99	108.40	90.24	1.94	1.30
miR-218	1.03	0.00	6.27	0.00	0.00
miR-218-5p	0.83	0.00	5.26	0.00	0.00
miR-218a	0.55	0.00	3.94	0.00	0.00
miR-218b	0.14	0.00	1.21	0.00	0.00
miR-219	3819.86	81.63	23.39	53.50	67.88
miR-219-5p	1936.60	43.38	10.33	25.31	29.78
miR-219a	204.70	4.54	1.01	2.78	3.34
miR-219a-5p	406.17	9.43	2.03	4.95	5.39
miR-219b	1.48	0.02	0.22	0.62	1.15
miR-219b-3p	177.43	4.34	0.71	1.94	1.80
miR-219b-5p	140.44	2.91	0.96	2.03	2.69
miR-219c-5p	140.44	2.91	0.96	2.03	2.69
miR-21a-5p	0.65	7.23	6.90	0.15	0.10
miR-22	54.48	29.12	4831.33	6.38	5.49
miR-221	4.13	21.66	1.21	1.68	0.00
miR-221-3p	4.41	23.15	1.37	1.79	0.00
miR-221-5p	0.28	1.36	0.05	0.11	0.00
miR-223	0.00	1.33	3.04	0.00	0.00

miR-223-3p	0.00	0.44	1.07	0.00	0.00
miR-22-3p	38.67	20.95	3350.65	4.67	4.79
miR-22-5p	0.83	0.00	5.94	0.00	0.00
miR-22a	4.17	2.32	374.87	0.49	0.40
miR-22a-3p	0.00	0.05	1.70	0.00	0.00
miR-22b	4.30	2.22	374.76	0.49	0.40
miR-22b-3p	0.07	0.00	1.64	0.00	0.00
miR-23-3p	0.10	0.00	1.01	0.00	0.00
miR-236	1036.68	656.41	156.97	142.81	86.88
miR-236-3p	252.78	224.35	14.79	4.63	2.99
miR-23a	11.02	2.66	27.45	5.53	5.99
miR-23a-3p	5.44	1.23	13.53	2.52	2.74
miR-23b	1.62	0.00	23.56	0.02	0.00
miR-23b-3p	1.34	0.00	16.14	0.00	0.00
miR-24	1.24	1.11	20.96	0.00	0.00
miR-24-3p	2.24	2.02	37.37	0.00	0.00
miR-2478	0.38	2.62	0.41	0.00	0.15
miR-24a	0.14	0.12	2.33	0.00	0.00
miR-24a-3p	0.17	0.17	2.44	0.00	0.00
miR-25	8.78	11.77	18.16	0.00	0.00
miR-25-3p	4.13	5.53	8.55	0.00	0.00
miR-26	1.45	2.05	109.36	0.04	0.00
miR-263a	1.31	0.44	2.19	1.49	3.19
miR-263a-5p	0.76	0.22	1.42	0.99	3.79
miR-26-5p	1.76	2.34	123.30	0.06	0.00
miR-26a	7.30	8.86	509.13	0.26	0.00
miR-26a-5p	4.79	5.82	338.02	0.17	0.00
miR-26b	0.14	3.04	106.51	0.26	0.35
miR-26b-5p	0.14	3.04	105.72	0.26	0.35
miR-26c	1.03	1.23	72.46	0.04	0.00
miR-27-3p	0.14	0.64	5.48	0.04	0.00
miR-275	1.86	0.89	3.45	0.00	2.69
miR-276	2.58	6.00	0.05	0.13	5.84
miR-276-3p	1.79	4.47	0.16	0.09	2.59
miR-276-5p	0.55	0.22	0.00	0.45	8.88
miR-276a	2.76	6.71	0.00	0.00	3.19
miR-276a-3p	1.38	3.36	0.00	0.00	1.60
miR-276a-5p	0.52	0.22	0.00	0.39	8.83
miR-276b-5p	0.52	0.22	0.00	0.39	8.83
miR-277	1.83	0.94	0.00	0.71	0.00
miR-277a	67.57	28.25	15.51	22.14	22.39
miR-277c-3p	30.51	26.45	12.22	14.90	17.91
miR-278	1.34	0.64	0.00	0.00	0.00

miR-279	1.34	3.04	0.00	0.00	2.29
miR-279a	0.10	1.38	0.00	0.00	0.65
miR-27a	0.59	1.68	9.94	0.00	0.00
miR-27a-3p	0.55	1.38	8.66	0.00	0.00
miR-27b	1.65	7.80	65.77	0.45	0.00
miR-27b-3p	2.20	10.34	87.66	0.60	0.00
miR-27d	0.00	0.15	3.94	0.00	0.00
miR-28	0.00	0.02	12.16	0.00	0.00
miR-281	116.16	144.30	424.89	116.97	89.03
miR-281-2-5p	1.03	0.49	0.00	0.00	1.00
miR-281-3p	6.65	0.47	1.34	0.82	1.65
miR-281a	0.72	0.39	4.05	1.40	0.65
miR-282	3.79	0.00	0.00	0.00	0.00
miR-28-5p	0.00	0.00	8.44	0.00	0.00
miR-28a-5p	0.00	0.00	1.21	0.00	0.00
miR-29	0.00	0.00	4.55	0.00	0.00
miR-296	0.38	0.00	2.44	0.00	0.00
miR-296-3p	1.89	0.00	10.60	0.00	0.00
miR-296-5p	2.76	0.00	0.82	0.00	0.00
miR-298-5p	0.38	0.00	1.78	0.00	0.00
miR-29a	14.46	2.10	514.22	1.64	0.00
miR-29a-3p	7.34	1.09	262.88	0.71	0.00
miR-29b	12.57	3.43	2833.50	2.09	0.00
miR-29b-3p	11.81	3.08	2547.77	2.20	0.00
miR-29c	3.00	0.17	158.48	1.01	0.00
miR-29c-3p	1.38	0.00	26.98	0.45	0.00
miR-29c-5p	0.14	0.00	1.10	0.00	0.00
miR-2a	4.58	6.39	0.38	0.71	4.14
miR-2a-3p	1.76	0.64	0.11	0.30	0.95
miR-2b	9.02	3.31	0.16	2.17	16.56
miR-2b-3p	1165.24	4136.35	36.00	217.50	176.11
miR-2c	0.41	0.00	0.00	0.09	1.15
miR-2c-3p	32.51	15.94	96.87	99.83	101.95
miR-301-3p	0.41	0.15	1.23	0.00	0.00
miR-301a	0.86	0.30	2.68	0.00	0.00
miR-301a-3p	1.10	0.39	3.29	0.00	0.00
miR-304	6.51	0.00	0.00	0.00	1.35
miR-305	10.88	1.58	0.00	0.00	20.75
miR-305-5p	3.10	0.54	0.00	0.00	6.28
miR-3068-5p	0.00	0.00	1.81	0.00	0.00
miR-308	0.34	0.00	0.00	0.00	1.50
miR-30a	0.48	0.05	6.60	0.00	0.00
miR-30a-3p	1.65	0.07	51.42	0.00	0.00

miR-30a-5p	6.58	1.14	46.79	0.00	0.00
miR-30b	13.88	0.44	28.33	0.00	0.00
miR-30b-3p	0.07	0.00	2.25	0.00	0.00
miR-30b-5p	20.08	0.74	47.37	0.00	0.00
miR-30c	1.00	0.00	1.07	0.00	0.00
miR-30c-3p	0.31	0.00	3.75	0.00	0.00
miR-30c-5p	1.14	0.10	3.64	0.00	0.00
miR-30d	4.96	0.49	33.17	0.00	0.00
miR-30d-3p	0.10	0.00	4.49	0.00	0.00
miR-30d-5p	3.31	0.42	24.85	0.00	0.00
miR-30e	2.27	0.69	22.66	0.00	0.00
miR-30e-3p	0.41	0.59	41.64	0.00	0.00
miR-30e-5p	3.34	1.16	23.09	0.00	0.00
miR-31	3.62	0.44	7.31	1.64	0.55
miR-312-3p	0.03	0.02	0.00	0.00	1.30
miR-313-5p	0.00	0.00	0.00	0.00	1.10
miR-314	3.79	0.00	0.00	0.00	0.00
miR-31-5p	5.51	0.62	9.37	2.58	0.70
miR-317	7.06	0.54	1.04	1.06	0.00
miR-317-3p	1.86	0.15	0.33	0.34	0.00
miR-318	5.30	1.09	0.00	0.00	6.03
miR-3184-3p	0.03	0.05	1.29	0.02	0.00
miR-31a	2.69	0.10	1.48	0.45	1.10
miR-320	0.62	8.88	6.57	1.68	1.15
miR-320-3p	0.62	8.88	6.41	1.68	1.05
miR-320a	1.45	20.73	14.96	3.92	2.44
miR-320b	0.83	11.35	4.82	2.24	1.40
miR-322-5p	0.07	0.05	16.66	0.00	0.00
miR-324	0.34	0.00	19.70	0.00	0.00
miR-324-5p	0.86	0.00	51.47	0.00	0.00
miR-328	1.10	0.00	15.56	0.00	0.00
miR-328-3p	0.41	0.00	5.84	0.00	0.00
miR-328a-3p	0.14	0.00	1.95	0.00	0.00
miR-33	15.70	1.11	5.73	1.23	0.95
miR-335	0.00	0.00	2.47	0.00	0.00
miR-335-5p	0.00	0.00	1.31	0.00	0.00
miR-33-5p	22.32	1.73	7.89	2.09	1.85
miR-338	0.00	0.69	3.07	0.00	0.00
miR-338-3p	0.00	0.39	2.08	0.00	0.00
miR-339	0.52	0.00	4.93	0.00	0.00
miR-339-5p	1.45	0.00	15.45	0.00	0.00
miR-339a	0.24	0.00	2.03	0.00	0.00
miR-339b	0.17	0.00	1.15	0.00	0.00

miR-33a	5.92	0.42	2.14	0.47	0.30
miR-33a-5p	7.99	0.57	2.93	0.63	0.55
miR-33b	3.48	0.00	0.00	0.00	0.05
miR-33b-5p	1.52	0.10	0.58	0.09	0.10
miR-34	25.28	2.94	21.56	8.64	35.66
miR-340	0.28	0.52	12.14	0.00	0.00
miR-340-5p	0.48	0.86	20.14	0.00	0.00
miR-342	0.21	0.00	17.42	0.00	0.00
miR-342-3p	0.31	0.00	33.20	0.00	0.00
miR-34-5p	12.88	1.55	0.68	4.72	18.70
miR-3473b	0.17	0.00	17.72	0.06	0.00
miR-34a	4.06	1.51	394.86	0.00	0.00
miR-34a-5p	41.02	1.92	378.04	0.58	2.04
miR-34b	40.84	0.96	196.72	0.09	0.00
miR-34b-3p	5.68	0.00	6.52	0.00	0.00
miR-34b-5p	92.12	0.07	154.59	0.00	0.00
miR-34c	109.93	2.89	549.34	0.28	0.00
miR-34c-3p	0.72	0.00	1.15	0.00	0.00
miR-34c-5p	356.55	9.62	1742.35	0.93	0.00
miR-351-5p	0.00	0.00	3.45	0.00	0.00
miR-3529-3p	0.17	0.62	2.33	0.00	0.55
miR-3571	111.75	23.22	199.73	118.48	139.00
miR-3586-3p	0.69	0.07	18.38	0.00	0.00
miR-3587	0.07	0.02	20.68	0.26	0.00
miR-3588	0.48	0.05	11.04	0.00	0.05
miR-3591-3p	0.00	4.61	0.00	0.00	0.00
miR-3596	0.38	0.91	65.64	0.56	0.20
miR-3596a	1.52	1.11	82.54	0.26	3.04
miR-3596c	0.00	0.02	2.79	0.00	0.00
miR-3596d	0.03	0.05	5.18	0.00	0.00
miR-3600	4.17	2.22	371.47	0.49	0.40
miR-3604	0.03	0.22	5.78	0.00	0.00
miR-362-5p	0.28	0.00	1.75	0.00	0.00
miR-369-3p	0.00	1.63	0.00	0.00	0.00
miR-374b-5p	0.00	0.30	1.12	0.00	0.00
miR-375	1425.91	3679.76	1582.53	1586.77	1007.33
miR-375-3p	657.99	1688.06	811.48	784.88	441.55
miR-375a-3p	80.04	207.17	85.31	88.45	55.66
miR-375b-3p	79.66	207.05	85.17	88.39	55.66
miR-378	0.17	0.89	1.29	0.00	0.00
miR-379	0.00	0.00	1.53	0.00	0.00
miR-379-5p	0.00	0.00	1.15	0.00	0.00
miR-380-3p	0.00	1.41	0.00	0.00	0.00

miR395	0.00	0.00	1.89	0.00	0.00
miR395a	0.00	0.00	8.19	0.00	0.00
miR395b	0.00	0.00	7.56	0.00	0.00
miR395c	0.00	0.00	6.93	0.00	0.00
miR395d	0.00	0.00	6.36	0.00	0.00
miR395d-3p	0.00	0.00	1.26	0.00	0.00
miR395e	0.00	0.00	5.10	0.00	0.00
miR395f	0.00	0.00	3.84	0.00	0.00
miR395g	0.00	0.00	3.21	0.00	0.00
miR395h	0.00	0.00	3.21	0.00	0.00
miR395i	0.00	0.00	3.15	0.00	0.00
miR395j	0.00	0.00	2.52	0.00	0.00
miR395k	0.00	0.00	1.89	0.00	0.00
miR395l	0.00	0.00	1.26	0.00	0.00
miR395m	0.00	0.00	1.26	0.00	0.00
miR396	0.00	1.78	0.41	0.00	0.00
miR396a	0.00	2.02	0.27	0.00	0.00
miR396a-5p	0.00	1.28	0.27	0.00	0.00
miR396b	0.00	3.58	1.10	0.00	0.00
miR396b-5p	0.00	1.31	0.41	0.00	0.00
miR396c	0.00	3.13	1.23	0.00	0.00
miR396d	0.00	1.46	0.55	0.00	0.00
miR396e	0.00	1.73	0.68	0.00	0.00
miR396e-5p	0.00	1.09	0.41	0.00	0.00
miR403a	0.00	1.58	0.79	0.34	0.00
miR403b	0.00	1.23	0.63	0.26	0.00
miR-423	0.10	0.07	1.73	0.04	0.00
miR-423-3p	0.76	0.27	1.81	0.00	0.00
miR-423-5p	0.34	0.49	12.88	0.19	0.00
miR-423a	0.03	0.05	1.29	0.02	0.00
miR-424	0.00	0.00	3.29	0.00	0.00
miR-424-5p	0.00	0.00	3.94	0.00	0.00
miR-425	3.58	0.20	16.00	0.00	0.00
miR-425-3p	0.00	0.00	1.10	0.00	0.00
miR-425-5p	8.95	0.49	40.08	0.00	0.00
miR-429	0.00	0.00	16.44	0.00	0.00
miR-429-3p	0.00	0.00	7.81	0.00	0.00
miR-429a	0.00	0.00	2.11	0.00	0.00
miR-4334-3p	0.17	0.00	1.15	0.00	0.00
miR-449	7.03	0.10	60.90	0.00	0.00
miR-449a	34.65	0.49	311.09	0.00	0.00
miR-449a-5p	27.79	0.39	247.43	0.00	0.00
miR-450a	0.00	0.00	2.55	0.00	0.00

miR-450a-5p	0.00	0.00	1.70	0.00	0.00
miR-451	1.93	1.38	10.57	0.00	0.20
miR-451-??	0.24	0.17	1.40	0.00	0.05
miR-451-5p	0.28	0.20	1.42	0.00	0.00
miR-451a	0.28	0.20	1.42	0.00	0.00
miR-465a-3p	0.38	0.00	2.16	0.00	0.00
miR-465a-5p	0.21	0.00	3.29	0.00	0.00
miR-465b-3p	0.38	0.00	2.16	0.00	0.00
miR-465b-5p	0.07	0.07	1.40	0.00	0.00
miR-465c-3p	0.38	0.00	2.16	0.00	0.00
miR-465c-5p	0.38	0.10	12.52	0.00	0.00
miR-466i-5p	1.31	0.22	1.29	0.80	1.75
miR-467e-5p	0.24	0.00	3.04	0.00	0.00
miR-470-5p	0.10	0.12	14.27	0.00	0.00
miR-471-5p	0.28	0.00	3.62	0.00	0.00
miR-497	1.45	0.00	6.93	0.00	0.00
miR-497-5p	1.24	0.00	5.34	0.00	0.00
miR-497a-5p	0.31	0.00	1.01	0.00	0.00
miR-499	0.00	0.30	1.81	0.00	0.00
miR-499-5p	0.00	0.59	3.62	0.00	0.00
miR-500-3p	0.00	0.00	2.36	0.00	0.00
miR-501-3p	0.00	0.00	1.64	0.00	0.00
miR-503	0.07	0.00	14.55	0.00	0.00
miR-503-5p	0.07	0.00	14.55	0.00	0.00
miR-511-3p	0.00	0.00	1.04	0.00	0.00
miR-532	0.03	0.00	2.63	0.00	0.05
miR-532-3p	0.28	0.00	1.48	0.00	0.40
miR-532-5p	0.00	0.00	6.90	0.00	0.00
miR-547-3p	0.00	0.00	2.27	0.00	0.00
miR5658	3.38	3.60	0.71	5.10	2.09
miR-652	0.00	0.20	16.22	0.75	0.40
miR-652-3p	0.00	0.12	10.11	0.47	0.25
miR-669c-5p	0.00	0.02	1.07	0.00	0.00
miR-672	0.07	0.00	5.86	0.00	0.00
miR-672-5p	0.07	0.00	5.86	0.00	0.00
miR-674-5p	0.00	0.00	2.41	0.00	0.00
miR-7	6.92	12.21	31.04	0.00	4.34
miR-708	0.00	0.00	1.51	0.00	0.00
miR-708-5p	0.00	0.00	1.92	0.00	0.00
miR-71	263342.35	79755.92	103297.86	250059.68	190127.93
miR-71-5p	217919.72	43457.20	81683.87	201079.56	166888.04
miR-71a-5p	52.93	2.71	8.46	20.96	13.87
miR-71c-5p	32675.80	5179.45	10848.90	28103.60	24600.30

miR-72	11.16	0.44	13.70	3.36	1.30
miR-72-5p	17.22	0.72	21.29	5.26	2.00
miR-72a	0.00	0.05	1.12	0.13	0.05
miR-741-3p	0.48	0.02	18.98	0.00	0.00
miR-743a-3p	0.45	0.00	10.82	0.00	0.00
miR-743b-3p	0.14	0.00	1.07	0.00	0.00
miR-744	0.00	0.00	5.89	0.00	0.00
miR-744-5p	0.00	0.00	2.99	0.00	0.00
miR-7-5p	2.89	6.64	20.35	0.00	3.84
miR-79	0.76	0.00	0.00	0.17	14.91
miR-79-3p	0.28	0.00	0.08	0.13	8.58
miR-7a	0.86	2.05	6.47	0.00	1.25
miR-7a-5p	0.69	1.09	2.41	0.00	0.20
miR-7b	0.45	0.64	2.77	0.02	0.55
miR-7c	0.17	0.62	2.33	0.00	0.55
miR-8	61436.45	11024.57	17462.96	45754.43	29461.97
miR-8-3p	121.74	15.52	30.33	133.75	145.69
miR-8-5p	0.48	0.17	0.00	0.78	7.33
miR-871-5p	0.28	0.00	4.96	0.00	0.00
miR-872-5p	0.52	0.00	1.48	0.00	0.00
miR-878-3p	0.17	0.00	1.07	0.00	0.00
miR-878-5p	0.00	0.00	1.34	0.00	0.00
miR-880-3p	0.38	0.00	6.93	0.00	0.00
miR-881-3p	0.45	0.22	1.26	0.00	0.00
miR-9	2.03	0.81	7.12	1.03	2.89
miR-92	18.94	35.36	59.97	0.00	0.05
miR-92-3p	1.93	3.68	5.62	0.00	0.10
miR-92a	16.67	31.29	49.61	0.00	0.65
miR-92a-3p	18.05	33.24	54.90	0.00	0.10
miR-92b	3.00	9.77	6.99	0.00	1.45
miR-92b-3p	1.03	2.37	1.64	0.00	0.75
miR-93	4.17	0.79	27.39	0.00	0.00
miR-93-3p	0.00	0.00	1.37	0.00	0.00
miR-93-5p	6.89	1.33	40.22	0.00	0.00
miR-9-5p	2.86	1.21	10.60	1.49	5.19
miR-970	0.21	0.15	0.00	0.00	1.65
miR-970-3p	0.34	0.25	0.00	0.00	2.74
miR-98	0.00	0.32	69.80	0.00	0.00
miR-98-5p	0.00	0.15	35.23	0.00	0.00
miR-989	0.96	0.67	0.00	0.00	15.46
miR-989-3p	0.34	0.54	0.00	0.00	10.67
miR-989a	0.07	0.12	0.00	0.00	3.29
miR-99	0.38	0.07	76.16	0.00	0.00

miR-993	26.93	6.17	103.11	7.95	34.31
miR-993-3p	0.52	0.00	1.23	0.09	0.75
miR-993a-3p	14.98	3.16	51.47	4.11	16.86
miR-993b-3p	18.29	0.05	0.22	0.04	0.10
miR-994-5p	0.21	0.00	0.00	0.00	6.43
miR-995-3p	0.10	0.10	0.00	0.00	7.73
miR-99-5p	0.24	0.07	72.35	0.00	0.00
miR-996-3p	0.83	0.00	0.00	0.02	2.44
miR-99a	1.76	0.27	290.77	0.00	0.00
miR-99a-3p	0.00	0.00	1.04	0.00	0.30
miR-99a-5p	1.48	0.27	281.78	0.00	0.00
miR-99b	0.17	0.32	45.28	0.00	0.00
miR-99b-5p	0.00	0.30	19.83	0.00	0.00
miR-9a	3.10	1.33	9.37	1.34	3.59
miR-9a-5p	81.41	42.32	71.97	25.85	17.61
miR-9b	36.13	5.16	26.71	13.50	52.97
miR-9b-5p	0.76	0.62	1.81	0.26	10.32
miR-9c	0.34	0.99	0.00	0.00	8.98
miR-9c-5p	0.10	0.30	0.00	0.00	2.69
miR-iab-4-3p	1.65	0.00	0.00	0.00	0.00

Supplementary Table 2 List of piRNA clusters across the *M. lignano* genome assembly.

Contig ID	Start	End	Length
unitig_26198	567	8586	8019
unitig_26950	2173	8693	6520
unitig_29363	5564	12590	7026
unitig_37027	2358	9065	6707
uti_cns_0000018	10	22253	22243
uti_cns_0000046	189620	195217	5597
uti_cns_0000063	45527	80217	34690
uti_cns_0000063	87038	96526	9488
uti_cns_0000106	99886	106341	6455
uti_cns_0000109	235064	246616	11552
uti_cns_0000109	252387	279494	27107
uti_cns_0000109	293043	340413	47370
uti_cns_0000136	2286	13271	10985
uti_cns_0000149	264143	286066	21923
uti_cns_0000149	292034	299797	7763
uti_cns_0000149	307289	324944	17655
uti_cns_0000184	59008	105411	46403
uti_cns_0000184	117018	125733	8715
uti_cns_0000184	133517	140248	6731

uti_cns_0000190	24179	31944	7765
uti_cns_0000197	29045	43383	14338
uti_cns_0000197	58193	66033	7840
uti_cns_0000205	305584	316238	10654
uti_cns_0000206	39045	56095	17050
uti_cns_0000206	62880	78353	15473
uti_cns_0000206	84142	90813	6671
uti_cns_0000217	195393	222398	27005
uti_cns_0000233	46448	72415	25967
uti_cns_0000233	78329	116027	37698
uti_cns_0000240	29543	34800	5257
uti_cns_0000242	129611	135360	5749
uti_cns_0000242	163464	173062	9598
uti_cns_0000244	100700	116763	16063
uti_cns_0000244	127819	156640	28821
uti_cns_0000276	158589	193344	34755
uti_cns_0000276	205363	213621	8258
uti_cns_0000276	219509	227207	7698
uti_cns_0000276	239838	304381	64543
uti_cns_0000297	151852	164093	12241
uti_cns_0000297	188618	223399	34781
uti_cns_0000308	71787	91662	19875
uti_cns_0000308	170226	178912	8686
uti_cns_0000308	196373	213716	17343
uti_cns_0000314	52330	59016	6686
uti_cns_0000360	44918	53977	9059
uti_cns_0000371	92835	118007	25172
uti_cns_0000371	126732	134444	7712
uti_cns_0000395	149355	165321	15966
uti_cns_0000395	201641	215616	13975
uti_cns_0000419	52262	63802	11540
uti_cns_0000419	79299	86786	7487
uti_cns_0000419	96700	110119	13419
uti_cns_0000419	120882	129608	8726
uti_cns_0000419	137260	147453	10193
uti_cns_0000419	161702	175782	14080
uti_cns_0000502	177930	234986	57056
uti_cns_0000502	241754	254348	12594
uti_cns_0000503	1981	17098	15117
uti_cns_0000517	212828	219529	6701
uti_cns_0000518	68936	79314	10378
uti_cns_0000518	88090	117942	29852
uti_cns_0000518	136592	165386	28794

uti_cns_0000527	93070	98607	5537
uti_cns_0000527	126775	220508	93733
uti_cns_0000588	194461	229012	34551
uti_cns_0000593	151853	161375	9522
uti_cns_0000597	43637	49291	5654
uti_cns_0000614	176971	206000	29029
uti_cns_0000633	44646	50206	5560
uti_cns_0000633	74469	99389	24920
uti_cns_0000636	6783	13497	6714
uti_cns_0000655	33922	55788	21866
uti_cns_0000655	71116	92727	21611
uti_cns_0000660	1	5818	5817
uti_cns_0000661	60939	92845	31906
uti_cns_0000662	183762	228073	44311
uti_cns_0000662	237170	245620	8450
uti_cns_0000694	27525	34634	7109
uti_cns_0000694	44482	60408	15926
uti_cns_0000722	34876	40626	5750
uti_cns_0000722	65814	88812	22998
uti_cns_0000722	94786	115893	21107
uti_cns_0000722	123000	129594	6594
uti_cns_0000750	24248	30924	6676
uti_cns_0000762	1179	25168	23989
uti_cns_0000768	73856	79276	5420
uti_cns_0000768	87050	139278	52228
uti_cns_0000788	49339	59690	10351
uti_cns_0000788	68794	80868	12074
uti_cns_0000788	87235	100593	13358
uti_cns_0000814	114132	154735	40603
uti_cns_0000814	161492	185479	23987
uti_cns_0000852	19425	25049	5624
uti_cns_0000867	47415	83162	35747
uti_cns_0000867	90939	96622	5683
uti_cns_0000867	111302	117944	6642
uti_cns_0000887	52373	79327	26954
uti_cns_0000905	25520	32882	7362
uti_cns_0000908	77945	99585	21640
uti_cns_0000908	106676	139267	32591
uti_cns_0000941	88147	104274	16127
uti_cns_0000941	120901	129419	8518
uti_cns_0000941	135418	149772	14354
uti_cns_0000941	155702	177870	22168
uti_cns_0000959	4911	10477	5566

uti_cns_0000984	33847	43547	9700
uti_cns_0000984	88064	121869	33805
uti_cns_0000984	148939	156526	7587
uti_cns_0001056	12081	26647	14566
uti_cns_0001056	33080	50267	17187
uti_cns_0001088	65020	77374	12354
uti_cns_0001095	48445	55151	6706
uti_cns_0001157	77546	85112	7566
uti_cns_0001160	39761	59019	19258
uti_cns_0001160	101648	129245	27597
uti_cns_0001163	89931	98606	8675
uti_cns_0001163	115078	157633	42555
uti_cns_0001186	13539	57064	43525
uti_cns_0001186	73515	84119	10604
uti_cns_0001217	23211	29019	5808
uti_cns_0001217	42817	51209	8392
uti_cns_0001217	78381	85113	6732
uti_cns_0001217	91910	104464	12554
uti_cns_0001217	128660	139280	10620
uti_cns_0001217	146987	154732	7745
uti_cns_0001247	74785	81244	6459
uti_cns_0001264	9603	20086	10483
uti_cns_0001292	60941	66756	5815
uti_cns_0001298	10006	16402	6396
uti_cns_0001332	29235	35291	6056
uti_cns_0001340	40738	48367	7629
uti_cns_0001345	32070	38705	6635
uti_cns_0001389	70591	76398	5807
uti_cns_0001389	103526	111167	7641
uti_cns_0001393	34812	41594	6782
uti_cns_0001393	49333	58022	8689
uti_cns_0001397	19351	42555	23204
uti_cns_0001397	81266	90898	9632
uti_cns_0001397	105433	118891	13458
uti_cns_0001418	85132	109967	24835
uti_cns_0001437	25166	36707	11541
uti_cns_0001465	9809	22208	12399
uti_cns_0001465	59988	78267	18279
uti_cns_0001465	89050	105356	16306
uti_cns_0001465	119059	136379	17320
uti_cns_0001492	76402	97679	21277
uti_cns_0001503	35025	45289	10264
uti_cns_0001544	35814	61913	26099

uti_cns_0001544	78381	129537	51156
uti_cns_0001551	60613	130267	69654
uti_cns_0001554	54598	59957	5359
uti_cns_0001554	106373	115996	9623
uti_cns_0001554	121862	155561	33699
uti_cns_0001558	25197	40468	15271
uti_cns_0001558	89174	102524	13350
uti_cns_0001558	114433	124774	10341
uti_cns_0001558	131636	144099	12463
uti_cns_0001570	17604	31939	14335
uti_cns_0001593	17406	22916	5510
uti_cns_0001598	70636	78352	7716
uti_cns_0001611	8129	29993	21864
uti_cns_0001611	37120	42501	5381
uti_cns_0001611	51252	78357	27105
uti_cns_0001623	15893	21266	5373
uti_cns_0001623	27078	53201	26123
uti_cns_0001632	7845	13013	5168
uti_cns_0001738	28099	72473	44374
uti_cns_0001739	68971	75439	6468
uti_cns_0001768	16575	22273	5698
uti_cns_0001802	78334	88029	9695
uti_cns_0001811	7166	16293	9127
uti_cns_0001837	7767	57057	49290
uti_cns_0001852	133473	146021	12548
uti_cns_0001879	29065	48255	19190
uti_cns_0001879	56528	137083	80555
uti_cns_0001902	55234	63509	8275
uti_cns_0001948	10204	41557	31353
uti_cns_0001948	52420	67677	15257
uti_cns_0001982	30958	37350	6392
uti_cns_0002022	24186	45469	21283
uti_cns_0002037	41630	47321	5691
uti_cns_0002038	27135	39671	12536
uti_cns_0002125	13555	20334	6779
uti_cns_0002138	18501	48339	29838
uti_cns_0002228	10792	16435	5643
uti_cns_0002230	13538	54732	41194
uti_cns_0002230	76396	95623	19227
uti_cns_0002305	98649	112167	13518
uti_cns_0002305	144347	150792	6445
uti_cns_0002307	21352	28001	6649
uti_cns_0002323	75471	82154	6683

uti_cns_0002391	31912	40550	8638
uti_cns_0002410	82287	104456	22169
uti_cns_0002412	18537	24645	6108
uti_cns_0002505	13734	19359	5625
uti_cns_0002521	22241	34823	12582
uti_cns_0002538	39170	47277	8107
uti_cns_0002585	32905	39677	6772
uti_cns_0002598	24414	41542	17128
uti_cns_0002598	82295	101543	19248
uti_cns_0002598	111246	117040	5794
uti_cns_0002604	95770	104445	8675
uti_cns_0002604	115151	127650	12499
uti_cns_0002613	90916	96098	5182
uti_cns_0002622	24218	32882	8664
uti_cns_0002629	43532	49301	5769
uti_cns_0002641	15481	21296	5815
uti_cns_0002665	89005	103370	14365
uti_cns_0002740	31063	36756	5693
uti_cns_0002749	35114	74377	39263
uti_cns_0002749	80264	103449	23185
uti_cns_0002749	114542	122746	8204
uti_cns_0002749	143134	148897	5763
uti_cns_0002752	95745	102510	6765
uti_cns_0002757	22277	31934	9657
uti_cns_0002846	18393	30977	12584
uti_cns_0002857	71567	78296	6729
uti_cns_0002864	108494	117994	9500
uti_cns_0002876	19522	58053	38531
uti_cns_0002876	64446	76079	11633
uti_cns_0002943	25155	31942	6787
uti_cns_0002960	30980	42353	11373
uti_cns_0002964	68853	122742	53889
uti_cns_0002992	85200	92575	7375
uti_cns_0003072	93820	105330	11510
uti_cns_0003076	24269	32825	8556
uti_cns_0003076	41614	49224	7610
uti_cns_0003076	55354	89923	34569
uti_cns_0003100	19348	33811	14463
uti_cns_0003124	19369	33878	14509
uti_cns_0003124	57057	69446	12389
uti_cns_0003124	82398	87883	5485
uti_cns_0003152	80292	91865	11573
uti_cns_0003233	37716	57084	19368

uti_cns_0003233	64067	75452	11385
uti_cns_0003233	93922	110078	16156
uti_cns_0003243	82230	88985	6755
uti_cns_0003254	33864	60942	27078
uti_cns_0003254	70604	113170	42566
uti_cns_0003257	27124	40593	13469
uti_cns_0003269	6776	14380	7604
uti_cns_0003387	71642	84111	12469
uti_cns_0003393	5867	76231	70364
uti_cns_0003414	20308	32326	12018
uti_cns_0003572	22255	32872	10617
uti_cns_0003584	119088	126589	7501
uti_cns_0003625	20336	29736	9400
uti_cns_0003645	92420	103498	11078
uti_cns_0003645	109329	117941	8612
uti_cns_0003729	47433	93790	46357
uti_cns_0003729	103471	110271	6800
uti_cns_0003852	34892	43437	8545
uti_cns_0003919	59043	69577	10534
uti_cns_0003931	13538	22271	8733
uti_cns_0003944	13605	40531	26926
uti_cns_0003944	50343	59018	8675
uti_cns_0003944	73497	91587	18090
uti_cns_0003944	107351	116053	8702
uti_cns_0003966	17412	28055	10643
uti_cns_0003966	35780	68489	32709
uti_cns_0003973	85541	90926	5385
uti_cns_0003974	16447	24884	8437
uti_cns_0004010	80389	87032	6643
uti_cns_0004094	28416	76379	47963
uti_cns_0004101	73626	82130	8504
uti_cns_0004150	58205	66723	8518
uti_cns_0004208	96785	104186	7401
uti_cns_0004296	12188	53640	41452
uti_cns_0004323	58991	70618	11627
uti_cns_0004356	33013	42578	9565
uti_cns_0004471	89246	97371	8125
uti_cns_0004531	39818	53214	13396
uti_cns_0004671	15532	23241	7709
uti_cns_0004685	23225	36208	12983
uti_cns_0004691	11620	42400	30780
uti_cns_0004691	50640	66713	16073
uti_cns_0004711	31937	38712	6775

uti_cns_0004711	46464	59785	13321
uti_cns_0004817	22275	39667	17392
uti_cns_0004890	37345	47896	10551
uti_cns_0004891	42613	51131	8518
uti_cns_0005008	12683	26142	13459
uti_cns_0005147	64031	74402	10371
uti_cns_0005215	22344	31924	9580
uti_cns_0005223	67982	77101	9119
uti_cns_0005358	23220	29027	5807
uti_cns_0005367	15783	25097	9314
uti_cns_0005371	38748	48231	9483
uti_cns_0005376	50390	61608	11218
uti_cns_0005442	32881	38633	5752
uti_cns_0005656	52305	60820	8515
uti_cns_0005911	9734	15483	5749
uti_cns_0005936	12610	18221	5611
uti_cns_0005956	61107	66725	5618
uti_cns_0005987	46595	64611	18016
uti_cns_0006064	29085	37640	8555
uti_cns_0006513	36779	44447	7668
uti_cns_0006921	5839	11637	5798
uti_cns_0007054	23224	30775	7551
uti_cns_0007227	7874	13552	5678
uti_cns_0007235	44742	52247	7505
uti_cns_0007245	38019	49288	11269
uti_cns_0007386	11669	18228	6559
uti_cns_0007416	38705	45475	6770
uti_cns_0007471	37717	43465	5748
uti_cns_0007471	55361	63526	8165
uti_cns_0007710	32933	43546	10613
uti_cns_0007796	27123	41582	14459
uti_cns_0007853	21398	28741	7343
uti_cns_0007895	30119	37158	7039
uti_cns_0007934	23215	33584	10369
uti_cns_0007972	42553	52220	9667
uti_cns_0008181	22270	27905	5635
uti_cns_0008428	5837	37504	31667
uti_cns_0008577	21311	28046	6735
uti_cns_0008638	17868	24052	6184
uti_cns_0009017	36757	45457	8700
uti_cns_0009434	16479	29987	13508
uti_cns_0009825	13130	24095	10965
uti_cns_0010104	15557	23946	8389

uti_cns_0010480	37913	43339	5426
uti_cns_0010502	39714	45431	5717
uti_cns_0010506	46418	52903	6485
uti_cns_0010743	32899	45280	12381
uti_cns_0010761	26254	37692	11438
uti_cns_0010855	14648	20280	5632
uti_cns_0010871	16488	25955	9467
uti_cns_0011446	11980	20292	8312
uti_cns_0011476	18380	25058	6678
uti_cns_0011749	5064	13480	8416
uti_cns_0011932	15492	23226	7734
uti_cns_0012120	13699	19235	5536
uti_cns_0012401	17538	22998	5460
uti_cns_0012479	9671	21880	12209
uti_cns_0012554	2368	8580	6212
uti_cns_0012609	14624	43406	28782
uti_cns_0012777	2034	11596	9562
uti_cns_0013208	16632	23223	6591
uti_cns_0013275	5808	13567	7759
uti_cns_0013750	14544	20945	6401
uti_cns_0013827	43622	51840	8218
uti_cns_0013846	13093	22246	9153
uti_cns_0014133	6434	11607	5173
uti_cns_0014782	13547	20322	6775
uti_cns_0014889	7771	15392	7621
uti_cns_0015551	3033	8708	5675
uti_cns_0045366	103491	110133	6642
uti_cns_0045366	125717	135995	10278
uti_cns_0045367	238859	245623	6764
uti_cns_0045374	21305	27987	6682
uti_cns_0045387	60929	85123	24194
uti_cns_0045388	93875	117015	23140
uti_cns_0045388	170335	187535	17200
uti_cns_0045388	193611	211761	18150
uti_cns_0045388	217575	227238	9663
uti_cns_0045388	243222	258988	15766
uti_cns_0045388	297849	307339	9490
uti_cns_0045390	14785	29022	14237
uti_cns_0045390	61889	122696	60807
uti_cns_0045390	260127	277543	17416
uti_cns_0045390	283334	291093	7759
uti_cns_0045390	305607	313316	7709
uti_cns_0045403	36834	42515	5681

uti_cns_0045431	360714	370046	9332
uti_cns_0045480	19353	29970	10617
uti_cns_0045485	271906	281340	9434
uti_cns_0045486	114109	135402	21293
uti_cns_0045489	130594	140241	9647
uti_cns_0045494	146034	207769	61735
uti_cns_0045611	288232	293824	5592
uti_cns_0045637	12637	54880	42243
uti_cns_0045638	21527	29967	8440
uti_cns_0045654	42615	52047	9432
uti_cns_0045672	25295	39679	14384
uti_cns_0045714	47689	88982	41293
uti_cns_0045714	101611	118697	17086
uti_cns_0045747	94784	100422	5638
uti_cns_0045800	125183	131279	6096
uti_cns_0045843	40665	53023	12358
uti_cns_0045849	120876	173923	53047
uti_cns_0045855	270821	278431	7610
uti_cns_0045977	62867	68682	5815
uti_cns_0045977	77364	86307	8943
uti_cns_0045977	109885	118973	9088
uti_cns_0045981	150991	156508	5517
uti_cns_0045981	162494	173004	10510
uti_cns_0045983	71570	95350	23780
uti_cns_0045983	107406	114138	6732
uti_cns_0045983	126678	139064	12386
uti_cns_0045997	133544	147754	14210
uti_cns_0045997	174060	207864	33804
uti_cns_0046010	226471	233999	7528
uti_cns_0046030	101593	127644	26051
uti_cns_0046030	157623	163439	5816
uti_cns_0046031	18480	82768	64288
uti_cns_0046031	91914	102286	10372
uti_cns_0046031	109687	118959	9272
uti_cns_0046031	128472	134407	5935
uti_cns_0046087	86069	98646	12577
uti_cns_0046118	67386	78322	10936
uti_cns_0046130	142149	200202	58053
uti_cns_0046134	24196	33850	9654
uti_cns_0046145	72546	79305	6759
uti_cns_0046185	18477	27109	8632
uti_cns_0046185	63005	91795	28790
uti_cns_0046236	76450	87892	11442

uti_cns_0046251	74500	84020	9520
uti_cns_0046258	97683	104394	6711
uti_cns_0046287	75474	82136	6662
uti_cns_0046368	83166	90845	7679
uti_cns_0046369	22285	32900	10615
uti_cns_0046481	59132	72495	13363
uti_cns_0046520	65862	71453	5591
uti_cns_0046572	17451	56115	38664
uti_cns_0046572	62868	75447	12579
uti_cns_0046643	65837	72414	6577
uti_cns_0046650	99905	106376	6471
uti_cns_0046814	21325	43530	22205
uti_cns_0046814	51285	60922	9637
uti_cns_0046835	64878	72541	7663
uti_cns_0047112	61164	74442	13278
uti_cns_0047128	29083	38682	9599
uti_cns_0047510	42067	53100	11033
uti_cns_0047575	19343	25148	5805
uti_cns_0047761	40617	60867	20250
uti_cns_0047778	18387	31937	13550
uti_cns_0047809	9670	14742	5072
uti_cns_0047810	37929	60952	23023
uti_cns_0047867	28349	38699	10350
uti_cns_0047952	61997	67465	5468
uti_cns_0047986	69628	75885	6257
uti_cns_0048012	967	11635	10668
uti_cns_0048155	44716	60568	15852
uti_cns_0048232	4973	12479	7506
uti_cns_0048261	16489	37687	21198
uti_cns_0048529	36079	42562	6483

Supplementary Table 3 List of piRNA-producing transcripts from the *de novo* transcriptome and their piRNA levels.

Transcript ID	Length	PPM	RPKM
c100094_g1_i1	295.00	237.06	803.59
c100111_g1_i1	530.00	122.43	230.99
c100158_g1_i1	225.00	26.71	118.72
c100291_g1_i1	1091.00	124.65	114.25
c100358_g2_i1	327.00	33.39	102.11
c100358_g3_i1	328.00	53.42	162.87
c100458_g1_i1	219.00	25.60	116.89
c100475_g1_i2	334.00	47.86	143.29
c100505_g1_i1	291.00	36.73	126.21

c100525_g1_i1	268.00	287.14	1071.43
c100525_g2_i1	303.00	107.96	356.29
c100569_g1_i1	513.00	77.91	151.87
c100646_g2_i1	292.00	207.01	708.94
c100646_g3_i1	495.00	94.60	191.11
c100672_g1_i1	302.00	41.18	136.36
c100730_g1_i1	637.00	84.58	132.79
c100730_g2_i1	428.00	148.02	345.85
c100730_g3_i1	1033.00	110.18	106.66
c100760_g1_i1	398.00	76.79	192.95
c100791_g1_i1	208.00	72.34	347.80
c100792_g1_i1	988.00	142.46	144.19
c100804_g1_i1	823.00	244.85	297.51
c100804_g2_i1	694.00	251.53	362.43
c100830_g1_i1	1052.00	115.75	110.03
c100830_g2_i1	546.00	96.83	177.34
c100837_g1_i1	464.00	186.98	402.97
c100860_g1_i1	343.00	317.19	924.76
c100860_g2_i1	444.00	343.90	774.56
c100883_g1_i1	278.00	183.64	660.57
c100883_g2_i1	239.00	576.51	2412.18
c100889_g2_i1	413.00	54.53	132.05
c100892_g1_i1	300.00	55.65	185.49
c100944_g1_i1	549.00	56.76	103.39
c100970_g1_i1	373.00	310.52	832.48
c100980_g1_i1	427.00	361.71	847.10
c100980_g2_i1	685.00	110.18	160.85
c101001_g1_i1	588.00	94.60	160.89
c101013_g1_i1	330.00	44.52	134.90
c101034_g1_i1	271.00	40.07	147.85
c101034_g2_i1	314.00	65.66	209.12
c101034_g3_i1	281.00	45.63	162.39
c101047_g1_i2	220.00	52.31	237.77
c101054_g1_i1	629.00	94.60	150.40
c101054_g2_i1	672.00	329.44	490.23
c101100_g1_i1	431.00	411.79	955.44
c101111_g1_i1	254.00	100.17	394.36
c101128_g1_i1	225.00	142.46	633.15
c101128_g2_i1	259.00	152.48	588.71
c101264_g1_i1	306.00	267.11	872.91
c101264_g2_i1	451.00	76.79	170.28
c101264_g3_i2	545.00	151.36	277.73
c101278_g1_i1	676.00	312.74	462.64

c101310_g2_i1	361.00	42.29	117.15
c101365_g1_i1	455.00	113.52	249.50
c101365_g2_i1	221.00	156.93	710.08
c101420_g1_i1	231.00	23.37	101.18
c101431_g1_i1	209.00	25.60	122.48
c101440_g3_i1	377.00	45.63	121.04
c101520_g2_i1	261.00	65.66	251.59
c101556_g2_i1	270.00	60.10	222.59
c101556_g3_i1	430.00	135.78	315.77
c101556_g4_i1	536.00	165.83	309.39
c101556_g5_i1	285.00	32.28	113.25
c101556_g6_i1	304.00	38.95	128.14
c101556_g7_i1	613.00	82.36	134.35
c101565_g1_i1	297.00	33.39	112.42
c101565_g1_i2	606.00	96.83	159.78
c101584_g1_i1	412.00	133.56	324.16
c10167_g1_i1	214.00	41.18	192.43
c101717_g1_i2	840.00	460.76	548.53
c101739_g1_i1	221.00	50.08	226.62
c101739_g2_i1	370.00	47.86	129.34
c101776_g1_i1	270.00	75.68	280.30
c101800_g1_i1	372.00	77.91	209.43
c101811_g1_i1	410.00	123.54	301.31
c101868_g1_i1	355.00	53.42	150.48
c101891_g4_i1	420.00	61.21	145.74
c10192_g1_i1	229.00	23.37	102.06
c101941_g1_i1	207.00	79.02	381.74
c101945_g2_i2	268.00	66.78	249.17
c101993_g1_i1	1665.00	115.75	69.52
c101999_g1_i1	551.00	64.55	117.15
c102002_g1_i1	741.00	122.43	165.22
c102013_g1_i2	1553.00	126.88	81.70
c102118_g1_i1	384.00	106.84	278.24
c102118_g2_i1	313.00	38.95	124.45
c102185_g1_i1	803.00	150.25	187.11
c102247_g4_i1	691.00	199.22	288.31
c102351_g1_i1	987.00	181.41	183.80
c102351_g2_i1	617.00	127.99	207.44
c102390_g3_i1	224.00	46.74	208.68
c102471_g1_i1	211.00	46.74	221.54
c102501_g1_i1	328.00	58.99	179.84
c102502_g1_i1	234.00	56.76	242.57
c102502_g2_i1	405.00	50.08	123.66

c102634_g1_i2	269.00	37.84	140.67
c102656_g1_i1	215.00	47.86	222.59
c102695_g1_i1	402.00	56.76	141.20
c102711_g1_i1	228.00	126.88	556.48
c102718_g1_i1	243.00	28.94	119.08
c102757_g1_i1	706.00	250.42	354.70
c102757_g2_i1	210.00	41.18	196.09
c102796_g1_i3	218.00	23.37	107.21
c102800_g1_i1	317.00	845.85	2668.29
c102824_g2_i1	247.00	36.73	148.70
c102849_g1_i1	431.00	111.30	258.23
c102849_g2_i1	378.00	131.33	347.43
c102971_g1_i1	438.00	159.15	363.36
c103018_g1_i1	456.00	61.21	134.24
c103144_g1_i1	383.00	70.12	183.07
c10316_g1_i1	531.00	63.44	119.47
c103174_g1_i2	733.00	86.81	118.43
c103206_g2_i1	494.00	84.58	171.22
c103246_g1_i1	644.00	70.12	108.88
c103253_g1_i1	635.00	110.18	173.52
c103307_g2_i1	278.00	218.14	784.68
c103327_g1_i1	2746.00	578.74	210.76
c103331_g1_i1	392.00	134.67	343.54
c103350_g1_i1	758.00	170.28	224.65
c103350_g3_i2	421.00	42.29	100.46
c103350_g4_i1	452.00	332.77	736.23
c103361_g1_i1	2102.00	204.78	97.42
c103361_g2_i1	826.00	189.20	229.06
c103372_g2_i1	302.00	50.08	165.84
c103427_g1_i1	1396.00	1016.13	727.89
c103449_g2_i1	226.00	23.37	103.42
c10344_g1_i1	298.00	172.51	578.89
c103509_g1_i1	656.00	186.98	285.03
c103509_g2_i2	971.00	125.76	129.52
c103519_g1_i1	557.00	307.18	551.48
c103658_g1_i1	686.00	125.76	183.33
c103661_g1_i1	527.00	115.75	219.64
c103688_g1_i1	422.00	92.38	218.90
c103713_g1_i1	706.00	148.02	209.67
c103726_g1_i1	282.00	43.41	153.92
c103773_g1_i1	529.00	293.82	555.43
c103776_g1_i1	303.00	82.36	271.81
c103776_g2_i1	690.00	225.93	327.44

c103787_g1_i1	615.00	145.80	237.07
c103805_g1_i1	594.00	63.44	106.80
c103819_g1_i1	341.00	71.23	208.88
c103832_g1_i1	234.00	50.08	214.03
c103921_g1_i1	891.00	97.94	109.92
c103924_g1_i1	350.00	94.60	270.29
c103943_g1_i1	413.00	101.28	245.23
c103956_g2_i1	564.00	76.79	136.16
c104125_g1_i1	1071.00	376.18	351.24
c104125_g2_i1	351.00	83.47	237.81
c104166_g1_i1	449.00	50.08	111.54
c104220_g1_i1	271.00	110.18	406.58
c104245_g1_i1	820.00	244.85	298.60
c104246_g1_i1	222.00	247.08	1112.96
c104251_g2_i1	269.00	111.30	413.74
c104275_g2_i1	739.00	148.02	200.30
c104311_g1_i1	617.00	71.23	115.45
c104327_g1_i2	422.00	52.31	123.96
c104437_g1_i1	525.00	215.91	411.26
c104437_g2_i1	305.00	260.43	853.88
c104459_g1_i1	328.00	281.58	858.47
c10449_g1_i1	365.00	178.07	487.87
c104556_g1_i1	207.00	144.68	698.96
c104605_g1_i1	469.00	102.39	218.32
c104631_g1_i1	255.00	99.05	388.44
c104658_g1_i1	395.00	62.33	157.79
c104662_g1_i1	497.00	92.38	185.87
c104725_g1_i1	301.00	301.61	1002.03
c104737_g1_i1	715.00	509.73	712.92
c104750_g1_i1	410.00	144.68	352.89
c104758_g1_i1	620.00	168.06	271.06
c104758_g3_i1	279.00	42.29	151.59
c104802_g1_i1	396.00	43.41	109.61
c104819_g1_i1	476.00	62.33	130.94
c104826_g1_i1	292.00	48.97	167.71
c104838_g1_i1	560.00	159.15	284.20
c104841_g1_i1	263.00	42.29	160.81
c104844_g2_i1	483.00	120.20	248.86
c104859_g1_i1	348.00	130.22	374.18
c104956_g1_i1	327.00	96.83	296.11
c104956_g2_i1	766.00	244.85	319.65
c104957_g1_i1	238.00	297.16	1248.57
c105017_g1_i1	598.00	103.51	173.09

c105031_g1_i1	572.00	91.26	159.55
c105037_g1_i1	307.00	363.94	1185.46
c105041_g1_i1	345.00	36.73	106.46
c105056_g1_i1	577.00	105.73	183.24
c105070_g1_i1	251.00	520.86	2075.16
c105070_g2_i1	212.00	274.90	1296.70
c105134_g2_i1	646.00	513.07	794.23
c105139_g1_i1	547.00	83.47	152.60
c105146_g1_i1	853.00	97.94	114.82
c105164_g2_i1	231.00	60.10	260.17
c105172_g2_i1	1020.00	119.09	116.75
c105270_g1_i1	911.00	97.94	107.51
c105302_g1_i1	776.00	282.69	364.29
c105312_g2_i1	534.00	116.86	218.84
c105312_g3_i1	202.00	89.04	440.78
c105413_g1_i1	1227.00	373.95	304.77
c105419_g1_i1	704.00	353.92	502.73
c105434_g2_i1	355.00	44.52	125.40
c105501_g1_i1	1309.00	303.84	232.11
c105501_g2_i1	291.00	36.73	126.21
c105515_g1_i3	1743.00	825.81	473.79
c105563_g1_i1	285.00	207.01	726.35
c105576_g1_i1	555.00	65.66	118.31
c105626_g1_i1	611.00	431.83	706.76
c105626_g2_i1	591.00	694.49	1175.10
c105640_g1_i1	209.00	71.23	340.81
c105673_g1_i1	375.00	50.08	133.56
c105685_g1_i1	1137.00	309.40	272.12
c105685_g2_i1	387.00	65.66	169.68
c105753_g1_i1	336.00	159.15	473.67
c105754_g1_i1	234.00	32.28	137.93
c105805_g2_i1	203.00	150.25	740.14
c105834_g1_i1	449.00	76.79	171.03
c105834_g2_i1	296.00	136.89	462.48
c10588_g1_i1	343.00	41.18	120.06
c105912_g1_i1	225.00	65.66	291.84
c105912_g2_i1	798.00	123.54	154.81
c105933_g1_i2	2161.00	136.89	63.35
c105933_g2_i1	926.00	345.02	372.59
c105933_g2_i2	397.00	65.66	165.40
c105945_g1_i1	437.00	62.33	142.62
c105957_g1_i2	795.00	91.26	114.80
c105957_g2_i1	339.00	37.84	111.62

c106028_g2_i1	601.00	501.94	835.18
c106039_g1_i1	589.00	73.46	124.71
c106039_g2_i1	782.00	159.15	203.52
c106048_g1_i1	512.00	57.87	113.04
c106102_g2_i1	212.00	27.82	131.25
c106166_g1_i1	689.00	105.73	153.46
c106193_g1_i1	538.00	84.58	157.22
c106199_g1_i1	743.00	649.97	874.79
c106260_g1_i1	454.00	154.70	340.75
c106275_g2_i1	843.00	131.33	155.79
c106293_g1_i1	510.00	455.20	892.55
c106293_g3_i1	374.00	202.56	541.60
c106307_g1_i1	464.00	302.72	652.42
c106321_g1_i1	504.00	169.17	335.65
c106326_g1_i1	638.00	117.97	184.91
c106346_g1_i1	698.00	122.43	175.39
c106350_g1_i1	292.00	32.28	110.53
c106383_g1_i1	473.00	103.51	218.83
c106383_g2_i1	273.00	54.53	199.76
c106383_g3_i1	351.00	77.91	221.96
c106390_g1_i1	570.00	110.18	193.30
c106390_g1_i2	740.00	134.67	181.98
c106390_g2_i1	273.00	27.82	101.92
c106573_g4_i1	1045.00	153.59	146.97
c106576_g1_i1	1134.00	186.98	164.88
c106594_g1_i1	958.00	302.72	316.00
c106676_g1_i1	255.00	30.05	117.84
c106702_g1_i2	644.00	85.70	133.07
c106711_g1_i1	444.00	141.35	318.35
c106776_g2_i1	1512.00	195.88	129.55
c106842_g1_i1	225.00	23.37	103.88
c106953_g1_i1	486.00	158.04	325.19
c106960_g2_i1	553.00	129.10	233.46
c106967_g1_i1	1734.00	175.85	101.41
c107014_g1_i1	349.00	66.78	191.34
c107018_g1_i1	236.00	107.96	457.44
c107018_g2_i1	428.00	143.57	335.45
c107018_g3_i1	310.00	115.75	373.38
c107018_g4_i1	229.00	74.57	325.63
c107051_g1_i1	657.00	426.26	648.80
c107051_g2_i1	233.00	143.57	616.19
c107083_g2_i1	2075.00	331.66	159.84
c107084_g1_i1	828.00	135.78	163.99

c107113_g1_i1	557.00	75.68	135.87
c107186_g1_i1	229.00	24.49	106.92
c107333_g1_i1	268.00	369.50	1378.74
c107393_g1_i1	361.00	136.89	379.21
c107411_g1_i1	599.00	106.84	178.37
c107479_g1_i1	405.00	82.36	203.36
c107482_g1_i1	327.00	260.43	796.43
c107495_g1_i1	479.00	150.25	313.67
c107537_g1_i1	201.00	37.84	188.26
c107537_g2_i1	297.00	35.61	119.92
c107570_g2_i1	455.00	53.42	117.41
c107614_g1_i1	685.00	274.90	401.32
c107685_g1_i1	2005.00	556.48	277.55
c107686_g1_i1	592.00	278.24	470.00
c107690_g1_i1	390.00	182.53	468.01
c107696_g1_i1	281.00	74.57	265.37
c107709_g1_i3	840.00	262.66	312.69
c107728_g1_i1	696.00	194.77	279.84
c107751_g1_i1	478.00	61.21	128.06
c107752_g1_i4	1171.00	115.75	98.85
c107752_g1_i6	784.00	198.11	252.69
c107752_g2_i1	370.00	53.42	144.38
c107761_g1_i1	251.00	33.39	133.02
c107790_g1_i1	560.00	111.30	198.74
c107790_g2_i1	904.00	169.17	187.13
c107790_g3_i1	238.00	96.83	406.84
c107796_g1_i2	338.00	378.41	1119.54
c107802_g1_i1	287.00	46.74	162.87
c107822_g1_i1	986.00	99.05	100.46
c107923_g2_i1	417.00	149.14	357.64
c107933_g1_i1	836.00	188.09	224.99
c10794_g1_i1	261.00	53.42	204.68
c107980_g2_i1	669.00	596.55	891.70
c107980_g3_i2	541.00	352.81	652.14
c107980_g4_i1	605.00	173.62	286.98
c107980_g4_i2	770.00	422.92	549.25
c107989_g1_i1	390.00	249.30	639.24
c107989_g2_i1	220.00	113.52	516.01
c107998_g1_i1	675.00	73.46	108.82
c108037_g2_i1	280.00	175.85	628.03
c108078_g1_i1	342.00	62.33	182.24
c108110_g1_i1	356.00	73.46	206.34
c108129_g1_i1	226.00	231.50	1024.31

c108145_g1_i1	563.00	117.97	209.54
c108150_g1_i1	284.00	46.74	164.59
c108168_g1_i1	399.00	707.84	1774.04
c108175_g1_i1	1092.00	608.79	557.50
c108199_g1_i1	6092.00	140.23	23.02
c108217_g1_i1	650.00	212.58	327.04
c108246_g1_i1	218.00	27.82	127.63
c108246_g2_i1	587.00	84.58	144.10
c108291_g1_i1	273.00	30.05	110.07
c108291_g2_i1	214.00	27.82	130.02
c108291_g3_i1	620.00	99.05	159.76
c108291_g4_i1	748.00	91.26	122.01
c108301_g1_i1	248.00	64.55	260.29
c108350_g1_i1	981.00	1070.67	1091.40
c108353_g1_i1	238.00	64.55	271.23
c108353_g2_i1	342.00	103.51	302.65
c108382_g1_i1	232.00	81.25	350.20
c108402_g1_i1	619.00	116.86	188.79
c10844_g1_i1	243.00	67.89	279.38
c108486_g1_i1	878.00	243.74	277.61
c108486_g2_i1	485.00	64.55	133.10
c108565_g1_i1	213.00	47.86	224.68
c108565_g2_i1	765.00	198.11	258.96
c108675_g1_i2	779.00	141.35	181.45
c108675_g2_i1	405.00	371.73	917.85
c108707_g1_i1	249.00	25.60	102.80
c108712_g1_i1	387.00	46.74	120.79
c108731_g1_i1	338.00	92.38	273.30
c108731_g2_i1	324.00	182.53	563.35
c108746_g1_i1	258.00	67.89	263.14
c108749_g1_i1	305.00	42.29	138.66
c10880_g1_i1	251.00	41.18	164.06
c108852_g1_i1	654.00	92.38	141.25
c108858_g1_i1	1049.00	298.27	284.34
c108904_g1_i1	378.00	160.27	423.98
c108904_g2_i1	536.00	153.59	286.55
c108965_g1_i1	472.00	47.86	101.39
c108969_g1_i1	736.00	635.50	863.45
c109031_g1_i3	202.00	195.88	969.71
c109035_g1_i1	268.00	43.41	161.96
c109037_g1_i1	450.00	86.81	192.91
c109042_g1_i1	409.00	51.20	125.17
c109101_g1_i1	423.00	132.44	313.10

c109101_g2_i1	478.00	184.75	386.51
c109101_g3_i1	555.00	172.51	310.83
c109107_g2_i1	775.00	221.48	285.78
c109107_g3_i1	239.00	164.72	689.20
c109113_g1_i1	510.00	82.36	161.49
c109147_g1_i1	294.00	31.16	106.00
c109147_g1_i2	316.00	47.86	151.45
c109152_g1_i1	244.00	53.42	218.94
c109186_g1_i1	620.00	83.47	134.63
c109250_g1_i1	245.00	50.08	204.42
c109297_g1_i1	566.00	954.92	1687.13
c109319_g1_i1	523.00	269.34	514.98
c109360_g1_i1	215.00	99.05	460.71
c109360_g2_i1	953.00	585.42	614.29
c109360_g2_i3	582.00	100.17	172.11
c109360_g3_i1	242.00	169.17	699.05
c109360_g4_i1	959.00	101.28	105.61
c109360_g4_i3	929.00	104.62	112.61
c109360_g5_i1	663.00	272.68	411.27
c109371_g1_i1	1530.00	565.38	369.53
c109396_g1_i1	412.00	77.91	189.10
c109454_g1_i1	608.00	352.81	580.28
c109478_g1_i1	216.00	28.94	133.97
c109485_g1_i1	947.00	499.72	527.69
c109485_g1_i2	417.00	94.60	226.86
c109491_g1_i3	665.00	624.37	938.90
c109492_g1_i3	504.00	69.00	136.91
c109550_g2_i1	1732.00	116.86	67.47
c109614_g1_i1	385.00	79.02	205.25
c109680_g1_i1	455.00	105.73	232.38
c109680_g2_i1	933.00	97.94	104.97
c109681_g1_i1	449.00	63.44	141.29
c109692_g1_i1	477.00	81.25	170.33
c109755_g1_i1	798.00	126.88	158.99
c109755_g2_i1	982.00	211.46	215.34
c109763_g2_i2	377.00	105.73	280.45
c109807_g1_i1	621.00	84.58	136.21
c109887_g1_i1	1110.00	109.07	98.26
c109931_g2_i1	227.00	58.99	259.85
c109953_g1_i1	271.00	146.91	542.11
c110014_g1_i1	273.00	69.00	252.76
c110014_g2_i1	408.00	126.88	310.97
c110049_g1_i1	457.00	61.21	133.95

c110120_g3_i1	419.00	111.30	265.62
c110120_g5_i1	244.00	55.65	228.07
c110136_g1_i1	559.00	376.18	672.95
c110136_g2_i1	1386.00	116.86	84.32
c110136_g3_i1	420.00	308.29	734.02
c110136_g4_i2	1164.00	161.38	138.64
c110136_g5_i1	1090.00	725.65	665.73
c110150_g2_i1	1569.00	299.39	190.81
c11028_g1_i1	656.00	104.62	159.48
c110297_g1_i1	830.00	156.93	189.07
c110347_g1_i1	396.00	105.73	267.00
c110347_g1_i2	277.00	32.28	116.52
c110347_g1_i3	268.00	40.07	149.50
c110401_g1_i1	1238.00	207.01	167.21
c110405_g1_i1	273.00	31.16	114.15
c110405_g2_i1	339.00	52.31	154.30
c110422_g1_i1	643.00	966.05	1502.41
c110422_g2_i1	1072.00	1800.77	1679.82
c110426_g1_i1	281.00	111.30	396.07
c110431_g1_i2	665.00	69.00	103.76
c11045_g1_i1	245.00	48.97	199.88
c110520_g1_i4	738.00	89.04	120.65
c110520_g1_i5	201.00	28.94	143.97
c110524_g1_i1	297.00	41.18	138.65
c110524_g2_i1	331.00	286.03	864.14
c110544_g3_i1	625.00	132.44	211.91
c110571_g1_i1	251.00	35.61	141.89
c110573_g1_i1	324.00	151.36	467.17
c110573_g2_i1	859.00	341.68	397.76
c110573_g3_i1	608.00	262.66	432.00
c110599_g1_i1	213.00	63.44	297.83
c110599_g1_i2	213.00	62.33	292.61
c110599_g2_i1	549.00	437.39	796.71
c110627_g1_i1	249.00	64.55	259.24
c110627_g1_i2	319.00	176.96	554.73
c110701_g1_i1	918.00	166.94	181.86
c110706_g2_i1	249.00	72.34	290.53
c110734_g1_i1	472.00	119.09	252.30
c110735_g1_i1	698.00	73.46	105.24
c110788_g1_i2	445.00	51.20	115.05
c110789_g1_i2	401.00	125.76	313.63
c110855_g1_i1	1219.00	227.04	186.25
c110950_g1_i1	629.00	112.41	178.71

c11096_g1_i1	705.00	119.09	168.92
c110981_g1_i2	221.00	74.57	337.41
c111010_g1_i1	482.00	53.42	110.83
c111011_g1_i1	906.00	904.83	998.71
c111076_g1_i1	892.00	205.90	230.83
c111076_g1_i2	502.00	130.22	259.39
c11108_g1_i1	208.00	35.61	171.22
c111128_g1_i1	1412.00	110.18	78.03
c111162_g1_i1	800.00	116.86	146.08
c111166_g1_i1	210.00	24.49	116.60
c111213_g1_i1	710.00	112.41	158.32
c111214_g1_i2	642.00	104.62	162.96
c111259_g1_i1	218.00	38.95	178.69
c111329_g1_i1	309.00	194.77	630.32
c111339_g1_i1	1099.00	123.54	112.41
c111383_g2_i2	1728.00	379.52	219.63
c111426_g1_i1	408.00	185.86	455.55
c111426_g2_i1	635.00	961.60	1514.32
c111426_g3_i1	338.00	210.35	622.33
c111462_g2_i1	693.00	119.09	171.84
c111499_g6_i1	240.00	36.73	153.03
c111502_g1_i1	240.00	135.78	565.75
c111513_g1_i1	539.00	348.36	646.30
c111513_g2_i1	605.00	123.54	204.20
c111515_g3_i1	479.00	67.89	141.73
c111546_g1_i1	210.00	142.46	678.37
c111547_g1_i1	563.00	124.65	221.41
c111547_g4_i1	1124.00	129.10	114.86
c111547_g6_i1	466.00	80.13	171.96
c111574_g2_i1	1352.00	110.18	81.50
c111621_g1_i1	297.00	94.60	318.52
c111621_g1_i2	362.00	41.18	113.76
c11162_g1_i1	230.00	50.08	217.75
c111703_g1_i1	369.00	112.41	304.63
c111727_g1_i1	245.00	141.35	576.92
c111740_g1_i1	756.00	282.69	373.93
c111740_g2_i1	1421.00	376.18	264.73
c111740_g3_i1	812.00	169.17	208.34
c111740_g4_i1	814.00	304.95	374.63
c111782_g1_i2	362.00	109.07	301.30
c111788_g2_i1	547.00	75.68	138.36
c111788_g4_i1	826.00	97.94	118.57
c111788_g6_i1	290.00	44.52	153.51

c11178_g1_i1	201.00	37.84	188.26
c111790_g2_i1	324.00	45.63	140.84
c111796_g2_i1	204.00	22.26	109.11
c111845_g1_i1	3187.00	13761.70	4318.08
c111851_g2_i1	541.00	142.46	263.32
c111889_g1_i2	907.00	172.51	190.20
c111891_g1_i1	918.00	239.29	260.66
c111891_g5_i1	435.00	168.06	386.34
c111935_g1_i2	331.00	42.29	127.77
c111935_g2_i1	237.00	266.00	1122.35
c111940_g1_i1	635.00	85.70	134.96
c111963_g1_i1	497.00	56.76	114.21
c111988_g2_i1	914.00	113.52	124.20
c111988_g2_i4	532.00	79.02	148.53
c112012_g2_i1	207.00	25.60	123.66
c112043_g1_i1	602.00	65.66	109.08
c112055_g2_i1	896.00	99.05	110.55
c112075_g3_i1	319.00	138.01	432.62
c112091_g1_i1	1545.00	397.33	257.17
c112091_g2_i1	593.00	90.15	152.02
c112130_g1_i1	1113.00	902.61	810.97
c112130_g2_i1	287.00	74.57	259.82
c112154_g1_i1	201.00	50.08	249.17
c112154_g2_i1	1801.00	477.46	265.11
c112253_g1_i1	244.00	52.31	214.38
c112267_g1_i1	709.00	145.80	205.64
c112332_g1_i1	432.00	302.72	700.75
c112332_g2_i1	446.00	444.07	995.67
c112399_g1_i3	206.00	84.58	410.61
c112399_g1_i4	216.00	31.16	144.27
c112413_g1_i1	310.00	58.99	190.28
c112413_g2_i1	446.00	124.65	279.49
c112413_g3_i1	707.00	393.99	557.27
c112413_g4_i1	300.00	54.53	181.78
c112414_g1_i1	565.00	617.69	1093.26
c112435_g1_i1	247.00	570.95	2311.53
c112452_g1_i1	252.00	48.97	194.33
c112493_g1_i3	1161.00	322.76	278.00
c112493_g2_i1	985.00	703.39	714.10
c112569_g1_i1	515.00	383.97	745.57
c112617_g1_i1	971.00	309.40	318.64
c112618_g1_i1	569.00	58.99	103.67
c112645_g1_i1	287.00	161.38	562.30

c112646_g1_i1	506.00	53.42	105.58
c112652_g1_i1	2210.00	156.93	71.01
c112668_g2_i1	418.00	50.08	119.82
c112676_g1_i1	376.00	74.57	198.32
c112676_g1_i2	738.00	411.79	557.99
c112682_g1_i1	333.00	91.26	274.06
c112682_g1_i2	278.00	233.72	840.72
c112682_g2_i1	408.00	142.46	349.16
c112734_g2_i1	220.00	38.95	177.06
c112764_g1_i1	1731.00	222.59	128.59
c112851_g1_i1	949.00	142.46	150.11
c112899_g1_i1	1434.00	491.93	343.05
c112899_g2_i1	529.00	109.07	206.18
c11289_g1_i1	333.00	107.96	324.20
c112909_g1_i1	287.00	58.99	205.53
c112909_g2_i1	266.00	52.31	196.65
c112915_g1_i2	457.00	71.23	155.86
c112915_g2_i1	450.00	243.74	541.64
c112922_g1_i1	223.00	31.16	139.74
c112957_g1_i1	292.00	121.31	415.45
c112971_g1_i1	1526.00	126.88	83.14
c112991_g1_i1	335.00	306.06	913.62
c112991_g1_i2	290.00	144.68	498.91
c113060_g1_i1	1167.00	106.84	91.55
c113068_g1_i1	259.00	54.53	210.56
c113071_g2_i1	693.00	117.97	170.24
c113130_g1_i1	1297.00	676.68	521.73
c113143_g1_i1	237.00	379.52	1601.34
c113143_g2_i1	566.00	806.89	1425.61
c11315_g1_i1	1477.00	195.88	132.62
c113163_g1_i1	700.00	188.09	268.70
c113244_g1_i1	1069.00	171.40	160.33
c113275_g1_i1	1263.00	353.92	280.22
c113275_g2_i1	352.00	106.84	303.53
c113310_g1_i2	497.00	149.14	300.07
c113316_g1_i1	978.00	124.65	127.46
c113337_g1_i1	555.00	224.82	405.08
c113337_g2_i2	1190.00	152.48	128.13
c113337_g3_i1	1461.00	435.17	297.86
c113343_g1_i1	358.00	95.71	267.36
c113405_g3_i2	401.00	47.86	119.35
c113409_g1_i1	404.00	96.83	239.67
c113409_g2_i1	791.00	319.42	403.82

c113423_g1_i1	471.00	60.10	127.60
c113515_g1_i1	1125.00	107.96	95.96
c113525_g2_i1	623.00	150.25	241.17
c113529_g1_i1	205.00	221.48	1080.38
c113534_g1_i1	1139.00	120.20	105.53
c11353_g1_i1	204.00	33.39	163.67
c113560_g2_i1	545.00	211.46	388.00
c113560_g2_i2	7306.00	6983.81	955.90
c113570_g1_i1	1808.00	142.46	78.79
c11359_g2_i1	250.00	27.82	111.30
c113604_g1_i1	1190.00	178.07	149.64
c113639_g1_i1	297.00	90.15	303.53
c113661_g1_i1	939.00	387.31	412.47
c113746_g2_i1	300.00	105.73	352.44
c113822_g1_i3	885.00	102.39	115.70
c113874_g2_i1	1405.00	100.17	71.29
c113883_g1_i1	333.00	62.33	187.16
c113888_g1_i2	670.00	75.68	112.96
c113945_g3_i1	716.00	126.88	177.20
c113945_g6_i1	552.00	135.78	245.98
c114013_g1_i1	421.00	116.86	277.58
c114013_g2_i1	1034.00	337.23	326.14
c114093_g1_i2	868.00	115.75	133.35
c11410_g1_i1	204.00	92.38	452.82
c114141_g2_i3	398.00	41.18	103.47
c114141_g3_i1	206.00	21.15	102.65
c114145_g2_i1	217.00	93.49	430.82
c114157_g1_i1	712.00	371.73	522.09
c114157_g1_i2	578.00	143.57	248.39
c114162_g1_i1	227.00	122.43	539.32
c114162_g1_i2	227.00	37.84	166.70
c114249_g1_i2	687.00	159.15	231.66
c114343_g1_i1	257.00	179.19	697.22
c114350_g4_i2	263.00	40.07	152.34
c114355_g1_i1	786.00	94.60	120.36
c114510_g1_i1	868.00	223.70	257.72
c114520_g2_i1	1132.00	250.42	221.22
c114541_g4_i1	1612.00	106.84	66.28
c114578_g1_i5	482.00	99.05	205.51
c114586_g1_i1	723.00	125.76	173.95
c114615_g1_i1	491.00	398.44	811.48
c114615_g2_i1	558.00	107.96	193.47
c114663_g1_i2	253.00	35.61	140.77

c114734_g1_i1	640.00	164.72	257.37
c114734_g1_i2	523.00	150.25	287.28
c114798_g1_i1	3781.00	23694.90	6266.82
c114877_g1_i1	268.00	124.65	465.12
c115004_g1_i1	2652.00	704.50	265.65
c115004_g1_i2	817.00	113.52	138.95
c115039_g1_i1	607.00	213.69	352.04
c115039_g2_i1	408.00	47.86	117.30
c115039_g3_i1	265.00	54.53	205.79
c115040_g1_i1	398.00	50.08	125.84
c115040_g1_i2	1249.00	711.18	569.40
c115040_g2_i1	1364.00	243.74	178.69
c115040_g3_i1	1051.00	657.76	625.84
c115046_g1_i1	1182.00	518.64	438.78
c115055_g1_i1	319.00	41.18	129.09
c115055_g1_i2	255.00	43.41	170.22
c115125_g1_i1	227.00	32.28	142.18
c115125_g2_i1	855.00	168.06	196.56
c115125_g3_i1	353.00	60.10	170.25
c115125_g4_i1	2163.00	575.40	266.02
c115125_g5_i1	221.00	58.99	266.91
c115166_g3_i1	219.00	33.39	152.46
c115220_g1_i1	267.00	89.04	333.47
c115220_g2_i2	950.00	199.22	209.71
c115225_g1_i2	2568.00	124.65	48.54
c11525_g1_i1	222.00	76.79	345.92
c115320_g1_i1	738.00	1523.64	2064.55
c115342_g1_i1	286.00	67.89	237.38
c115342_g2_i1	586.00	58.99	100.66
c115390_g1_i1	264.00	69.00	261.38
c115425_g1_i1	316.00	69.00	218.37
c115445_g1_i3	1094.00	113.52	103.77
c115535_g1_i1	278.00	54.53	196.17
c115597_g1_i1	331.00	37.84	114.32
c115597_g1_i2	309.00	47.86	154.88
c115628_g1_i1	282.00	37.84	134.19
c115628_g4_i2	920.00	93.49	101.62
c115628_g5_i1	579.00	60.10	103.80
c115628_g6_i1	336.00	110.18	327.93
c115673_g1_i1	911.00	1135.22	1246.12
c115710_g1_i1	1182.00	274.90	232.57
c115728_g1_i1	632.00	111.30	176.10
c115764_g1_i1	289.00	86.81	300.38

c115764_g2_i2	418.00	61.21	146.44
c115921_g1_i1	363.00	45.63	125.71
c115984_g1_i1	276.00	82.36	298.40
c116121_g1_i1	388.00	136.89	352.82
c116121_g1_i2	346.00	145.80	421.38
c116153_g1_i1	226.00	1257.64	5564.79
c116262_g1_i2	783.00	103.51	132.19
c116263_g1_i2	258.00	33.39	129.41
c116263_g1_i6	213.00	102.39	480.71
c116381_g2_i2	361.00	43.41	120.24
c116399_g1_i3	279.00	32.28	115.68
c116400_g1_i1	203.00	48.97	241.23
c116408_g1_i1	564.00	129.10	228.91
c116418_g4_i1	1214.00	102.39	84.34
c116471_g1_i1	258.00	46.74	181.18
c116471_g2_i1	1196.00	132.44	110.74
c116485_g2_i1	655.00	84.58	129.14
c116485_g3_i1	484.00	94.60	195.46
c116485_g6_i1	308.00	35.61	115.63
c116527_g3_i1	277.00	35.61	128.57
c116559_g3_i1	448.00	102.39	228.55
c116563_g2_i4	404.00	64.55	159.78
c116577_g1_i2	2306.00	104.62	45.37
c116577_g3_i1	1337.00	145.80	109.05
c116592_g1_i1	717.00	284.92	397.37
c116592_g2_i1	412.00	50.08	121.56
c116632_g1_i1	946.00	266.00	281.18
c116632_g2_i1	213.00	27.82	130.63
c116668_g1_i1	343.00	434.05	1265.46
c116681_g1_i1	1108.00	566.50	511.28
c116691_g1_i1	316.00	361.71	1144.66
c11670_g1_i1	392.00	227.04	579.19
c116722_g2_i1	255.00	38.95	152.76
c116742_g3_i1	221.00	23.37	105.76
c116747_g2_i1	951.00	445.18	468.12
c116754_g1_i1	211.00	35.61	168.79
c116754_g1_i2	292.00	211.46	724.19
c116754_g2_i1	262.00	417.36	1592.97
c116760_g1_i1	338.00	50.08	148.18
c116760_g2_i1	287.00	31.16	108.58
c116856_g1_i1	971.00	429.60	442.43
c116910_g1_i1	464.00	66.78	143.92
c117013_g1_i1	1349.00	854.75	633.62

c117020_g1_i1	234.00	25.60	109.39
c117053_g1_i1	667.00	331.66	497.24
c117085_g1_i1	626.00	440.73	704.04
c117088_g1_i1	204.00	67.89	332.80
c117088_g1_i2	205.00	52.31	255.17
c117163_g1_i1	936.00	1026.15	1096.31
c117188_g4_i1	1220.00	131.33	107.65
c117273_g1_i1	715.00	92.38	129.20
c117285_g1_i1	457.00	200.33	438.36
c117285_g2_i1	245.00	107.96	440.64
c117335_g1_i3	806.00	174.73	216.79
c117335_g2_i1	377.00	109.07	289.31
c117354_g2_i1	290.00	106.84	368.43
c117354_g3_i1	355.00	85.70	241.40
c117356_g1_i1	389.00	154.70	397.69
c117356_g1_i3	243.00	75.68	311.45
c117363_g2_i1	813.00	107.96	132.79
c117368_g2_i1	722.00	171.40	237.39
c117415_g2_i2	1106.00	109.07	98.62
c117417_g1_i2	3146.00	122.43	38.91
c117426_g1_i1	250.00	865.88	3463.52
c117473_g2_i1	1232.00	153.59	124.67
c11747_g1_i1	399.00	93.49	234.31
c11747_g2_i1	1014.00	194.77	192.08
c117594_g1_i1	1441.00	402.89	279.59
c117614_g1_i1	375.00	159.15	424.41
c117614_g2_i1	297.00	178.07	599.57
c117667_g1_i1	703.00	261.55	372.04
c117715_g1_i1	204.00	92.38	452.82
c117743_g1_i1	583.00	790.20	1355.40
c117754_g2_i1	1612.00	154.70	95.97
c117754_g4_i1	314.00	50.08	159.50
c117754_g6_i1	211.00	27.82	131.87
c117822_g1_i1	211.00	28.94	137.14
c117896_g1_i1	281.00	38.95	138.63
c117906_g1_i1	366.00	45.63	124.68
c117927_g2_i1	319.00	122.43	383.78
c117938_g1_i1	1529.00	499.72	326.83
c117975_g1_i1	664.00	173.62	261.48
c1179_g1_i1	236.00	31.16	132.05
c118077_g1_i1	339.00	527.54	1556.17
c118098_g2_i1	529.00	65.66	124.13
c118122_g2_i1	358.00	62.33	174.09

c118122_g3_i1	414.00	64.55	155.92
c118144_g1_i1	824.00	105.73	128.31
c118152_g1_i1	867.00	277.13	319.64
c118188_g1_i1	2055.00	456.31	222.05
c118189_g7_i1	316.00	83.47	264.15
c118225_g1_i1	392.00	180.30	459.95
c118234_g1_i1	721.00	190.32	263.96
c118385_g1_i1	226.00	48.97	216.68
c118385_g2_i1	330.00	48.97	148.39
c118385_g4_i1	236.00	91.26	386.71
c118537_g1_i3	1872.00	155.81	83.23
c11856_g1_i1	288.00	304.95	1058.86
c118591_g1_i1	282.00	65.66	232.85
c118613_g2_i1	475.00	290.48	611.54
c118613_g3_i1	235.00	71.23	303.10
c118622_g2_i1	211.00	31.16	147.69
c118655_g1_i1	577.00	483.02	837.13
c118684_g1_i1	451.00	200.33	444.20
c118684_g2_i1	217.00	368.39	1697.64
c118696_g1_i3	5847.00	140.23	23.98
c118732_g1_i1	1026.00	100.17	97.63
c118732_g1_i2	764.00	93.49	122.37
c118925_g1_i1	250.00	33.39	133.56
c118926_g2_i1	368.00	115.75	314.53
c118995_g1_i1	268.00	46.74	174.42
c119009_g2_i1	700.00	241.51	345.02
c119009_g3_i1	306.00	32.28	105.48
c119014_g2_i2	1749.00	1328.87	759.79
c119091_g1_i1	239.00	211.46	884.78
c119106_g1_i1	208.00	1523.64	7325.19
c119106_g2_i1	206.00	171.40	832.02
c119107_g1_i1	1054.00	234.83	222.80
c119120_g1_i2	773.00	105.73	136.78
c119120_g3_i1	288.00	62.33	216.41
c119148_g1_i1	1851.00	286.03	154.53
c119153_g1_i1	2940.00	1425.70	484.93
c119153_g2_i1	821.00	220.37	268.41
c119162_g1_i1	313.00	66.78	213.35
c119164_g1_i1	653.00	240.40	368.15
c119164_g3_i2	2360.00	159.15	67.44
c119238_g2_i1	488.00	77.91	159.65
c119251_g1_i1	726.00	184.75	254.48
c119251_g2_i1	270.00	42.29	156.64

c119251_g3_i2	688.00	77.91	113.24
c119325_g2_i6	275.00	47.86	174.03
c119356_g3_i2	2829.00	142.46	50.36
c119390_g1_i1	884.00	152.48	172.48
c119453_g1_i1	2138.00	393.99	184.28
c119471_g1_i1	716.00	101.28	141.45
c119500_g1_i1	229.00	32.28	140.94
c119502_g1_i1	1860.00	245.96	132.24
c119574_g1_i2	4140.00	116.86	28.23
c119611_g2_i1	311.00	164.72	529.64
c119627_g1_i1	585.00	283.80	485.14
c119675_g2_i1	685.00	249.30	363.95
c119675_g3_i1	531.00	64.55	121.57
c119675_g4_i1	380.00	52.31	137.66
c119675_g5_i1	254.00	25.60	100.78
c119708_g2_i1	447.00	52.31	117.02
c119744_g1_i1	1971.00	608.79	308.87
c119749_g1_i1	664.00	220.37	331.88
c119749_g2_i1	555.00	87.92	158.42
c11978_g1_i1	207.00	23.37	112.91
c119869_g2_i1	208.00	395.10	1899.52
c119879_g1_i1	260.00	26.71	102.74
c119879_g5_i1	481.00	162.49	337.82
c119879_g6_i1	225.00	66.78	296.79
c119918_g1_i1	1111.00	178.07	160.28
c119934_g1_i1	1054.00	358.37	340.01
c119989_g1_i1	220.00	42.29	192.24
c119998_g1_i2	503.00	73.46	146.03
c120014_g1_i1	826.00	142.46	172.47
c120014_g2_i2	688.00	95.71	139.12
c120024_g2_i1	205.00	40.07	195.45
c120078_g1_i1	1155.00	125.76	108.89
c120095_g1_i1	333.00	41.18	123.66
c120095_g1_i2	456.00	73.46	161.09
c120179_g2_i1	429.00	51.20	119.34
c120222_g2_i1	2077.00	119.09	57.34
c12024_g1_i1	321.00	308.29	960.40
c120421_g1_i1	633.00	171.40	270.77
c120421_g2_i1	387.00	69.00	178.30
c120437_g1_i3	227.00	23.37	102.96
c120473_g1_i1	798.00	353.92	443.51
c120473_g2_i1	966.00	104.62	108.30
c120506_g1_i1	349.00	45.63	130.75

c120506_g2_i1	244.00	189.20	775.42
c120539_g1_i1	2322.00	363.94	156.73
c120595_g1_i1	1485.00	563.16	379.23
c120595_g4_i1	718.00	162.49	226.31
c120595_g5_i1	620.00	63.44	102.32
c120670_g1_i1	501.00	69.00	137.73
c120680_g1_i1	2949.00	500.83	169.83
c120713_g1_i1	333.00	87.92	264.04
c120713_g1_i3	308.00	234.83	762.45
c120713_g1_i4	298.00	183.64	616.24
c120770_g1_i1	219.00	33.39	152.46
c120770_g2_i1	718.00	301.61	420.07
c120770_g3_i1	643.00	109.07	169.63
c120819_g1_i1	296.00	43.41	146.64
c120819_g1_i6	726.00	142.46	196.22
c120819_g1_i7	684.00	319.42	466.99
c120819_g1_i9	236.00	31.16	132.05
c120819_g3_i1	206.00	62.33	302.55
c120828_g1_i2	987.00	103.51	104.87
c120852_g1_i1	497.00	69.00	138.84
c120913_g2_i1	626.00	317.19	506.70
c120985_g1_i1	330.00	42.29	128.16
c120985_g2_i1	1064.00	119.09	111.92
c121019_g2_i2	938.00	180.30	192.22
c121093_g1_i1	1988.00	139.12	69.98
c121095_g1_i1	1073.00	112.41	104.76
c121095_g1_i2	338.00	50.08	148.18
c121106_g1_i1	229.00	65.66	286.74
c121106_g2_i1	1072.00	191.43	178.57
c121106_g4_i1	286.00	32.28	112.85
c121107_g1_i1	486.00	61.21	125.95
c121145_g1_i1	538.00	166.94	310.30
c121145_g3_i4	1166.00	117.97	101.18
c121145_g4_i1	462.00	104.62	226.45
c121152_g3_i1	792.00	103.51	130.69
c121159_g2_i1	430.00	55.65	129.41
c121159_g2_i3	561.00	80.13	142.84
c12115_g1_i1	571.00	149.14	261.18
c12115_g2_i1	203.00	55.65	274.13
c121311_g1_i1	1355.00	253.75	187.27
c121311_g2_i1	2679.00	542.01	202.32
c121311_g5_i1	1800.00	183.64	102.02
c121326_g1_i1	1298.00	144.68	111.47

c121326_g2_i1	303.00	56.76	187.33
c121326_g4_i1	329.00	218.14	663.04
c121326_g5_i1	577.00	105.73	183.24
c121349_g3_i1	1309.00	133.56	102.03
c121553_g4_i1	365.00	257.09	704.37
c121648_g1_i2	1827.00	163.61	89.55
c121648_g3_i1	986.00	144.68	146.74
c121693_g2_i1	259.00	33.39	128.91
c121704_g1_i1	755.00	189.20	250.60
c121704_g1_i2	305.00	81.25	266.38
c121719_g1_i1	721.00	536.45	744.03
c121719_g1_i2	515.00	230.38	447.34
c121758_g1_i1	323.00	84.58	261.87
c121812_g1_i1	379.00	202.56	534.45
c121812_g2_i1	963.00	198.11	205.72
c121824_g1_i1	1244.00	173.62	139.57
c121857_g1_i2	540.00	90.15	166.94
c121888_g1_i1	259.00	38.95	150.40
c121894_g1_i1	1831.00	376.18	205.45
c121897_g1_i1	623.00	188.09	301.91
c121905_g2_i1	522.00	53.42	102.34
c121905_g3_i1	332.00	64.55	194.43
c121923_g1_i1	217.00	55.65	256.44
c121923_g2_i1	280.00	30.05	107.32
c121923_g3_i1	389.00	148.02	380.52
c121923_g3_i2	208.00	63.44	304.99
c121923_g4_i1	1174.00	1784.07	1519.65
c121972_g1_i2	1691.00	242.63	143.48
c121972_g2_i1	456.00	51.20	112.27
c121976_g4_i1	352.00	85.70	243.46
c122024_g11_i1	230.00	31.16	135.49
c122060_g1_i1	517.00	917.08	1773.84
c122060_g1_i2	348.00	74.57	214.28
c122086_g1_i1	264.00	40.07	151.77
c122091_g1_i1	211.00	24.49	116.04
c122174_g3_i1	415.00	182.53	439.82
c122174_g4_i1	437.00	66.78	152.81
c122174_g5_i1	285.00	44.52	156.21
c122174_g5_i2	595.00	129.10	216.98
c122174_g6_i1	201.00	144.68	719.82
c122174_g7_i1	592.00	447.41	755.76
c122178_g4_i1	224.00	24.49	109.31
c122212_g2_i1	214.00	43.41	202.83

c122212_g3_i1	1027.00	273.79	266.59
c122307_g2_i1	459.00	211.46	460.70
c122307_g3_i1	392.00	178.07	454.27
c122307_g4_i1	977.00	363.94	372.51
c122370_g1_i1	251.00	119.09	474.45
c122370_g1_i2	495.00	112.41	227.09
c122370_g1_i3	492.00	397.33	807.57
c122370_g2_i1	240.00	476.35	1984.77
c122370_g3_i1	392.00	106.84	272.56
c122370_g3_i2	220.00	53.42	242.83
c122404_g1_i1	854.00	127.99	149.87
c122419_g1_i2	1069.00	142.46	133.26
c122455_g1_i1	808.00	214.80	265.84
c122465_g2_i1	653.00	119.09	182.37
c122489_g1_i1	1735.00	771.28	444.54
c122490_g2_i1	233.00	125.76	539.76
c122517_g1_i1	1031.00	179.19	173.80
c122518_g1_i2	1804.00	113.52	62.93
c122579_g4_i1	261.00	26.71	102.34
c122656_g4_i1	350.00	36.73	104.94
c122708_g3_i2	667.00	518.64	777.57
c122715_g1_i1	487.00	180.30	370.22
c122728_g1_i1	1196.00	172.51	144.24
c122741_g3_i1	1719.00	127.99	74.46
c122743_g1_i1	2947.00	2196.98	745.50
c122787_g2_i1	1925.00	224.82	116.79
c12284_g1_i1	212.00	25.60	120.75
c122863_g3_i1	911.00	91.26	100.18
c122912_g3_i1	2216.00	336.11	151.68
c122999_g3_i1	673.00	111.30	165.37
c123008_g1_i1	854.00	156.93	183.76
c123010_g5_i1	611.00	114.64	187.62
c123022_g1_i1	1799.00	337.23	187.45
c123094_g8_i2	599.00	81.25	135.64
c123095_g1_i3	404.00	72.34	179.07
c123105_g2_i1	392.00	151.36	386.13
c123112_g1_i1	2196.00	146.91	66.90
c123137_g4_i1	425.00	61.21	144.03
c123209_g3_i1	405.00	67.89	167.63
c123231_g1_i2	799.00	84.58	105.86
c123231_g3_i1	2150.00	861.43	400.67
c123237_g1_i1	1513.00	994.98	657.62
c123237_g2_i1	471.00	89.04	189.04

c123237_g2_i2	2095.00	1486.91	709.74
c123263_g7_i1	422.00	121.31	287.47
c123263_g8_i1	251.00	45.63	181.80
c123362_g13_i1	365.00	57.87	158.56
c123379_g1_i2	2605.00	119.09	45.71
c123381_g1_i1	289.00	33.39	115.53
c123386_g3_i1	203.00	24.49	120.62
c123394_g2_i1	254.00	38.95	153.36
c123432_g1_i1	901.00	203.67	226.05
c123440_g4_i1	227.00	34.50	151.99
c123470_g2_i1	240.00	52.31	217.95
c12348_g1_i1	272.00	97.94	360.07
c123492_g1_i1	226.00	67.89	300.40
c123492_g3_i1	1297.00	161.38	124.43
c123492_g3_i4	1952.00	4273.76	2189.42
c123495_g2_i3	893.00	131.33	147.07
c123495_g3_i2	226.00	33.39	147.74
c123495_g5_i1	2892.00	192.54	66.58
c123501_g4_i1	666.00	1539.22	2311.14
c123501_g5_i1	251.00	366.16	1458.82
c123501_g7_i1	297.00	558.71	1881.16
c123507_g2_i1	255.00	61.21	240.05
c123515_g3_i1	264.00	392.87	1488.16
c123543_g4_i1	1378.00	254.87	184.95
c123543_g7_i1	818.00	87.92	107.49
c123554_g1_i2	754.00	106.84	141.70
c123572_g1_i2	222.00	63.44	285.76
c123572_g1_i3	2434.00	154.70	63.56
c123642_g1_i1	906.00	132.44	146.18
c123644_g1_i1	310.00	40.07	129.25
c123644_g3_i1	606.00	77.91	128.56
c123657_g1_i2	3561.00	1242.06	348.80
c123688_g4_i4	493.00	69.00	139.97
c123732_g1_i1	1732.00	468.56	270.53
c123742_g1_i2	485.00	112.41	231.77
c123750_g1_i1	1083.00	306.06	282.61
c123766_g1_i1	998.00	106.84	107.06
c123820_g3_i2	242.00	55.65	229.95
c123820_g4_i2	250.00	47.86	191.43
c123820_g9_i1	296.00	32.28	109.04
c123888_g1_i1	2235.00	546.46	244.50
c123888_g5_i1	749.00	102.39	136.71
c123905_g3_i1	753.00	83.47	110.85

c123905_g5_i1	854.00	208.12	243.70
c123905_g6_i1	943.00	166.94	177.04
c123912_g1_i1	866.00	122.43	141.37
c123921_g1_i2	406.00	142.46	350.88
c123921_g3_i1	425.00	148.02	348.29
c123921_g5_i3	582.00	259.32	445.57
c123923_g1_i1	2915.00	271.56	93.16
c123930_g2_i1	351.00	40.07	114.15
c123930_g2_i2	290.00	93.49	322.37
c123945_g2_i2	1955.00	2348.34	1201.20
c123945_g2_i3	484.00	215.91	446.10
c123945_g3_i2	604.00	92.38	152.94
c123945_g5_i1	765.00	414.02	541.20
c123956_g1_i1	313.00	106.84	341.35
c123966_g1_i1	738.00	369.50	500.68
c123967_g1_i2	1934.00	135.78	70.21
c124000_g3_i1	663.00	123.54	186.33
c124003_g2_i1	1431.00	166.94	116.66
c124027_g1_i3	231.00	23.37	101.18
c124060_g1_i1	1484.00	248.19	167.24
c124084_g1_i1	1126.00	446.30	396.36
c124094_g3_i2	252.00	25.60	101.58
c124123_g1_i1	2667.00	908.17	340.52
c124123_g1_i2	1376.00	438.51	318.68
c124123_g2_i1	501.00	62.33	124.40
c124123_g2_i2	245.00	110.18	449.73
c124123_g3_i1	349.00	369.50	1058.74
c124124_g3_i4	924.00	303.84	328.83
c124133_g1_i1	257.00	56.76	220.86
c124133_g2_i1	1034.00	180.30	174.37
c124152_g2_i1	236.00	131.33	556.48
c124156_g2_i1	372.00	38.95	104.71
c124156_g3_i1	1183.00	188.09	158.99
c124169_g1_i1	728.00	208.12	285.88
c124169_g2_i2	552.00	58.99	106.86
c124188_g3_i1	213.00	341.68	1604.12
c124221_g1_i1	511.00	76.79	150.28
c124221_g4_i1	583.00	61.21	105.00
c124256_g3_i1	1462.00	185.86	127.13
c124297_g1_i1	1165.00	193.66	166.23
c124297_g2_i2	663.00	152.48	229.98
c124297_g3_i1	1509.00	119.09	78.92
c124297_g4_i2	332.00	80.13	241.36

c124297_g5_i1	269.00	94.60	351.68
c124297_g6_i1	270.00	34.50	127.78
c124302_g4_i1	386.00	80.13	207.60
c124402_g1_i1	208.00	71.23	342.45
c124402_g1_i3	439.00	110.18	250.99
c124436_g1_i4	332.00	50.08	150.85
c124436_g2_i1	310.00	48.97	157.97
c124436_g3_i2	429.00	107.96	251.65
c124436_g3_i3	519.00	66.78	128.67
c124472_g2_i8	919.00	93.49	101.73
c124482_g2_i1	1279.00	199.22	155.76
c124482_g3_i1	201.00	40.07	199.34
c124496_g3_i1	795.00	303.84	382.19
c124496_g5_i1	351.00	38.95	110.98
c124500_g1_i1	236.00	24.49	103.75
c124500_g3_i1	212.00	33.39	157.49
c124549_g6_i1	515.00	57.87	112.38
c124558_g2_i1	707.00	716.75	1013.78
c124566_g3_i1	221.00	23.37	105.76
c124570_g1_i1	223.00	71.23	319.41
c124635_g1_i2	1315.00	148.02	112.57
c124651_g5_i1	1547.00	455.20	294.25
c124654_g1_i1	519.00	63.44	122.23
c124654_g2_i1	976.00	258.21	264.56
c124688_g1_i1	1638.00	204.78	125.02
c124720_g3_i1	2743.00	388.42	141.61
c124759_g1_i2	1124.00	115.75	102.98
c124759_g2_i6	1252.00	160.27	128.01
c124759_g3_i1	207.00	43.41	209.69
c124782_g2_i1	359.00	166.94	465.02
c124782_g3_i1	295.00	84.58	286.73
c124790_g2_i1	948.00	101.28	106.84
c124790_g2_i4	1955.00	253.75	129.80
c124792_g1_i2	339.00	53.42	157.59
c124795_g18_i1	394.00	116.86	296.60
c124826_g1_i1	230.00	26.71	116.14
c124826_g2_i1	1027.00	498.61	485.50
c124849_g1_i1	1112.00	372.84	335.29
c124849_g2_i2	1634.00	204.78	125.33
c124849_g3_i1	716.00	76.79	107.25
c124855_g1_i1	2170.00	109.07	50.26
c124872_g1_i1	225.00	64.55	286.90
c124872_g2_i1	1379.00	170.28	123.48

c124872_g5_i1	239.00	48.97	204.90
c124877_g1_i1	248.00	152.48	614.82
c124877_g2_i1	706.00	444.07	628.99
c124877_g3_i1	377.00	208.12	552.05
c124877_g4_i1	470.00	279.35	594.37
c124897_g1_i1	616.00	205.90	334.25
c124906_g1_i4	1482.00	242.63	163.71
c124939_g5_i2	208.00	93.49	449.46
c124939_g6_i2	256.00	86.81	339.10
c124997_g3_i1	2020.00	291.60	144.35
c125010_g1_i1	482.00	258.21	535.70
c125010_g3_i1	455.00	475.23	1044.47
c125010_g5_i1	349.00	143.57	411.38
c125024_g2_i1	661.00	83.47	126.28
c125053_g1_i2	587.00	179.19	305.26
c125061_g1_i1	800.00	261.55	326.93
c125061_g4_i1	228.00	54.53	239.19
c125080_g1_i1	230.00	80.13	348.40
c125080_g2_i5	529.00	62.33	117.82
c125080_g4_i1	299.00	609.90	2039.80
c125092_g1_i1	770.00	87.92	114.19
c125092_g1_i4	1593.00	395.10	248.02
c125092_g1_i6	833.00	121.31	145.63
c125117_g3_i1	206.00	63.44	307.95
c125117_g4_i1	593.00	75.68	127.62
c125117_g4_i2	429.00	61.21	142.69
c125117_g6_i1	1153.00	153.59	133.21
c125137_g2_i2	507.00	73.46	144.88
c125138_g1_i1	784.00	133.56	170.35
c125168_g2_i3	779.00	81.25	104.30
c125168_g4_i1	425.00	56.76	133.56
c125168_g7_i1	1492.00	106.84	71.61
c125207_g1_i1	248.00	30.05	121.17
c125219_g10_i1	223.00	52.31	234.57
c125260_g1_i1	554.00	58.99	106.47
c125338_g2_i2	527.00	57.87	109.82
c125338_g3_i1	652.00	149.14	228.74
c125338_g4_i1	498.00	186.98	375.46
c125356_g1_i4	250.00	86.81	347.24
c125359_g1_i1	367.00	40.07	109.17
c125359_g1_i2	486.00	56.76	116.79
c125366_g3_i1	1288.00	170.28	132.21
c125373_g1_i1	229.00	112.41	490.87

c125373_g2_i1	723.00	761.26	1052.92
c125373_g3_i1	251.00	55.65	221.71
c125374_g4_i1	972.00	120.20	123.66
c125378_g1_i3	1801.00	133.56	74.16
c125476_g1_i2	1051.00	144.68	137.66
c125479_g2_i1	466.00	50.08	107.47
c125484_g6_i1	885.00	90.15	101.86
c1254_g1_i1	252.00	48.97	194.33
c125517_g1_i1	225.00	31.16	138.50
c125517_g9_i1	425.00	52.31	123.08
c125522_g1_i1	2465.00	684.47	277.68
c125535_g2_i1	546.00	81.25	148.80
c125606_g5_i1	319.00	44.52	139.56
c125608_g1_i3	1364.00	120.20	88.12
c125616_g1_i1	1439.00	339.45	235.89
c125616_g1_i2	715.00	757.92	1060.03
c125637_g1_i1	357.00	46.74	130.94
c125637_g4_i1	251.00	33.39	133.02
c125646_g1_i1	4708.00	191.43	40.66
c125693_g2_i1	419.00	84.58	201.87
c125693_g3_i1	3337.00	890.37	266.82
c125708_g2_i1	698.00	94.60	135.53
c125708_g2_i2	1988.00	393.99	198.18
c125741_g1_i2	3692.00	231.50	62.70
c125764_g2_i1	429.00	207.01	482.54
c125789_g1_i1	253.00	286.03	1130.55
c125789_g2_i2	2255.00	327.21	145.10
c125789_g3_i1	307.00	44.52	145.01
c125825_g1_i1	243.00	92.38	380.15
c125833_g3_i1	317.00	159.15	502.06
c125833_g4_i1	209.00	150.25	718.90
c125913_g4_i2	1586.00	269.34	169.82
c125913_g4_i3	399.00	140.23	351.46
c125913_g7_i4	2454.00	270.45	110.21
c125913_g9_i1	479.00	72.34	151.03
c125918_g1_i1	1562.00	168.06	107.59
c125961_g1_i1	985.00	751.25	762.69
c125983_g1_i1	1123.00	429.60	382.55
c125983_g2_i1	2939.00	1129.65	384.37
c126010_g4_i1	714.00	81.25	113.79
c126051_g1_i1	1826.00	266.00	145.67
c126051_g2_i1	1818.00	264.88	145.70
c126051_g3_i1	2549.00	457.43	179.45

c126073_g10_i1	1197.00	141.35	118.08
c126075_g1_i2	1652.00	385.08	233.10
c126075_g3_i1	1069.00	1642.73	1536.69
c126107_g1_i1	263.00	45.63	173.50
c126107_g5_i1	940.00	155.81	165.76
c126138_g2_i1	282.00	80.13	284.16
c126138_g2_i2	841.00	176.96	210.42
c126142_g2_i1	700.00	79.02	112.89
c126149_g1_i1	3785.00	121.31	32.05
c126157_g1_i1	516.00	81.25	157.45
c126165_g1_i2	3343.00	100.17	29.96
c126171_g2_i6	456.00	129.10	283.12
c126175_g3_i1	476.00	91.26	191.73
c126187_g3_i1	224.00	26.71	119.25
c126225_g3_i1	868.00	156.93	180.79
c126228_g1_i1	754.00	152.48	202.22
c126228_g2_i1	1308.00	858.09	656.03
c126228_g3_i1	747.00	248.19	332.25
c126232_g1_i1	3942.00	257.09	65.22
c126238_g2_i3	2196.00	185.86	84.64
c126248_g2_i1	2706.00	169.17	62.52
c126250_g1_i1	448.00	53.42	119.25
c126252_g1_i2	1998.00	639.95	320.30
c126255_g1_i2	1422.00	188.09	132.27
c126264_g1_i2	668.00	90.15	134.95
c126264_g1_i4	1278.00	224.82	175.91
c126274_g1_i1	554.00	205.90	371.66
c126287_g3_i7	306.00	31.16	101.84
c126288_g4_i1	254.00	75.68	297.96
c126288_g6_i1	397.00	235.95	594.33
c126288_g7_i1	226.00	111.30	492.46
c126289_g2_i1	889.00	184.75	207.82
c126316_g1_i1	370.00	55.65	150.40
c126325_g1_i1	1781.00	172.51	96.86
c126325_g2_i1	1883.00	168.06	89.25
c126325_g3_i1	241.00	91.26	378.68
c126327_g3_i4	652.00	191.43	293.60
c126331_g1_i1	1190.00	501.94	421.80
c126336_g7_i4	477.00	75.68	158.66
c126336_g8_i1	561.00	148.02	263.86
c126340_g2_i1	313.00	50.08	160.01
c126358_g1_i1	549.00	192.54	350.71
c126358_g1_i3	308.00	141.35	458.91

c126358_g2_i1	556.00	136.89	246.21
c126385_g1_i1	1462.00	219.25	149.97
c126392_g1_i1	226.00	64.55	285.63
c126392_g2_i1	893.00	606.56	679.24
c126415_g5_i2	347.00	132.44	381.68
c126459_g2_i1	964.00	140.23	145.47
c126459_g2_i3	1874.00	209.24	111.65
c126494_g1_i1	304.00	92.38	303.87
c126497_g1_i1	775.00	144.68	186.69
c126497_g2_i1	933.00	115.75	124.06
c126507_g1_i5	241.00	43.41	180.11
c126518_g1_i1	937.00	1366.71	1458.60
c126518_g1_i2	908.00	1002.77	1104.38
c126518_g1_i3	658.00	845.85	1285.48
c126528_g4_i5	3194.00	142.46	44.60
c126539_g6_i2	711.00	159.15	223.84
c126552_g1_i1	2328.00	209.24	89.88
c126552_g2_i1	817.00	203.67	249.29
c126552_g3_i1	1505.00	249.30	165.65
c126552_g5_i1	4142.00	2607.66	629.57
c126563_g1_i2	827.00	203.67	246.28
c126563_g2_i1	505.00	185.86	368.05
c126564_g1_i1	245.00	66.78	272.56
c126566_g2_i1	1945.00	398.44	204.85
c126568_g3_i1	1804.00	163.61	90.69
c126568_g5_i1	4939.00	259.32	52.50
c126589_g1_i1	321.00	54.53	169.89
c126589_g2_i1	1430.00	1228.70	859.23
c126589_g3_i1	232.00	205.90	887.49
c126589_g4_i1	241.00	26.71	110.83
c126614_g1_i2	552.00	269.34	487.93
c126632_g5_i2	1232.00	115.75	93.95
c126641_g1_i1	274.00	37.84	138.10
c126664_g4_i4	3184.00	248.19	77.95
c126708_g1_i1	297.00	37.84	127.41
c126708_g1_i2	1186.00	106.84	90.09
c126708_g1_i3	1334.00	283.80	212.75
c126711_g1_i4	247.00	28.94	117.15
c126719_g2_i1	1016.00	404.00	397.64
c126725_g1_i3	1515.00	277.13	182.92
c126725_g1_i5	1073.00	145.80	135.88
c126725_g2_i1	205.00	37.84	184.59
c126725_g4_i1	992.00	294.93	297.31

c126725_g5_i1	228.00	119.09	522.31
c126745_g1_i1	453.00	251.53	555.25
c126745_g2_i1	457.00	1179.73	2581.48
c126745_g3_i1	265.00	44.52	167.99
c126745_g3_i5	310.00	42.29	136.43
c126745_g3_i8	1177.00	362.82	308.26
c126745_g4_i1	247.00	524.20	2122.28
c126745_g5_i1	239.00	527.54	2207.29
c126749_g3_i2	585.00	83.47	142.69
c126760_g2_i1	1049.00	1245.40	1187.23
c126760_g2_i2	208.00	33.39	160.52
c126760_g2_i4	1704.00	449.64	263.87
c126784_g2_i7	1280.00	405.12	316.50
c126784_g3_i1	375.00	47.86	127.62
c126791_g5_i2	230.00	38.95	169.36
c126807_g2_i1	337.00	37.84	112.29
c126825_g1_i1	853.00	340.57	399.26
c126825_g1_i2	1983.00	241.51	121.79
c126825_g2_i1	282.00	201.45	714.35
c126830_g1_i2	1093.00	1887.58	1726.97
c126834_g1_i1	964.00	134.67	139.70
c126834_g2_i2	1243.00	290.48	233.69
c126834_g2_i5	1351.00	311.63	230.67
c126834_g2_i6	776.00	102.39	131.95
c126834_g3_i2	854.00	129.10	151.18
c126859_g1_i2	1983.00	111.30	56.12
c126864_g2_i2	975.00	160.27	164.38
c126876_g2_i1	2896.00	1285.47	443.88
c126876_g4_i1	560.00	82.36	147.07
c126876_g6_i1	226.00	67.89	300.40
c126884_g1_i3	2076.00	122.43	58.97
c126894_g1_i14	434.00	116.86	269.26
c126894_g1_i2	873.00	888.14	1017.34
c126894_g1_i3	491.00	544.24	1108.42
c126894_g1_i7	528.00	1570.38	2974.21
c126894_g1_i9	613.00	381.74	622.75
c126995_g1_i1	710.00	75.68	106.59
c127002_g1_i6	5727.00	4078.99	712.24
c127017_g5_i1	804.00	255.98	318.38
c127018_g1_i1	679.00	229.27	337.66
c127021_g1_i1	752.00	534.22	710.40
c127021_g2_i1	433.00	148.02	341.86
c127021_g5_i3	3007.00	225.93	75.13

c127040_g2_i1	302.00	41.18	136.36
c127046_g1_i2	3984.00	816.91	205.05
c127062_g1_i1	1088.00	763.49	701.74
c127065_g2_i1	300.00	41.18	137.27
c127099_g12_i1	226.00	35.61	157.59
c127112_g5_i1	1108.00	171.40	154.69
c127117_g2_i2	1884.00	552.03	293.01
c127122_g1_i1	1187.00	217.03	182.84
c127122_g1_i2	283.00	42.29	149.44
c127122_g1_i3	530.00	65.66	123.90
c127140_g3_i1	2961.00	1176.40	397.30
c127140_g4_i1	233.00	125.76	539.76
c127148_g1_i1	705.00	195.88	277.85
c127176_g3_i1	838.00	146.91	175.31
c127176_g4_i5	531.00	165.83	312.30
c127197_g5_i1	347.00	37.84	109.05
c127208_g1_i3	383.00	54.53	142.39
c127217_g1_i4	4294.00	123.54	28.77
c127227_g2_i1	1956.00	154.70	79.09
c127251_g1_i1	1989.00	101.28	50.92
c127265_g1_i1	906.00	92.38	101.96
c127265_g2_i1	213.00	28.94	135.85
c127277_g8_i1	669.00	75.68	113.13
c127278_g2_i11	367.00	56.76	154.66
c127293_g6_i1	300.00	46.74	155.81
c127293_g8_i1	885.00	202.56	228.88
c127293_g9_i1	682.00	235.95	345.96
c127297_g1_i5	362.00	42.29	116.83
c127297_g1_i6	1086.00	103.51	95.31
c127297_g2_i1	237.00	41.18	173.75
c127325_g11_i1	366.00	56.76	155.08
c127325_g2_i1	263.00	178.07	677.08
c127325_g2_i2	736.00	766.83	1041.89
c127325_g3_i1	1253.00	957.14	763.88
c127325_g4_i1	472.00	340.57	721.54
c127325_g5_i1	250.00	481.91	1927.64
c127325_g6_i1	853.00	127.99	150.05
c127329_g4_i4	225.00	62.33	277.00
c127330_g1_i1	1676.00	119.09	71.05
c127352_g4_i1	606.00	77.91	128.56
c127357_g1_i7	388.00	229.27	590.90
c127357_g1_i8	652.00	94.60	145.09
c127363_g1_i2	742.00	809.12	1090.46

c127363_g1_i4	214.00	26.71	124.82
c127363_g5_i2	472.00	404.00	855.94
c127367_g2_i2	2728.00	1084.02	397.37
c127372_g1_i4	1270.00	493.04	388.22
c127372_g3_i1	370.00	82.36	222.59
c127372_g5_i1	929.00	564.27	607.39
c127375_g2_i1	616.00	67.89	110.21
c127375_g2_i4	637.00	431.83	677.91
c127375_g3_i1	385.00	593.21	1540.80
c127388_g7_i1	819.00	182.53	222.86
c127392_g2_i1	263.00	44.52	169.27
c127402_g1_i1	1220.00	175.85	144.14
c127459_g11_i1	3302.00	134.67	40.78
c127470_g4_i7	2333.00	232.61	99.70
c127475_g1_i3	745.00	77.91	104.57
c127508_g3_i2	932.00	140.23	150.46
c127508_g4_i1	1295.00	408.46	315.41
c127531_g4_i1	313.00	71.23	227.57
c127531_g5_i1	739.00	164.72	222.89
c127551_g1_i1	2139.00	923.76	431.86
c127568_g2_i1	530.00	540.90	1020.56
c127568_g3_i1	886.00	101.28	114.31
c127568_g5_i1	226.00	114.64	507.23
c127576_g1_i1	261.00	130.22	498.91
c127576_g1_i3	497.00	1286.58	2588.69
c127576_g1_i4	474.00	124.65	262.98
c127582_g3_i1	467.00	53.42	114.39
c127654_g5_i2	1871.00	101.28	54.13
c127659_g2_i2	420.00	145.80	347.14
c127659_g2_i3	551.00	56.76	103.01
c127679_g3_i1	203.00	61.21	301.54
c127686_g2_i1	976.00	111.30	114.03
c127686_g3_i1	623.00	1067.33	1713.20
c127686_g4_i1	1095.00	317.19	289.67
c127686_g4_i4	391.00	135.78	347.27
c127686_g5_i1	362.00	101.28	279.78
c127689_g5_i1	464.00	85.70	184.69
c127732_g6_i1	385.00	83.47	216.81
c127741_g2_i1	204.00	73.46	360.07
c127762_g3_i1	988.00	116.86	118.28
c127762_g3_i2	211.00	33.39	158.24
c127762_g5_i1	323.00	35.61	110.26
c127833_g2_i8	385.00	80.13	208.14

c127860_g3_i3	2738.00	670.00	244.70
c127869_g1_i3	553.00	66.78	120.76
c127869_g2_i1	826.00	2100.15	2542.56
c127869_g2_i10	229.00	201.45	879.67
c127869_g2_i11	1029.00	397.33	386.13
c127869_g2_i12	1092.00	791.31	724.65
c127869_g2_i13	977.00	357.26	365.67
c127869_g2_i3	1321.00	445.18	337.01
c127869_g2_i4	557.00	1431.26	2569.59
c127869_g2_i5	417.00	82.36	197.50
c127869_g2_i6	1333.00	458.54	343.99
c127869_g2_i7	379.00	54.53	143.89
c127869_g2_i8	1029.00	117.97	114.65
c127869_g3_i1	625.00	300.50	480.80
c127869_g4_i1	268.00	590.98	2205.15
c127872_g1_i2	2603.00	356.15	136.82
c127888_g1_i1	6795.00	143.57	21.13
c127919_g1_i1	626.00	106.84	170.68
c127922_g2_i1	4093.00	283.80	69.34
c127937_g2_i1	590.00	95.71	162.23
c127943_g2_i1	1034.00	438.51	424.09
c127943_g3_i2	1832.00	505.28	275.81
c127943_g5_i1	581.00	449.64	773.90
c127944_g2_i1	845.00	91.26	108.00
c127951_g2_i1	246.00	72.34	294.07
c127951_g2_i3	1237.00	133.56	107.97
c127952_g1_i5	1047.00	250.42	239.17
c127952_g1_i6	443.00	46.74	105.52
c127952_g1_i7	585.00	125.76	214.98
c127960_g1_i1	230.00	52.31	227.43
c127960_g2_i1	1537.00	593.21	385.95
c127973_g4_i3	1172.00	110.18	94.01
c127973_g4_i4	798.00	89.04	111.58
c127977_g11_i1	345.00	271.56	787.14
c127977_g13_i1	287.00	718.97	2505.12
c127977_g2_i1	729.00	1361.15	1867.14
c127977_g2_i2	245.00	1186.41	4842.50
c127977_g3_i1	735.00	938.22	1276.49
c127977_g3_i2	974.00	1022.81	1050.11
c127977_g3_i3	268.00	133.56	498.34
c127977_g4_i1	562.00	530.88	944.63
c127977_g5_i1	485.00	330.55	681.54
c127977_g6_i1	849.00	258.21	304.13

c127981_g1_i3	786.00	572.06	727.81
c127981_g2_i1	217.00	34.50	158.99
c127981_g3_i1	323.00	238.17	737.38
c128012_g1_i1	212.00	45.63	215.24
c128012_g2_i1	5401.00	496.38	91.91
c128017_g1_i5	3028.00	270.45	89.32
c128064_g1_i1	498.00	190.32	382.16
c12807_g2_i1	297.00	44.52	149.89
c128144_g5_i2	607.00	81.25	133.85
c128146_g1_i1	1130.00	283.80	251.15
c128146_g1_i2	1103.00	113.52	102.92
c128147_g2_i1	425.00	75.68	178.07
c128149_g2_i4	374.00	92.38	246.99
c128168_g3_i1	357.00	43.41	121.58
c128174_g2_i2	2084.00	212.58	102.00
c128179_g4_i4	2122.00	397.33	187.24
c128196_g10_i1	397.00	417.36	1051.28
c128196_g11_i1	1148.00	1087.36	947.18
c128196_g1_i1	399.00	451.86	1132.48
c128196_g2_i2	277.00	27.82	100.45
c128196_g3_i1	756.00	1350.02	1785.74
c128196_g4_i1	368.00	202.56	550.43
c128196_g5_i1	706.00	411.79	583.28
c128196_g6_i1	614.00	1167.49	1901.45
c128196_g6_i2	1389.00	222.59	160.25
c128196_g7_i1	241.00	70.12	290.94
c128196_g8_i1	348.00	112.41	323.01
c128196_g9_i1	909.00	174.73	192.23
c128197_g2_i1	3886.00	122.43	31.50
c128212_g3_i1	1007.00	365.05	362.51
c128215_g1_i1	1819.00	136.89	75.26
c128215_g4_i1	2142.00	242.63	113.27
c128220_g1_i2	2089.00	468.56	224.30
c128220_g1_i3	453.00	46.74	103.19
c128220_g3_i1	1580.00	242.63	153.56
c128220_g6_i1	379.00	152.48	402.31
c128220_g8_i1	211.00	50.08	237.36
c128232_g2_i8	278.00	27.82	100.09
c128251_g1_i1	379.00	261.55	690.09
c128251_g2_i1	2606.00	270.45	103.78
c128251_g2_i2	2741.00	172.51	62.94
c128269_g14_i1	245.00	87.92	358.87
c128269_g15_i1	321.00	55.65	173.36

c128269_g6_i3	276.00	111.30	403.25
c128269_g7_i1	321.00	81.25	253.10
c128283_g4_i1	762.00	90.15	118.31
c128285_g1_i1	514.00	121.31	236.02
c128285_g2_i2	788.00	119.09	151.13
c128285_g2_i3	690.00	288.26	417.76
c128285_g2_i4	2716.00	1000.55	368.39
c128285_g3_i1	1303.00	342.79	263.08
c128285_g4_i1	1420.00	1508.06	1062.01
c128286_g1_i2	603.00	134.67	223.33
c128286_g2_i2	313.00	33.39	106.67
c128286_g6_i1	209.00	34.50	165.08
c128292_g1_i1	288.00	31.16	108.20
c12829_g1_i1	487.00	87.92	180.54
c128312_g1_i1	273.00	97.94	358.76
c128312_g2_i2	2379.00	383.97	161.40
c128312_g3_i5	972.00	168.06	172.90
c128312_g3_i6	3421.00	1421.25	415.45
c128317_g1_i1	1994.00	106.84	53.58
c128336_g1_i1	2517.00	212.58	84.46
c128336_g4_i1	402.00	132.44	329.46
c128336_g5_i1	1329.00	400.67	301.48
c128336_g6_i1	394.00	172.51	437.84
c128349_g1_i1	245.00	642.18	2621.13
c128349_g2_i1	255.00	846.96	3321.41
c128349_g3_i1	2489.00	3666.08	1472.91
c128349_g4_i1	451.00	1426.81	3163.66
c128353_g1_i1	2313.00	164.72	71.21
c128363_g3_i1	1942.00	103.51	53.30
c128366_g1_i3	1737.00	204.78	117.90
c128375_g2_i1	222.00	60.10	270.72
c128390_g2_i2	379.00	131.33	346.51
c128390_g6_i1	668.00	1286.58	1926.02
c128392_g6_i1	341.00	54.53	159.93
c128403_g2_i1	2414.00	253.75	105.12
c128422_g1_i2	1492.00	121.31	81.31
c128436_g3_i5	904.00	221.48	245.00
c128440_g1_i1	898.00	538.67	599.86
c128440_g2_i1	242.00	47.86	197.76
c128440_g3_i1	244.00	45.63	187.01
c128440_g4_i4	1334.00	166.94	125.15
c128459_g7_i1	685.00	127.99	186.85
c128459_g9_i2	219.00	37.84	172.79

c128492_g1_i1	559.00	260.43	465.89
c128492_g3_i2	2557.00	802.44	313.82
c128492_g4_i3	357.00	38.95	109.11
c128495_g2_i1	1255.00	223.70	178.25
c128495_g2_i2	237.00	70.12	295.85
c128495_g2_i3	1255.00	185.86	148.10
c128499_g5_i1	223.00	53.42	239.56
c128510_g1_i1	1054.00	1313.29	1246.01
c128510_g1_i3	472.00	441.84	936.11
c128510_g1_i5	1623.00	565.38	348.36
c128510_g1_i7	1368.00	1501.38	1097.50
c128510_g3_i1	536.00	97.94	182.72
c128510_g3_i2	537.00	314.97	586.53
c128512_g5_i1	290.00	156.93	541.13
c128530_g6_i3	1669.00	149.14	89.36
c128553_g2_i1	960.00	897.04	934.42
c128553_g2_i2	636.00	74.57	117.25
c128553_g4_i1	1110.00	1240.95	1117.97
c128553_g5_i1	541.00	72.34	133.72
c128561_g1_i1	730.00	471.89	646.43
c128561_g2_i2	620.00	309.40	499.04
c128561_g3_i2	1544.00	988.31	640.10
c128561_g4_i1	1196.00	415.13	347.10
c128561_g5_i1	301.00	45.63	151.60
c128566_g2_i1	632.00	72.34	114.47
c128570_g2_i1	456.00	65.66	144.00
c128584_g2_i1	220.00	28.94	131.53
c128605_g1_i2	452.00	63.44	140.35
c128610_g1_i1	574.00	148.02	257.88
c128610_g1_i2	2487.00	2698.92	1085.21
c128610_g1_i5	1515.00	459.65	303.40
c128610_g1_i6	278.00	360.60	1297.12
c128610_g5_i1	642.00	409.57	637.96
c128610_g9_i1	326.00	865.88	2656.08
c128618_g1_i2	1366.00	141.35	103.47
c128658_g3_i2	1570.00	312.74	199.20
c128660_g1_i1	240.00	262.66	1094.41
c128660_g2_i8	5442.00	1174.17	215.76
c128674_g1_i1	4081.00	626.60	153.54
c128680_g2_i3	210.00	25.60	121.90
c128680_g5_i1	1048.00	278.24	265.50
c128693_g4_i1	3442.00	259.32	75.34
c128703_g1_i1	1044.00	643.29	616.18

c128703_g2_i3	4008.00	461.88	115.24
c128703_g3_i1	366.00	199.22	544.32
c128714_g5_i1	203.00	23.37	115.13
c128718_g2_i1	1420.00	362.82	255.51
c128724_g1_i2	892.00	320.53	359.34
c128724_g1_i3	557.00	248.19	445.58
c128724_g1_i4	506.00	109.07	215.55
c128724_g1_i5	1827.00	772.39	422.77
c128724_g1_i6	494.00	1194.20	2417.42
c128724_g2_i1	414.00	94.60	228.51
c128724_g2_i3	240.00	349.47	1456.12
c128728_g1_i2	3011.00	292.71	97.21
c128737_g2_i1	803.00	156.93	195.43
c128739_g1_i5	763.00	228.16	299.03
c128752_g5_i1	478.00	52.31	109.43
c128780_g2_i6	225.00	33.39	148.39
c128799_g10_i1	427.00	231.50	542.14
c128799_g4_i1	705.00	110.18	156.29
c128803_g1_i1	502.00	70.12	139.67
c128803_g1_i3	798.00	200.33	251.04
c128817_g1_i3	339.00	92.38	272.49
c128821_g3_i1	997.00	125.76	126.14
c128829_g1_i1	2344.00	555.37	236.93
c128829_g1_i2	2981.00	383.97	128.81
c128829_g1_i5	1049.00	648.85	618.55
c128829_g1_i6	2100.00	1515.85	721.83
c128829_g2_i7	1628.00	267.11	164.07
c128829_g3_i2	1082.00	111.30	102.86
c128829_g4_i1	589.00	91.26	154.95
c128829_g6_i1	369.00	393.99	1067.72
c128834_g2_i1	1946.00	528.66	271.66
c128836_g3_i1	506.00	201.45	398.11
c128861_g5_i6	930.00	156.93	168.74
c128861_g8_i1	866.00	136.89	158.08
c128861_g8_i2	519.00	65.66	126.52
c128868_g1_i1	437.00	104.62	239.40
c128868_g2_i1	261.00	34.50	132.19
c128868_g3_i1	443.00	369.50	834.09
c128868_g3_i2	511.00	220.37	431.24
c128868_g3_i3	217.00	37.84	174.38
c128868_g4_i1	302.00	52.31	173.21
c128868_g5_i2	243.00	56.76	233.58
c128868_g7_i1	363.00	80.13	220.75

c128883_g1_i1	2707.00	151.36	55.92
c128883_g3_i1	223.00	62.33	279.49
c128945_g1_i1	1785.00	143.57	80.43
c128962_g2_i1	464.00	145.80	314.22
c128962_g3_i1	488.00	218.14	447.01
c128973_g1_i3	1987.00	747.91	376.40
c128989_g1_i1	2729.00	566.50	207.58
c128998_g1_i1	804.00	191.43	238.10
c128998_g3_i1	439.00	103.51	235.78
c128998_g5_i1	516.00	52.31	101.37
c129006_g3_i1	242.00	76.79	317.33
c129006_g4_i1	253.00	122.43	483.90
c129026_g2_i1	1360.00	2200.32	1617.88
c129030_g3_i1	444.00	70.12	157.92
c129043_g1_i1	2916.00	314.97	108.01
c129046_g1_i1	297.00	48.97	164.88
c129046_g3_i4	837.00	84.58	101.06
c129048_g2_i3	3599.00	622.14	172.87
c129063_g2_i1	1392.00	589.87	423.76
c129063_g2_i2	390.00	112.41	288.23
c129063_g2_i3	3209.00	4329.40	1349.14
c129063_g2_i5	1015.00	808.01	796.07
c129063_g2_i6	752.00	438.51	583.12
c129063_g2_i7	861.00	476.35	553.25
c129063_g2_i8	305.00	58.99	193.40
c129064_g1_i2	1793.00	473.01	263.81
c129070_g1_i1	367.00	43.41	118.27
c129080_g4_i1	843.00	121.31	143.91
c129103_g1_i1	252.00	41.18	163.41
c129116_g2_i1	300.00	38.95	129.85
c129116_g5_i1	735.00	302.72	411.87
c129116_g6_i1	523.00	288.26	551.16
c129117_g2_i1	323.00	319.42	988.91
c129129_g1_i1	224.00	120.20	536.60
c129133_g1_i1	2055.00	1662.76	809.13
c129133_g2_i1	377.00	181.41	481.20
c129136_g2_i3	378.00	48.97	129.55
c129136_g4_i1	323.00	81.25	251.54
c129141_g1_i2	558.00	63.44	113.69
c129141_g1_i4	528.00	76.79	145.44
c12914_g2_i1	371.00	41.18	111.00
c129183_g2_i1	3350.00	107.96	32.23
c129225_g1_i3	2996.00	884.80	295.33

c129225_g2_i1	501.00	231.50	462.07
c129236_g1_i2	791.00	309.40	391.15
c129236_g1_i3	218.00	76.79	352.27
c129236_g1_i4	320.00	212.58	664.30
c129236_g2_i1	306.00	119.09	389.17
c129236_g2_i2	251.00	53.42	212.84
c129246_g1_i2	1249.00	100.17	80.20
c129248_g1_i3	3739.00	194.77	52.09
c129257_g3_i1	946.00	282.69	298.83
c129261_g7_i1	414.00	61.21	147.86
c129264_g5_i1	298.00	48.97	164.33
c129274_g1_i2	3708.00	171.40	46.22
c129281_g1_i1	282.00	47.86	169.71
c129281_g3_i1	1881.00	511.96	272.18
c129283_g1_i1	1881.00	324.98	172.77
c12928_g1_i1	864.00	339.45	392.88
c129300_g11_i1	234.00	31.16	133.17
c129300_g6_i1	640.00	189.20	295.63
c129300_g8_i1	702.00	133.56	190.25
c129307_g3_i2	607.00	70.12	115.51
c129312_g1_i7	864.00	132.44	153.29
c129315_g1_i1	1227.00	592.09	482.55
c129315_g1_i4	897.00	1382.29	1541.02
c129336_g1_i2	270.00	56.76	210.23
c129336_g2_i1	275.00	35.61	129.51
c129336_g8_i1	404.00	101.28	250.69
c129339_g12_i1	236.00	31.16	132.05
c129346_g1_i1	246.00	64.55	262.41
c129346_g1_i2	1340.00	131.33	98.01
c129346_g1_i3	416.00	129.10	310.34
c129361_g2_i1	758.00	81.25	107.19
c129361_g3_i1	295.00	64.55	218.82
c129361_g4_i1	1903.00	172.51	90.65
c129363_g5_i1	1551.00	1500.27	967.29
c129363_g5_i7	1210.00	170.28	140.73
c129371_g1_i3	584.00	400.67	686.07
c129371_g1_i6	1238.00	122.43	98.89
c129392_g1_i1	345.00	57.87	167.75
c129392_g1_i2	219.00	46.74	213.44
c129406_g1_i1	2055.00	173.62	84.49
c129406_g1_i3	1827.00	284.92	155.95
c129411_g1_i3	1008.00	462.99	459.32
c129411_g3_i1	987.00	339.45	343.92

c129415_g1_i1	2728.00	725.65	266.00
c129417_g5_i3	1844.00	510.85	277.03
c129464_g1_i1	351.00	35.61	101.47
c129464_g1_i3	387.00	178.07	460.14
c129464_g2_i1	355.00	164.72	463.99
c129464_g2_i3	393.00	47.86	121.77
c129470_g3_i1	235.00	87.92	374.14
c129470_g5_i2	556.00	86.81	156.13
c129470_g8_i1	1370.00	122.43	89.36
c129473_g1_i1	1147.00	693.37	604.51
c129473_g2_i2	1813.00	351.70	193.99
c129473_g3_i1	221.00	31.16	141.01
c129473_g4_i1	427.00	62.33	145.96
c129476_g1_i1	885.00	442.96	500.52
c129476_g3_i1	686.00	133.56	194.69
c129476_g4_i1	441.00	238.17	540.08
c129476_g5_i1	250.00	97.94	391.76
c129484_g1_i1	4335.00	400.67	92.43
c129485_g1_i1	901.00	606.56	673.21
c129492_g6_i1	437.00	72.34	165.54
c129504_g2_i2	1782.00	294.93	165.51
c129525_g10_i2	769.00	130.22	169.33
c129527_g3_i1	496.00	90.15	181.75
c129532_g2_i1	302.00	66.78	221.12
c129533_g1_i3	1506.00	176.96	117.50
c129533_g1_i4	1495.00	111.30	74.45
c129540_g2_i1	796.00	516.41	648.76
c129540_g2_i2	469.00	95.71	204.08
c129540_g2_i3	391.00	55.65	142.32
c129540_g2_i4	332.00	271.56	817.96
c129540_g4_i1	473.00	101.28	214.12
c129547_g2_i1	1274.00	231.50	181.71
c129549_g8_i1	264.00	112.41	425.79
c129555_g3_i1	311.00	56.76	182.51
c129556_g1_i1	373.00	62.33	167.09
c129565_g2_i3	2518.00	917.08	364.21
c129571_g4_i1	4651.00	578.74	124.43
c129571_g4_i3	3545.00	189.20	53.37
c129571_g6_i1	491.00	69.00	140.54
c129572_g1_i2	1212.00	173.62	143.25
c129572_g2_i1	302.00	81.25	269.03
c129572_g3_i1	1636.00	414.02	253.07
c129572_g4_i1	3567.00	133.56	37.44

c129572_g4_i2	4627.00	713.41	154.18
c129574_g1_i1	224.00	23.37	104.34
c129574_g2_i2	1375.00	560.93	407.95
c129574_g2_i3	784.00	184.75	235.65
c129583_g3_i1	650.00	67.89	104.45
c129583_g4_i1	649.00	73.46	113.18
c129588_g2_i1	1168.00	132.44	113.39
c129588_g7_i1	1202.00	205.90	171.30
c129596_g3_i10	2015.00	164.72	81.75
c129597_g1_i3	1752.00	120.20	68.61
c129616_g1_i2	898.00	251.53	280.10
c129616_g1_i3	2490.00	800.22	321.37
c129616_g2_i2	904.00	801.33	886.43
c129616_g2_i3	467.00	929.32	1989.98
c129616_g3_i1	548.00	535.33	976.88
c129616_g4_i1	839.00	182.53	217.55
c129619_g2_i1	4932.00	139.12	28.21
c129624_g4_i1	922.00	203.67	220.90
c129628_g1_i1	1454.00	632.16	434.77
c129628_g3_i1	633.00	123.54	195.16
c129628_g4_i1	1146.00	124.65	108.77
c129632_g3_i1	278.00	72.34	260.22
c129642_g2_i1	1448.00	299.39	206.76
c129646_g1_i1	258.00	27.82	107.85
c129656_g2_i1	208.00	22.26	107.02
c129656_g4_i2	250.00	40.07	160.27
c129656_g5_i2	364.00	126.88	348.56
c129656_g5_i3	233.00	149.14	640.07
c129656_g8_i1	773.00	396.21	512.57
c129656_g8_i4	274.00	51.20	186.85
c129656_g8_i6	472.00	95.71	202.79
c129666_g1_i6	755.00	254.87	337.57
c129670_g4_i1	2486.00	186.98	75.21
c129670_g6_i1	762.00	188.09	246.84
c129677_g1_i1	319.00	132.44	415.18
c129677_g3_i1	366.00	170.28	465.25
c129677_g5_i1	1425.00	302.72	212.44
c129679_g3_i1	699.00	214.80	307.30
c129684_g1_i1	528.00	469.67	889.52
c129684_g7_i1	440.00	666.66	1515.14
c129684_g8_i1	403.00	396.21	983.16
c129687_g1_i1	1130.00	103.51	91.60
c129687_g2_i4	3966.00	105.73	26.66

c129687_g3_i1	500.00	232.61	465.22
c129690_g2_i3	2308.00	176.96	76.67
c129690_g2_i4	3449.00	1631.60	473.06
c129690_g2_i5	880.00	142.46	161.89
c129690_g3_i1	892.00	191.43	214.61
c129692_g4_i7	544.00	135.78	249.60
c129698_g1_i3	1225.00	169.17	138.10
c129698_g2_i1	259.00	48.97	189.07
c129698_g3_i1	360.00	52.31	145.30
c129709_g5_i9	574.00	87.92	153.18
c129717_g1_i1	623.00	127.99	205.44
c129717_g6_i1	911.00	166.94	183.25
c129730_g4_i1	331.00	51.20	154.67
c129734_g4_i1	207.00	45.63	220.44
c129734_g7_i1	355.00	74.57	210.05
c129737_g4_i1	561.00	102.39	182.52
c129744_g1_i4	1172.00	112.41	95.91
c129744_g2_i1	754.00	621.03	823.65
c129744_g4_i2	276.00	110.18	399.21
c129756_g1_i1	897.00	310.52	346.17
c129763_g1_i1	1007.00	696.71	691.87
c129763_g3_i1	283.00	35.61	125.85
c129768_g1_i2	3447.00	385.08	111.72
c129776_g2_i6	349.00	69.00	197.72
c129783_g5_i1	229.00	74.57	325.63
c129802_g2_i1	540.00	301.61	558.54
c129802_g4_i1	255.00	112.41	440.82
c129802_g6_i1	854.00	101.28	118.59
c129806_g5_i1	280.00	54.53	194.77
c129815_g3_i2	2463.00	100.17	40.67
c129816_g2_i10	2185.00	260.43	119.19
c129816_g2_i2	908.00	253.75	279.47
c129818_g4_i3	522.00	93.49	179.10
c129825_g3_i2	2153.00	122.43	56.86
c129837_g1_i5	1469.00	125.76	85.61
c129841_g3_i1	788.00	191.43	242.93
c129848_g2_i1	2176.00	182.53	83.88
c129848_g3_i1	2163.00	792.43	366.36
c129849_g1_i3	474.00	101.28	213.67
c129850_g1_i1	254.00	82.36	324.25
c129855_g1_i4	2306.00	435.17	188.71
c129869_g3_i1	868.00	86.81	100.01
c129870_g5_i3	522.00	83.47	159.91

c129882_g1_i2	2317.00	546.46	235.85
c129885_g2_i1	2541.00	143.57	56.50
c129888_g1_i4	1694.00	114.64	67.67
c129892_g1_i3	5532.00	168.06	30.38
c129895_g1_i1	509.00	615.47	1209.17
c129895_g2_i2	1431.00	2752.34	1923.37
c129905_g5_i1	5593.00	101.28	18.11
c129918_g1_i2	606.00	109.07	179.98
c129918_g2_i2	2507.00	151.36	60.38
c129926_g3_i1	211.00	30.05	142.42
c129937_g1_i1	462.00	921.53	1994.65
c129937_g2_i1	677.00	81.25	120.01
c129937_g2_i2	448.00	46.74	104.34
c129937_g4_i1	1105.00	202.56	183.31
c129937_g4_i2	995.00	235.95	237.13
c129937_g4_i4	1146.00	180.30	157.33
c129937_g5_i1	877.00	2233.71	2546.98
c129940_g4_i1	227.00	44.52	196.12
c129940_g6_i2	2582.00	302.72	117.24
c129940_g7_i1	213.00	44.52	209.01
c129945_g1_i1	773.00	272.68	352.75
c129945_g1_i3	828.00	429.60	518.84
c129945_g2_i1	439.00	248.19	565.35
c129945_g3_i1	470.00	671.11	1427.90
c129950_g1_i1	276.00	200.33	725.84
c129950_g2_i2	1690.00	150.25	88.90
c129950_g3_i1	614.00	367.28	598.17
c129953_g2_i2	631.00	76.79	121.70
c129953_g2_i3	500.00	57.87	115.75
c129953_g3_i1	419.00	74.57	177.97
c129962_g1_i3	912.00	639.95	701.70
c129962_g1_i4	456.00	66.78	146.44
c129962_g1_i5	208.00	61.21	294.29
c129962_g2_i1	557.00	60.10	107.90
c129984_g2_i1	1143.00	390.65	341.77
c129992_g1_i2	264.00	28.94	109.61
c129995_g2_i3	5549.00	107.96	19.46
c129998_g1_i1	861.00	188.09	218.46
c130003_g4_i1	1138.00	1329.98	1168.70
c130003_g4_i2	1043.00	469.67	450.31
c130029_g1_i1	3165.00	257.09	81.23
c130032_g1_i1	2068.00	141.35	68.35
c130043_g1_i2	5765.00	131.33	22.78

c130054_g1_i1	682.00	1914.29	2806.87
c130055_g3_i1	228.00	81.25	356.34
c130058_g1_i1	237.00	634.39	2676.73
c130058_g1_i3	3136.00	5778.47	1842.63
c130058_g2_i1	243.00	124.65	512.97
c130066_g1_i1	263.00	100.17	380.86
c130066_g2_i2	1521.00	245.96	161.71
c130066_g3_i1	418.00	97.94	234.31
c130066_g3_i2	753.00	87.92	116.76
c130066_g3_i4	1095.00	560.93	512.27
c130066_g3_i5	424.00	162.49	383.24
c130066_g4_i1	309.00	112.41	363.78
c130066_g5_i1	1489.00	130.22	87.45
c130067_g2_i1	202.00	237.06	1173.56
c130067_g2_i2	370.00	267.11	721.92
c130067_g2_i3	419.00	231.50	552.49
c130067_g4_i1	204.00	33.39	163.67
c130073_g1_i1	489.00	220.37	450.65
c130073_g2_i2	1067.00	220.37	206.53
c130073_g2_i3	1818.00	303.84	167.13
c130073_g2_i6	669.00	119.09	178.01
c130073_g5_i1	555.00	1834.15	3304.78
c130073_g6_i1	683.00	69.00	101.03
c130074_g1_i1	396.00	40.07	101.18
c13007_g1_i1	256.00	42.29	165.21
c130084_g1_i2	4704.00	243.74	51.82
c130086_g2_i1	243.00	66.78	274.80
c130086_g3_i1	371.00	105.73	284.99
c130086_g4_i1	353.00	54.53	154.49
c130086_g4_i2	1241.00	1088.47	877.09
c130086_g4_i5	726.00	220.37	303.53
c130087_g1_i1	340.00	65.66	193.13
c130087_g2_i1	812.00	81.25	100.06
c130087_g2_i2	1255.00	280.47	223.48
c130087_g2_i3	1753.00	703.39	401.25
c130087_g2_i4	1330.00	202.56	152.30
c130087_g2_i5	284.00	40.07	141.08
c130093_g5_i1	1175.00	257.09	218.80
c130104_g2_i1	1168.00	164.72	141.03
c130104_g2_i2	614.00	112.41	183.08
c130108_g9_i1	318.00	54.53	171.49
c130119_g1_i2	804.00	91.26	113.51
c130119_g1_i3	2176.00	139.12	63.93

c130121_g2_i2	268.00	52.31	195.18
c130121_g2_i4	1168.00	102.39	87.66
c130121_g2_i5	664.00	447.41	673.81
c130121_g2_i6	473.00	67.89	143.53
c130121_g3_i1	565.00	203.67	360.48
c130128_g5_i3	2396.00	182.53	76.18
c130137_g1_i1	500.00	1035.05	2070.10
c130137_g4_i2	379.00	227.04	599.06
c130137_g4_i3	720.00	221.48	307.61
c130137_g4_i4	2292.00	554.25	241.82
c130138_g1_i1	212.00	45.63	215.24
c130144_g1_i1	236.00	124.65	528.18
c130150_g1_i3	488.00	131.33	269.12
c130150_g1_i7	1070.00	1787.41	1670.48
c130150_g2_i1	332.00	52.31	157.56
c130150_g6_i1	300.00	80.13	267.11
c130152_g1_i1	11088.00	111.30	10.04
c130154_g6_i1	211.00	93.49	443.07
c130154_g7_i1	436.00	230.38	528.40
c130156_g1_i1	642.00	515.30	802.65
c130156_g1_i2	761.00	605.45	795.60
c130156_g2_i3	576.00	317.19	550.68
c130167_g3_i1	213.00	30.05	141.08
c130167_g7_i1	904.00	240.40	265.93
c130174_g1_i2	3122.00	725.65	232.43
c130185_g1_i3	2593.00	648.85	250.23
c130185_g4_i1	267.00	42.29	158.40
c130185_g5_i1	459.00	73.46	160.03
c130189_g1_i1	770.00	627.71	815.21
c130189_g1_i2	224.00	220.37	983.78
c130189_g1_i3	423.00	314.97	744.60
c130195_g1_i1	269.00	281.58	1046.76
c130195_g1_i2	280.00	134.67	480.96
c130195_g2_i1	738.00	267.11	361.94
c130195_g3_i2	2394.00	928.21	387.72
c130195_g3_i5	1172.00	350.58	299.13
c130200_g1_i2	4205.00	233.72	55.58
c130202_g1_i1	224.00	47.86	213.65
c130203_g1_i1	1921.00	268.22	139.63
c130203_g3_i1	854.00	525.32	615.12
c130205_g1_i1	1214.00	266.00	219.11
c130207_g2_i1	470.00	92.38	196.54
c130207_g2_i4	514.00	63.44	123.42

c130207_g2_i6	287.00	75.68	263.70
c130207_g4_i1	1315.00	1575.95	1198.44
c130210_g1_i2	2608.00	473.01	181.37
c130211_g2_i3	3783.00	149.14	39.42
c130219_g1_i1	3880.00	2161.36	557.05
c130220_g2_i3	2198.00	346.13	157.48
c130220_g3_i1	247.00	40.07	162.21
c130221_g1_i3	3332.00	227.04	68.14
c130233_g3_i1	4387.00	4003.31	912.54
c130235_g1_i1	233.00	34.50	148.08
c130237_g2_i1	221.00	95.71	433.10
c130237_g3_i1	456.00	469.67	1029.97
c130245_g2_i2	830.00	340.57	410.32
c130246_g1_i1	267.00	278.24	1042.09
c130246_g1_i3	267.00	46.74	175.07
c130246_g1_i4	338.00	66.78	197.57
c130246_g2_i3	324.00	99.05	305.72
c130246_g2_i4	1588.00	165.83	104.43
c130246_g4_i1	324.00	297.16	917.16
c130250_g5_i1	253.00	117.97	466.30
c130254_g1_i1	2252.00	183.64	81.54
c130256_g4_i2	3205.00	151.36	47.23
c130256_g5_i1	515.00	57.87	112.38
c130256_g6_i1	1610.00	1031.71	640.82
c130259_g1_i1	4306.00	6134.62	1424.67
c130259_g1_i2	467.00	582.08	1246.42
c130260_g1_i1	294.00	58.99	200.64
c130260_g1_i2	1085.00	308.29	284.14
c130260_g1_i3	359.00	65.66	182.91
c130260_g1_i4	596.00	63.44	106.44
c130260_g7_i2	415.00	96.83	233.32
c130262_g1_i10	1189.00	203.67	171.30
c130262_g1_i2	327.00	94.60	289.30
c130265_g2_i1	285.00	38.95	136.68
c130268_g2_i1	260.00	56.76	218.31
c130268_g3_i3	411.00	52.31	127.27
c130268_g3_i5	1236.00	341.68	276.44
c130268_g4_i1	417.00	238.17	571.16
c130268_g5_i2	275.00	70.12	254.97
c130268_g6_i1	268.00	169.17	631.23
c130273_g1_i3	598.00	125.76	210.31
c130273_g3_i1	282.00	227.04	805.12
c130273_g4_i1	390.00	90.15	231.15

c130273_g5_i1	756.00	282.69	373.93
c130276_g1_i1	579.00	85.70	148.01
c130276_g7_i1	288.00	28.94	100.48
c130277_g2_i1	1579.00	297.16	188.20
c130277_g2_i2	305.00	54.53	178.80
c130287_g2_i1	324.00	338.34	1044.26
c130287_g2_i2	328.00	189.20	576.84
c130288_g3_i1	4918.00	6064.50	1233.12
c130292_g1_i1	4289.00	504.17	117.55
c130292_g1_i2	1412.00	176.96	125.33
c130292_g1_i3	384.00	42.29	110.14
c130295_g6_i1	1871.00	215.91	115.40
c130310_g1_i10	1602.00	284.92	177.85
c130310_g1_i2	682.00	69.00	101.18
c130311_g2_i3	244.00	34.50	141.40
c130314_g5_i1	890.00	140.23	157.57
c130319_g1_i2	223.00	27.82	124.77
c130322_g1_i1	4092.00	1727.31	422.12
c130324_g1_i3	1757.00	268.22	152.66
c130327_g2_i1	4552.00	352.81	77.51
c130331_g1_i2	743.00	82.36	110.85
c130331_g2_i1	241.00	138.01	572.64
c130331_g3_i1	636.00	107.96	169.74
c130331_g3_i2	2895.00	3869.75	1336.70
c130339_g1_i3	3948.00	111.30	28.19
c130339_g4_i1	1395.00	107.96	77.39
c130343_g2_i1	278.00	337.23	1213.04
c130343_g2_i2	854.00	1886.46	2208.97
c130344_g1_i2	2227.00	144.68	64.97
c130344_g1_i7	677.00	349.47	516.20
c130345_g6_i1	307.00	32.28	105.13
c130346_g1_i1	245.00	52.31	213.51
c130349_g1_i1	6331.00	121.31	19.16
c130349_g1_i2	6184.00	129.10	20.88
c130351_g1_i3	8020.00	126.88	15.82
c130354_g1_i2	3285.00	4304.92	1310.48
c130356_g1_i1	851.00	109.07	128.17
c130357_g1_i1	2606.00	1283.24	492.42
c130365_g1_i1	2609.00	10920.30	4185.64
c130365_g1_i2	360.00	643.29	1786.91
c130367_g2_i3	1683.00	475.23	282.37
c130367_g3_i1	348.00	97.94	281.44
c130367_g3_i2	600.00	270.45	450.75

c130377_g1_i1	5903.00	964.93	163.47
c130378_g1_i1	1434.00	176.96	123.40
c130379_g2_i1	1344.00	282.69	210.34
c130379_g2_i2	633.00	66.78	105.49
c130379_g3_i2	348.00	46.74	134.32
c130380_g1_i1	574.00	219.25	381.97
c130380_g1_i2	219.00	25.60	116.89
c130380_g2_i1	279.00	37.84	135.63
c130380_g5_i1	597.00	631.05	1057.03
c130382_g1_i1	3424.00	2444.05	713.80
c130388_g1_i1	207.00	26.71	129.04
c130388_g2_i1	1430.00	773.51	540.91
c130399_g1_i1	4244.00	1097.38	258.57
c1303_g1_i1	254.00	80.13	315.48
c130401_g1_i1	874.00	5256.50	6014.30
c130401_g1_i2	982.00	4170.25	4246.69
c130403_g1_i1	359.00	93.49	260.41
c130403_g2_i1	408.00	194.77	477.37
c130403_g2_i2	237.00	198.11	835.89
c130403_g2_i3	307.00	445.18	1450.11
c130403_g2_i4	202.00	50.08	247.94
c130403_g3_i1	262.00	113.52	433.29
c130403_g4_i1	210.00	21.15	100.70
c130405_g3_i1	1428.00	1139.67	798.09
c130405_g3_i2	352.00	40.07	113.83
c130406_g1_i1	5884.00	554.25	94.20
c130406_g3_i1	350.00	96.83	276.65
c130412_g1_i1	6846.00	272.68	39.83
c130413_g2_i4	5690.00	4106.81	721.76
c130415_g1_i1	4497.00	7442.35	1654.96
c130415_g1_i2	340.00	38.95	114.57
c130424_g1_i1	389.00	111.30	286.11
c130424_g2_i1	242.00	43.41	179.36
c130428_g2_i1	2246.00	8741.17	3891.88
c130428_g3_i1	4814.00	6664.39	1384.38
c130428_g4_i1	758.00	688.92	908.87
c130428_g4_i2	1100.00	2316.06	2105.51
c130428_g5_i1	497.00	619.92	1247.32
c130430_g1_i1	1496.00	429.60	287.17
c130430_g1_i2	368.00	52.31	142.14
c130430_g2_i1	4913.00	455.20	92.65
c130430_g2_i3	5584.00	405.12	72.55
c130452_g1_i1	558.00	85.70	153.58

c130507_g1_i1	232.00	46.74	201.48
c130508_g1_i1	395.00	54.53	138.06
c130521_g1_i1	314.00	65.66	209.12
c130540_g1_i1	297.00	60.10	202.36
c13057_g1_i1	293.00	50.08	170.93
c130589_g1_i1	366.00	130.22	355.78
c130595_g1_i1	522.00	208.12	398.70
c130627_g1_i1	227.00	30.05	132.38
c130633_g1_i1	212.00	30.05	141.75
c130693_g1_i1	659.00	84.58	128.35
c130710_g1_i1	204.00	23.37	114.57
c130755_g1_i1	221.00	61.21	276.98
c130763_g1_i1	296.00	109.07	368.48
c130791_g1_i1	258.00	28.94	112.16
c130811_g1_i1	238.00	61.21	257.20
c130873_g1_i1	308.00	45.63	148.15
c130947_g1_i1	754.00	218.14	289.31
c130979_g1_i1	377.00	60.10	159.42
c131042_g1_i1	757.00	393.99	520.46
c131050_g1_i1	287.00	133.56	465.35
c131057_g1_i1	450.00	65.66	145.92
c131069_g1_i1	213.00	30.05	141.08
c131084_g1_i1	367.00	41.18	112.21
c131118_g1_i1	223.00	26.71	119.78
c131125_g1_i1	320.00	87.92	274.76
c131132_g1_i1	267.00	70.12	262.61
c131137_g1_i1	333.00	123.54	370.99
c131173_g1_i1	300.00	93.49	311.63
c131221_g1_i1	304.00	84.58	278.24
c131240_g1_i1	954.00	244.85	256.66
c131252_g1_i1	361.00	43.41	120.24
c131277_g1_i1	295.00	36.73	124.50
c131285_g1_i1	205.00	30.05	146.59
c131325_g1_i1	286.00	225.93	789.97
c131355_g1_i1	372.00	60.10	161.56
c131368_g1_i1	755.00	82.36	109.09
c131458_g1_i1	372.00	510.85	1373.25
c131481_g1_i1	406.00	44.52	109.65
c131485_g1_i1	253.00	34.50	136.37
c131528_g1_i1	269.00	121.31	450.98
c131536_g1_i1	214.00	64.55	301.64
c131565_g1_i1	227.00	107.96	475.58
c131569_g1_i1	204.00	87.92	431.00

c131616_g1_i1	327.00	40.07	122.53
c131654_g1_i1	451.00	124.65	276.39
c131656_g1_i1	205.00	43.41	211.73
c131666_g1_i1	225.00	41.18	183.02
c131674_g1_i1	398.00	110.18	276.84
c131751_g1_i1	551.00	70.12	127.25
c131816_g1_i1	409.00	44.52	108.85
c131847_g1_i1	407.00	66.78	164.07
c131865_g1_i1	367.00	138.01	376.04
c131891_g1_i1	328.00	95.71	291.81
c131904_g1_i1	317.00	66.78	210.65
c131987_g1_i1	442.00	76.79	173.74
c132023_g1_i1	238.00	164.72	692.09
c132059_g1_i1	309.00	103.51	334.97
c132088_g1_i1	219.00	33.39	152.46
c132118_g1_i1	253.00	81.25	321.13
c132136_g1_i1	740.00	455.20	615.14
c132180_g1_i1	270.00	35.61	131.91
c132228_g1_i1	230.00	144.68	629.06
c132244_g1_i1	203.00	44.52	219.30
c132332_g1_i1	234.00	57.87	247.32
c132370_g1_i1	234.00	130.22	556.48
c132629_g1_i1	297.00	117.97	397.22
c132675_g1_i1	245.00	31.16	127.20
c132758_g1_i1	340.00	44.52	130.94
c132767_g1_i1	228.00	31.16	136.68
c132778_g1_i1	220.00	156.93	713.31
c132791_g1_i1	297.00	144.68	487.15
c132798_g1_i1	257.00	94.60	368.10
c132803_g1_i1	251.00	86.81	345.86
c132814_g1_i1	240.00	38.95	162.31
c132859_g1_i1	256.00	85.70	334.76
c132864_g1_i1	384.00	159.15	414.46
c132911_g1_i1	280.00	76.79	274.26
c132964_g1_i1	248.00	25.60	103.22
c133003_g1_i1	248.00	28.94	116.68
c133019_g1_i1	207.00	46.74	225.82
c133184_g1_i1	418.00	105.73	252.95
c133283_g1_i1	345.00	43.41	125.81
c133327_g1_i1	202.00	89.04	440.78
c133350_g1_i1	408.00	382.86	938.38
c133367_g1_i1	249.00	102.39	411.21
c133428_g1_i1	228.00	34.50	151.32

c133465_g1_i1	310.00	76.79	247.72
c133490_g1_i1	349.00	54.53	156.26
c133521_g1_i1	355.00	45.63	128.54
c133630_g1_i1	247.00	53.42	216.28
c133669_g1_i1	288.00	54.53	189.36
c133719_g1_i1	224.00	40.07	178.87
c133806_g1_i1	470.00	74.57	158.66
c13383_g2_i1	228.00	45.63	200.14
c133884_g1_i1	208.00	21.15	101.66
c133989_g1_i1	245.00	32.28	131.74
c134016_g1_i1	218.00	25.60	117.42
c134018_g1_i1	202.00	60.10	297.52
c134023_g1_i1	230.00	55.65	241.95
c134035_g1_i1	444.00	61.21	137.87
c134040_g1_i1	245.00	126.88	517.87
c134088_g1_i1	308.00	45.63	148.15
c134199_g1_i1	206.00	23.37	113.46
c134277_g1_i1	261.00	198.11	759.03
c134389_g1_i1	213.00	55.65	261.26
c134577_g1_i1	334.00	64.55	193.27
c134601_g1_i1	301.00	65.66	218.15
c134613_g1_i1	214.00	41.18	192.43
c134702_g1_i1	239.00	33.39	139.70
c134731_g1_i1	220.00	76.79	349.06
c134771_g1_i1	247.00	38.95	157.71
c134807_g1_i1	209.00	24.49	117.15
c134832_g1_i1	372.00	41.18	110.70
c134847_g1_i1	237.00	47.86	201.93
c134873_g1_i1	214.00	60.10	280.84
c134952_g1_i1	228.00	93.49	410.04
c134993_g1_i1	208.00	322.76	1551.72
c135000_g1_i1	270.00	42.29	156.64
c135055_g1_i1	274.00	43.41	158.41
c135248_g1_i1	215.00	35.61	165.65
c135250_g1_i1	244.00	37.84	155.08
c135269_g1_i1	362.00	73.46	202.92
c135315_g1_i1	303.00	280.47	925.63
c135344_g1_i1	274.00	50.08	182.79
c135410_g1_i1	243.00	36.73	151.14
c135493_g1_i1	297.00	69.00	232.34
c135557_g1_i1	554.00	143.57	259.15
c135711_g1_i1	240.00	36.73	153.03
c135731_g1_i1	260.00	28.94	111.30

c135765_g1_i1	213.00	53.42	250.81
c135779_g1_i1	240.00	56.76	236.50
c135836_g1_i1	246.00	28.94	117.63
c135879_g1_i1	250.00	44.52	178.07
c135996_g1_i1	258.00	73.46	284.71
c136013_g1_i1	217.00	34.50	158.99
c13603_g1_i1	288.00	36.73	127.53
c136146_g1_i1	289.00	40.07	138.64
c136195_g1_i1	208.00	65.66	315.70
c136205_g1_i1	350.00	50.08	143.10
c136256_g1_i1	256.00	32.28	126.08
c136407_g1_i1	258.00	124.65	483.14
c136486_g1_i1	245.00	53.42	218.05
c136536_g1_i1	223.00	32.28	144.73
c136711_g1_i1	226.00	64.55	285.63
c136782_g1_i1	384.00	73.46	191.29
c136785_g1_i1	483.00	50.08	103.69
c136795_g1_i1	310.00	41.18	132.84
c136826_g1_i1	272.00	210.35	773.34
c136846_g1_i1	347.00	38.95	112.26
c136854_g1_i1	374.00	46.74	124.99
c136857_g1_i1	321.00	45.63	142.15
c136892_g1_i1	744.00	94.60	127.15
c136907_g1_i1	207.00	23.37	112.91
c136952_g1_i1	217.00	23.37	107.71
c136967_g1_i1	251.00	40.07	159.63
c137001_g1_i1	409.00	109.07	266.67
c137044_g1_i1	265.00	28.94	109.20
c137049_g1_i1	517.00	213.69	413.32
c137259_g1_i1	625.00	67.89	108.63
c137265_g1_i1	239.00	41.18	172.30
c137343_g1_i1	201.00	24.49	121.82
c137377_g1_i1	206.00	33.39	162.08
c13738_g1_i1	204.00	31.16	152.76
c137449_g1_i1	391.00	53.42	136.63
c137479_g1_i1	322.00	155.81	483.90
c137494_g1_i1	351.00	121.31	345.62
c137520_g1_i1	258.00	74.57	289.02
c137564_g1_i1	395.00	56.76	143.70
c137655_g1_i1	223.00	42.29	189.65
c137660_g1_i1	212.00	32.28	152.24
c137711_g1_i1	298.00	248.19	832.85
c137736_g1_i1	1410.00	291.60	206.81

c137738_g1_i1	249.00	32.28	129.62
c137746_g1_i1	979.00	234.83	239.87
c137800_g1_i1	222.00	41.18	185.49
c137880_g1_i1	296.00	48.97	165.44
c137910_g1_i1	237.00	142.46	601.09
c137911_g1_i1	242.00	219.25	906.00
c137934_g1_i1	266.00	28.94	108.79
c137946_g1_i1	242.00	41.18	170.16
c137950_g1_i1	215.00	27.82	129.41
c137960_g1_i1	511.00	54.53	106.72
c137989_g1_i1	246.00	43.41	176.44
c138002_g1_i1	218.00	28.94	132.74
c138062_g1_i1	240.00	75.68	315.34
c138078_g1_i1	268.00	28.94	107.97
c138081_g1_i1	548.00	107.96	197.00
c138093_g1_i1	284.00	30.05	105.81
c13830_g1_i1	336.00	44.52	132.50
c138333_g1_i1	363.00	38.95	107.31
c13833_g1_i1	283.00	31.16	110.12
c138417_g1_i1	270.00	82.36	305.03
c13849_g1_i1	331.00	48.97	147.95
c138583_g1_i1	241.00	282.69	1172.99
c138599_g1_i1	245.00	47.86	195.34
c138632_g1_i1	205.00	37.84	184.59
c138668_g1_i1	205.00	48.97	238.88
c138687_g1_i1	256.00	52.31	204.33
c138707_g1_i1	278.00	53.42	192.17
c138719_g1_i1	205.00	33.39	162.87
c138721_g1_i1	207.00	64.55	311.84
c138724_g1_i1	232.00	48.97	211.08
c138757_g1_i1	252.00	47.86	189.91
c138782_g1_i1	230.00	24.49	106.46
c138785_g1_i1	243.00	24.49	100.76
c138847_g1_i1	309.00	117.97	381.79
c138850_g1_i1	205.00	24.49	119.44
c138878_g1_i1	207.00	31.16	150.55
c138893_g1_i1	307.00	44.52	145.01
c138923_g1_i1	289.00	62.33	215.66
c138928_g1_i1	219.00	47.86	218.53
c139048_g1_i1	229.00	227.04	991.46
c139103_g1_i1	247.00	30.05	121.66
c139140_g1_i1	466.00	257.09	551.70
c139192_g1_i1	551.00	333.89	605.97

c139235_g1_i1	215.00	22.26	103.53
c139240_g1_i1	275.00	34.50	125.46
c139357_g1_i1	414.00	64.55	155.92
c139370_g1_i1	312.00	111.30	356.72
c139428_g1_i1	312.00	126.88	406.66
c139432_g1_i1	213.00	32.28	151.53
c139473_g1_i1	297.00	42.29	142.40
c139545_g1_i1	220.00	24.49	111.30
c139661_g1_i1	232.00	24.49	105.54
c139673_g1_i1	241.00	58.99	244.76
c139726_g1_i1	246.00	267.11	1085.81
c139833_g1_i1	553.00	72.34	130.82
c13983_g1_i1	250.00	25.60	102.39
c139867_g1_i1	293.00	41.18	140.54
c139914_g1_i1	203.00	52.31	257.68
c139934_g1_i1	291.00	75.68	260.07
c139983_g1_i1	208.00	21.15	101.66
c140105_g1_i1	228.00	30.05	131.80
c140115_g1_i1	266.00	190.32	715.47
c140138_g1_i1	276.00	81.25	294.37
c140234_g1_i1	214.00	120.20	561.68
c140282_g1_i1	346.00	41.18	119.02
c140355_g1_i1	217.00	153.59	707.78
c140369_g1_i1	245.00	74.57	304.36
c140404_g1_i1	229.00	35.61	155.52
c140481_g1_i1	224.00	50.08	223.59
c140544_g1_i1	218.00	43.41	199.11
c140558_g1_i1	254.00	42.29	166.51
c140565_g1_i1	347.00	41.18	118.67
c140632_g1_i1	258.00	60.10	232.95
c140667_g1_i1	204.00	35.61	174.58
c140705_g1_i1	233.00	93.49	401.24
c140843_g1_i1	301.00	205.90	684.04
c140873_g1_i1	290.00	189.20	652.42
c140894_g1_i1	205.00	25.60	124.87
c140998_g1_i1	201.00	21.15	105.21
c141065_g1_i1	213.00	31.16	146.30
c141081_g1_i1	246.00	82.36	334.79
c141219_g1_i1	215.00	272.68	1268.25
c141222_g1_i1	288.00	174.73	606.72
c141262_g1_i1	217.00	46.74	215.41
c141269_g1_i1	226.00	63.44	280.70
c141293_g1_i1	252.00	27.82	110.41

c141368_g1_i1	226.00	119.09	526.93
c14139_g1_i1	322.00	148.02	459.70
c141441_g1_i1	390.00	101.28	259.69
c141516_g1_i1	299.00	35.61	119.11
c141519_g1_i1	214.00	25.60	119.62
c141521_g1_i1	271.00	44.52	164.27
c141523_g1_i1	396.00	97.94	247.32
c141575_g1_i1	234.00	27.82	118.91
c141581_g1_i1	500.00	66.78	133.56
c141583_g1_i1	280.00	31.16	111.30
c141598_g1_i1	227.00	120.20	529.51
c141599_g1_i1	331.00	61.21	184.93
c141614_g1_i1	227.00	50.08	220.63
c141696_g1_i1	279.00	31.16	111.70
c141752_g1_i1	206.00	21.15	102.65
c141794_g1_i1	242.00	25.60	105.78
c14185_g1_i1	284.00	83.47	293.92
c141875_g1_i1	270.00	51.20	189.62
c141910_g1_i1	207.00	38.95	188.18
c141914_g1_i1	261.00	115.75	443.48
c142015_g1_i1	204.00	31.16	152.76
c142229_g1_i1	204.00	22.26	109.11
c142285_g1_i1	218.00	22.26	102.11
c142337_g1_i1	229.00	28.94	126.36
c142380_g1_i1	292.00	198.11	678.45
c142442_g1_i1	236.00	25.60	108.47
c142473_g1_i1	218.00	30.05	137.84
c142483_g1_i1	277.00	101.28	365.63
c142628_g1_i1	348.00	102.39	294.23
c142712_g1_i1	290.00	46.74	161.19
c142754_g1_i1	209.00	38.95	186.38
c142796_g1_i1	202.00	161.38	798.91
c142913_g1_i1	249.00	52.31	210.08
c142931_g1_i1	210.00	28.94	137.80
c14295_g1_i1	482.00	113.52	235.52
c14301_g1_i1	229.00	123.54	539.47
c143059_g1_i1	227.00	28.94	127.48
c143164_g1_i1	241.00	32.28	133.92
c143192_g1_i1	224.00	23.37	104.34
c143207_g1_i1	388.00	52.31	134.82
c143273_g1_i1	244.00	121.31	497.18
c143280_g1_i1	243.00	31.16	128.24
c143307_g1_i1	325.00	101.28	311.63

c143330_g1_i1	302.00	46.74	154.78
c143335_g1_i1	319.00	75.68	237.25
c143362_g1_i1	273.00	111.30	407.68
c143368_g1_i1	254.00	31.16	122.69
c143396_g1_i1	367.00	80.13	218.35
c143438_g1_i1	455.00	117.97	259.28
c143452_g1_i1	329.00	67.89	206.35
c143600_g1_i1	531.00	237.06	446.44
c143618_g1_i1	469.00	50.08	106.79
c143766_g1_i1	242.00	41.18	170.16
c143777_g1_i1	291.00	36.73	126.21
c143836_g1_i1	488.00	53.42	109.47
c143851_g1_i1	331.00	43.41	131.13
c143923_g1_i1	362.00	55.65	153.72
c144001_g1_i1	230.00	77.91	338.73
c144084_g1_i1	241.00	65.66	272.47
c144122_g1_i1	211.00	43.41	205.71
c144153_g1_i1	393.00	333.89	849.59
c144183_g1_i1	211.00	242.63	1149.88
c144190_g1_i1	1230.00	717.86	583.62
c144347_g1_i1	278.00	40.07	144.12
c144416_g1_i1	201.00	65.66	326.69
c144466_g1_i1	235.00	40.07	170.50
c144470_g1_i1	217.00	24.49	112.83
c144481_g1_i1	416.00	56.76	136.44
c144507_g1_i1	279.00	129.10	462.74
c144540_g1_i1	268.00	75.68	282.39
c144552_g1_i1	270.00	36.73	136.03
c144561_g1_i1	329.00	46.74	142.08
c144591_g1_i1	443.00	50.08	113.05
c144604_g1_i1	219.00	99.05	452.30
c144624_g1_i1	243.00	42.29	174.04
c144649_g1_i1	319.00	65.66	205.85
c144655_g1_i1	395.00	57.87	146.52
c14467_g1_i1	272.00	117.97	433.73
c144715_g1_i1	298.00	107.96	362.27
c144720_g1_i1	314.00	65.66	209.12
c144756_g1_i1	389.00	77.91	200.28
c144771_g1_i1	600.00	83.47	139.12
c144845_g1_i1	294.00	133.56	454.27
c144892_g1_i1	370.00	117.97	318.85
c144951_g1_i1	290.00	40.07	138.16
c145009_g1_i1	296.00	139.12	470.00

c145092_g1_i1	233.00	150.25	644.85
c145124_g1_i1	255.00	60.10	235.69
c145125_g1_i1	201.00	41.18	204.87
c145132_g1_i1	256.00	75.68	295.63
c145193_g1_i1	248.00	36.73	148.10
c145205_g1_i1	211.00	40.07	189.89
c145254_g1_i1	212.00	58.99	278.24
c145276_g1_i1	250.00	26.71	106.84
c145286_g1_i1	244.00	26.71	109.47
c145305_g1_i1	208.00	36.73	176.58
c145351_g1_i1	264.00	41.18	155.98
c145369_g1_i1	217.00	22.26	102.58
c145395_g1_i1	420.00	174.73	416.03
c145404_g1_i1	250.00	34.50	138.01
c145421_g1_i1	204.00	26.71	130.94
c145480_g1_i1	221.00	67.89	307.20
c145502_g1_i1	248.00	80.13	323.12
c145548_g1_i1	443.00	48.97	110.54
c145577_g1_i1	308.00	111.30	361.35
c145650_g1_i1	237.00	35.61	150.27
c145684_g1_i1	247.00	56.76	229.80
c145699_g1_i1	232.00	184.75	796.34
c145701_g1_i1	305.00	76.79	251.78
c145795_g1_i1	201.00	119.09	592.47
c145803_g1_i1	220.00	35.61	161.89
c145844_g1_i1	273.00	37.84	138.61
c145845_g1_i1	280.00	191.43	683.67
c145857_g1_i1	226.00	153.59	679.59
c145971_g1_i1	445.00	57.87	130.05
c14615_g1_i1	344.00	70.12	203.83
c146164_g1_i1	252.00	57.87	229.66
c146172_g1_i1	212.00	52.31	246.74
c146204_g1_i1	328.00	45.63	139.12
c146211_g1_i1	331.00	33.39	100.87
c146234_g1_i1	329.00	103.51	314.61
c146247_g1_i1	225.00	35.61	158.29
c14626_g1_i1	304.00	41.18	135.46
c146333_g1_i1	221.00	22.26	100.72
c146507_g1_i1	564.00	58.99	104.59
c146582_g1_i1	216.00	38.95	180.34
c14659_g1_i1	226.00	58.99	261.00
c146687_g1_i1	281.00	35.61	126.74
c146753_g1_i1	220.00	24.49	111.30

c146783_g1_i1	285.00	62.33	218.69
c146907_g1_i1	223.00	84.58	379.30
c146914_g1_i1	349.00	130.22	373.11
c147085_g1_i1	244.00	32.28	132.28
c147150_g1_i1	210.00	24.49	116.60
c147206_g1_i1	262.00	34.50	131.69
c147224_g1_i1	237.00	62.33	262.98
c147265_g1_i1	280.00	42.29	151.04
c147267_g1_i1	220.00	24.49	111.30
c147318_g1_i1	242.00	38.95	160.97
c147339_g1_i1	223.00	79.02	354.35
c147454_g1_i1	262.00	73.46	280.36
c147474_g1_i1	468.00	54.53	116.53
c147538_g1_i1	202.00	112.41	556.48
c147541_g1_i1	215.00	105.73	491.77
c147567_g1_i1	201.00	112.41	559.25
c147588_g1_i1	210.00	21.15	100.70
c147596_g1_i1	220.00	41.18	187.18
c147620_g1_i1	221.00	28.94	130.94
c147650_g1_i1	472.00	196.99	417.36
c147684_g1_i1	231.00	32.28	139.72
c147697_g1_i1	223.00	47.86	214.61
c147911_g1_i1	251.00	92.38	368.03
c147913_g1_i1	320.00	33.39	104.34
c147985_g1_i1	233.00	28.94	124.19
c148012_g1_i1	258.00	67.89	263.14
c148105_g1_i1	222.00	70.12	315.84
c148261_g1_i1	212.00	30.05	141.75
c148297_g1_i1	367.00	358.37	976.49
c148368_g1_i1	252.00	101.28	401.90
c148581_g1_i1	205.00	46.74	228.02
c148582_g1_i1	212.00	32.28	152.24
c148593_g1_i1	288.00	92.38	320.75
c14863_g1_i1	374.00	40.07	107.13
c148640_g1_i1	247.00	44.52	180.24
c148847_g1_i1	302.00	33.39	110.56
c148877_g1_i1	267.00	27.82	104.21
c149007_g1_i1	239.00	28.94	121.08
c149079_g1_i1	210.00	55.65	264.99
c149212_g1_i1	247.00	86.81	351.46
c149308_g1_i1	363.00	179.19	493.63
c149369_g1_i1	212.00	37.84	178.49
c149422_g1_i1	387.00	352.81	911.65

c149451_g1_i1	478.00	186.98	391.17
c149495_g1_i1	227.00	48.97	215.73
c149505_g1_i1	220.00	47.86	217.53
c149535_g1_i1	346.00	48.97	141.53
c149576_g1_i1	747.00	114.64	153.46
c149611_g1_i1	232.00	60.10	259.05
c149685_g1_i1	213.00	253.75	1191.33
c149708_g1_i1	661.00	145.80	220.57
c149729_g1_i1	415.00	65.66	158.23
c149761_g1_i1	210.00	47.86	227.89
c149789_g1_i1	418.00	48.97	117.15
c149898_g1_i1	209.00	22.26	106.50
c149939_g1_i1	326.00	83.47	256.05
c150144_g1_i1	234.00	26.71	114.15
c150182_g1_i1	246.00	166.94	678.63
c150256_g1_i1	496.00	129.10	260.29
c150395_g1_i1	862.00	210.35	244.02
c150416_g1_i1	347.00	43.41	125.09
c150439_g1_i1	232.00	41.18	177.50
c150440_g1_i1	283.00	117.97	416.87
c150457_g1_i1	307.00	119.09	387.90
c150466_g1_i1	240.00	56.76	236.50
c150553_g1_i1	219.00	25.60	116.89
c150590_g1_i1	235.00	63.44	269.95
c150627_g1_i1	235.00	34.50	146.82
c150763_g1_i1	367.00	38.95	106.14
c150774_g1_i1	278.00	50.08	180.16
c150785_g1_i1	223.00	65.66	294.46
c150840_g1_i1	379.00	107.96	284.85
c150884_g1_i1	215.00	71.23	331.30
c150920_g1_i1	252.00	42.29	167.83
c150922_g1_i1	249.00	27.82	111.74
c150978_g1_i1	575.00	84.58	147.10
c151077_g1_i1	421.00	55.65	132.18
c151159_g1_i1	250.00	80.13	320.53
c151215_g1_i1	241.00	43.41	180.11
c151228_g1_i1	387.00	75.68	195.56
c151245_g1_i1	251.00	127.99	509.92
c151246_g1_i1	276.00	174.73	633.10
c151267_g1_i1	350.00	38.95	111.30
c151309_g1_i1	217.00	185.86	856.52
c151400_g1_i1	228.00	37.84	165.97
c151530_g1_i1	322.00	44.52	138.26

c151562_g1_i1	218.00	43.41	199.11
c151577_g1_i1	559.00	76.79	137.38
c151587_g1_i1	328.00	169.17	515.76
c151661_g1_i1	355.00	56.76	159.89
c151732_g1_i1	316.00	36.73	116.23
c151747_g1_i1	424.00	151.36	356.99
c151767_g1_i1	223.00	27.82	124.77
c151892_g1_i1	307.00	32.28	105.13
c151946_g1_i1	604.00	123.54	204.53
c151951_g1_i1	227.00	70.12	308.88
c151964_g1_i1	236.00	31.16	132.05
c152024_g1_i1	202.00	23.37	115.70
c152059_g1_i1	228.00	112.41	493.02
c152150_g1_i1	264.00	37.84	143.34
c15221_g1_i1	277.00	31.16	112.50
c152243_g1_i1	217.00	45.63	210.28
c152268_g1_i1	203.00	25.60	126.10
c152291_g1_i1	367.00	114.64	312.36
c152337_g1_i1	311.00	62.33	200.40
c152420_g1_i1	242.00	214.80	887.61
c152478_g1_i1	425.00	86.81	204.26
c152500_g1_i1	221.00	123.54	559.00
c152540_g1_i1	244.00	89.04	364.90
c152601_g1_i1	221.00	33.39	151.08
c152604_g1_i1	208.00	82.36	395.96
c152633_g1_i1	315.00	79.02	250.86
c152654_g1_i1	376.00	89.04	236.80
c152806_g1_i1	208.00	56.76	272.89
c152808_g1_i1	235.00	66.78	284.16
c152910_g1_i1	367.00	154.70	421.53
c152920_g1_i1	417.00	154.70	370.99
c153015_g1_i1	323.00	53.42	165.39
c153023_g1_i1	410.00	93.49	228.02
c153053_g1_i1	344.00	62.33	181.18
c153093_g1_i1	300.00	30.05	100.17
c153136_g1_i1	271.00	45.63	168.38
c153147_g1_i1	252.00	87.92	348.90
c153164_g1_i1	275.00	45.63	165.93
c153219_g1_i1	333.00	36.73	110.29
c153250_g1_i1	289.00	50.08	173.30
c153374_g1_i1	400.00	176.96	442.40
c153375_g1_i1	202.00	25.60	126.72
c153396_g1_i1	249.00	61.21	245.83

c15339_g1_i1	574.00	77.91	135.73
c153417_g1_i1	356.00	97.94	275.11
c153429_g1_i1	222.00	25.60	115.31
c153521_g1_i1	210.00	55.65	264.99
c153543_g1_i1	309.00	125.76	407.00
c153592_g1_i1	705.00	214.80	304.68
c153627_g1_i1	205.00	33.39	162.87
c153719_g1_i1	274.00	316.08	1153.58
c153744_g1_i1	204.00	32.28	158.22
c153855_g1_i1	215.00	46.74	217.42
c153889_g1_i1	363.00	55.65	153.30
c153962_g1_i1	268.00	30.05	112.13
c153968_g1_i1	250.00	132.44	529.77
c15397_g1_i1	220.00	121.31	551.42
c154046_g1_i1	251.00	37.84	150.76
c154104_g1_i1	241.00	53.42	221.67
c154159_g1_i1	251.00	66.78	266.05
c154163_g1_i1	279.00	139.12	498.64
c154229_g1_i1	318.00	34.50	108.50
c15423_g1_i1	552.00	516.41	935.53
c154261_g1_i1	282.00	51.20	181.55
c154262_g1_i1	203.00	22.26	109.65
c154312_g1_i1	206.00	43.41	210.71
c154332_g1_i1	347.00	44.52	128.30
c154368_g1_i1	203.00	43.41	213.82
c154378_g1_i1	337.00	80.13	237.78
c154531_g1_i1	243.00	54.53	224.42
c154567_g1_i1	283.00	45.63	161.24
c154619_g1_i1	204.00	23.37	114.57
c154652_g1_i1	294.00	96.83	329.35
c154708_g1_i1	210.00	22.26	106.00
c154742_g1_i1	275.00	42.29	153.79
c154755_g1_i1	284.00	38.95	137.16
c154783_g1_i1	222.00	46.74	210.56
c154785_g1_i1	290.00	83.47	287.83
c154898_g1_i1	245.00	38.95	158.99
c154992_g1_i1	202.00	23.37	115.70
c155077_g1_i1	261.00	47.86	183.36
c155201_g1_i1	307.00	61.21	199.39
c155209_g1_i1	237.00	27.82	117.40
c155286_g1_i1	205.00	34.50	168.30
c155386_g1_i1	230.00	63.44	275.82
c155428_g1_i1	210.00	34.50	164.29

c155541_g1_i1	487.00	84.58	173.69
c155564_g1_i1	405.00	65.66	162.14
c155579_g1_i1	591.00	194.77	329.56
c155664_g1_i1	209.00	41.18	197.03
c155679_g1_i1	228.00	86.81	380.75
c155681_g1_i1	320.00	34.50	107.82
c155698_g1_i1	627.00	76.79	122.48
c155707_g1_i1	280.00	41.18	147.07
c155737_g1_i1	242.00	37.84	156.37
c155828_g1_i1	294.00	82.36	280.13
c155845_g1_i1	442.00	124.65	282.02
c155858_g1_i1	408.00	64.55	158.22
c155874_g1_i1	474.00	190.32	401.51
c155904_g1_i1	236.00	52.31	221.65
c155920_g1_i1	215.00	22.26	103.53
c156006_g1_i1	374.00	55.65	148.79
c15601_g1_i1	280.00	52.31	186.82
c156066_g1_i1	232.00	41.18	177.50
c156190_g1_i1	391.00	74.57	190.71
c156214_g1_i1	312.00	37.84	121.28
c156323_g1_i1	442.00	86.81	196.40
c156328_g1_i1	481.00	48.97	101.81
c156384_g1_i1	210.00	146.91	699.57
c156493_g1_i1	212.00	33.39	157.49
c156640_g1_i1	232.00	31.16	134.32
c156700_g1_i1	317.00	34.50	108.84
c156705_g1_i1	320.00	251.53	786.03
c156754_g1_i1	245.00	43.41	177.17
c156769_g1_i1	361.00	42.29	117.15
c156781_g1_i1	275.00	52.31	190.22
c156847_g1_i1	230.00	90.15	391.96
c156849_g1_i1	228.00	41.18	180.61
c156865_g1_i1	215.00	34.50	160.47
c156868_g1_i1	218.00	90.15	413.53
c156882_g1_i1	379.00	184.75	487.47
c156954_g1_i1	335.00	50.08	149.50
c157020_g1_i1	396.00	44.52	112.42
c157049_g1_i1	343.00	199.22	580.81
c157079_g1_i1	576.00	74.57	129.46
c157160_g1_i1	232.00	75.68	326.21
c157161_g1_i1	249.00	32.28	129.62
c157192_g1_i1	209.00	26.71	127.80
c157193_g1_i1	436.00	396.21	908.75

c157201_g1_i1	306.00	109.07	356.44
c157238_g1_i1	240.00	41.18	171.58
c157252_g1_i1	557.00	235.95	423.60
c15732_g1_i1	341.00	107.96	316.59
c157417_g1_i1	240.00	70.12	292.15
c157444_g1_i1	344.00	50.08	145.59
c157458_g1_i1	317.00	82.36	259.81
c157459_g1_i1	400.00	53.42	133.56
c157472_g1_i1	241.00	62.33	258.61
c157500_g1_i1	212.00	36.73	173.24
c157523_g1_i1	362.00	38.95	107.61
c15755_g1_i1	246.00	44.52	180.97
c157570_g1_i1	302.00	99.05	327.99
c157589_g1_i1	259.00	38.95	150.40
c157688_g1_i1	210.00	25.60	121.90
c157767_g1_i1	232.00	100.17	431.75
c157788_g1_i1	203.00	90.15	444.09
c157863_g1_i1	249.00	30.05	120.68
c157897_g1_i1	306.00	97.94	320.07
c157992_g1_i1	207.00	40.07	193.56
c158039_g1_i1	440.00	307.18	698.13
c1580_g1_i1	211.00	34.50	163.52
c158136_g1_i1	417.00	71.23	170.81
c158219_g1_i1	358.00	140.23	391.71
c158224_g1_i1	207.00	50.08	241.95
c158225_g1_i1	388.00	63.44	163.50
c158239_g1_i1	280.00	56.76	202.72
c158261_g1_i1	257.00	67.89	264.17
c158263_g1_i1	236.00	89.04	377.27
c158316_g1_i1	380.00	56.76	149.37
c158319_g1_i1	255.00	63.44	248.78
c158358_g1_i1	248.00	38.95	157.07
c158364_g1_i1	253.00	99.05	391.52
c158425_g1_i1	320.00	100.17	313.02
c158433_g1_i1	233.00	70.12	300.93
c15845_g1_i1	336.00	95.71	284.86
c158489_g1_i1	207.00	27.82	134.42
c158515_g1_i1	319.00	119.09	373.31
c158536_g1_i1	220.00	35.61	161.89
c158631_g1_i1	316.00	74.57	235.98
c158820_g1_i1	392.00	77.91	198.74
c158844_g1_i1	454.00	110.18	242.69
c158845_g1_i1	305.00	66.78	218.94

c158859_g1_i1	259.00	35.61	137.51
c158866_g1_i1	207.00	56.76	274.21
c158875_g1_i1	278.00	34.50	124.11
c158929_g1_i1	266.00	36.73	138.07
c158941_g1_i1	388.00	52.31	134.82
c158965_g1_i1	335.00	249.30	744.19
c158977_g1_i1	215.00	60.10	279.53
c158983_g1_i1	257.00	60.10	233.85
c159025_g1_i1	375.00	80.13	213.69
c159028_g1_i1	369.00	54.53	147.79
c159046_g1_i1	494.00	89.04	180.24
c159052_g1_i1	205.00	61.21	298.60
c159054_g1_i1	240.00	31.16	129.85
c159094_g1_i1	612.00	146.91	240.05
c159114_g1_i1	211.00	27.82	131.87
c159116_g1_i1	224.00	33.39	149.06
c159124_g1_i1	255.00	54.53	213.86
c159185_g1_i1	250.00	58.99	235.95
c159218_g1_i1	315.00	37.84	120.13
c159242_g1_i1	219.00	70.12	320.17
c159305_g1_i1	249.00	43.41	174.32
c159316_g1_i1	374.00	66.78	178.55
c159385_g1_i1	220.00	45.63	207.42
c159420_g1_i1	363.00	37.84	104.24
c159488_g1_i1	218.00	32.28	148.05
c159500_g1_i1	346.00	158.04	456.76
c159513_g1_i1	239.00	31.16	130.39
c159562_g1_i1	345.00	38.95	112.91
c159567_g1_i1	233.00	35.61	152.85
c159570_g1_i1	254.00	99.05	389.97
c159593_g1_i1	353.00	67.89	192.32
c159665_g1_i1	265.00	253.75	957.56
c159684_g1_i1	221.00	30.05	135.97
c159696_g1_i1	328.00	71.23	217.16
c159739_g1_i1	217.00	38.95	179.51
c159785_g1_i1	362.00	56.76	156.80
c159894_g1_i1	248.00	28.94	116.68
c159959_g1_i1	286.00	42.29	147.88
c15996_g1_i1	256.00	204.78	799.94
c15996_g2_i1	222.00	87.92	396.05
c159988_g1_i1	214.00	113.52	530.48
c160046_g1_i1	225.00	36.73	163.23
c160050_g1_i1	206.00	41.18	199.90

c160062_g1_i1	262.00	141.35	539.49
c160166_g1_i1	234.00	50.08	214.03
c160181_g1_i1	315.00	40.07	127.20
c160241_g1_i1	217.00	64.55	297.47
c160254_g1_i1	341.00	34.50	101.18
c160396_g1_i1	232.00	123.54	532.49
c160399_g1_i1	209.00	42.29	202.36
c160426_g1_i1	274.00	58.99	215.28
c160498_g1_i1	213.00	36.73	172.43
c160555_g1_i1	522.00	81.25	155.64
c160556_g1_i1	240.00	24.49	102.02
c160593_g1_i1	236.00	66.78	282.96
c160624_g1_i1	202.00	62.33	308.54
c160708_g1_i1	301.00	531.99	1767.42
c160720_g1_i1	229.00	96.83	422.83
c160747_g1_i1	248.00	170.28	686.62
c160768_g1_i1	214.00	58.99	275.64
c160771_g1_i1	229.00	115.75	505.45
c160827_g1_i1	215.00	72.34	336.48
c160828_g1_i1	209.00	225.93	1081.01
c160832_g1_i1	221.00	25.60	115.83
c160837_g1_i1	237.00	47.86	201.93
c160863_g1_i1	214.00	61.21	286.04
c160968_g1_i1	276.00	93.49	338.73
c160985_g1_i1	213.00	94.60	444.14
c160989_g1_i1	272.00	42.29	155.49
c161038_g1_i1	409.00	77.91	190.48
c161050_g1_i1	280.00	53.42	190.79
c161074_g1_i1	265.00	53.42	201.59
c161133_g1_i1	363.00	138.01	380.18
c161176_g1_i1	242.00	26.71	110.38
c161200_g1_i1	206.00	52.31	253.93
c161229_g1_i1	216.00	35.61	164.88
c161271_g1_i1	265.00	105.73	398.99
c161530_g1_i1	212.00	22.26	105.00
c161550_g1_i1	238.00	48.97	205.76
c161793_g1_i1	210.00	22.26	106.00
c161820_g1_i1	206.00	54.53	264.73
c16191_g1_i1	205.00	30.05	146.59
c16196_g1_i1	234.00	26.71	114.15
c162053_g1_i1	340.00	117.97	346.98
c162066_g1_i1	290.00	43.41	149.67
c162075_g1_i1	293.00	32.28	110.16

c16207_g1_i1	256.00	35.61	139.12
c162103_g1_i1	208.00	52.31	251.49
c162104_g1_i1	635.00	254.87	401.37
c162120_g1_i1	222.00	94.60	426.13
c162245_g1_i1	298.00	30.05	100.84
c162251_g1_i1	237.00	71.23	300.55
c162260_g1_i1	1986.00	113.52	57.16
c162294_g1_i1	581.00	101.28	174.32
c16229_g1_i1	251.00	66.78	266.05
c162333_g1_i1	238.00	54.53	229.14
c162347_g1_i1	533.00	106.84	200.46
c162348_g1_i1	312.00	57.87	185.49
c1623_g1_i1	236.00	33.39	141.48
c1623_g2_i1	471.00	210.35	446.60
c162410_g1_i1	540.00	93.49	173.13
c162416_g1_i1	613.00	97.94	159.77
c16242_g1_i1	265.00	113.52	428.38
c162508_g1_i1	406.00	77.91	191.89
c162538_g1_i1	316.00	50.08	158.49
c162615_g1_i1	508.00	84.58	166.51
c162626_g1_i1	550.00	141.35	256.99
c162682_g1_i1	322.00	43.41	134.80
c162766_g1_i1	634.00	262.66	414.29
c162829_g1_i1	267.00	32.28	120.88
c162980_g1_i1	215.00	38.95	181.18
c163034_g1_i1	458.00	80.13	174.96
c163052_g1_i1	202.00	27.82	137.74
c163064_g1_i1	287.00	40.07	139.60
c163241_g1_i1	280.00	53.42	190.79
c163376_g1_i1	203.00	211.46	1041.68
c163390_g1_i1	228.00	28.94	126.92
c163413_g1_i1	215.00	91.26	424.48
c163533_g1_i1	441.00	58.99	133.76
c163536_g1_i1	250.00	45.63	182.53
c163551_g1_i1	363.00	41.18	113.44
c163555_g1_i1	218.00	43.41	199.11
c163627_g1_i1	231.00	37.84	163.81
c163640_g1_i1	328.00	110.18	335.92
c163772_g1_i1	326.00	73.46	225.32
c163796_g1_i1	252.00	26.71	106.00
c163834_g1_i1	285.00	44.52	156.21
c163840_g1_i1	255.00	58.99	231.32
c163961_g1_i1	236.00	60.10	254.66

c163974_g1_i1	261.00	42.29	162.04
c163997_g1_i1	237.00	73.46	309.94
c164057_g1_i1	355.00	67.89	191.24
c164082_g1_i1	231.00	76.79	332.44
c164095_g1_i1	485.00	54.53	112.44
c164130_g1_i1	222.00	149.14	671.79
c164157_g1_i1	293.00	44.52	151.94
c164181_g1_i1	423.00	109.07	257.85
c164189_g1_i1	221.00	113.52	513.67
c164208_g1_i1	256.00	94.60	369.54
c164232_g1_i1	219.00	127.99	584.43
c164242_g1_i1	603.00	65.66	108.90
c164316_g1_i1	404.00	57.87	143.25
c164350_g1_i1	448.00	64.55	144.09
c164358_g1_i1	308.00	76.79	249.33
c164502_g1_i1	233.00	30.05	128.97
c164504_g1_i1	254.00	69.00	271.67
c164616_g1_i1	222.00	25.60	115.31
c164682_g1_i1	267.00	45.63	170.90
c164688_g1_i1	206.00	31.16	151.28
c164692_g1_i1	226.00	105.73	467.84
c164799_g1_i1	242.00	52.31	216.15
c164969_g1_i1	201.00	22.26	110.74
c164981_g1_i1	225.00	43.41	192.91
c165073_g1_i1	245.00	109.07	445.18
c165082_g1_i1	363.00	44.52	122.64
c165224_g1_i1	211.00	21.15	100.22
c165227_g1_i1	593.00	77.91	131.38
c165336_g1_i1	254.00	85.70	337.39
c165394_g1_i1	226.00	83.47	369.34
c16569_g1_i1	320.00	53.42	166.94
c165730_g1_i1	220.00	58.99	268.12
c165768_g1_i1	264.00	73.46	278.24
c165791_g1_i1	293.00	36.73	125.35
c165853_g1_i1	264.00	46.74	177.06
c165909_g1_i1	249.00	25.60	102.80
c165930_g1_i1	417.00	211.46	507.10
c166033_g1_i1	246.00	65.66	266.93
c166147_g1_i1	629.00	291.60	463.59
c166178_g1_i1	230.00	25.60	111.30
c166185_g1_i1	229.00	32.28	140.94
c166209_g1_i1	385.00	176.96	459.64
c166218_g1_i1	235.00	86.81	369.41

c166236_g1_i1	295.00	30.05	101.86
c166292_g1_i1	249.00	54.53	219.02
c166359_g1_i1	401.00	114.64	285.87
c166365_g1_i1	211.00	52.31	247.91
c166391_g1_i1	342.00	34.50	100.88
c166579_g1_i1	427.00	71.23	166.81
c166608_g1_i1	208.00	22.26	107.02
c166615_g1_i1	382.00	87.92	230.17
c166723_g1_i1	209.00	38.95	186.38
c166729_g1_i1	263.00	42.29	160.81
c166885_g1_i1	279.00	54.53	195.47
c167037_g1_i1	202.00	95.71	473.83
c167071_g1_i1	201.00	26.71	132.89
c167127_g1_i1	201.00	22.26	110.74
c167153_g1_i1	219.00	38.95	177.87
c167182_g1_i1	281.00	35.61	126.74
c167249_g1_i1	295.00	40.07	135.82
c167280_g1_i1	211.00	43.41	205.71
c167319_g1_i1	233.00	26.71	114.64
c167393_g1_i1	209.00	109.07	521.87
c167416_g1_i1	245.00	148.02	604.18
c167429_g1_i1	218.00	22.26	102.11
c167430_g1_i1	328.00	263.77	804.18
c167439_g1_i1	227.00	37.84	166.70
c167475_g1_i1	332.00	80.13	241.36
c167514_g1_i1	222.00	34.50	155.41
c167684_g1_i1	237.00	62.33	262.98
c167729_g1_i1	273.00	109.07	399.52
c167731_g1_i1	266.00	37.84	142.26
c167744_g1_i1	205.00	80.13	390.89
c167855_g1_i1	220.00	23.37	106.24
c167886_g1_i1	258.00	47.86	185.49
c16828_g1_i1	346.00	101.28	292.71
c17137_g1_i1	830.00	106.84	128.73
c17241_g1_i1	360.00	61.21	170.04
c17249_g1_i1	230.00	57.87	251.63
c17596_g1_i1	268.00	41.18	153.66
c17774_g1_i1	241.00	35.61	147.78
c17823_g1_i1	413.00	123.54	299.12
c17886_g1_i1	267.00	56.76	212.59
c17939_g1_i1	208.00	159.15	765.16
c17999_g1_i1	523.00	57.87	110.66
c18093_g1_i1	354.00	75.68	213.79

c18460_g1_i1	213.00	162.49	762.87
c18581_g1_i1	205.00	21.15	103.15
c19015_g1_i1	1146.00	277.13	241.82
c19040_g1_i1	398.00	70.12	176.17
c19058_g1_i1	333.00	52.31	157.08
c19093_g1_i1	523.00	217.03	414.97
c19269_g1_i1	283.00	33.39	117.98
c19302_g1_i1	435.00	48.97	112.58
c1944_g1_i1	315.00	50.08	158.99
c19519_g1_i1	217.00	71.23	328.25
c19581_g1_i1	267.00	55.65	208.42
c19807_g1_i1	243.00	26.71	109.92
c19875_g1_i1	214.00	30.05	140.42
c19894_g1_i1	251.00	77.91	310.39
c20318_g1_i1	304.00	46.74	153.76
c20368_g1_i1	276.00	63.44	229.85
c20370_g1_i1	387.00	171.40	442.88
c20370_g2_i1	403.00	253.75	629.66
c20542_g1_i1	206.00	72.34	351.18
c20832_g1_i1	432.00	212.58	492.07
c20901_g1_i1	242.00	82.36	340.33
c20910_g1_i1	267.00	27.82	104.21
c20987_g1_i1	415.00	235.95	568.55
c21018_g1_i1	219.00	25.60	116.89
c21051_g1_i1	262.00	37.84	144.43
c21116_g1_i1	307.00	34.50	112.38
c21337_g1_i1	442.00	402.89	911.52
c21489_g1_i1	208.00	45.63	219.38
c21515_g1_i1	278.00	27.82	100.09
c21611_g1_i1	329.00	47.86	145.46
c21814_g1_i1	260.00	30.05	115.58
c21821_g1_i1	212.00	40.07	188.99
c21867_g1_i1	243.00	57.87	238.16
c2186_g1_i1	205.00	76.79	374.61
c21873_g1_i1	225.00	130.22	578.74
c21894_g1_i1	458.00	87.92	191.97
c21956_g1_i1	382.00	89.04	233.08
c21994_g1_i1	272.00	30.05	110.48
c22018_g1_i1	205.00	31.16	152.01
c22153_g1_i1	209.00	65.66	314.18
c22790_g1_i1	299.00	112.41	375.95
c22898_g1_i1	218.00	196.99	903.64
c22962_g1_i1	578.00	60.10	103.98

c23017_g1_i1	589.00	62.33	105.82
c23179_g1_i1	246.00	53.42	217.16
c23251_g1_i1	205.00	67.89	331.17
c23409_g1_i1	280.00	152.48	544.55
c23419_g1_i1	762.00	211.46	277.51
c23430_g1_i1	254.00	38.95	153.36
c23552_g1_i1	217.00	25.60	117.96
c23583_g1_i1	410.00	57.87	141.16
c23592_g1_i1	412.00	151.36	367.38
c23836_g1_i1	280.00	38.95	139.12
c23851_g1_i1	584.00	214.80	367.81
c23864_g1_i1	359.00	72.34	201.51
c23997_g1_i1	205.00	25.60	124.87
c24085_g1_i1	647.00	92.38	142.78
c24100_g1_i1	243.00	37.84	155.72
c24139_g1_i1	204.00	58.99	289.15
c24222_g1_i1	301.00	99.05	329.08
c24231_g2_i1	353.00	63.44	179.71
c24302_g1_i1	778.00	95.71	123.03
c2453_g1_i1	278.00	109.07	392.34
c24577_g1_i1	203.00	30.05	148.03
c24600_g1_i1	323.00	43.41	134.38
c24612_g1_i1	238.00	32.28	135.61
c24673_g1_i1	304.00	60.10	197.70
c24706_g1_i1	207.00	65.66	317.22
c24755_g1_i1	246.00	53.42	217.16
c24820_g1_i1	217.00	25.60	117.96
c24844_g1_i1	226.00	26.71	118.19
c24952_g1_i1	545.00	164.72	302.23
c24956_g1_i1	309.00	47.86	154.88
c25010_g1_i1	485.00	54.53	112.44
c25049_g1_i1	526.00	97.94	186.20
c25076_g1_i1	847.00	335.00	395.51
c25205_g1_i1	239.00	37.84	158.33
c25280_g1_i1	316.00	42.29	133.84
c25313_g1_i2	713.00	79.02	110.83
c25413_g1_i1	432.00	50.08	115.93
c25437_g1_i1	470.00	144.68	307.84
c25616_g1_i1	274.00	63.44	231.53
c25620_g1_i1	481.00	71.23	148.09
c25958_g1_i1	690.00	145.80	211.30
c25958_g2_i1	242.00	32.28	133.37
c26080_g1_i1	362.00	106.84	295.15

c26148_g1_i1	404.00	51.20	126.72
c26148_g2_i1	319.00	89.04	279.11
c26149_g1_i1	319.00	224.82	704.76
c26320_g1_i1	286.00	82.36	287.97
c26320_g2_i1	214.00	112.41	525.27
c26323_g1_i1	312.00	48.97	156.96
c26346_g1_i1	272.00	107.96	396.90
c26381_g1_i1	389.00	56.76	145.92
c26470_g1_i1	460.00	47.86	104.04
c26480_g1_i1	226.00	64.55	285.63
c26495_g1_i1	220.00	27.82	126.47
c26748_g1_i1	430.00	50.08	116.47
c26773_g1_i1	319.00	79.02	247.71
c26836_g1_i1	343.00	72.34	210.91
c2705_g1_i1	362.00	44.52	122.98
c27061_g1_i1	331.00	70.12	211.83
c27092_g1_i1	565.00	109.07	193.04
c27125_g1_i1	349.00	35.61	102.05
c27220_g1_i1	413.00	274.90	665.62
c2725_g1_i1	238.00	35.61	149.64
c2725_g2_i1	460.00	114.64	249.21
c27260_g1_i1	238.00	96.83	406.84
c27337_g1_i1	262.00	43.41	165.67
c27398_g1_i1	256.00	141.35	552.13
c27675_g1_i1	309.00	33.39	108.05
c27747_g1_i1	309.00	46.74	151.28
c27817_g1_i1	267.00	40.07	150.06
c2790_g1_i1	271.00	112.41	414.79
c28011_g1_i1	317.00	85.70	270.34
c2803_g1_i1	221.00	67.89	307.20
c28088_g1_i1	432.00	188.09	435.39
c28195_g1_i1	238.00	26.71	112.23
c28323_g1_i1	446.00	127.99	286.97
c2836_g1_i1	223.00	37.84	169.69
c28373_g2_i1	502.00	89.04	177.36
c28377_g1_i1	528.00	229.27	434.22
c28385_g1_i1	286.00	86.81	303.53
c28422_g1_i1	254.00	173.62	683.55
c28522_g1_i1	228.00	52.31	229.43
c28589_g1_i1	249.00	30.05	120.68
c28711_g1_i1	425.00	61.21	144.03
c28771_g1_i1	558.00	64.55	115.68
c28826_g1_i1	217.00	35.61	164.12

c28869_g1_i1	291.00	134.67	462.78
c28875_g1_i1	331.00	130.22	393.40
c28973_g2_i1	218.00	32.28	148.05
c28986_g1_i1	281.00	52.31	186.15
c28987_g1_i1	569.00	60.10	105.62
c29056_g1_i1	407.00	41.18	101.18
c29095_g1_i1	289.00	30.05	103.98
c29123_g1_i1	483.00	103.51	214.30
c29235_g1_i1	433.00	231.50	534.63
c29372_g1_i1	221.00	26.71	120.86
c2938_g1_i1	435.00	44.52	102.34
c29673_g1_i1	401.00	297.16	741.05
c29673_g2_i1	759.00	424.04	558.68
c29684_g1_i1	215.00	36.73	170.83
c29868_g1_i1	241.00	26.71	110.83
c29914_g1_i1	456.00	104.62	229.43
c29943_g1_i1	357.00	77.91	218.23
c30037_g1_i1	327.00	111.30	340.35
c3014_g1_i1	399.00	50.08	125.52
c30326_g2_i1	692.00	125.76	181.74
c3037_g1_i1	245.00	52.31	213.51
c30426_g1_i1	267.00	124.65	466.86
c30479_g1_i1	213.00	47.86	224.68
c3049_g1_i1	242.00	104.62	432.31
c30521_g1_i1	456.00	358.37	785.90
c305_g1_i1	257.00	94.60	368.10
c305_g2_i1	257.00	133.56	519.67
c30607_g1_i1	267.00	31.16	116.72
c30627_g1_i1	588.00	60.10	102.21
c30964_g1_i1	418.00	508.62	1216.80
c31014_g1_i1	377.00	54.53	144.66
c31075_g1_i1	366.00	40.07	109.47
c31397_g1_i2	311.00	48.97	157.46
c31518_g1_i2	560.00	62.33	111.30
c31611_g1_i1	564.00	144.68	256.53
c31727_g1_i1	326.00	60.10	184.36
c3188_g1_i1	437.00	470.78	1077.30
c32078_g1_i1	382.00	152.48	399.15
c32356_g1_i1	213.00	34.50	161.98
c3245_g1_i1	292.00	56.76	194.39
c32604_g1_i1	213.00	103.51	485.94
c32703_g1_i1	205.00	33.39	162.87
c32885_g1_i1	341.00	851.41	2496.81

c33073_g1_i1	325.00	73.46	226.02
c33084_g1_i1	415.00	42.29	101.91
c33126_g1_i1	208.00	24.49	117.72
c33191_g2_i1	254.00	26.71	105.16
c33242_g1_i1	247.00	72.34	292.88
c33389_g1_i1	671.00	121.31	180.79
c33424_g1_i1	243.00	24.49	100.76
c33601_g1_i1	216.00	42.29	195.80
c33790_g1_i1	207.00	100.17	483.90
c3390_g1_i1	326.00	95.71	293.60
c34048_g1_i1	291.00	55.65	191.23
c34203_g1_i1	453.00	75.68	167.07
c34248_g1_i1	288.00	56.76	197.09
c34280_g1_i1	313.00	61.21	195.57
c34288_g1_i1	228.00	73.46	322.17
c34431_g1_i1	415.00	62.33	150.18
c34467_g2_i1	465.00	48.97	105.31
c34629_g1_i1	201.00	173.62	863.79
c34649_g1_i1	380.00	53.42	140.58
c34670_g1_i1	382.00	89.04	233.08
c34990_g1_i1	469.00	291.60	621.74
c3502_g1_i1	358.00	171.40	478.76
c35243_g1_i1	355.00	169.17	476.53
c3542_g1_i1	453.00	196.99	434.86
c3542_g2_i1	453.00	120.20	265.34
c35825_g1_i1	219.00	204.78	935.09
c35974_g1_i1	231.00	148.02	640.79
c36003_g1_i1	229.00	92.38	403.39
c36086_g1_i1	206.00	25.60	124.26
c3609_g1_i1	270.00	42.29	156.64
c36150_g1_i1	239.00	55.65	232.84
c36217_g1_i1	223.00	60.10	269.51
c36309_g1_i1	372.00	62.33	167.54
c36384_g1_i1	315.00	120.20	381.59
c36576_g1_i1	465.00	69.00	148.39
c36791_g1_i1	221.00	22.26	100.72
c3690_g1_i1	435.00	127.99	294.23
c36913_g1_i1	429.00	113.52	264.62
c37578_g1_i1	284.00	99.05	348.78
c37675_g1_i1	206.00	87.92	426.81
c37712_g1_i1	215.00	41.18	191.53
c37748_g1_i1	266.00	32.28	121.34
c37798_g1_i1	312.00	84.58	271.11

c37798_g2_i1	670.00	92.38	137.87
c37816_g1_i1	304.00	44.52	146.44
c37884_g1_i1	380.00	71.23	187.45
c37888_g1_i1	242.00	28.94	119.57
c38148_g1_i1	796.00	199.22	250.28
c38273_g1_i1	308.00	35.61	115.63
c38342_g1_i1	529.00	164.72	311.38
c38468_g1_i1	208.00	64.55	310.34
c38500_g1_i1	216.00	55.65	257.63
c38518_g1_i1	326.00	1208.67	3707.58
c38526_g1_i1	321.00	130.22	405.66
c38527_g1_i1	279.00	42.29	151.59
c38631_g1_i1	271.00	38.95	143.74
c38666_g1_i1	336.00	47.86	142.43
c38867_g1_i1	250.00	61.21	244.85
c38966_g1_i1	441.00	83.47	189.28
c39004_g1_i1	441.00	242.63	550.17
c39030_g1_i1	463.00	52.31	112.98
c39036_g1_i1	398.00	217.03	545.29
c39080_g1_i1	251.00	32.28	128.59
c39567_g1_i1	291.00	42.29	145.34
c39590_g1_i1	405.00	48.97	120.91
c39778_g1_i1	376.00	47.86	127.28
c39778_g2_i1	480.00	201.45	419.68
c39951_g1_i1	287.00	131.33	457.59
c40006_g1_i1	232.00	54.53	235.06
c40134_g1_i1	276.00	32.28	116.94
c40200_g1_i1	299.00	105.73	353.62
c40200_g2_i1	254.00	66.78	262.90
c40256_g1_i1	370.00	75.68	204.54
c40366_g1_i1	206.00	69.00	334.97
c40500_g1_i1	403.00	104.62	259.60
c40516_g2_i1	209.00	35.61	170.41
c40549_g1_i1	248.00	33.39	134.63
c40575_g1_i1	245.00	169.17	690.49
c40589_g1_i1	478.00	81.25	169.97
c40739_g2_i1	297.00	60.10	202.36
c40761_g1_i1	210.00	53.42	254.39
c40761_g2_i1	264.00	58.99	223.44
c40833_g1_i1	417.00	146.91	352.30
c40833_g2_i1	213.00	50.08	235.13
c40895_g1_i1	247.00	101.28	410.04
c408_g1_i1	221.00	103.51	468.35

c40966_g1_i1	640.00	84.58	132.16
c41108_g1_i1	245.00	51.20	208.96
c41491_g1_i1	371.00	248.19	668.97
c41525_g1_i1	252.00	50.08	198.74
c41528_g1_i1	207.00	53.42	258.08
c4161_g1_i1	202.00	245.96	1217.64
c41679_g1_i1	410.00	99.05	241.59
c42003_g1_i1	217.00	720.08	3318.36
c42009_g1_i2	537.00	100.17	186.53
c42048_g1_i1	413.00	178.07	431.17
c42229_g1_i1	292.00	30.05	102.91
c42250_g1_i1	286.00	32.28	112.85
c42278_g1_i1	225.00	106.84	474.86
c42290_g1_i1	204.00	55.65	272.78
c42348_g1_i1	243.00	53.42	219.84
c42366_g1_i1	223.00	23.37	104.81
c42378_g1_i1	228.00	55.65	244.07
c42459_g1_i1	375.00	51.20	136.52
c42533_g1_i1	210.00	56.76	270.29
c42589_g1_i1	321.00	44.52	138.69
c42706_g1_i1	296.00	34.50	116.56
c42827_g1_i1	206.00	36.73	178.29
c42879_g1_i1	214.00	56.76	265.24
c43027_g1_i1	230.00	38.95	169.36
c43083_g2_i1	268.00	40.07	149.50
c43259_g1_i1	201.00	32.28	160.58
c43296_g1_i1	294.00	66.78	227.13
c43392_g1_i1	359.00	54.53	151.91
c43568_g1_i1	377.00	81.25	215.51
c43767_g1_i1	1630.00	115.75	71.01
c43795_g1_i1	440.00	84.58	192.24
c43860_g1_i1	499.00	51.20	102.60
c43881_g1_i1	340.00	45.63	134.21
c44018_g1_i1	331.00	41.18	124.41
c44074_g1_i1	306.00	76.79	250.96
c44074_g2_i1	490.00	71.23	145.37
c44134_g1_i1	677.00	411.79	608.26
c44137_g1_i1	238.00	31.16	130.94
c44193_g1_i1	273.00	81.25	297.60
c44253_g1_i1	334.00	43.41	129.96
c44434_g1_i1	224.00	34.50	154.03
c44707_g1_i1	1990.00	914.85	459.72
c44875_g1_i1	212.00	123.54	582.73

c44907_g1_i1	340.00	35.61	104.75
c45021_g1_i1	228.00	71.23	312.41
c45147_g1_i1	288.00	43.41	150.71
c45194_g1_i1	219.00	28.94	132.13
c45555_g1_i1	390.00	55.65	142.69
c45593_g1_i1	253.00	82.36	325.53
c46019_g1_i1	264.00	65.66	248.73
c4620_g1_i1	897.00	180.30	201.00
c46284_g1_i1	207.00	235.95	1139.84
c46359_g1_i1	509.00	62.33	122.45
c46568_g1_i1	437.00	129.10	295.43
c46568_g2_i1	201.00	32.28	160.58
c46678_g1_i1	285.00	100.17	351.46
c46713_g1_i1	376.00	47.86	127.28
c46862_g1_i1	201.00	32.28	160.58
c47180_g1_i1	1093.00	298.27	272.89
c47350_g1_i1	208.00	161.38	775.86
c47540_g1_i1	244.00	46.74	191.58
c47540_g2_i1	231.00	46.74	202.36
c47733_g1_i1	212.00	35.61	167.99
c47789_g1_i1	303.00	125.76	415.06
c48004_g1_i1	211.00	47.86	226.81
c48017_g1_i1	399.00	64.55	161.78
c48110_g1_i1	409.00	476.35	1164.66
c48395_g1_i1	277.00	28.94	104.47
c48589_g1_i1	617.00	296.05	479.82
c48899_g1_i1	352.00	45.63	129.63
c48999_g1_i1	239.00	54.53	228.18
c49108_g1_i1	204.00	28.94	141.85
c49265_g1_i2	243.00	90.15	370.99
c49521_g1_i1	466.00	174.73	374.97
c49896_g1_i1	270.00	99.05	366.86
c50075_g1_i1	235.00	41.18	175.23
c50168_g1_i1	225.00	25.60	113.77
c50198_g1_i1	237.00	45.63	192.54
c50281_g1_i1	1011.00	327.21	323.65
c50298_g1_i1	355.00	41.18	116.00
c50459_g1_i1	226.00	48.97	216.68
c50574_g1_i1	246.00	93.49	380.03
c50812_g1_i1	290.00	89.04	307.02
c50885_g1_i1	207.00	54.53	263.45
c50898_g1_i1	342.00	249.30	728.96
c50904_g1_i1	233.00	38.95	167.18

c50955_g1_i1	202.00	158.04	782.38
c50955_g2_i1	289.00	164.72	569.96
c51043_g1_i1	275.00	105.73	384.48
c51069_g1_i1	225.00	40.07	178.07
c51093_g1_i1	405.00	72.34	178.62
c51219_g1_i1	247.00	57.87	234.31
c51325_g1_i1	203.00	47.86	235.75
c51378_g1_i1	424.00	110.18	259.87
c51436_g1_i1	271.00	155.81	574.96
c51456_g1_i1	212.00	129.10	608.98
c51649_g1_i1	203.00	96.83	476.98
c51732_g1_i1	236.00	25.60	108.47
c51857_g1_i1	433.00	277.13	640.02
c51974_g1_i1	265.00	211.46	797.97
c52048_g1_i1	208.00	53.42	256.84
c52089_g1_i1	407.00	58.99	144.93
c52130_g1_i1	333.00	61.21	183.82
c52139_g1_i1	473.00	54.53	115.30
c52161_g1_i1	239.00	61.21	256.12
c52532_g1_i1	350.00	37.84	108.12
c52532_g2_i1	215.00	24.49	113.88
c5297_g1_i1	222.00	65.66	295.79
c52984_g1_i1	287.00	67.89	236.55
c53066_g2_i1	338.00	46.74	138.30
c53224_g1_i1	209.00	28.94	138.45
c53387_g1_i1	339.00	34.50	101.78
c53471_g1_i1	273.00	70.12	256.84
c53479_g1_i1	215.00	92.38	429.65
c5376_g1_i1	508.00	64.55	127.07
c54006_g1_i1	240.00	65.66	273.60
c54105_g1_i1	220.00	41.18	187.18
c54105_g2_i1	349.00	38.95	111.62
c54222_g1_i1	342.00	54.53	159.46
c54434_g1_i1	220.00	44.52	202.36
c54736_g1_i1	336.00	99.05	294.80
c54780_g1_i1	372.00	40.07	107.71
c54785_g1_i1	374.00	218.14	583.26
c54889_g1_i1	215.00	75.68	352.01
c55593_g1_i1	1915.00	357.26	186.56
c55633_g1_i1	274.00	80.13	292.46
c55853_g1_i1	267.00	28.94	108.38
c55930_g1_i1	220.00	74.57	338.95
c55931_g1_i1	429.00	62.33	145.28

c55999_g1_i1	479.00	230.38	480.97
c56001_g1_i1	233.00	87.92	377.36
c56400_g1_i1	323.00	48.97	151.61
c56629_g1_i1	1259.00	1007.23	800.02
c56709_g1_i1	204.00	34.50	169.13
c56765_g1_i1	237.00	126.88	535.35
c57072_g1_i1	222.00	38.95	175.47
c57105_g1_i1	284.00	173.62	611.34
c57536_g1_i1	245.00	58.99	240.76
c57556_g1_i1	329.00	36.73	111.63
c57685_g1_i1	283.00	30.05	106.18
c57812_g1_i1	206.00	42.29	205.30
c578_g1_i1	225.00	62.33	277.00
c58116_g1_i1	206.00	145.80	707.75
c58131_g1_i1	318.00	35.61	112.00
c58212_g1_i1	319.00	35.61	111.65
c58530_g1_i1	207.00	186.98	903.27
c58647_g1_i1	258.00	46.74	181.18
c58888_g1_i1	261.00	34.50	132.19
c5900_g1_i1	305.00	51.20	167.86
c59057_g1_i1	295.00	173.62	588.55
c59303_g1_i1	203.00	84.58	416.67
c5959_g1_i1	203.00	47.86	235.75
c59710_g1_i1	274.00	121.31	442.75
c59978_g1_i1	318.00	35.61	112.00
c60017_g1_i1	263.00	109.07	414.71
c60021_g1_i1	344.00	37.84	110.00
c6050_g1_i1	225.00	30.05	133.56
c60538_g1_i1	387.00	152.48	393.99
c60538_g2_i1	237.00	100.17	422.64
c60543_g1_i1	289.00	80.13	277.28
c6056_g1_i1	255.00	342.79	1344.28
c606_g1_i1	300.00	42.29	140.98
c61124_g1_i1	249.00	66.78	268.18
c6118_g1_i1	362.00	205.90	568.78
c61194_g1_i1	420.00	375.07	893.02
c61271_g1_i1	309.00	60.10	194.50
c61320_g1_i1	297.00	130.22	438.44
c61324_g1_i1	217.00	31.16	143.61
c61352_g1_i1	605.00	93.49	154.53
c61493_g1_i1	273.00	111.30	407.68
c61512_g1_i1	257.00	67.89	264.17
c6158_g1_i1	228.00	27.82	122.04

c61704_g1_i1	381.00	251.53	660.18
c61766_g1_i1	234.00	41.18	175.98
c61805_g1_i1	219.00	64.55	294.76
c61900_g1_i1	299.00	34.50	115.39
c61918_g1_i1	270.00	87.92	325.64
c62246_g1_i1	211.00	32.28	152.97
c62433_g1_i1	331.00	66.78	201.75
c62566_g1_i1	328.00	133.56	407.18
c62586_g1_i1	241.00	106.84	443.34
c62679_g1_i1	233.00	106.84	458.56
c62735_g1_i1	222.00	115.75	521.39
c62913_g1_i1	228.00	27.82	122.04
c63006_g1_i1	213.00	95.71	449.36
c6303_g1_i1	335.00	34.50	102.99
c63100_g1_i2	371.00	71.23	191.99
c63198_g1_i1	300.00	35.61	118.72
c63286_g1_i1	386.00	47.86	123.98
c63691_g1_i1	215.00	69.00	320.95
c6369_g2_i1	299.00	55.65	186.11
c63703_g1_i1	217.00	65.66	302.60
c63851_g1_i1	216.00	38.95	180.34
c63884_g1_i1	230.00	40.07	174.20
c6404_g1_i1	573.00	109.07	190.35
c6417_g1_i1	403.00	45.63	113.23
c6434_g1_i1	210.00	58.99	280.89
c64360_g1_i1	274.00	42.29	154.35
c64432_g1_i1	333.00	60.10	180.48
c64522_g1_i1	211.00	26.71	126.59
c64544_g1_i1	243.00	34.50	141.98
c64722_g1_i1	547.00	204.78	374.38
c64917_g1_i1	556.00	66.78	120.10
c64_g1_i1	212.00	142.46	671.97
c64_g2_i1	257.00	283.80	1104.30
c65117_g1_i1	334.00	496.38	1486.16
c65359_g1_i1	256.00	52.31	204.33
c65425_g1_i1	233.00	61.21	262.72
c65614_g1_i1	281.00	102.39	364.39
c66169_g1_i1	232.00	60.10	259.05
c66373_g1_i1	424.00	82.36	194.24
c6643_g1_i1	330.00	44.52	134.90
c66768_g1_i1	503.00	287.14	570.86
c66956_g1_i1	314.00	56.76	180.77
c67030_g1_i1	447.00	51.20	114.53

c67148_g1_i1	224.00	36.73	163.96
c67183_g1_i1	270.00	64.55	239.08
c67380_g1_i1	288.00	57.87	200.95
c6742_g1_i1	248.00	28.94	116.68
c67576_g1_i1	267.00	79.02	295.96
c67713_g1_i1	211.00	37.84	179.34
c67732_g1_i1	324.00	121.31	374.42
c68061_g2_i1	430.00	74.57	173.41
c68267_g1_i1	286.00	28.94	101.18
c68361_g1_i1	931.00	406.23	436.34
c68361_g2_i1	320.00	55.65	173.90
c68555_g1_i1	332.00	44.52	134.09
c68680_g1_i1	380.00	117.97	310.46
c68830_g1_i1	307.00	33.39	108.76
c68961_g1_i1	241.00	123.54	512.61
c69031_g1_i1	257.00	155.81	606.28
c69052_g1_i1	221.00	51.20	231.66
c69066_g1_i1	350.00	64.55	184.43
c69134_g1_i1	245.00	35.61	145.37
c69152_g1_i1	389.00	116.86	300.41
c69152_g2_i1	257.00	70.12	272.83
c69166_g1_i1	330.00	540.90	1639.08
c69190_g1_i1	353.00	57.87	163.95
c69226_g1_i1	235.00	37.84	161.02
c69363_g1_i1	586.00	65.66	112.06
c69374_g1_i1	213.00	30.05	141.08
c69551_g1_i1	205.00	182.53	890.37
c69551_g2_i1	268.00	259.32	967.61
c69614_g1_i1	360.00	54.53	151.49
c69660_g1_i2	460.00	77.91	169.36
c69675_g1_i1	358.00	76.79	214.51
c69678_g1_i1	469.00	80.13	170.86
c69678_g2_i1	306.00	48.97	160.03
c69782_g1_i1	203.00	34.50	169.96
c69791_g1_i1	426.00	106.84	250.81
c69791_g2_i1	400.00	73.46	183.64
c69882_g1_i1	335.00	34.50	102.99
c69884_g1_i1	278.00	67.89	244.21
c69906_g2_i1	278.00	33.39	120.10
c69906_g3_i1	219.00	81.25	370.99
c69952_g1_i1	232.00	55.65	239.86
c69952_g2_i1	581.00	155.81	268.18
c70081_g1_i1	266.00	146.91	552.30

c70109_g1_i1	431.00	90.15	209.16
c70311_g1_i1	254.00	36.73	144.60
c70340_g1_i1	412.00	44.52	108.05
c7034_g1_i1	358.00	36.73	102.59
c70363_g1_i1	290.00	64.55	222.59
c70405_g1_i1	223.00	26.71	119.78
c70439_g1_i1	355.00	43.41	122.27
c7049_g1_i1	244.00	144.68	592.97
c70503_g1_i1	671.00	574.29	855.87
c70553_g1_i1	616.00	388.42	630.56
c70584_g1_i1	217.00	33.39	153.87
c70646_g1_i1	245.00	25.60	104.48
c70712_g1_i1	217.00	64.55	297.47
c70712_g2_i1	242.00	94.60	390.92
c70726_g1_i1	473.00	77.91	164.71
c70726_g2_i1	673.00	160.27	238.14
c70736_g1_i1	251.00	36.73	146.33
c70779_g1_i1	423.00	173.62	410.45
c70825_g1_i1	325.00	392.87	1208.84
c70867_g1_i1	269.00	89.04	330.99
c70877_g1_i1	295.00	142.46	482.91
c70877_g2_i1	292.00	131.33	449.76
c70890_g2_i1	640.00	129.10	201.72
c70929_g2_i1	227.00	40.07	176.50
c70929_g3_i1	380.00	54.53	143.51
c70976_g1_i1	491.00	89.04	181.34
c70976_g2_i1	283.00	28.94	102.25
c70993_g1_i1	286.00	34.50	120.64
c71005_g1_i1	446.00	66.78	149.73
c71063_g1_i1	416.00	104.62	251.49
c71102_g1_i1	357.00	74.57	208.87
c71102_g3_i1	215.00	28.94	134.59
c71139_g1_i1	323.00	86.81	268.76
c71262_g1_i1	226.00	57.87	256.08
c71297_g2_i1	287.00	70.12	244.31
c71349_g2_i1	213.00	40.07	188.11
c71412_g1_i2	672.00	166.94	248.43
c71546_g2_i1	216.00	32.28	149.43
c71622_g1_i1	241.00	85.70	355.59
c71659_g1_i1	237.00	53.42	225.41
c71691_g1_i1	272.00	122.43	450.09
c71725_g1_i1	305.00	60.10	197.05
c71865_g2_i1	246.00	46.74	190.02

c71897_g1_i1	535.00	172.51	322.45
c71949_g1_i1	316.00	34.50	109.18
c71949_g1_i2	369.00	57.87	156.84
c72155_g1_i1	362.00	210.35	581.07
c72248_g1_i1	229.00	24.49	106.92
c72268_g1_i1	244.00	217.03	889.45
c72268_g2_i1	547.00	114.64	209.57
c72302_g1_i1	414.00	125.76	303.78
c72308_g1_i1	475.00	47.86	100.75
c72354_g1_i1	434.00	166.94	384.66
c72354_g2_i1	572.00	64.55	112.85
c7243_g2_i1	276.00	30.05	108.88
c72503_g1_i1	207.00	398.44	1924.82
c72583_g1_i1	207.00	41.18	198.93
c72654_g1_i1	207.00	54.53	263.45
c72654_g2_i1	648.00	122.43	188.93
c72757_g1_i1	280.00	31.16	111.30
c72836_g1_i1	360.00	66.78	185.49
c72853_g1_i1	637.00	110.18	172.97
c7287_g1_i1	337.00	328.32	974.25
c72979_g1_i1	203.00	22.26	109.65
c72987_g1_i1	421.00	50.08	118.96
c73068_g1_i1	325.00	35.61	109.58
c7318_g1_i1	235.00	48.97	208.38
c73216_g1_i1	220.00	27.82	126.47
c73236_g2_i1	773.00	181.41	234.69
c73249_g1_i1	236.00	251.53	1065.80
c73286_g1_i1	524.00	162.49	310.10
c73286_g2_i1	417.00	84.58	202.84
c73306_g1_i1	280.00	35.61	127.20
c73306_g3_i1	296.00	57.87	195.52
c73348_g1_i1	204.00	44.52	218.23
c73403_g1_i1	206.00	28.94	140.47
c73426_g1_i1	630.00	411.79	653.64
c73427_g1_i1	224.00	26.71	119.25
c73427_g2_i1	1045.00	233.72	223.66
c73447_g1_i2	608.00	73.46	120.81
c73498_g1_i1	298.00	72.34	242.76
c73546_g1_i1	285.00	65.66	230.40
c73553_g1_i1	315.00	84.58	268.52
c7355_g1_i1	266.00	35.61	133.89
c73617_g1_i1	259.00	41.18	158.99
c74148_g1_i1	252.00	37.84	150.16

c74410_g1_i1	250.00	28.94	115.75
c74476_g1_i1	506.00	54.53	107.78
c74480_g1_i1	523.00	60.10	114.91
c74509_g1_i1	1059.00	154.70	146.08
c74565_g1_i1	255.00	28.94	113.48
c74589_g1_i2	334.00	45.63	136.62
c74682_g1_i1	345.00	62.33	180.65
c74741_g1_i1	316.00	40.07	126.79
c74777_g1_i2	370.00	38.95	105.28
c7483_g1_i1	209.00	72.34	346.14
c74841_g1_i1	297.00	34.50	116.17
c74941_g1_i1	336.00	56.76	168.93
c75107_g1_i1	543.00	111.30	204.97
c75158_g1_i1	1034.00	251.53	243.26
c75235_g1_i1	314.00	46.74	148.87
c75318_g1_i1	306.00	37.84	123.66
c75339_g1_i1	378.00	84.58	223.77
c75383_g1_i1	470.00	81.25	172.86
c75383_g2_i1	281.00	65.66	233.68
c75440_g1_i1	212.00	94.60	446.23
c7547_g1_i1	208.00	36.73	176.58
c75519_g1_i1	393.00	683.36	1738.82
c75664_g1_i1	740.00	253.75	342.91
c75664_g2_i1	562.00	188.09	334.68
c75752_g1_i1	277.00	146.91	530.36
c75761_g1_i1	205.00	65.66	320.32
c75761_g2_i1	1117.00	397.33	355.71
c75812_g1_i1	219.00	109.07	498.04
c75860_g1_i1	205.00	80.13	390.89
c76080_g1_i1	384.00	46.74	121.73
c76096_g1_i1	390.00	215.91	553.63
c76224_g1_i1	283.00	132.44	467.99
c76330_g1_i1	205.00	34.50	168.30
c76356_g1_i1	451.00	104.62	231.97
c76427_g1_i1	285.00	65.66	230.40
c76427_g2_i1	398.00	56.76	142.62
c76487_g3_i1	667.00	95.71	143.50
c76548_g1_i1	481.00	410.68	853.81
c76548_g2_i1	410.00	237.06	578.20
c76577_g1_i1	201.00	74.57	370.99
c76593_g1_i1	347.00	55.65	160.37
c76854_g1_i1	829.00	397.33	479.28
c76887_g2_i1	315.00	74.57	236.72

c76945_g1_i1	255.00	113.52	445.18
c7703_g1_i1	312.00	41.18	131.99
c77059_g1_i1	224.00	125.76	561.45
c77071_g1_i1	227.00	64.55	284.37
c77098_g1_i1	453.00	79.02	174.44
c77142_g1_i1	210.00	33.39	158.99
c77178_g1_i1	498.00	179.19	359.81
c77278_g1_i1	233.00	45.63	195.84
c77370_g1_i1	345.00	54.53	158.07
c77370_g2_i1	270.00	72.34	267.93
c77500_g1_i1	216.00	60.10	278.24
c77602_g1_i1	279.00	74.57	267.27
c77934_g1_i1	214.00	26.71	124.82
c77957_g1_i1	316.00	71.23	225.41
c77969_g2_i2	208.00	85.70	412.01
c77999_g1_i1	607.00	94.60	155.85
c78049_g1_i1	461.00	76.79	166.58
c78211_g1_i1	800.00	151.36	189.20
c78270_g1_i1	269.00	75.68	281.34
c78295_g1_i1	249.00	48.97	196.67
c78304_g1_i1	266.00	116.86	439.33
c78406_g1_i1	215.00	50.08	232.95
c78406_g2_i1	316.00	44.52	140.88
c78443_g1_i1	244.00	82.36	337.54
c78563_g1_i1	681.00	79.02	116.04
c78622_g1_i1	735.00	186.98	254.39
c78787_g1_i1	417.00	66.78	160.14
c78811_g1_i1	581.00	69.00	118.77
c78864_g1_i1	334.00	117.97	353.21
c78893_g1_i1	235.00	62.33	265.22
c78893_g1_i2	238.00	102.39	430.22
c78893_g2_i1	205.00	175.85	857.79
c78914_g1_i1	548.00	106.84	194.97
c78933_g1_i1	302.00	71.23	235.86
c78933_g2_i1	314.00	46.74	148.87
c79016_g1_i1	1048.00	107.96	103.01
c79028_g1_i1	591.00	89.04	150.65
c79098_g1_i1	245.00	31.16	127.20
c79098_g2_i1	230.00	36.73	159.69
c79166_g1_i1	259.00	58.99	227.75
c79206_g1_i1	518.00	176.96	341.62
c79372_g1_i1	345.00	92.38	267.76
c79450_g1_i1	223.00	41.18	184.66

c79526_g1_i1	208.00	48.97	235.43
c79526_g2_i1	435.00	66.78	153.51
c79535_g1_i1	377.00	43.41	115.13
c79583_g1_i1	276.00	44.52	161.30
c79583_g2_i1	274.00	54.53	199.03
c79637_g1_i1	405.00	50.08	123.66
c79686_g1_i1	310.00	212.58	685.73
c79796_g1_i1	281.00	55.65	198.04
c79834_g1_i1	465.00	99.05	213.02
c79869_g1_i1	207.00	57.87	279.58
c79877_g1_i1	1111.00	141.35	127.22
c79888_g1_i1	282.00	41.18	146.03
c79888_g3_i1	324.00	41.18	127.10
c79958_g1_i1	289.00	35.61	123.23
c80061_g1_i1	210.00	117.97	561.78
c80223_g1_i1	202.00	30.05	148.76
c80264_g1_i1	348.00	133.56	383.78
c80273_g1_i1	204.00	61.21	300.06
c80276_g1_i1	601.00	251.53	418.52
c80276_g2_i1	219.00	83.47	381.15
c80284_g1_i1	330.00	491.93	1490.69
c80345_g1_i1	286.00	138.01	482.54
c80392_g1_i1	353.00	45.63	129.27
c80403_g1_i1	972.00	150.25	154.58
c80429_g1_i1	292.00	80.13	274.43
c80429_g2_i1	220.00	93.49	424.95
c80598_g1_i1	241.00	33.39	138.54
c80606_g1_i1	208.00	82.36	395.96
c80606_g2_i1	392.00	63.44	161.83
c80620_g1_i1	477.00	71.23	149.33
c80678_g1_i1	455.00	47.86	105.18
c80689_g1_i1	475.00	70.12	147.61
c80713_g1_i1	425.00	61.21	144.03
c80818_g1_i1	231.00	38.95	168.63
c80897_g1_i1	206.00	44.52	216.11
c80927_g1_i1	215.00	101.28	471.07
c80987_g1_i1	237.00	34.50	145.58
c81035_g1_i1	283.00	82.36	291.02
c81390_g1_i1	422.00	65.66	155.60
c81422_g1_i1	400.00	71.23	178.07
c81422_g2_i1	954.00	170.28	178.49
c81481_g1_i1	202.00	25.60	126.72
c81586_g1_i1	882.00	417.36	473.20

c81681_g1_i2	244.00	55.65	228.07
c81699_g1_i1	440.00	209.24	475.54
c8177_g1_i1	310.00	56.76	183.10
c81930_g1_i1	203.00	21.15	104.17
c81953_g1_i1	223.00	411.79	1846.61
c82045_g1_i1	362.00	154.70	427.35
c82150_g1_i1	337.00	112.41	333.56
c82159_g1_i1	222.00	26.71	120.32
c82214_g1_i1	240.00	196.99	820.81
c82243_g1_i1	270.00	65.66	243.20
c82243_g1_i2	374.00	146.91	392.81
c82309_g1_i1	467.00	57.87	123.93
c82331_g1_i1	356.00	45.63	128.18
c82341_g1_i1	280.00	92.38	329.91
c82368_g1_i1	204.00	64.55	316.43
c82454_g1_i1	454.00	104.62	230.44
c82457_g1_i2	285.00	44.52	156.21
c82464_g1_i1	373.00	101.28	271.53
c82513_g2_i1	459.00	80.13	174.58
c8251_g1_i1	243.00	67.89	279.38
c82546_g1_i1	212.00	70.12	330.74
c82546_g2_i1	510.00	245.96	482.28
c82568_g1_i1	541.00	122.43	226.29
c82570_g1_i1	239.00	64.55	270.09
c82594_g1_i1	204.00	22.26	109.11
c8261_g1_i1	246.00	468.56	1904.70
c82643_g1_i1	413.00	71.23	172.47
c82643_g2_i1	1117.00	129.10	115.58
c82718_g1_i1	709.00	284.92	401.86
c82738_g1_i1	320.00	41.18	128.69
c82831_g1_i1	578.00	72.34	125.16
c82841_g1_i1	216.00	30.05	139.12
c82933_g1_i1	410.00	44.52	108.58
c82967_g2_i1	203.00	162.49	800.45
c8301_g1_i1	298.00	50.08	168.06
c83029_g1_i1	294.00	33.39	113.57
c83073_g1_i1	368.00	72.34	196.58
c83073_g2_i1	227.00	48.97	215.73
c83129_g1_i1	303.00	36.73	121.21
c8314_g1_i1	560.00	119.09	212.65
c83151_g1_i1	208.00	23.37	112.37
c83190_g1_i1	275.00	133.56	485.65
c83190_g2_i1	332.00	62.33	187.73

c83201_g1_i1	346.00	240.40	694.79
c83247_g1_i1	876.00	259.32	296.03
c83247_g2_i1	1663.00	276.01	165.97
c83250_g1_i1	345.00	95.71	277.43
c83280_g1_i1	341.00	53.42	156.66
c83292_g1_i1	231.00	28.94	125.27
c83327_g1_i1	401.00	43.41	108.24
c83345_g1_i1	342.00	69.00	201.76
c83376_g1_i1	535.00	82.36	153.94
c83378_g1_i1	776.00	102.39	131.95
c83394_g1_i1	284.00	83.47	293.92
c83426_g1_i1	389.00	53.42	137.33
c83476_g1_i1	1452.00	316.08	217.69
c83574_g1_i1	841.00	89.04	105.87
c83600_g1_i1	532.00	151.36	284.52
c8363_g1_i1	202.00	34.50	170.80
c83654_g1_i1	201.00	24.49	121.82
c83660_g1_i1	207.00	23.37	112.91
c83701_g1_i1	211.00	22.26	105.49
c84021_g1_i1	267.00	52.31	195.91
c84023_g2_i1	261.00	30.05	115.13
c84065_g1_i1	634.00	261.55	412.53
c84065_g2_i1	283.00	51.20	180.91
c84067_g1_i1	663.00	156.93	236.69
c84157_g1_i1	371.00	121.31	326.99
c84157_g2_i1	430.00	117.97	274.36
c84239_g1_i1	311.00	83.47	268.40
c84290_g1_i1	644.00	190.32	295.52
c84295_g1_i1	410.00	99.05	241.59
c84330_g2_i1	257.00	31.16	121.26
c84446_g1_i1	1099.00	383.97	349.38
c84446_g2_i1	215.00	339.45	1578.85
c84469_g1_i1	387.00	114.64	296.21
c84469_g2_i1	465.00	53.42	114.89
c84495_g1_i1	434.00	63.44	146.17
c84574_g1_i1	350.00	201.45	575.56
c84601_g1_i1	329.00	85.70	260.48
c84625_g2_i1	262.00	32.28	123.19
c84637_g1_i1	239.00	86.81	363.23
c84637_g2_i1	268.00	30.05	112.13
c84646_g1_i1	354.00	74.57	210.64
c84810_g1_i1	377.00	44.52	118.09
c84875_g1_i1	699.00	317.19	453.78

c8493_g1_i1	442.00	142.46	322.30
c84940_g1_i2	1497.00	214.80	143.49
c85003_g1_i1	420.00	79.02	188.14
c85007_g1_i1	312.00	298.27	956.00
c85024_g1_i1	299.00	36.73	122.84
c85050_g1_i1	675.00	106.84	158.29
c85095_g1_i1	209.00	25.60	122.48
c85095_g2_i1	756.00	104.62	138.38
c85095_g4_i1	638.00	122.43	191.89
c850_g1_i1	324.00	103.51	319.46
c85273_g1_i1	271.00	47.86	176.60
c85298_g1_i2	1240.00	397.33	320.42
c85298_g2_i1	1153.00	141.35	122.59
c85316_g1_i1	375.00	66.78	178.07
c85352_g1_i1	251.00	247.08	984.37
c85357_g2_i1	483.00	102.39	211.99
c85426_g1_i1	385.00	231.50	601.29
c85504_g1_i2	505.00	60.10	119.01
c8550_g1_i1	457.00	65.66	143.69
c85517_g1_i1	444.00	218.14	491.31
c85518_g1_i1	219.00	53.42	243.94
c85522_g1_i1	402.00	63.44	157.81
c85545_g2_i1	240.00	27.82	115.93
c85557_g2_i1	567.00	63.44	111.89
c85648_g1_i1	458.00	66.78	145.80
c85780_g1_i1	316.00	32.28	102.14
c85792_g1_i1	265.00	249.30	940.76
c85875_g1_i1	682.00	238.17	349.23
c85886_g1_i1	216.00	24.49	113.36
c85998_g1_i1	219.00	28.94	132.13
c86000_g1_i1	351.00	54.53	155.37
c86031_g1_i1	244.00	66.78	273.68
c86031_g2_i1	676.00	76.79	113.60
c86084_g1_i1	417.00	84.58	202.84
c86102_g1_i1	343.00	193.66	564.59
c86102_g2_i1	230.00	134.67	585.51
c86159_g2_i1	263.00	144.68	550.13
c86262_g1_i1	230.00	58.99	256.46
c86262_g2_i1	320.00	82.36	257.37
c86262_g3_i1	402.00	231.50	575.86
c86470_g1_i1	354.00	192.54	543.90
c86657_g1_i1	397.00	60.10	151.39
c86668_g1_i1	836.00	219.25	262.26

c8680_g1_i1	244.00	43.41	177.89
c86822_g1_i1	306.00	90.15	294.61
c86843_g1_i1	261.00	41.18	157.78
c87000_g1_i1	295.00	35.61	120.73
c87105_g1_i1	203.00	42.29	208.34
c87132_g1_i1	296.00	32.28	109.04
c87132_g2_i1	512.00	64.55	126.08
c87150_g1_i1	219.00	54.53	249.02
c87168_g1_i1	264.00	129.10	489.03
c87168_g2_i1	480.00	109.07	227.23
c87168_g3_i1	688.00	121.31	176.33
c87218_g1_i1	501.00	286.03	570.92
c8724_g1_i1	692.00	142.46	205.87
c87254_g1_i1	211.00	21.15	100.22
c87270_g1_i1	409.00	67.89	165.99
c87299_g1_i1	313.00	89.04	284.46
c87332_g1_i1	421.00	99.05	235.28
c87353_g1_i1	296.00	45.63	154.16
c87353_g2_i1	381.00	43.41	113.93
c87429_g1_i1	1376.00	1603.77	1165.53
c87650_g1_i1	367.00	69.00	188.02
c87661_g1_i1	628.00	180.30	287.10
c87681_g1_i1	203.00	54.53	268.65
c87702_g1_i1	564.00	93.49	165.76
c87722_g1_i1	585.00	247.08	422.35
c87761_g1_i1	308.00	33.39	108.41
c87772_g1_i1	310.00	56.76	183.10
c87800_g1_i1	285.00	40.07	140.58
c87877_g1_i1	428.00	48.97	114.42
c87901_g1_i1	235.00	83.47	355.20
c87901_g1_i2	289.00	123.54	427.47
c87922_g1_i1	780.00	124.65	159.81
c88071_g1_i1	539.00	116.86	216.81
c88120_g1_i1	206.00	1318.85	6402.21
c88133_g1_i2	564.00	61.21	108.53
c88142_g1_i1	451.00	45.63	101.18
c88148_g1_i1	610.00	61.21	100.35
c88166_g1_i1	251.00	65.66	261.61
c88184_g1_i1	287.00	47.86	166.75
c88313_g1_i1	330.00	94.60	286.67
c88329_g1_i1	228.00	44.52	195.26
c88335_g1_i1	372.00	76.79	206.44
c8833_g1_i1	241.00	235.95	979.03

c88395_g1_i1	212.00	47.86	225.74
c88395_g3_i1	296.00	48.97	165.44
c88428_g1_i1	830.00	481.91	580.62
c88525_g1_i1	274.00	46.74	170.60
c88543_g1_i1	342.00	46.74	136.68
c88637_g1_i1	237.00	115.75	488.39
c88676_g1_i1	395.00	47.86	121.16
c88704_g2_i1	220.00	26.71	121.41
c88746_g1_i1	227.00	41.18	181.41
c88808_g1_i1	402.00	52.31	130.12
c88821_g1_i1	322.00	38.95	120.97
c88833_g1_i1	223.00	58.99	264.52
c8884_g1_i1	294.00	93.49	317.99
c88994_g1_i1	290.00	182.53	629.40
c89075_g1_i1	258.00	40.07	155.30
c89315_g1_i1	286.00	152.48	533.13
c89350_g1_i1	229.00	25.60	111.78
c89499_g1_i1	517.00	64.55	124.86
c89511_g1_i1	305.00	85.70	280.98
c89587_g1_i1	220.00	82.36	374.36
c89696_g1_i1	318.00	45.63	143.50
c89719_g1_i1	386.00	42.29	109.57
c89867_g1_i1	504.00	165.83	329.03
c89867_g2_i1	323.00	209.24	647.79
c89916_g1_i1	481.00	57.87	120.32
c89936_g1_i1	266.00	55.65	209.20
c89936_g2_i1	316.00	134.67	426.16
c8993_g1_i1	214.00	82.36	384.85
c89968_g1_i2	2080.00	121.31	58.32
c9003_g1_i1	649.00	169.17	260.66
c90119_g1_i1	316.00	38.95	123.27
c90176_g1_i1	985.00	188.09	190.95
c9025_g1_i1	322.00	41.18	127.89
c90359_g1_i1	283.00	42.29	149.44
c90359_g3_i1	305.00	32.28	105.82
c90458_g1_i1	384.00	213.69	556.48
c90525_g1_i1	338.00	56.76	167.93
c90543_g1_i1	219.00	32.28	147.38
c90543_g2_i1	207.00	116.86	564.54
c90586_g1_i1	805.00	119.09	147.93
c90623_g1_i1	298.00	71.23	239.02
c90629_g2_i1	572.00	94.60	165.39
c90685_g1_i1	235.00	203.67	866.69

c90794_g1_i1	566.00	194.77	344.11
c90802_g1_i1	280.00	32.28	115.27
c90831_g1_i1	415.00	43.41	104.59
c90871_g2_i1	230.00	28.94	125.81
c90916_g1_i1	300.00	37.84	126.14
c90930_g1_i1	264.00	40.07	151.77
c90957_g1_i1	226.00	80.13	354.57
c91032_g2_i1	256.00	45.63	178.25
c91049_g1_i1	310.00	122.43	394.92
c91095_g1_i1	250.00	40.07	160.27
c91144_g1_i1	562.00	267.11	475.28
c91151_g1_i1	551.00	271.56	492.85
c91160_g1_i1	205.00	25.60	124.87
c91246_g1_i1	426.00	45.63	107.12
c91286_g1_i1	555.00	131.33	236.63
c9131_g1_i1	305.00	35.61	116.77
c91323_g1_i1	252.00	26.71	106.00
c91364_g1_i1	685.00	97.94	142.98
c9141_g1_i1	259.00	136.89	528.55
c91452_g1_i1	257.00	43.41	168.89
c91464_g1_i1	239.00	31.16	130.39
c91472_g1_i1	509.00	671.11	1318.49
c91484_g1_i1	248.00	45.63	184.00
c9148_g1_i1	239.00	42.29	176.96
c91532_g1_i1	804.00	141.35	175.80
c91627_g1_i1	209.00	44.52	213.01
c91653_g1_i2	770.00	102.39	132.98
c91656_g1_i1	406.00	74.57	183.67
c91715_g1_i1	280.00	189.20	675.72
c91739_g1_i2	644.00	91.26	141.71
c91749_g1_i1	1023.00	189.20	184.95
c91749_g2_i1	517.00	204.78	396.10
c91759_g1_i1	1224.00	179.19	146.39
c9177_g1_i1	450.00	93.49	207.75
c91790_g1_i1	448.00	138.01	308.05
c91859_g1_i1	437.00	171.40	392.21
c91859_g2_i1	1951.00	582.08	298.35
c91870_g1_i1	395.00	409.57	1036.88
c91876_g1_i1	251.00	154.70	616.34
c91916_g1_i1	387.00	41.18	106.41
c91943_g1_i1	262.00	200.33	764.63
c91959_g1_i1	815.00	87.92	107.88
c92018_g1_i1	549.00	73.46	133.80

c92019_g1_i1	275.00	66.78	242.83
c92025_g1_i1	204.00	30.05	147.30
c92052_g1_i1	926.00	99.05	106.97
c9205_g1_i1	240.00	42.29	176.22
c9205_g2_i1	511.00	116.86	228.69
c92136_g1_i1	878.00	106.84	121.69
c9219_g1_i1	207.00	120.20	580.67
c92207_g1_i1	1116.00	678.90	608.34
c92253_g1_i1	1051.00	514.19	489.24
c92305_g1_i1	280.00	30.05	107.32
c92314_g1_i1	213.00	69.00	323.96
c92334_g1_i1	401.00	66.78	166.53
c92360_g1_i1	208.00	54.53	262.19
c92430_g1_i1	404.00	64.55	159.78
c92471_g1_i1	507.00	204.78	403.91
c92497_g1_i1	412.00	43.41	105.35
c92546_g1_i1	614.00	109.07	177.64
c92550_g1_i1	1589.00	622.14	391.53
c92557_g1_i1	244.00	41.18	168.77
c92619_g1_i1	508.00	172.51	339.58
c92683_g1_i1	385.00	284.92	740.04
c92690_g1_i1	301.00	62.33	207.06
c92765_g1_i1	1465.00	222.59	151.94
c92765_g2_i1	533.00	62.33	116.93
c92765_g3_i1	585.00	130.22	222.59
c92765_g4_i1	778.00	142.46	183.11
c92770_g1_i1	382.00	430.72	1127.52
c92809_g2_i1	550.00	282.69	513.98
c92837_g1_i1	1236.00	134.67	108.96
c92854_g1_i1	554.00	178.07	321.43
c92898_g1_i1	336.00	45.63	135.81
c92924_g1_i1	246.00	53.42	217.16
c93007_g1_i1	505.00	90.15	178.51
c93029_g1_i1	232.00	153.59	662.02
c93035_g1_i1	400.00	148.02	370.06
c93043_g1_i1	297.00	43.41	146.15
c93054_g1_i1	562.00	56.76	101.00
c93077_g1_i1	210.00	74.57	355.09
c93091_g1_i1	236.00	42.29	179.21
c93302_g1_i1	292.00	32.28	110.53
c93314_g1_i1	360.00	446.30	1239.71
c93317_g1_i1	473.00	77.91	164.71
c93369_g1_i1	492.00	60.10	122.15

c93441_g1_i1	237.00	35.61	150.27
c93508_g1_i1	313.00	126.88	405.36
c93508_g2_i1	367.00	140.23	382.11
c93508_g3_i1	210.00	124.65	593.58
c93620_g1_i1	626.00	144.68	231.13
c93802_g1_i1	299.00	71.23	238.23
c93830_g1_i1	700.00	336.11	480.16
c93843_g1_i1	221.00	42.29	191.37
c93904_g1_i1	208.00	22.26	107.02
c93904_g2_i1	359.00	54.53	151.91
c93920_g1_i1	314.00	61.21	194.95
c93920_g1_i2	344.00	87.92	255.59
c93998_g1_i1	231.00	69.00	298.72
c94030_g1_i1	295.00	556.48	1886.37
c94058_g2_i1	532.00	120.20	225.94
c94092_g1_i1	1721.00	616.58	358.27
c94092_g2_i1	323.00	90.15	279.10
c94094_g2_i1	555.00	158.04	284.76
c94135_g1_i1	2220.00	430.72	194.02
c94135_g3_i1	660.00	90.15	136.59
c94227_g1_i1	511.00	97.94	191.66
c94227_g2_i1	272.00	30.05	110.48
c94227_g5_i1	489.00	93.49	191.18
c94295_g2_i1	411.00	48.97	119.15
c94318_g1_i1	262.00	31.16	118.94
c94419_g1_i1	662.00	125.76	189.98
c94465_g1_i1	354.00	79.02	223.22
c94516_g1_i1	550.00	298.27	542.31
c94536_g1_i1	381.00	85.70	224.93
c94539_g1_i1	213.00	34.50	161.98
c94552_g2_i1	266.00	54.53	205.02
c94587_g2_i1	230.00	27.82	120.97
c94591_g1_i1	516.00	53.42	103.53
c94595_g1_i1	408.00	132.44	324.61
c94595_g2_i1	528.00	114.64	217.11
c94615_g1_i1	447.00	90.15	201.68
c94615_g2_i1	206.00	85.70	416.01
c94620_g1_i1	994.00	110.18	110.85
c94691_g1_i1	316.00	79.02	250.06
c94714_g1_i1	202.00	57.87	286.50
c94822_g2_i1	202.00	95.71	473.83
c94822_g3_i1	237.00	130.22	549.44
c94892_g1_i1	788.00	93.49	118.64

c94892_g2_i1	479.00	150.25	313.67
c94892_g3_i1	462.00	67.89	146.95
c94892_g4_i1	322.00	84.58	262.69
c9491_g1_i1	223.00	45.63	204.62
c94950_g1_i1	311.00	110.18	354.29
c95006_g1_i1	562.00	73.46	130.70
c95094_g1_i1	220.00	27.82	126.47
c95119_g1_i1	279.00	40.07	143.61
c95177_g1_i1	242.00	158.04	653.06
c95188_g1_i1	280.00	76.79	274.26
c95188_g2_i1	353.00	105.73	299.52
c95279_g1_i1	412.00	1206.45	2928.27
c95298_g1_i1	379.00	45.63	120.40
c95349_g1_i1	471.00	176.96	375.71
c95349_g2_i1	236.00	76.79	325.40
c95349_g3_i1	216.00	46.74	216.41
c95357_g1_i1	492.00	90.15	183.23
c95357_g2_i1	478.00	90.15	188.60
c95361_g1_i2	257.00	35.61	138.58
c95455_g1_i1	608.00	207.01	340.48
c95492_g1_i1	281.00	135.78	483.21
c95510_g1_i1	821.00	153.59	187.07
c95554_g1_i1	285.00	58.99	206.97
c95633_g1_i1	688.00	79.02	114.86
c95651_g1_i2	307.00	192.54	627.17
c95684_g1_i1	412.00	154.70	375.49
c95701_g1_i1	443.00	140.23	316.55
c95703_g1_i1	814.00	143.57	176.38
c95773_g1_i1	320.00	70.12	219.11
c95773_g2_i1	201.00	30.05	149.50
c95776_g2_i1	357.00	76.79	215.11
c95858_g1_i1	1014.00	182.53	180.01
c95877_g1_i1	312.00	52.31	167.66
c95900_g1_i1	384.00	117.97	307.22
c95990_g1_i1	358.00	270.45	755.44
c96001_g1_i1	509.00	129.10	253.64
c96220_g2_i1	540.00	166.94	309.16
c96226_g1_i1	454.00	69.00	151.99
c96235_g1_i1	220.00	271.56	1234.37
c96283_g1_i2	300.00	51.20	170.65
c96344_g1_i1	268.00	503.06	1877.08
c96376_g1_i1	288.00	132.44	459.87
c96376_g2_i1	270.00	106.84	395.72

c96412_g1_i1	241.00	74.57	309.41
c96426_g2_i1	963.00	114.64	119.04
c96430_g1_i1	260.00	127.99	492.27
c96448_g3_i1	572.00	61.21	107.02
c96528_g1_i1	445.00	74.57	167.57
c96541_g2_i1	259.00	35.61	137.51
c96618_g1_i1	572.00	119.09	208.19
c96656_g1_i1	471.00	158.04	335.54
c96667_g2_i1	244.00	77.91	319.29
c96715_g1_i1	335.00	250.42	747.51
c96733_g1_i1	850.00	164.72	193.79
c96778_g1_i1	265.00	46.74	176.39
c96816_g2_i1	521.00	67.89	130.31
c96884_g2_i1	244.00	26.71	109.47
c96931_g1_i1	313.00	32.28	103.12
c97036_g1_i1	1160.00	135.78	117.05
c97037_g1_i1	221.00	26.71	120.86
c9705_g1_i1	241.00	27.82	115.45
c97070_g1_i1	202.00	369.50	1829.22
c97096_g1_i1	863.00	122.43	141.86
c97107_g1_i1	245.00	44.52	181.71
c97162_g2_i1	438.00	148.02	337.95
c97176_g1_i1	467.00	52.31	112.01
c97197_g1_i1	551.00	283.80	515.07
c97211_g1_i1	889.00	409.57	460.71
c97211_g2_i1	206.00	67.89	329.57
c97224_g1_i1	324.00	80.13	247.32
c97251_g2_i1	228.00	33.39	146.44
c9726_g1_i1	331.00	164.72	497.64
c9727_g1_i1	284.00	41.18	145.00
c97309_g1_i1	283.00	45.63	161.24
c97309_g2_i1	700.00	268.22	383.18
c97396_g1_i1	212.00	54.53	257.24
c9749_g1_i1	297.00	45.63	153.64
c97542_g1_i1	502.00	179.19	356.94
c97578_g1_i2	354.00	46.74	132.05
c97612_g1_i1	241.00	1259.87	5227.67
c97629_g2_i1	365.00	107.96	295.77
c97630_g1_i1	1149.00	173.62	151.11
c97667_g1_i1	529.00	270.45	511.25
c97688_g1_i1	457.00	107.96	236.23
c97688_g1_i2	666.00	77.91	116.98
c97688_g1_i3	280.00	86.81	310.04

c97695_g1_i1	222.00	33.39	150.40
c9776_g1_i1	405.00	61.21	151.14
c97883_g1_i1	343.00	141.35	412.09
c97914_g1_i1	202.00	23.37	115.70
c97949_g1_i1	229.00	26.71	116.64
c97980_g1_i1	251.00	69.00	274.91
c97980_g1_i2	243.00	72.34	297.71
c98023_g1_i1	221.00	22.26	100.72
c98103_g1_i2	1402.00	148.02	105.58
c98185_g1_i1	451.00	505.28	1120.36
c98185_g2_i1	322.00	79.02	245.40
c98187_g1_i1	301.00	86.81	288.41
c98187_g2_i2	350.00	196.99	562.84
c98250_g1_i1	759.00	106.84	140.77
c98256_g1_i2	310.00	37.84	122.07
c98261_g4_i1	248.00	28.94	116.68
c98304_g1_i1	685.00	81.25	118.61
c98401_g1_i1	314.00	34.50	109.88
c98470_g1_i1	712.00	74.57	104.73
c98479_g1_i1	292.00	76.79	262.99
c98549_g1_i1	244.00	38.95	159.65
c98549_g2_i1	398.00	77.91	195.75
c98560_g1_i2	248.00	33.39	134.63
c98576_g2_i1	273.00	28.94	106.00
c98592_g2_i1	209.00	23.37	111.83
c98595_g1_i1	221.00	66.78	302.16
c98661_g1_i1	290.00	34.50	118.97
c98666_g1_i1	453.00	221.48	488.92
c98674_g1_i1	322.00	195.88	608.33
c98674_g2_i1	522.00	330.55	633.23
c98680_g1_i1	567.00	58.99	104.03
c98719_g1_i1	252.00	61.21	242.91
c98757_g1_i1	227.00	58.99	259.85
c98817_g1_i1	242.00	127.99	528.89
c98817_g2_i1	247.00	161.38	653.36
c98836_g1_i1	1141.00	125.76	110.22
c98836_g2_i1	353.00	54.53	154.49
c98836_g3_i1	377.00	67.89	180.08
c98838_g1_i1	605.00	106.84	176.60
c98868_g1_i1	465.00	207.01	445.18
c98896_g1_i1	267.00	110.18	412.67
c98919_g1_i1	254.00	35.61	140.22
c99157_g1_i1	473.00	99.05	209.42

c99167_g2_i1	379.00	43.41	114.53
c99203_g1_i1	228.00	45.63	200.14
c99203_g2_i1	341.00	102.39	300.27
c99220_g1_i1	420.00	61.21	145.74
c99291_g1_i1	429.00	150.25	350.23
c99291_g2_i1	574.00	82.36	143.48
c99318_g1_i1	225.00	36.73	163.23
c99450_g1_i1	302.00	35.61	117.93
c99558_g1_i1	220.00	101.28	460.36
c99594_g1_i1	231.00	61.21	264.99
c99608_g1_i1	296.00	34.50	116.56
c99659_g2_i1	347.00	54.53	157.16
c99751_g2_i1	265.00	50.08	188.99
c99791_g2_i1	330.00	75.68	229.34
c99791_g3_i1	791.00	240.40	303.92
c99893_g1_i1	764.00	139.12	182.09
c99907_g1_i1	228.00	47.86	209.90
c99913_g1_i1	213.00	42.29	198.56
c99971_g2_i1	1012.00	127.99	126.47
c99979_g1_i1	687.00	207.01	301.33
c99979_g2_i1	202.00	61.21	303.03
c99979_g3_i1	233.00	123.54	530.21

Chapter 3
Summary and future directions

The discovery of small noncoding RNAs has revealed a whole new level of gene regulation in the past two decades. Among all small RNA pathways, PIWI/piRNA pathway is the most complex and fascinating in terms of both biogenesis and functions. First discovered as a factor required for *Drosophila* germline development, PIWI proteins and their piRNAs have been shown as essential gene expression regulators, in metazoans ranging from nematodes to human, through multiple mechanisms that are not yet fully understood. Despite the predominant presence of piRNAs in animal germline, increasing evidence points to the involvement of piRNAs pathway in soma, such as the somatic stem cells in flatworms. The flatworm somatic stem cell system, also known as neoblast, not only gives rise to its remarkable longevity and regeneration ability, but also shows vast potential in teaching us how to expand and harness the power of stem cells. In the emerging flatworm model, *M. lignano*, we showed the presence of a highly conserved canonical piRNA pathway using at least three PIWI proteins. One of the PIWIs, Macpiwi1, is required for stem cell maintenance. Its depletion results in the failure of stem cells and all stem cell-dependent activities. Interestingly, depletion of Macpiwi1 or piRNA biogenesis factor Macvasa disrupts transposon repression, however, silencing of Macvasa does not affect stem cell maintenance and further differentiation. The role of Macpiwi1 in stem cell maintenance seems separate from the best-known piRNA function, transposon silencing. While disclosing the potential significance, our findings raise more questions regarding the mechanisms of PIWI/piRNA pathway in the regulation of pluripotency. And to answer these questions, several technical limitations of this new model organism have to be overcome. Here are several directions worth taking following our study.

3.1 Access to the complete genomic landscape

Studies of piRNAs largely rely on deep sequencing data and the high quality of genome/transcriptome assemblies. Due to the unusually repetitive nature of *M. lignano* genome, efforts on the genome assembly have not yielded to satisfactory results. We recently combined PacBio long sequencing reads with Illumina short reads, aiming for the complete assembly of this genome (Wasik et al., submitted). Despite the significant improvement of contig length, our current assembly is still far from completion. For the

same reason, current transcriptome is only partially assembled. Besides the incomplete assembly, transcript annotation is another challenging task. Flatworms seem evolutionarily divergent from other well-studied metazoans; therefore, a large number of transcripts cannot be annotated based on similarity across species. In our *de novo* transcriptome, merely ~20% of the transcripts are annotated. This number is comparable to that for planarian transcriptomes (Abril et al. 2010). At epigenetic level, our preliminary data has shown a low level of CpG methylation in *M. lignano* (Wasik et al., submitted) in contrast to other common invertebrate models, such as *C. elegans* and *D. melanogaster*. DNA methylation, as a crucial regulator in pluripotency and differentiation, will certainly bring us clearer insight in neoblast functions. With advancement in sequencing technologies, we hope for the availability of complete genomic information for *M. lignano*.

3.2 Efficient genome editing in *M. lignano*

In addition to the fragmented genomic information, another major obstacle is the lack of efficient genome editing approach. RNAi knockdown, which enables loss-of-function studies to a large extent, has several drawbacks. First, depletion of protein expression is incomplete and residual expression often obscures phenotypes. Second, it is technically and economically difficult to scale up RNAi; therefore, experiments requiring a large number of worms are unfeasible in combination with RNAi knockdown. For instance, it is not practical to pull down PIWI protein after depleting a piRNA component, simply due to the large amount of worms needed for immunoprecipitation. Moreover, overexpression or targeted mutagenesis can only be achieved when genome editing is available. Several methods, including transposase and TALENs, have recently been applied to M. *lignano.* Although a proof-of-concept GFP line was successfully made (Marie-Orleach et al. 2014) all methods are far from efficient. In addition to the low efficiency related to the editing methods *per se*, the transgene expression seems rather unstable. During our group's attempts, in most cases, worms tend to lose GFP expression over time from all cell types other than neurons. This indicates either an unsuccessful integration or silencing of the transgene. Understanding the cause of unstable expression will provide us clues to improve the editing methods. Alternatively, the highly efficient CRISPR-Cas9 system is undoubtedly worth trying.

3.3 Elucidating the biogenesis network of *M. lignano* piRNA pathway

M. lignano utilizes a canonical piRNA pathway with multiple PIWIs and secondary piRNA amplification. At least three PIWI proteins are encoded as well as a number of other essential piRNA pathway components. One of the PIWIs, Macpiwi1, is likely to interact with primary piRNAs and perform heterogenic ping-pong cycle with other PIWIs. While our data draws the outline of *M. lignano* piRNA network, many details remain elusive. During the search for piRNA components, we were unable to identify Zucchini, the enzyme required for the formation of primary piRNA precursors. One simple possibility is that our transcriptome is too fragmented to detect the Zuc homologue. Another possibility is that *M. lignano* uses a functional homologue that has

low sequence similarity to Zuc in other species. And this possibility is in line with the nearly 80% transcripts we are unable to annotate based on similarity to other species. Further genetic and biochemical experiments are needed to identify the Zuc counterpart in *M. lignano*. Besides the Zuc mystery, another question to be addressed is the hierarchy of PIWIs in piRNA biogenesis. Despite the evidence showing Macpiwi1 as the primary piRNA donor during heterogenic ping-pong, it remains unclear which PIWI(s) receive primary piRNAs and mediate the secondary piRNA formation. We faced multiple technical issues while trying to answer this question. To demonstrate the role of each PIWI, the associated piRNAs have to be examined following PIWI immunoprecipitation. Unfortunately, none of the antibodies against Macpiwi2 and Macpiwi3 were suitable for this purpose. Alternatively, we analyzed the change of piRNA composition with Macpiwi2 depletion, with hope to identify the Macpiwi2-associated population indirectly. However, the change of piRNAs seemed intricate due to the likely redundancy and compensation with other PIWIs. In our study, we identified a potential Macpiwi3 from transcriptome; however, we were not able to amplify the full-length transcripts using RACE. Instead, the product was a hybrid with the 5' half of ribosomal RNA and 3' half of putative Macpiwi3 sequence. As a result, we decided not to investigate further thus the identity of Macpiwi3 remains a mystery. We hope in the follow-up studies these technical difficulties will be overcome and these questions can be addressed eventually.

3.4 Understanding the roles of Macpiwi1 and piRNAs in stem cell maintenance

Our data suggests that transposon reactivation is unlikely to cause stem cell failure in the absence of Macpiwi1 since Macvasa depletion leads to more severe transposon reactivation with no impact on stem cell functions. Recently an increasing number of studies have pointed to piRNA/PIWI-medicated gene regulation beyond transposon silencing. This is likely to encompass Macpiwi1. Macpiwi1 might be involved in the silencing of genes related to stem cell renewal at transcriptional or post-transcriptional level. A more comprehensive examination of transcription and epigenetic modification in Macpiwi1-null background will hopefully provide more clues. Although Macvasa knockdown does not affect stem cell functions, it does lower piRNAs to a nearly undetectable level. This leads us to ask whether Macpiwi1 function in stem cell maintenance is dependent on canonical piRNAs. In a genetic background with complete disruption of primary piRNA production, assuming such genetic condition can be achieved, one could investigate the stem cell phenotypes and Macpiwi1-associated piRNA population, in order to address this question.

3.5 Understanding the specific roles of small RNAs in different subpopulations and states of stem cells

PIWIs and piRNAs are present in dividing cells including both germline and somatic neoblasts, whereas in most metazoans they are restricted in germline only. In fact, flatworm somatic neoblasts are highly similar to germline. For instance, in planarian the only known distinguishable transcription factor between the two cell types is the germline-specific Nanos (Sato et al. 2006). We wonder whether piRNA pathway is

involved in defining the unique nature of somatic neoblasts in *M. lignano*. Even within somatic neoblasts, there exist different subgroups based on morphology and behaviors. Studies of neoblast dynamics suggest the presence of a pool of arrested G2-phase neoblasts that can quickly enter M-phase during regeneration. It would be of interest to investigate the roles of piRNAs in the activation of this pool of neoblasts. Unfortunately, based on the current knowledge, there is no good approach to separate the somatic neoblasts or even the G2-phase neoblasts. We hope as our knowledge grows, we will be able to isolate different populations and subpopulations and study the unique roles of their piRNAs. Besides piRNAs, our preliminary data also displays the differential expression of miRNAs in dividing cells and during regeneration, indicating the involvement of miRNAs in stem cell functions. This could be another interest entry point for future studies.

References

Abril JF, Cebria F, Rodriguez-Esteban G, Horn T, Fraguas S, Calvo B, Bartscherer K, Salo E. 2010. Smed454 dataset: unravelling the transcriptome of Schmidtea mediterranea. *BMC Genomics* **11**: 731.

Anand A, Kai T. 2012. The tudor domain protein kumo is required to assemble the nuage and to generate germline piRNAs in Drosophila. *Embo J* **31**: 870-882.

Andersen RA, Berges JA, P.J. H, Watanabe MM. 2005. Recipes for freshwater and seawater media. Elsevier, Amsterdam.

Aravin AA, Sachidanandam R, Girard A, Fejes-Toth K, Hannon GJ. 2007. Developmentally regulated piRNA clusters implicate MILI in transposon control. *Science* **316**: 744-747.

Aronica L, Bednenko J, Noto T, DeSouza LV, Siu KW, Loidl J, Pearlman RE, Gorovsky MA, Mochizuki K. 2008. Study of an RNA helicase implicates small RNA-noncoding RNA interactions in programmed DNA elimination in Tetrahymena. *Genes Dev* **22**: 2228-2241.

Babiarz JE, Ruby JG, Wang Y, Bartel DP, Blelloch R. 2008. Mouse ES cells express endogenous shRNAs, siRNAs, and other Microprocessor-independent, Dicer-dependent small RNAs. *Genes Dev* **22**: 2773-2785.

Baguna J. 2012. The planarian neoblast: the rambling history of its origin and some current black boxes. *Int J Dev Biol* **56**: 19-37.

Bernstein E, Caudy AA, Hammond SM, Hannon GJ. 2001. Role for a bidentate ribonuclease in the initiation step of RNA interference. *Nature* **409**: 363-366.

Biemont C. 2010. A brief history of the status of transposable elements: from junk DNA to major players in evolution. *Genetics* **186**: 1085-1093.

Bode A, Salvenmoser W, Nimeth K, Mahlknecht M, Adamski Z, Rieger RM, Peter R, Ladurner P. 2006. Immunogold-labeled S-phase neoblasts, total neoblast number, their distribution, and evidence for arrested neoblasts in Macrostomum lignano (Platyhelminthes, Rhabditophora). *Cell Tissue Res* **325**: 577-587.

Brennecke J, Aravin AA, Stark A, Dus M, Kellis M, Sachidanandam R, Hannon GJ. 2007. Discrete small RNA-generating loci as master regulators of transposon activity in Drosophila. *Cell* **128**: 1089-1103.

Brennecke J, Malone CD, Aravin AA, Sachidanandam R, Stark A, Hannon GJ. 2008. An epigenetic role for maternally inherited piRNAs in transposon silencing. *Science* **322**: 1387-1392.

Brennecke J, Stark A, Russell RB, Cohen SM. 2005. Principles of microRNA-target recognition. *PLoS Biol* **3**: e85.

Britten RJ, Davidson EH. 1969. Gene regulation for higher cells: a theory. *Science* **165**: 349-357.

Brower-Toland B, Findley SD, Jiang L, Liu L, Yin H, Dus M, Zhou P, Elgin SC, Lin H. 2007. Drosophila PIWI associates with chromatin and interacts directly with HP1a. *Genes Dev* **21**: 2300-2311.

Carmell MA, Xuan Z, Zhang MQ, Hannon GJ. 2002. The Argonaute family: tentacles that reach into RNAi, developmental control, stem cell maintenance, and tumorigenesis. *Genes Dev* **16**: 2733-2742.

Cerutti L, Mian N, Bateman A. 2000. Domains in gene silencing and cell differentiation proteins: the novel PAZ domain and redefinition of the Piwi domain. *Trends Biochem Sci* **25**: 481-482.

Chalker DL, Yao MC. 2011. DNA elimination in ciliates: transposon domestication and genome surveillance. *Annu Rev Genet* **45**: 227-246.

Chen C, Jin J, James DA, Adams-Cioaba MA, Park JG, Guo Y, Tenaglia E, Xu C, Gish G, Min J et al. 2009. Mouse Piwi interactome identifies binding mechanism of Tdrkh Tudor domain to arginine methylated Miwi. *Proc Natl Acad Sci U S A* **106**: 20336-20341.

Chen D, McKearin D. 2005. Gene circuitry controlling a stem cell niche. *Curr Biol* **15**: 179-184.

Chung WJ, Okamura K, Martin R, Lai EC. 2008. Endogenous RNA interference provides a somatic defense against Drosophila transposons. *Curr Biol* **18**: 795-802.

Cora E, Pandey RR, Xiol J, Taylor J, Sachidanandam R, McCarthy AA, Pillai RS. 2014. The MID-PIWI module of Piwi proteins specifies nucleotide- and strand-biases of piRNAs. *Rna* **20**: 773-781.

Cowley M, Oakey RJ. 2013. Transposable elements re-wire and fine-tune the transcriptome. *PLoS Genet* **9**: e1003234.

Cox DN, Chao A, Baker J, Chang L, Qiao D, Lin H. 1998. A novel class of evolutionarily conserved genes defined by piwi are essential for stem cell self-renewal. *Genes Dev* **12**: 3715-3727.

Cox DN, Chao A, Lin H. 2000. piwi encodes a nucleoplasmic factor whose activity modulates the number and division rate of germline stem cells. *Development* **127**: 503-514.

Crooks GE, Hon G, Chandonia JM, Brenner SE. 2004. WebLogo: a sequence logo generator. *Genome Res* **14**: 1188-1190.

Cullen BR. 2005. RNAi the natural way. *Nat Genet* **37**: 1163-1165.

Czech B, Malone CD, Zhou R, Stark A, Schlingeheyde C, Dus M, Perrimon N, Kellis M, Wohlschlegel JA, Sachidanandam R et al. 2008. An endogenous small interfering RNA pathway in Drosophila. *Nature* **453**: 798-802.

De Mulder K, Kuales G, Pfister D, Egger B, Seppi T, Eichberger P, Borgonie G, Ladurner P. 2010. Potential of Macrostomum lignano to recover from gamma-ray irradiation. *Cell Tissue Res* **339**: 527-542.

De Mulder K, Pfister D, Kuales G, Egger B, Salvenmoser W, Willems M, Steger J, Fauster K, Micura R, Borgonie G et al. 2009. Stem cells are differentially regulated during development, regeneration and homeostasis in flatworms. *Dev Biol* **334**: 198-212.

Demircan T, Berezikov E. 2013. The Hippo pathway regulates stem cells during homeostasis and regeneration of the flatworm Macrostomum lignano. *Stem Cells Dev* **22**: 2174-2185.

Doolittle WF, Sapienza C. 1980. Selfish genes, the phenotype paradigm and genome evolution. *Nature* **284**: 601-603.

Egger B, Gschwentner R, Hess MW, Nimeth KT, Adamski Z, Willems M, Rieger R, Salvenmoser W. 2009a. The caudal regeneration blastema is an accumulation of

rapidly proliferating stem cells in the flatworm Macrostomum lignano. *BMC Dev Biol* **9**: 41.
Egger B, Gschwentner R, Rieger R. 2007. Free-living flatworms under the knife: past and present. *Dev Genes Evol* **217**: 89-104.
Egger B, Ishida S. 2005. Chromosome fission or duplication in Macrostomum lignano (Macrostomorpha, Plathelminthes) - remarks on chromosome numbers in 'archoophoran turbellarians'. *J Zool Syst Evol Res* **43**: 127-132.
Egger B, Ladurner P, Nimeth K, Gschwentner R, Rieger R. 2006. The regeneration capacity of the flatworm Macrostomum lignano--on repeated regeneration, rejuvenation, and the minimal size needed for regeneration. *Dev Genes Evol* **216**: 565-577.
Egger B, Lapraz F, Tomiczek B, Muller S, Dessimoz C, Girstmair J, Skunca N, Rawlinson KA, Cameron CB, Beli E et al. 2015. A Transcriptomic-Phylogenomic Analysis of the Evolutionary Relationships of Flatworms. *Curr Biol*.
Egger B, Steinke D, Tarui H, De Mulder K, Arendt D, Borgonie G, Funayama N, Gschwentner R, Hartenstein V, Hobmayer B et al. 2009b. To be or not to be a flatworm: the acoel controversy. *PLoS One* **4**: e5502.
Eickbush TH. 1997. Telomerase and retrotransposons: which came first? *Science* **277**: 911-912.
Elbashir SM, Lendeckel W, Tuschl T. 2001. RNA interference is mediated by 21- and 22-nucleotide RNAs. *Genes Dev* **15**: 188-200.
Fang W, Wang X, Bracht JR, Nowacki M, Landweber LF. 2012. Piwi-interacting RNAs protect DNA against loss during Oxytricha genome rearrangement. *Cell* **151**: 1243-1255.
Feschotte C, Pritham EJ. 2007. DNA transposons and the evolution of eukaryotic genomes. *Annu Rev Genet* **41**: 331-368.
Filipowicz W, Bhattacharyya SN, Sonenberg N. 2008. Mechanisms of post-transcriptional regulation by microRNAs: are the answers in sight? *Nat Rev Genet* **9**: 102-114.
Findley SD, Tamanaha M, Clegg NJ, Ruohola-Baker H. 2003. Maelstrom, a Drosophila spindle-class gene, encodes a protein that colocalizes with Vasa and RDE1/AGO1 homolog, Aubergine, in nuage. *Development* **130**: 859-871.
Flutre T, Duprat E, Feuillet C, Quesneville H. 2011. Considering transposable element diversification in de novo annotation approaches. *PLoS One* **6**: e16526.
Frank F, Sonenberg N, Nagar B. 2010. Structural basis for 5'-nucleotide base-specific recognition of guide RNA by human AGO2. *Nature* **465**: 818-822.
Friedlander MR, Adamidi C, Han T, Lebedeva S, Isenbarger TA, Hirst M, Marra M, Nusbaum C, Lee WL, Jenkin JC et al. 2009. High-resolution profiling and discovery of planarian small RNAs. *Proc Natl Acad Sci U S A* **106**: 11546-11551.
Frost RJ, Hamra FK, Richardson JA, Qi X, Bassel-Duby R, Olson EN. 2010. MOV10L1 is necessary for protection of spermatocytes against retrotransposons by Piwi-interacting RNAs. *Proc Natl Acad Sci U S A* **107**: 11847-11852.
Ghildiyal M, Seitz H, Horwich MD, Li C, Du T, Lee S, Xu J, Kittler EL, Zapp ML, Weng Z et al. 2008. Endogenous siRNAs derived from transposons and mRNAs in Drosophila somatic cells. *Science* **320**: 1077-1081.

Grivna ST, Pyhtila B, Lin H. 2006. MIWI associates with translational machinery and PIWI-interacting RNAs (piRNAs) in regulating spermatogenesis. *Proc Natl Acad Sci U S A* **103**: 13415-13420.

Ha M, Kim VN. 2014. Regulation of microRNA biogenesis. *Nature reviews Molecular cell biology* **15**: 509-524.

Haase AD, Fenoglio S, Muerdter F, Guzzardo PM, Czech B, Pappin DJ, Chen C, Gordon A, Hannon GJ. 2010. Probing the initiation and effector phases of the somatic piRNA pathway in Drosophila. *Genes Dev* **24**: 2499-2504.

Hammond SM, Bernstein E, Beach D, Hannon GJ. 2000. An RNA-directed nuclease mediates post-transcriptional gene silencing in Drosophila cells. *Nature* **404**: 293-296.

Han BW, Wang W, Li C, Weng Z, Zamore PD. 2015a. Noncoding RNA. piRNA-guided transposon cleavage initiates Zucchini-dependent, phased piRNA production. *Science* **348**: 817-821.

Han BW, Wang W, Zamore PD, Weng Z. 2015b. piPipes: a set of pipelines for piRNA and transposon analysis via small RNA-seq, RNA-seq, degradome- and CAGE-seq, ChIP-seq and genomic DNA sequencing. *Bioinformatics* **31**: 593-595.

Handler D, Olivieri D, Novatchkova M, Gruber FS, Meixner K, Mechtler K, Stark A, Sachidanandam R, Brennecke J. 2011. A systematic analysis of Drosophila TUDOR domain-containing proteins identifies Vreteno and the Tdrd12 family as essential primary piRNA pathway factors. *Embo J* **30**: 3977-3993.

Harris AN, Macdonald PM. 2001. Aubergine encodes a Drosophila polar granule component required for pole cell formation and related to eIF2C. *Development* **128**: 2823-2832.

Hirano T, Iwasaki YW, Lin ZY, Imamura M, Seki NM, Sasaki E, Saito K, Okano H, Siomi MC, Siomi H. 2014. Small RNA profiling and characterization of piRNA clusters in the adult testes of the common marmoset, a model primate. *Rna* **20**: 1223-1237.

Hock J, Meister G. 2008. The Argonaute protein family. *Genome Biol* **9**: 210.

Horwich MD, Li C, Matranga C, Vagin V, Farley G, Wang P, Zamore PD. 2007. The Drosophila RNA methyltransferase, DmHen1, modifies germline piRNAs and single-stranded siRNAs in RISC. *Curr Biol* **17**: 1265-1272.

Hutvagner G, Zamore PD. 2002. A microRNA in a multiple-turnover RNAi enzyme complex. *Science* **297**: 2056-2060.

Ipsaro JJ, Haase AD, Knott SR, Joshua-Tor L, Hannon GJ. 2012. The structural biochemistry of Zucchini implicates it as a nuclease in piRNA biogenesis. *Nature* **491**: 279-283.

Ishizu H, Siomi H, Siomi MC. 2012. Biology of PIWI-interacting RNAs: new insights into biogenesis and function inside and outside of germlines. *Genes Dev* **26**: 2361-2373.

Izumi N, Kawaoka S, Yasuhara S, Suzuki Y, Sugano S, Katsuma S, Tomari Y. 2013. Hsp90 facilitates accurate loading of precursor piRNAs into PIWI proteins. *Rna* **19**: 896-901.

Jones JM, Gellert M. 2004. The taming of a transposon: V(D)J recombination and the immune system. *Immunol Rev* **200**: 233-248.

Juliano C, Wang J, Lin H. 2011. Uniting germline and stem cells: the function of Piwi proteins and the piRNA pathway in diverse organisms. *Annu Rev Genet* **45**: 447-469.

Kapitonov VV, Jurka J. 2005. RAG1 core and V(D)J recombination signal sequences were derived from Transib transposons. *PLoS Biol* **3**: e181.

Kawamura Y, Saito K, Kin T, Ono Y, Asai K, Sunohara T, Okada TN, Siomi MC, Siomi H. 2008. Drosophila endogenous small RNAs bind to Argonaute 2 in somatic cells. *Nature* **453**: 793-797.

Kazazian HH, Jr., Wong C, Youssoufian H, Scott AF, Phillips DG, Antonarakis SE. 1988. Haemophilia A resulting from de novo insertion of L1 sequences represents a novel mechanism for mutation in man. *Nature* **332**: 164-166.

Khurana JS, Theurkauf W. 2010. piRNAs, transposon silencing, and Drosophila germline development. *J Cell Biol* **191**: 905-913.

Kidwell MG, Lisch DR. 2001. Perspective: transposable elements, parasitic DNA, and genome evolution. *Evolution* **55**: 1-24.

Kim VN, Han J, Siomi MC. 2009. Biogenesis of small RNAs in animals. *Nature reviews Molecular cell biology* **10**: 126-139.

Klattenhoff C, Bratu DP, McGinnis-Schultz N, Koppetsch BS, Cook HA, Theurkauf WE. 2007. Drosophila rasiRNA pathway mutations disrupt embryonic axis specification through activation of an ATR/Chk2 DNA damage response. *Dev Cell* **12**: 45-55.

Klattenhoff C, Theurkauf W. 2008. Biogenesis and germline functions of piRNAs. *Development* **135**: 3-9.

Klenov MS, Sokolova OA, Yakushev EY, Stolyarenko AD, Mikhaleva EA, Lavrov SA, Gvozdev VA. 2011. Separation of stem cell maintenance and transposon silencing functions of Piwi protein. *Proc Natl Acad Sci U S A* **108**: 18760-18765.

Krek A, Grun D, Poy MN, Wolf R, Rosenberg L, Epstein EJ, MacMenamin P, da Piedade I, Gunsalus KC, Stoffel M et al. 2005. Combinatorial microRNA target predictions. *Nat Genet* **37**: 495-500.

Ku HY, Lin H. 2014. PIWI proteins and their interactors in piRNA biogenesis, germline development and gene expression. *National science review* **1**: 205-218.

Kuales G, De Mulder K, Glashauser J, Salvenmoser W, Takashima S, Hartenstein V, Berezikov E, Salzburger W, Ladurner P. 2011. Boule-like genes regulate male and female gametogenesis in the flatworm Macrostomum lignano. *Dev Biol* **357**: 117-132.

Kuramochi-Miyagawa S, Watanabe T, Gotoh K, Takamatsu K, Chuma S, Kojima-Kita K, Shiromoto Y, Asada N, Toyoda A, Fujiyama A et al. 2010. MVH in piRNA processing and gene silencing of retrotransposons. *Genes Dev* **24**: 887-892.

Kuramochi-Miyagawa S, Watanabe T, Gotoh K, Totoki Y, Toyoda A, Ikawa M, Asada N, Kojima K, Yamaguchi Y, Ijiri TW et al. 2008. DNA methylation of retrotransposon genes is regulated by Piwi family members MILI and MIWI2 in murine fetal testes. *Genes Dev* **22**: 908-917.

Ladurner P, Scharer L, Salvenmoser W, Rieger RM. 2005. A new model organism among the lower Bilateria and the use of digital microscopy in taxonomy of meiobenthic Platyhelminthes: Macrostomum lignano, n. sp (Rhabditophora, Macrostomorpha). *J Zool Syst Evol Res* **43**: 114-126.

Ladurner P, Egger B, De Mulder K, Pfister D, Kuales G, Salvenmoser W, Schärer L. 2008. The stem cell system of the basal flatworm *Macrostomum lignano*. In: Bosch, T.C. (Ed.), *Stem cell: from Hydra to Man.* Springer, pp. 75–94.

Langmead B. 2010. Aligning short sequencing reads with Bowtie. Curr Protoc *Bioinformatics* **Chapter 11**: Unit 11 17.

Lau NC, Lim LP, Weinstein EG, Bartel DP. 2001. An abundant class of tiny RNAs with probable regulatory roles in Caenorhabditis elegans. *Science* **294**: 858-862.

Lau NC, Robine N, Martin R, Chung WJ, Niki Y, Berezikov E, Lai EC. 2009. Abundant primary piRNAs, endo-siRNAs, and microRNAs in a Drosophila ovary cell line. *Genome Res* **19**: 1776-1785.

Laumer CE, Hejnol A, Giribet G. 2015. Nuclear genomic signals of the 'microturbellarian' roots of platyhelminth evolutionary innovation. *Elife* **4**.

Le Thomas A, Rogers AK, Webster A, Marinov GK, Liao SE, Perkins EM, Hur JK, Aravin AA, Toth KF. 2013. Piwi induces piRNA-guided transcriptional silencing and establishment of a repressive chromatin state. *Genes Dev* **27**: 390-399.

Lee RC, Feinbaum RL, Ambros V. 1993. The C. elegans heterochronic gene lin-4 encodes small RNAs with antisense complementarity to lin-14. *Cell* **75**: 843-854.

Lee Y, Ahn C, Han J, Choi H, Kim J, Yim J, Lee J, Provost P, Radmark O, Kim S et al. 2003. The nuclear RNase III Drosha initiates microRNA processing. *Nature* **425**: 415-419.

Lee Y, Kim M, Han J, Yeom KH, Lee S, Baek SH, Kim VN. 2004a. MicroRNA genes are transcribed by RNA polymerase II. *Embo J* **23**: 4051-4060.

Lee YS, Nakahara K, Pham JW, Kim K, He Z, Sontheimer EJ, Carthew RW. 2004b. Distinct roles for Drosophila Dicer-1 and Dicer-2 in the siRNA/miRNA silencing pathways. *Cell* **117**: 69-81.

Leng N, Dawson JA, Thomson JA, Ruotti V, Rissman AI, Smits BM, Haag JD, Gould MN, Stewart RM, Kendziorski C. 2013. EBSeq: an empirical Bayes hierarchical model for inference in RNA-seq experiments. *Bioinformatics* **29**: 1035-1043.

Lengerer B, Pjeta R, Wunderer J, Rodrigues M, Arbore R, Scharer L, Berezikov E, Hess MW, Pfaller K, Egger B et al. 2014. Biological adhesion of the flatworm Macrostomum lignano relies on a duo-gland system and is mediated by a cell type-specific intermediate filament protein. *Front Zool* **11**: 12.

Lewis BP, Burge CB, Bartel DP. 2005. Conserved seed pairing, often flanked by adenosines, indicates that thousands of human genes are microRNA targets. *Cell* **120**: 15-20.

Lewis BP, Shih IH, Jones-Rhoades MW, Bartel DP, Burge CB. 2003. Prediction of mammalian microRNA targets. *Cell* **115**: 787-798.

Li B, Dewey CN. 2011. RSEM: accurate transcript quantification from RNA-Seq data with or without a reference genome. *BMC Bioinformatics* **12**: 323.

Li H, Handsaker B, Wysoker A, Fennell T, Ruan J, Homer N, Marth G, Abecasis G, Durbin R, Genome Project Data Processing S. 2009. The Sequence Alignment/Map format and SAMtools. *Bioinformatics* **25**: 2078-2079.

Li XZ, Roy CK, Dong X, Bolcun-Filas E, Wang J, Han BW, Xu J, Moore MJ, Schimenti JC, Weng Z et al. 2013. An ancient transcription factor initiates the burst of piRNA production during early meiosis in mouse testes. *Mol Cell* **50**: 67-81.

Liang L, Diehl-Jones W, Lasko P. 1994. Localization of vasa protein to the Drosophila pole plasm is independent of its RNA-binding and helicase activities. *Development* **120**: 1201-1211.
Lim AK, Kai T. 2007. Unique germ-line organelle, nuage, functions to repress selfish genetic elements in Drosophila melanogaster. *Proc Natl Acad Sci U S A* **104**: 6714-6719.
Lin H, Spradling AC. 1997. A novel group of pumilio mutations affects the asymmetric division of germline stem cells in the Drosophila ovary. *Development* **124**: 2463-2476.
Lingel A, Simon B, Izaurralde E, Sattler M. 2003. Structure and nucleic-acid binding of the Drosophila Argonaute 2 PAZ domain. *Nature* **426**: 465-469.
Lippman Z, Gendrel AV, Black M, Vaughn MW, Dedhia N, McCombie WR, Lavine K, Mittal V, May B, Kasschau KD et al. 2004. Role of transposable elements in heterochromatin and epigenetic control. *Nature* **430**: 471-476.
Liu L, Qi H, Wang J, Lin H. 2011. PAPI, a novel TUDOR-domain protein, complexes with AGO3, ME31B and TRAL in the nuage to silence transposition. *Development* **138**: 1863-1873.
Liu Q, Paroo Z. 2010. Biochemical principles of small RNA pathways. *Annu Rev Biochem* **79**: 295-319.
Liu Q, Rand TA, Kalidas S, Du F, Kim HE, Smith DP, Wang X. 2003. R2D2, a bridge between the initiation and effector steps of the Drosophila RNAi pathway. *Science* **301**: 1921-1925.
Luteijn MJ, Ketting RF. 2013. PIWI-interacting RNAs: from generation to transgenerational epigenetics. *Nat Rev Genet* **14**: 523-534.
Macfarlan TS, Gifford WD, Agarwal S, Driscoll S, Lettieri K, Wang J, Andrews SE, Franco L, Rosenfeld MG, Ren B et al. 2011. Endogenous retroviruses and neighboring genes are coordinately repressed by LSD1/KDM1A. *Genes Dev* **25**: 594-607.
Macfarlan TS, Gifford WD, Driscoll S, Lettieri K, Rowe HM, Bonanomi D, Firth A, Singer O, Trono D, Pfaff SL. 2012. Embryonic stem cell potency fluctuates with endogenous retrovirus activity. *Nature* **487**: 57-63.
Malone CD, Brennecke J, Dus M, Stark A, McCombie WR, Sachidanandam R, Hannon GJ. 2009. Specialized piRNA pathways act in germline and somatic tissues of the Drosophila ovary. *Cell* **137**: 522-535.
Marie-Orleach L, Janicke T, Vizoso DB, Eichmann M, Scharer L. 2014. Fluorescent sperm in a transparent worm: validation of a GFP marker to study sexual selection. *BMC Evol Biol* **14**: 148.
Markham NR, Zuker M. 2008. UNAFold: software for nucleic acid folding and hybridization. *Methods Mol Biol* **453**: 3-31.
McClintock B. 1951. Chromosome organization and genic expression. *Cold Spring Harb Symp Quant Biol* **16**: 13-47.
Megosh HB, Cox DN, Campbell C, Lin H. 2006. The role of PIWI and the miRNA machinery in Drosophila germline determination. *Curr Biol* **16**: 1884-1894.
Mochizuki K, Fine NA, Fujisawa T, Gorovsky MA. 2002. Analysis of a piwi-related gene implicates small RNAs in genome rearrangement in tetrahymena. *Cell* **110**: 689-699.

Mochizuki K, Gorovsky MA. 2005. A Dicer-like protein in Tetrahymena has distinct functions in genome rearrangement, chromosome segregation, and meiotic prophase. *Genes Dev* **19**: 77-89.

Mohn F, Handler D, Brennecke J. 2015. Noncoding RNA. piRNA-guided slicing specifies transcripts for Zucchini-dependent, phased piRNA biogenesis. *Science* **348**: 812-817.

Mohn F, Sienski G, Handler D, Brennecke J. 2014. The rhino-deadlock-cutoff complex licenses noncanonical transcription of dual-strand piRNA clusters in Drosophila. *Cell* **157**: 1364-1379.

Montgomery MK, Fire A. 1998. Double-stranded RNA as a mediator in sequence-specific genetic silencing and co-suppression. *Trends Genet* **14**: 255-258.

Morgan HD, Sutherland HG, Martin DI, Whitelaw E. 1999. Epigenetic inheritance at the agouti locus in the mouse. *Nat Genet* **23**: 314-318.

Morris J, Cardona A, De Miguel-Bonet Mdel M, Hartenstein V. 2007. Neurobiology of the basal platyhelminth Macrostomum lignano: map and digital 3D model of the juvenile brain neuropile. *Dev Genes Evol* **217**: 569-584.

Morris J, Ladurner P, Rieger R, Pfister D, Del Mar De Miguel-Bonet M, Jacobs D, Hartenstein V. 2006. The Macrostomum lignano EST database as a molecular resource for studying platyhelminth development and phylogeny. *Dev Genes Evol* **216**: 695-707.

Mourelatos Z, Dostie J, Paushkin S, Sharma A, Charroux B, Abel L, Rappsilber J, Mann M, Dreyfuss G. 2002. miRNPs: a novel class of ribonucleoproteins containing numerous microRNAs. *Genes Dev* **16**: 720-728.

Mouton S, Willems M, Back P, Braeckman BP, Borgonie G. 2009a. Demographic analysis reveals gradual senescence in the flatworm Macrostomum lignano. *Front Zool* **6**: 15.

Mouton S, Willems M, Braeckman BP, Egger B, Ladurner P, Scharer L, Borgonie G. 2009b. The free-living flatworm Macrostomum lignano: a new model organism for ageing research. *Exp Gerontol* **44**: 243-249.

Nagao A, Sato K, Nishida KM, Siomi H, Siomi MC. 2011. Gender-Specific Hierarchy in Nuage Localization of PIWI-Interacting RNA Factors in Drosophila. *Frontiers in genetics* **2**: 55.

Nimeth KT, Egger B, Rieger R, Salvenmoser W, Peter R, Gschwentner R. 2007. Regeneration in Macrostomum lignano (Platyhelminthes): cellular dynamics in the neoblast stem cell system. *Cell Tissue Res* **327**: 637-646.

Nimeth KT, Mahlknecht M, Mezzanato A, Peter R, Rieger R, Ladurner P. 2004. Stem cell dynamics during growth, feeding, and starvation in the basal flatworm Macrostomum sp. (Platyhelminthes). *Dev Dyn* **230**: 91-99.

Nishida KM, Okada TN, Kawamura T, Mituyama T, Kawamura Y, Inagaki S, Huang H, Chen D, Kodama T, Siomi H et al. 2009. Functional involvement of Tudor and dPRMT5 in the piRNA processing pathway in Drosophila germlines. *Embo J* **28**: 3820-3831.

Nishimasu H, Ishizu H, Saito K, Fukuhara S, Kamatani MK, Bonnefond L, Matsumoto N, Nishizawa T, Nakanaga K, Aoki J et al. 2012. Structure and function of Zucchini endoribonuclease in piRNA biogenesis. *Nature* **491**: 284-287.

Ohno S. 1972. So much "junk" DNA in our genome. *Brookhaven Symp Biol* **23**: 366-370.

Okamura K, Balla S, Martin R, Liu N, Lai EC. 2008a. Two distinct mechanisms generate endogenous siRNAs from bidirectional transcription in Drosophila melanogaster. *Nat Struct Mol Biol* **15**: 581-590.

Okamura K, Chung WJ, Ruby JG, Guo H, Bartel DP, Lai EC. 2008b. The Drosophila hairpin RNA pathway generates endogenous short interfering RNAs. *Nature* **453**: 803-806.

Olivieri D, Senti KA, Subramanian S, Sachidanandam R, Brennecke J. 2012. The cochaperone shutdown defines a group of biogenesis factors essential for all piRNA populations in Drosophila. *Mol Cell* **47**: 954-969.

Olivieri D, Sykora MM, Sachidanandam R, Mechtler K, Brennecke J. 2010. An in vivo RNAi assay identifies major genetic and cellular requirements for primary piRNA biogenesis in Drosophila. *Embo J* **29**: 3301-3317.

Orgel LE, Crick FH. 1980. Selfish DNA: the ultimate parasite. *Nature* **284**: 604-607.

Pal-Bhadra M, Leibovitch BA, Gandhi SG, Chikka MR, Bhadra U, Birchler JA, Elgin SC. 2004. Heterochromatic silencing and HP1 localization in Drosophila are dependent on the RNAi machinery. *Science* **303**: 669-672.

Palakodeti D, Smielewska M, Lu YC, Yeo GW, Graveley BR. 2008. The PIWI proteins SMEDWI-2 and SMEDWI-3 are required for stem cell function and piRNA expression in planarians. *Rna* **14**: 1174-1186.

Pan J, Goodheart M, Chuma S, Nakatsuji N, Page DC, Wang PJ. 2005. RNF17, a component of the mammalian germ cell nuage, is essential for spermiogenesis. *Development* **132**: 4029-4039.

Pandey RR, Tokuzawa Y, Yang Z, Hayashi E, Ichisaka T, Kajita S, Asano Y, Kunieda T, Sachidanandam R, Chuma S et al. 2013. Tudor domain containing 12 (TDRD12) is essential for secondary PIWI interacting RNA biogenesis in mice. *Proc Natl Acad Sci U S A* **110**: 16492-16497.

Pantano L, Jodar M, Bak M, Ballesca JL, Tommerup N, Oliva R, Vavouri T. 2015. The small RNA content of human sperm reveals pseudogene-derived piRNAs complementary to protein-coding genes. *Rna* **21**: 1085-1095.

Pardue ML, DeBaryshe PG. 2003. Retrotransposons provide an evolutionarily robust non-telomerase mechanism to maintain telomeres. *Annu Rev Genet* **37**: 485-511.

Patil VS, Kai T. 2010. Repression of retroelements in Drosophila germline via piRNA pathway by the Tudor domain protein Tejas. *Curr Biol* **20**: 724-730.

Pattamadilok J, Huapai N, Rattanatanyong P, Vasurattana A, Triratanachat S, Tresukosol D, Mutirangura A. 2008. LINE-1 hypomethylation level as a potential prognostic factor for epithelial ovarian cancer. *Int J Gynecol Cancer* **18**: 711-717.

Perrat PN, DasGupta S, Wang J, Theurkauf W, Weng Z, Rosbash M, Waddell S. 2013. Transposition-driven genomic heterogeneity in the Drosophila brain. *Science* **340**: 91-95.

Pfister D, De Mulder K, Hartenstein V, Kuales G, Borgonie G, Marx F, Morris J, Ladurner P. 2008. Flatworm stem cells and the germ line: developmental and evolutionary implications of macvasa expression in Macrostomum lignano. *Dev Biol* **319**: 146-159.

Pfister D, De Mulder K, Philipp I, Kuales G, Hrouda M, Eichberger P, Borgonie G, Hartenstein V, Ladurner P. 2007. The exceptional stem cell system of Macrostomum lignano: screening for gene expression and studying cell proliferation by hydroxyurea treatment and irradiation. *Front Zool* **4**: 9.

Pham JW, Pellino JL, Lee YS, Carthew RW, Sontheimer EJ. 2004. A Dicer-2-dependent 80s complex cleaves targeted mRNAs during RNAi in Drosophila. *Cell* **117**: 83-94.

Preall JB, Czech B, Guzzardo PM, Muerdter F, Hannon GJ. 2012. shutdown is a component of the Drosophila piRNA biogenesis machinery. *Rna* **18**: 1446-1457.

Qi H, Watanabe T, Ku HY, Liu N, Zhong M, Lin H. 2011. The Yb body, a major site for Piwi-associated RNA biogenesis and a gateway for Piwi expression and transport to the nucleus in somatic cells. *J Biol Chem* **286**: 3789-3797.

Quinlan AR, Hall IM. 2010. BEDTools: a flexible suite of utilities for comparing genomic features. *Bioinformatics* **26**: 841-842.

Rajasethupathy P, Antonov I, Sheridan R, Frey S, Sander C, Tuschl T, Kandel ER. 2012. A role for neuronal piRNAs in the epigenetic control of memory-related synaptic plasticity. *Cell* **149**: 693-707.

Ratcliff F, Harrison BD, Baulcombe DC. 1997. A similarity between viral defense and gene silencing in plants. *Science* **276**: 1558-1560.

Reddien PW, Oviedo NJ, Jennings JR, Jenkin JC, Sanchez Alvarado A. 2005. SMEDWI-2 is a PIWI-like protein that regulates planarian stem cells. *Science* **310**: 1327-1330.

Reddien PW, Sanchez Alvarado A. 2004. Fundamentals of planarian regeneration. *Annu Rev Cell Dev Biol* **20**: 725-757.

Rivas FV, Tolia NH, Song JJ, Aragon JP, Liu J, Hannon GJ, Joshua-Tor L. 2005. Purified Argonaute2 and an siRNA form recombinant human RISC. *Nat Struct Mol Biol* **12**: 340-349.

Rouget C, Papin C, Boureux A, Meunier AC, Franco B, Robine N, Lai EC, Pelisson A, Simonelig M. 2010. Maternal mRNA deadenylation and decay by the piRNA pathway in the early Drosophila embryo. *Nature* **467**: 1128-1132.

Rowe HM, Jakobsson J, Mesnard D, Rougemont J, Reynard S, Aktas T, Maillard PV, Layard-Liesching H, Verp S, Marquis J et al. 2010. KAP1 controls endogenous retroviruses in embryonic stem cells. *Nature* **463**: 237-240.

Saito K, Inagaki S, Mituyama T, Kawamura Y, Ono Y, Sakota E, Kotani H, Asai K, Siomi H, Siomi MC. 2009. A regulatory circuit for piwi by the large Maf gene traffic jam in Drosophila. *Nature* **461**: 1296-1299.

Saito K, Ishizu H, Komai M, Kotani H, Kawamura Y, Nishida KM, Siomi H, Siomi MC. 2010. Roles for the Yb body components Armitage and Yb in primary piRNA biogenesis in Drosophila. *Genes Dev* **24**: 2493-2498.

Saito K, Sakaguchi Y, Suzuki T, Suzuki T, Siomi H, Siomi MC. 2007. Pimet, the Drosophila homolog of HEN1, mediates 2'-O-methylation of Piwi- interacting RNAs at their 3' ends. *Genes Dev* **21**: 1603-1608.

Salo E, Baguna J. 1984. Regeneration and pattern formation in planarians. I. The pattern of mitosis in anterior and posterior regeneration in Dugesia (G) tigrina, and a new proposal for blastema formation. *Journal of embryology and experimental morphology* **83**: 63-80.

Sarot E, Payen-Groschene G, Bucheton A, Pelisson A. 2004. Evidence for a piwi-dependent RNA silencing of the gypsy endogenous retrovirus by the Drosophila melanogaster flamenco gene. *Genetics* **166**: 1313-1321.

Sato K, Iwasaki YW, Shibuya A, Piero C, Ishizu H, Siomi MC, Siomi H. 2013. Krimper enforces on piRNA pools an antisense bias by binding unmethylated AGO3 in the Drosophila germline. *Genes Genet Syst* **88**: 338-338.

Sato K, Nishida KM, Shibuya A, Siomi MC, Siomi H. 2011. Maelstrom coordinates microtubule organization during Drosophila oogenesis through interaction with components of the MTOC. *Genes Dev* **25**: 2361-2373.

Sato K, Shibata N, Orii H, Amikura R, Sakurai T, Agata K, Kobayashi S, Watanabe K. 2006. Identification and origin of the germline stem cells as revealed by the expression of nanos-related gene in planarians. *Dev Growth Differ* **48**: 615-628.

Saxe JP, Chen M, Zhao H, Lin H. 2013. Tdrkh is essential for spermatogenesis and participates in primary piRNA biogenesis in the germline. *Embo J* **32**: 1869-1885.

Sekii K, Salvenmoser W, De Mulder K, Scharer L, Ladurner P. 2009. Melav2, an elav-like gene, is essential for spermatid differentiation in the flatworm Macrostomum lignano. *BMC Dev Biol* **9**: 62.

Senti KA, Brennecke J. 2010. The piRNA pathway: a fly's perspective on the guardian of the genome. *Trends Genet* **26**: 499-509.

Shoji M, Tanaka T, Hosokawa M, Reuter M, Stark A, Kato Y, Kondoh G, Okawa K, Chujo T, Suzuki T et al. 2009. The TDRD9-MIWI2 complex is essential for piRNA-mediated retrotransposon silencing in the mouse male germline. *Dev Cell* **17**: 775-787.

Siddiqi S, Matushansky I. 2012. Piwis and piwi-interacting RNAs in the epigenetics of cancer. *J Cell Biochem* **113**: 373-380.

Siebel CW, Rio DC. 1990. Regulated splicing of the Drosophila P transposable element third intron in vitro: somatic repression. *Science* **248**: 1200-1208.

Smit, AFA, Hubley, R & Green, P. RepeatMasker Open-4.0. 2013-2015 <http://www.repeatmasker.org>.

Smulders-Srinivasan TK, Szakmary A, Lin H. 2010. A Drosophila chromatin factor interacts with the Piwi-interacting RNA mechanism in niche cells to regulate germline stem cell self-renewal. *Genetics* **186**: 573-583.

Song JJ, Liu J, Tolia NH, Schneiderman J, Smith SK, Martienssen RA, Hannon GJ, Joshua-Tor L. 2003. The crystal structure of the Argonaute2 PAZ domain reveals an RNA binding motif in RNAi effector complexes. *Nat Struct Biol* **10**: 1026-1032.

Song JJ, Smith SK, Hannon GJ, Joshua-Tor L. 2004. Crystal structure of Argonaute and its implications for RISC slicer activity. *Science* **305**: 1434-1437.

Soper SF, van der Heijden GW, Hardiman TC, Goodheart M, Martin SL, de Boer P, Bortvin A. 2008. Mouse maelstrom, a component of nuage, is essential for spermatogenesis and transposon repression in meiosis. *Dev Cell* **15**: 285-297.

Suzuki R, Honda S, Kirino Y. 2012. PIWI Expression and Function in Cancer. *Frontiers in genetics* **3**: 204.

Tam OH, Aravin AA, Stein P, Girard A, Murchison EP, Cheloufi S, Hodges E, Anger M, Sachidanandam R, Schultz RM et al. 2008. Pseudogene-derived small interfering RNAs regulate gene expression in mouse oocytes. *Nature* **453**: 534-538.

Tang W, Gunn TM, McLaughlin DF, Barsh GS, Schlossman SF, Duke-Cohan JS. 2000. Secreted and membrane attractin result from alternative splicing of the human ATRN gene. *Proc Natl Acad Sci U S A* **97**: 6025-6030.

Taverna SD, Coyne RS, Allis CD. 2002. Methylation of histone h3 at lysine 9 targets programmed DNA elimination in tetrahymena. *Cell* **110**: 701-711.

Thomson T, Lin H. 2009. The biogenesis and function of PIWI proteins and piRNAs: progress and prospect. *Annu Rev Cell Dev Biol* **25**: 355-376.

Unhavaithaya Y, Hao Y, Beyret E, Yin H, Kuramochi-Miyagawa S, Nakano T, Lin H. 2009. MILI, a PIWI-interacting RNA-binding protein, is required for germ line stem cell self-renewal and appears to positively regulate translation. *J Biol Chem* **284**: 6507-6519.

Vagin VV, Wohlschlegel J, Qu J, Jonsson Z, Huang X, Chuma S, Girard A, Sachidanandam R, Hannon GJ, Aravin AA. 2009. Proteomic analysis of murine Piwi proteins reveals a role for arginine methylation in specifying interaction with Tudor family members. *Genes Dev* **23**: 1749-1762.

Vagin VV, Yu Y, Jankowska A, Luo Y, Wasik KA, Malone CD, Harrison E, Rosebrock A, Wakimoto BT, Fagegaltier D et al. 2013. Minotaur is critical for primary piRNA biogenesis. *Rna* **19**: 1064-1077.

Verdoodt F, Bert W, Couvreur M, De Mulder K, Willems M. 2012. Proliferative response of the stem cell system during regeneration of the rostrum in Macrostomum lignano (Platyhelminthes). *Cell Tissue Res* **347**: 397-406.

Voigt F, Reuter M, Kasaruho A, Schulz EC, Pillai RS, Barabas O. 2012. Crystal structure of the primary piRNA biogenesis factor Zucchini reveals similarity to the bacterial PLD endonuclease Nuc. *Rna* **18**: 2128-2134.

Wagner DE, Wang IE, Reddien PW. 2011. Clonogenic neoblasts are pluripotent adult stem cells that underlie planarian regeneration. *Science* **332**: 811-816.

Wallace MR, Andersen LB, Saulino AM, Gregory PE, Glover TW, Collins FS. 1991. A de novo Alu insertion results in neurofibromatosis type 1. *Nature* **353**: 864-866.

Wang Y, Juranek S, Li H, Sheng G, Wardle GS, Tuschl T, Patel DJ. 2009. Nucleation, propagation and cleavage of target RNAs in Ago silencing complexes. *Nature* **461**: 754-761.

Wasik KA, Gurtowski J, Zhou X, Ramos OM, Delás MJ, El Demerdash O, Battistoni G, Falciatori I, Vizoso DB, Smith AD et al. 2015. The genome and transcriptome of the regeneration-competent flatworm, *Macrostomum lignano*. submitted.

Wasik KA, Tam OH, Knott SR, Falciatori I, Hammell M, Vagin VV, Hannon GJ. 2015. RNF17 blocks promiscuous activity of PIWI proteins in mouse testes. *Genes Dev* **29**: 1403-1415.

Watanabe T, Cheng EC, Zhong M, Lin H. 2015. Retrotransposons and pseudogenes regulate mRNAs and lncRNAs via the piRNA pathway in the germline. *Genome Res* **25**: 368-380.

Watanabe T, Takeda A, Tsukiyama T, Mise K, Okuno T, Sasaki H, Minami N, Imai H. 2006. Identification and characterization of two novel classes of small RNAs in the mouse germline: retrotransposon-derived siRNAs in oocytes and germline small RNAs in testes. *Genes Dev* **20**: 1732-1743.

Watanabe T, Totoki Y, Toyoda A, Kaneda M, Kuramochi-Miyagawa S, Obata Y, Chiba H, Kohara Y, Kono T, Nakano T et al. 2008. Endogenous siRNAs from naturally formed dsRNAs regulate transcripts in mouse oocytes. *Nature* **453**: 539-543.

Wicker T, Sabot F, Hua-Van A, Bennetzen JL, Capy P, Chalhoub B, Flavell A, Leroy P, Morgante M, Panaud O et al. 2007. A unified classification system for eukaryotic transposable elements. *Nat Rev Genet* **8**: 973-982.

Xie W, Donohue RC, Birchler JA. 2013. Quantitatively increased somatic transposition of transposable elements in Drosophila strains compromised for RNAi. *PLoS One* **8**: e72163.

Xiol J, Spinelli P, Laussmann MA, Homolka D, Yang Z, Cora E, Coute Y, Conn S, Kadlec J, Sachidanandam R et al. 2014. RNA clamping by Vasa assembles a piRNA amplifier complex on transposon transcripts. *Cell* **157**: 1698-1711.

Xu M, You Y, Hunsicker P, Hori T, Small C, Griswold MD, Hecht NB. 2008. Mice deficient for a small cluster of Piwi-interacting RNAs implicate Piwi-interacting RNAs in transposon control. *Biol Reprod* **79**: 51-57.

Yabuta Y, Ohta H, Abe T, Kurimoto K, Chuma S, Saitou M. 2011. TDRD5 is required for retrotransposon silencing, chromatoid body assembly, and spermiogenesis in mice. *J Cell Biol* **192**: 781-795.

Yekta S, Shih IH, Bartel DP. 2004. MicroRNA-directed cleavage of HOXB8 mRNA. *Science* **304**: 594-596.

Yi R, Qin Y, Macara IG, Cullen BR. 2003. Exportin-5 mediates the nuclear export of pre-microRNAs and short hairpin RNAs. *Genes Dev* **17**: 3011-3016.

Yin H, Lin H. 2007. An epigenetic activation role of Piwi and a Piwi-associated piRNA in Drosophila melanogaster. *Nature* **450**: 304-308.

Zambon RA, Vakharia VN, Wu LP. 2006. RNAi is an antiviral immune response against a dsRNA virus in Drosophila melanogaster. *Cell Microbiol* **8**: 880-889.

Zamparini AL, Davis MY, Malone CD, Vieira E, Zavadil J, Sachidanandam R, Hannon GJ, Lehmann R. 2011. Vreteno, a gonad-specific protein, is essential for germline development and primary piRNA biogenesis in Drosophila. *Development* **138**: 4039-4050.

Zhang F, Wang J, Xu J, Zhang Z, Koppetsch BS, Schultz N, Vreven T, Meignin C, Davis I, Zamore PD et al. 2012. UAP56 couples piRNA clusters to the perinuclear transposon silencing machinery. *Cell* **151**: 871-884.

Zhang Z, Wang J, Schultz N, Zhang F, Parhad SS, Tu S, Vreven T, Zamore PD, Weng Z, Theurkauf WE. 2014. The HP1 homolog rhino anchors a nuclear complex that suppresses piRNA precursor splicing. *Cell* **157**: 1353-1363.

Zhang Z, Xu J, Koppetsch BS, Wang J, Tipping C, Ma S, Weng Z, Theurkauf WE, Zamore PD. 2011. Heterotypic piRNA Ping-Pong requires qin, a protein with both E3 ligase and Tudor domains. *Mol Cell* **44**: 572-584.

Zheng K, Xiol J, Reuter M, Eckardt S, Leu NA, McLaughlin KJ, Stark A, Sachidanandam R, Pillai RS, Wang PJ. 2010. Mouse MOV10L1 associates with Piwi proteins and is an essential component of the Piwi-interacting RNA (piRNA) pathway. *Proc Natl Acad Sci U S A* **107**: 11841-11846.

Appendix A
A short hairpin-RNA (shRNA) backbone based on a Dicer-independent microRNA, miR-451

1.1 Abstract

Short hairpin RNA (shRNA) is a powerful tool for targeted stable gene silencing by reprogramming the endogenous microRNA (miRNA) pathway. A 22nt small RNA guide of any sequence can be embedded in and expressed from an endogenous miRNA backbone to silence genes with corresponding target sites. The current shRNA platform is based on the canonical miRNA, miR-30, which requires two RNase III enzymes – Drosha and Dicer – for biogenesis. Although the miR-30-based shRNA provides efficient silencing in a wide range of applications, the efficacy may be decreased in some contexts with reduced Dicer expression level, such as some types of cancers. Here, we report an alternative miRNA backbone for shRNA expression using the Dicer independent miR-451, aiming for efficient gene silencing in Dicer-null contexts. The miR-451-based shRNAs display comparable processing and knockdown efficiency to that of miR-30-based shRNAs. Interestingly, the two shRNA backbones seem to possess different preferences for guide sequences. Our miR-451-based shRNA system provides an alternative to the commonly used miR-30-based shRNAs and potentially enables the usage of shRNAs in Dicer-deficient background.

1.2 Introduction

The endogenous microRNA (miRNA) pathway provides a programmable mechanism for targeted gene silencing for loss-of-function studies. The biogenesis involves two RNase III-mediated processing steps (Figure 1.4). First, the primary miRNA transcript harboring a stem-loop structure is cleaved by Drosha near the junction between single-stranded and double-stranded regions (Lee et al. 2003; Han et al. 2006). This cleavage produces the precursor miRNA with a hairpin-like structure. Exported to the cytoplasm by Exportin-5 (Yi et al. 2003), the precursor is then processed by another RNase III, Dicer (Bernstein et al. 2001; Park et al. 2011), to

remove the loop and produce a ~22nt double-stranded RNA duplex, which is subsequently loaded into Argonaute. The passenger strand of the duplex is finally removed and the RNA-induced silencing complex (RISC) is formed with Argonaute and the guide small RNA being the main components (Hutvagner and Zamore 2002; Mourelatos et al. 2002). The nature of miRNA processing hints the possibility for artificial targeted gene silencing. An artificial small RNA guide can hijack the endogenous miRNA pathway from three entry points: the effector stage, the precursor stage and the primary miRNA stage (Cullen 2005). A siRNA duplex can be introduced into cells and bind Argonaute proteins to form a RISC (Elbashir et al. 2001). Alternatively, the small RNA guide can be expressed from a RNA polymerase III (pol III)-driven promoter as a precursor hairpin RNA (Brummelkamp et al. 2002; Paddison et al. 2002; Siolas et al. 2005). The most natural strategy is to mimic the entire processing of an endogenous miRNA (Zeng et al. 2002). An artificial small RNA guide with sequence of interest can be embedded into a pol II promoter-driven endogenous primary miRNA backbone. The miR-30 backbone has been successfully programmed for this purpose (Silva et al. 2005; Stegmeier et al. 2005). Compared to the previous two strategies, this miR-30-based shRNA strategy has several advantages. First, it mimics the natural miRNA biogenesis thus is unlikely to saturate the RNAi machinery. The toxicity is minimal compared to the other two strategies. Second, it enables stable and controllable gene silencing. The miR-30 cassette can be integrated into viral vectors and stable silencing can be achieved by viral transduction. Moreover, the shRNA expression can be made inducible for reversible gene expression regulation (Unwalla et al. 2004; Aagaard et al. 2007). The miR-30-based shRNA has been applied in a wide range of loss-of-function studies, from the studies of single genes in cell lines and mouse model to high throughput genetic screening for drug targets.

Despite the versatility and high efficiency, current shRNA technology faces technical limitations. Besides off-target effects and difficulty in identifying potent guide sequences, another limitation is linked to the biogenesis requirement. As a canonical miRNA, the processing of miR-30 requires Drosha and Dicer. In some contexts, the miRNA machinery is altered. For instance, suppression of miRNA biogenesis is often linked to cancer progression. Dicer loss has been observed in multiple cancer models (Khoshnaw et al. 2012; Ravi et al. 2012). In such context, miR-30-based shRNA is no more suitable due to insufficient biogenesis. Fortunately, not all miRNAs require Dicer for processing. A non-canonical miRNA, miR-451, has been found in mammals and zebrafish processed in a Dicer-independent manner (Cheloufi et al. 2010; Cifuentes et al. 2010). Instead of Dicer, it is Ago2 that processes the Drosha-produced precursor miR-451 (Figure 3.1). Ago2, the only Argonaute with catalytic activity in mammals, binds and cleaves the precursor miR-451 hairpin to generate a 30nt intermediate, which is further trimmed from 3' end and gives rise to the mature 23nt miR-451 guide strand as well as 26nt and 29nt small RNA. Transfection of synthetic miR-451 precursor mimic that targets p53 results in efficient p53 silencing (Figure 3.2), indicating the potential of miR-451 as an alternative shRNA tool. Moreover, miR-451 does not undergo strand selection in RISC, thus further avoids the off-target effect induced by the passenger strand. Here we develop a new shRNA backbone based on the Dicer-independent miR-451. The miR-451-based shRNAs show comparable knockdown efficiency to that of

miR-30-based shRNAs. Notably, the two shRNA expression systems seem to show different preferences for guide sequences. Our new shRNA expression tool may potentially serve as a complement to the current miR-30 based system and expand the territory of shRNA applications.

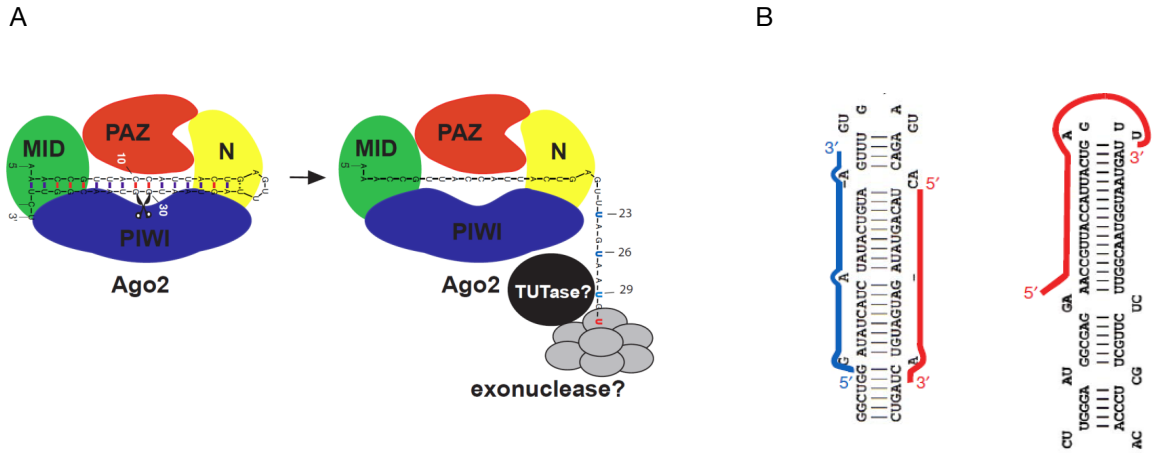

Figure 3.1 Biogenesis of mature miR-451 by Ago2. (A) The precursor miR-451 is loaded into Ago2 and cleaved after the 30th nucleotide from the 5' end. The 30nt intermediate is then trimmed from the 3' end by an unknown mechanism to generate the 22nt, 26nt and 29nt mature miR-451. (B) The secondary structures of miR-30 (left) and miR-451 (right) precursors. Red denotes guide strand and blue passenger strand. Adapted from (Cheloufi et al. 2010).

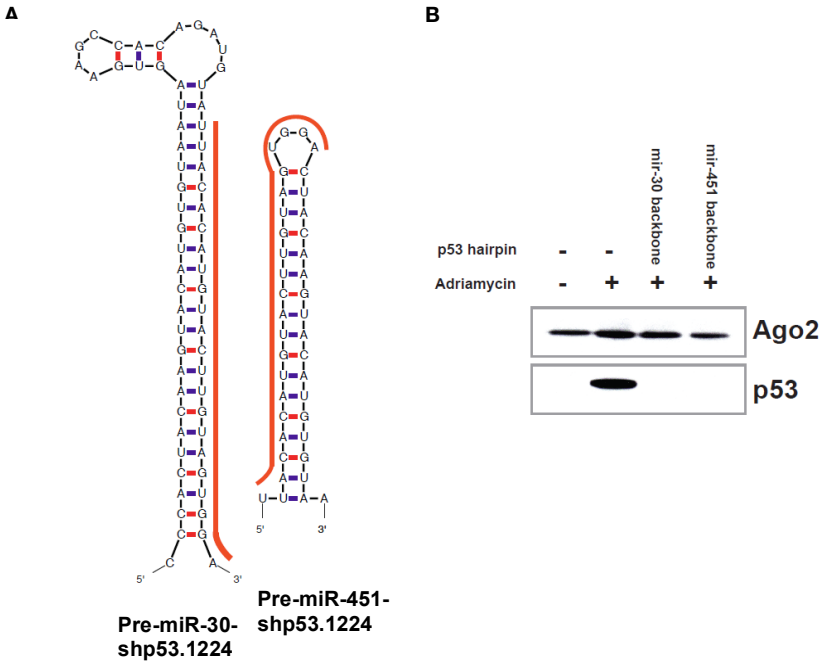

Figure 3.2 The precursor miR-451 can be programmed for targeted gene silencing. (A) The miR-30 and miR-451 precursor mimics targeting p53. Red denotes guide strands. (B) Western blot showing p53 knockdown efficiency and Ago2 expression level. Adapted from (Cheloufi et al. 2010).

1.3 Results

1.3.1 Dose dependence of synthetic miR-451 precursor mimics

A precursor miR-451 mimic targeting p53 has been shown previously capable of efficient silencing at high dose (100nM) (Cheloufi et al. 2010). In order to understand the dose dependence, we therefore tested knockdown efficiency of miR-451 precursor mimics at a series of concentrations in comparison to corresponding miR-30 precursor mimics. We selected three p53 guide sequences whose efficiencies were pre-defined in miR-30 backbone. While the general trend was consistent, there existed behavioral differences between miR-451 and miR-30 mimics. In miR-30, shp53.1224 (best efficiency) and shp53.279 (medium efficiency) both reached maximum knockdown starting at concentration as low as ~10nM, whereas shp53.1404 (poor efficiency) showed nearly no silencing effect. In miR-451, shp53.279 replicated the behavior in miR-30. However, shp53.1224 required a much higher dose for maximum knockdown. In contrast to miR-30, miR-451 precursor harboring shp53.1404 exhibited moderate silencing (~40%) at high concentrations. In general, the miR-451 precursor mimics showed comparable knockdown efficiency to miR-30, in spite of some behavioral differences that are likely to be the results of distinct nature of biogenesis in the two settings.

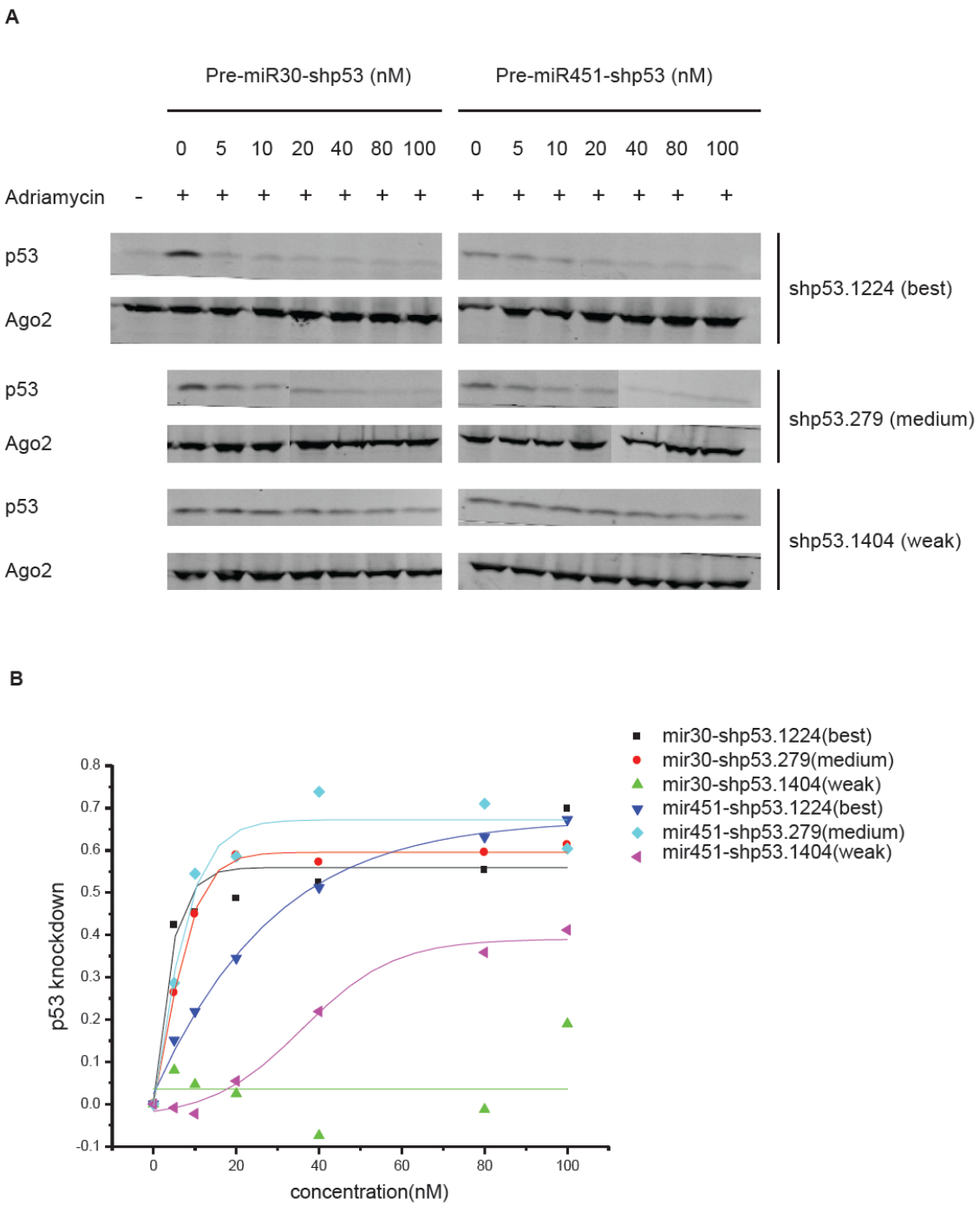

Figure 3.3 Titration of synthetic miR-451 precursor mimics targeting p53 in mouse ES cells. (A) Western blot showing knockdown of p53 at a series of transfected precursor RNA concentrations. Ago2 expression level is presented as a control. (B) Quantitative presentation of p53 silencing based on western blot.

1.3.2 Primary miR-451 mimics induce targeted gene silencing

We next explored the feasibility of programming the primary miR-451. We synthesized 200nt DNA fragments of miR-451 mimics with ~60nt flanking the stem-loop

on each side (5' and 3' miR). These primary miR-451 mimics were inserted into LMN vector to replace the miR-30 cassette (Figure 3.4A) and delivered into NIH3T3 cells by retroviral infection. With multiple copies (high MOI), all three guide sequences displayed efficient (>80%) silencing in miR-30 backbone while shp53.1224 (best) and shp53.279 (medium) performed well in miR-451. However, with single copy (low MOI), shp53.279 failed to silence the target gene in miR-451 and the shp53.1224 only exhibited moderate knockdown efficiency (~60%) (Figure 3.4B). To exclude the cell line-specific effects, we reproduced the single copy infections in primary MEF and obtained consistent results (Figure 3.4C). In addition to p53 hairpins, we tested four Renilla hairpins with different knockdown efficiency predefined in miR-30 (Figure 3.4D). All guide sequences except one (RN-1) showed comparable efficiency in miR-451. Silencing by RN-1 is significantly less efficient in miR-451 than in miR-30. Considered as a whole, our results showed the potential of miR-451 as an alternative shRNA backbone with differential preferences from miR-30. The efficiency in miR-451 backbone cannot be predicted based on the performance in miR-30, suggesting distinct rules during biogenesis and effector steps.

1.3.3 Primary miR-451 mimics are processed through the miR-451 biogenesis pathway

The biogenesis efficiency directly contributes to silencing efficiency. Therefore we examine the production of mature guide RNA, include 23nt, 26nt and 29nt small RNA, from miR-451 backbone. Compared between miR-451 and miR-30 backbones, each hairpin was produced at similar levels after single-copy (Figure 3.5A) or multiple-copy (Figure 3.5B) infections, with the exception of shp53.279 with single copy. This trend was well correlated with knockdown efficiency (Figure 3.4B). Since Ago2, but not other Ago proteins, is responsible for the formation of mature guide strand, we particularly examined the Ago2-bound hairpins and observed the similar trend (Figure 3.4C). The catalytic activity of Ago2, the only catalytically active Ago protein in mammals, is required for the cleavage of miR-451 precursor to form the mature RNA. In order to confirm the authenticity of our miR-451 mimics, we compared the mature strand formation in the presence of wild type and catalytically inactive Ago2. As expected, incapability of cleavage led to accumulation of the 40nt precursor of miR-451 mimic, while miR-30 mimic was unaffected by the Ago2 catalytic activity (Figure 3.6). These data combined prove that our miR-451 mimics are truly channeled into the endegonous miR-451 biogenesis pathway.

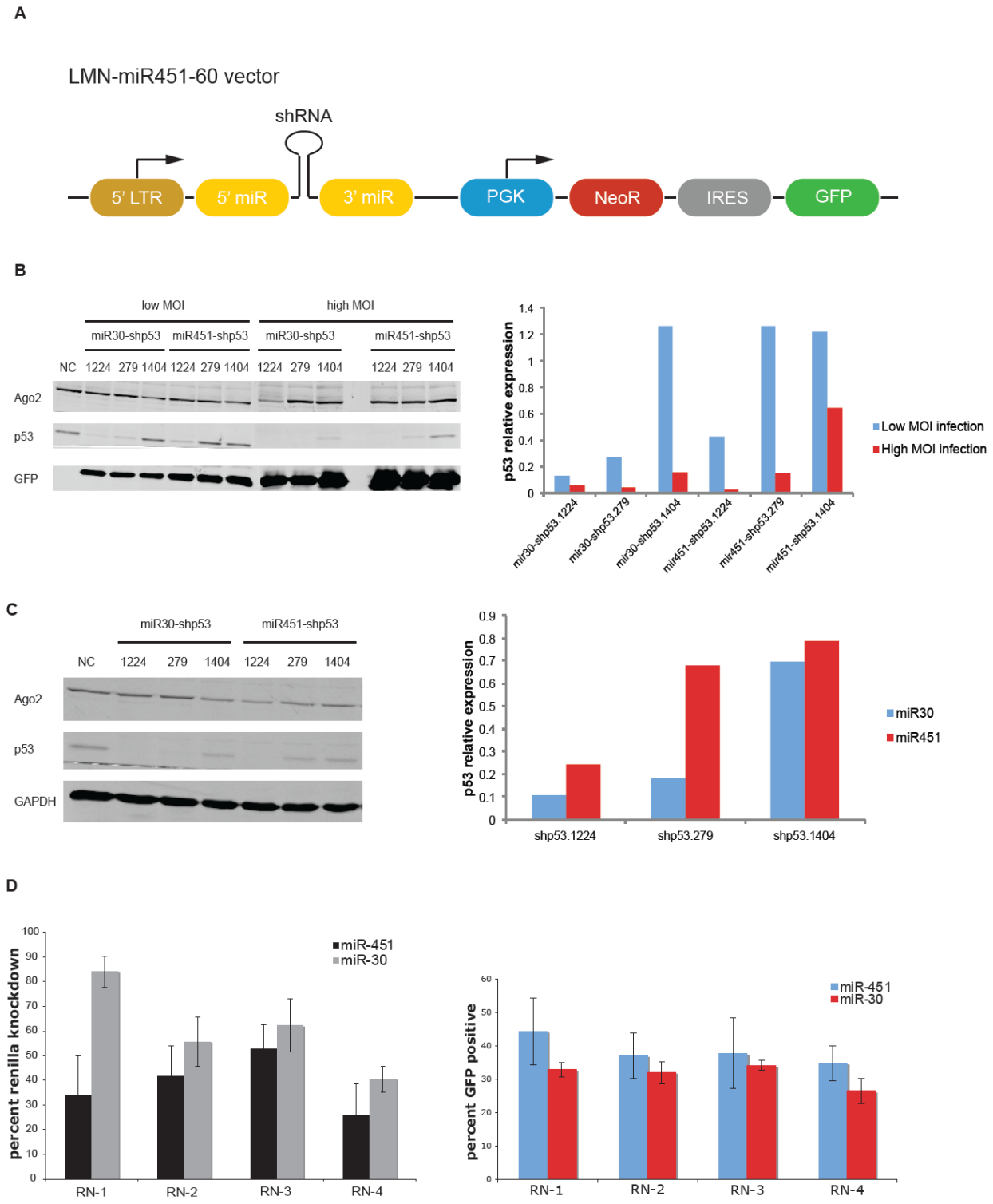

Figure 3.4 Targeted stable gene silencing mediated by primary miR-451 mimics. (A) Schematic presentation of LMN-miR451-60 retroviral vector. The primary miR-451 DNA fragment with ~60nt 5' and 3' miR replaces the original miR-30 cassette. (B) Western blot (left) and quantification (right) of p53 knockdown in NIH3T3 cells infected with p53 hairpins in miR-30 and miR-451 backbones. (C) Western blot (left) and quantification (right) of p53 knockdown in primary MEF infected with single copy of p53 hairpins in miR-30 and miR-451 backbones. (D) Renilla knockdown efficiency (left) in NIH3T3 cells infected with Renilla hairpins in miR-30 and miR451 backbones. Infection efficiency is shown on the right.

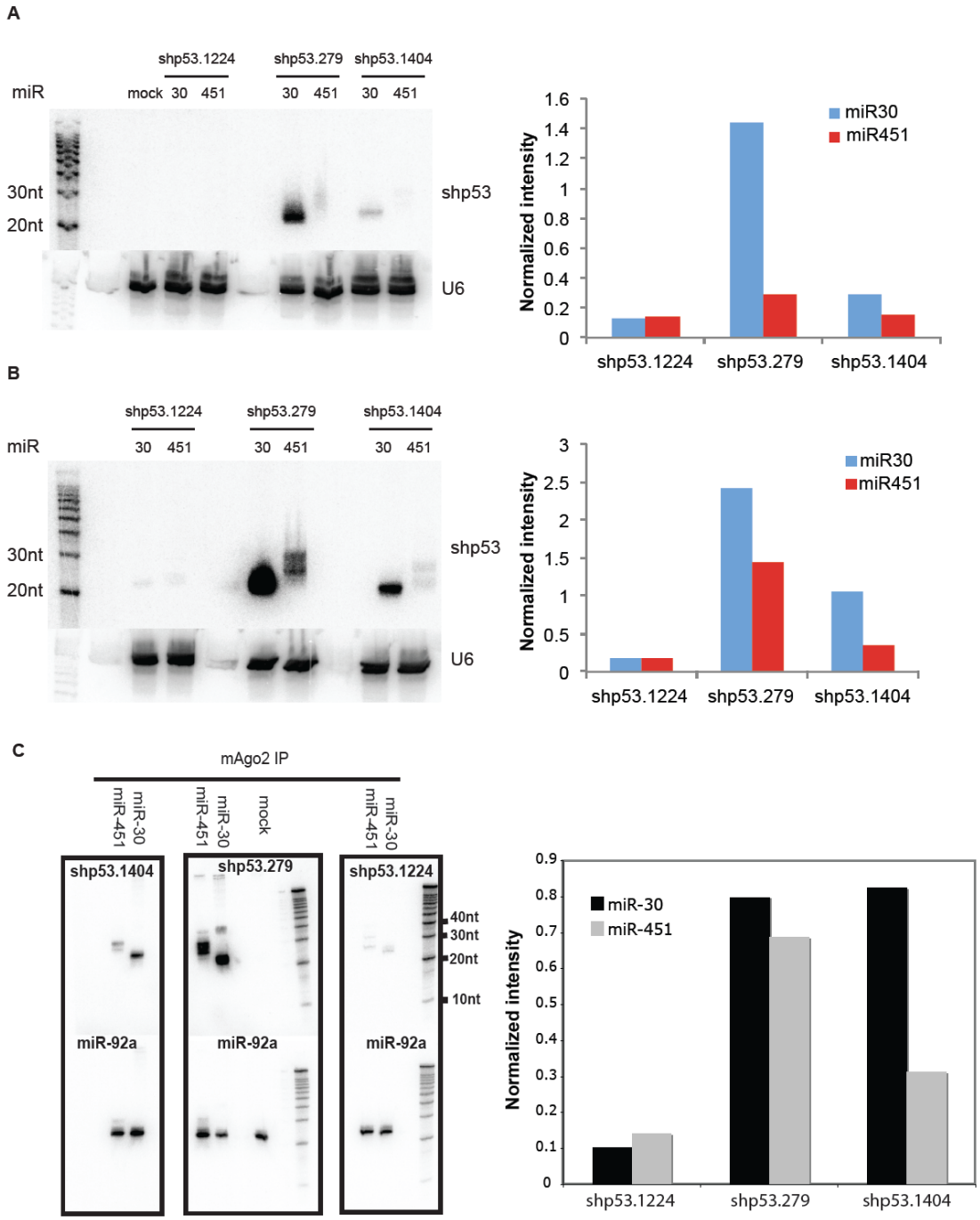

Figure 3.5 Production of mature guide RNA from miR-451-based backbone. Northern blot is performed (left) and quantified (right) to examine mature small RNA guides in NIH3T3 cells infected with p53 hairpins at low (A) and high (B) MOI or in HEK293 cells following p53 hairpin vector transfection and Ago2 IP (C).

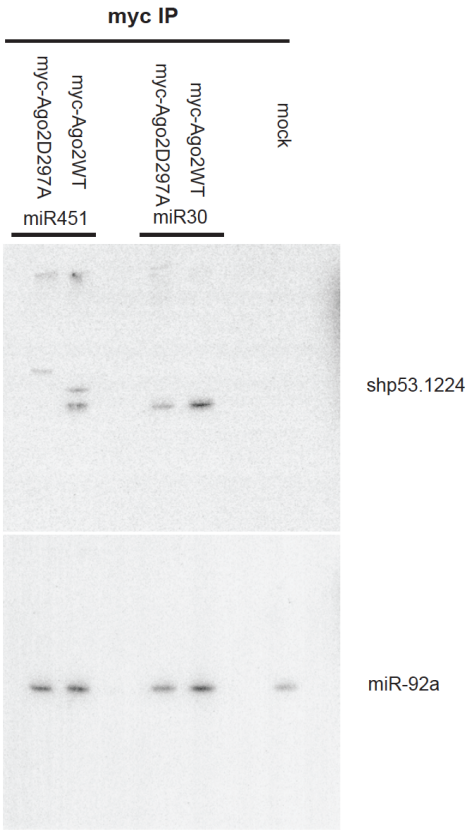

Figure 3.6 Processing of miR-451 mimics depends on the catalytic activity of Ago2. Northern blot for shp53.1224 hairpin following Myc IP from HEK293 cells cotransfected with hairpin vector and Myc-tagged Ago2 construct. WT: wild type; D297A: catalytically dead mutant.

1.3.4 Construction of a versatile miR-451 shRNA expression vector

In order to simplify cloning, we aimed at developing a miR-451 shRNA expression vector with restriction sites flanking the variable stem-loop region (LMN-144-451 vector). To ensure high processing efficiency, the flanking sequences were extended to 200nt on each side of the stem-loop. The 5' flanking region contains another miRNA, miR-144. To facilitate DNA cloning, we introduced sites by point mutations within the upstream and downstream regions near the stem-loop region (Figure 3.7A). The resulting endogenous primary miR-451 variants were then tested using a firefly luciferase sensor harboring miR-451 target sites in the 3'UTR. In any variant tested, introduction of restriction sites did not disrupt knockdown efficiency (Figure 3.7B). In conclusion, we constructed a flexible miR-451 shRNA backbone that can be easily adapted for targeted gene silencing.

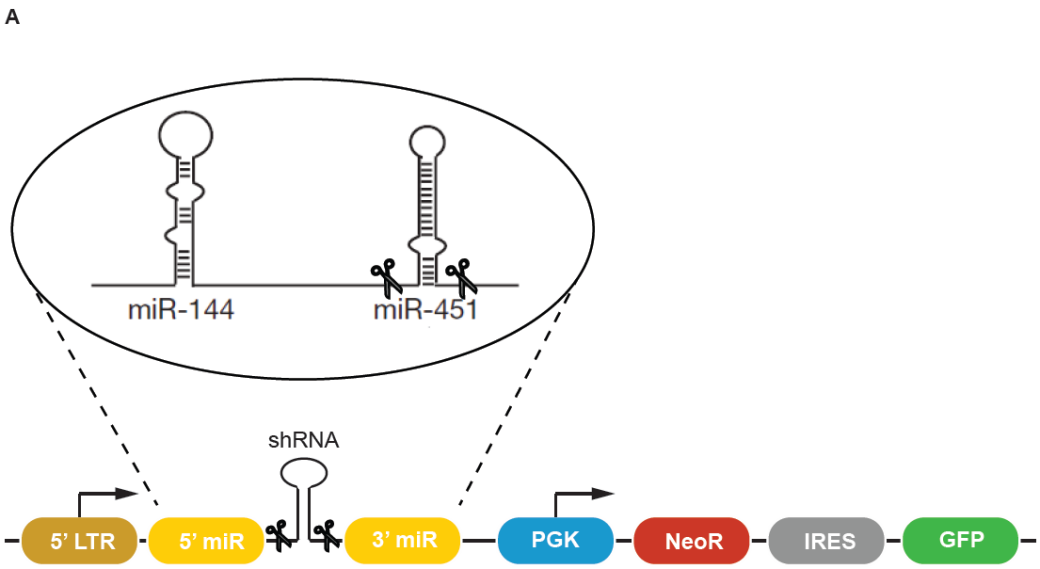

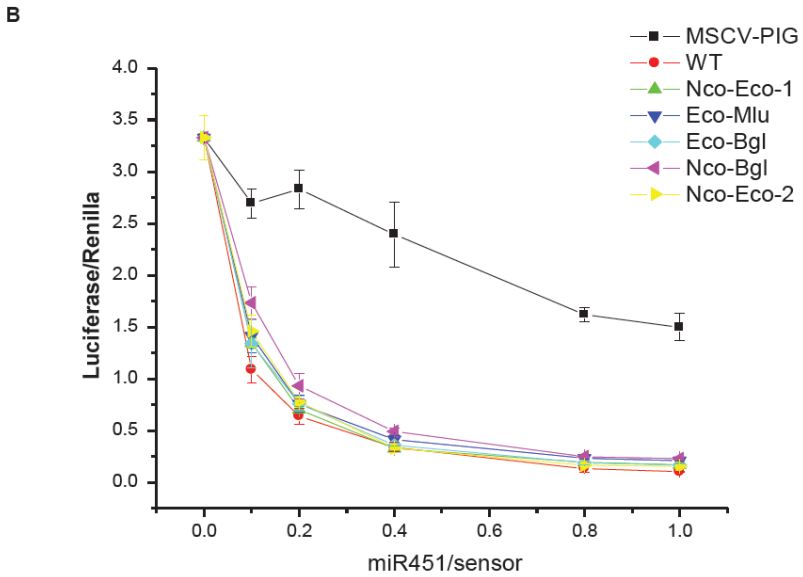

Figure 3.7 The miR-451 shRNA expression vector. (A) Schematic presentation of the construction of LMN-144-451 vector. Scissors denote restriction sites. (B) Knockdown efficiency of firefly luciferase sensor by primary miR-451 variants with introduced restriction sites. WT: wild type; Nco: NcoI; Eco: EcoRI; Mlu: MluI; Bgl: BglII. MSCV-PIG is the empty vector with no miR.

1.4 Contribution

This project is a collaboration between Sihem Cheloufi and me. Sihem and I designed all experiments. Sihem performed the northern blot following Ago2 and Myc IP, and characterization of Renilla hairpins. I performed all other experiments.

1.5 Discussion

In this study, we developed a new shRNA backbone based on the Dicer-independent non-canonical miR-451. This shRNA expression system exhibited comparable knockdown efficiency to that of the widely used miR-30-based shRNA system. Its Dicer independent nature potentially spans the shRNA applications to Dicer null contexts, such as shRNA screening in cancer cells with low Dicer expression.

Apart from the target accessibility (Brown et al. 2005), knockdown efficiency is mainly determined by two properties of shRNAs – processing efficiency and the guide-target interaction. We compared the processing ability of miR-451 backbone to that of miR-30. The two backbones do not always have similar mature guide production levels of the same guide sequences, indicating differential requirements for biogenesis beyond the known features of the two pathways. Further studies are required to understand how the biogenesis enzymes interact with substrates and what they prefer. Another consideration in this respect is the length of flanking sequences required for efficient biogenesis. 200nt from each side has been the rule of thumb, however further comparison is needed. In the case of miR-451, we included 200nt flanking each side, which includes another miRNA, miR144. It is unclear whether miR-451 processing is independent of the presence of miR-144. It is also highly likely that the guide sequences affect processing efficiency, although not much is understood regarding that. As much as miRNA processing, the guide-target interaction largely remains an open question. Moreover, the unique nature of miR-451 processing adds even more uncertainty to the question. In contrast to canonical miRNAs, miR-451 biogenesis yields mature miRNAs in different sizes (23nt, 26nt and 29nt) (Cheloufi et al. 2010). It is unknown whether the 26nt and 29nt small RNAs mediate target silencing as well and if so through which mechanisms.

1.6 Materials and methods

1.6.1 Construct cloning

LMN-miR451-60 vector was constructed by replacing the miR-30 cassette with the miR-451 mimics containing a 60nt flanking sequence on each side of the stem-loop. The LMN-144-451 vector was made by replacing the miR-30 cassette with the endogenous miR-451 cassette with a 200nt flanking sequence on each side of stem-loop. Restriction sites were introduced using the QuikChange lightning site-directed mutagenesis kit (Agilent). The Myc-tagged Ago2 wild type and D297A plasmids were described previously described.

1.6.2 Cell culture transfection, viral transduction and sensor assay

NIH3T3, HEK293 and primary MEFs were cultured in DMEM with 10% FBS. Mouse ES cells were cultured on gelatin without feeder cells following previously described protocol (Nagy et al. 2003). HEK293 cells were transfected with 20μg of hairpin plasmid or cotransfected with 20ug of hairpin plasmid and 10ug of Ago2 plasmid using Lipofectamine 2000 (Life technologies). Cells were collected for downstream assays after 48 hours. LMN-based retroviral vector was transfected into ecotropic

Phoenix cells using Lipofectamine 2000 for virus packaging. NIH3T3 cells were infected with low (<30%) or high MOI and selected by G418. Synthetic precursor RNAs (Dharmacon) were transfected into mouse ES cells at a series of concentrations using Lipofectamine 2000. Cells were collected for downstream assays 48 hours post-transfection. The sensor assay was conducted using a firefly luciferase reporter harboring four miR-451 target sites in the 3' UTR. HEK293 cells were cotransfected with the reporter plasmid, Renilla luciferase plasmid and LMN-144-451 variants or MSCV-PIG empty vector at different guide: sensor ratios. Bioluminescence was measured 48 hours post-transfection as readout of knockdown.

1.6.3 Western blot

Protein samples were resuspended in Laemmli buffer, boiled for 5min and run on 10% SDS-PAGE. Proteins were transferred onto a PVDF membrane using a wet transfer method at 35V overnight. Membranes were blocked in Odyssey blocking buffer (LI-COR) at room temperature for 1 hour and incubated with primary antibodies (1:1000) at 4°C overnight. Membranes were washed in TBS-T (3 x 5min) and incubated with IRDye-700 anti-mouse secondary antibody (LI-COR) at room temperature for 1 hour. After washes in TBS-T (5 x 5min), membrane was imaged on Odyssey CLx Imager. Primary antibodies were anti-eif2c2 mouse monoclonal antibody M01 (Abnova), anti-GFP mouse monoclonal antibody Pab240 (Santa Cruz) and anti-GAPDH mouse monoclonal antibody 6C5 (Millipore).

1.6.4 Immunoprecipitation, RNA extraction and northern blot

Ago2 and Myc immunoprecipitation was performed as previously described (Cheloufi et al. 2010). IP RNA was purified using acidic phenol: chloroform (Ambion) followed by chloroform and precipitated with ethanol. Total RNA was extracted using TRIzol reagent (Life Technologies) according to manufacturer's instruction. Northern blot was performed as previously described (Cheloufi et al. 2010).

References

Aagaard L, Amarzguioui M, Sun G, Santos LC, Ehsani A, Prydz H, Rossi JJ. 2007. A facile lentiviral vector system for expression of doxycycline-inducible shRNAs: knockdown of the pre-miRNA processing enzyme Drosha. *Mol Ther* **15**: 938-945.

Bernstein E, Caudy AA, Hammond SM, Hannon GJ. 2001. Role for a bidentate ribonuclease in the initiation step of RNA interference. *Nature* **409**: 363-366.

Brown KM, Chu CY, Rana TM. 2005. Target accessibility dictates the potency of human RISC. *Nat Struct Mol Biol* **12**: 469-470.

Brummelkamp TR, Bernards R, Agami R. 2002. A system for stable expression of short interfering RNAs in mammalian cells. *Science* **296**: 550-553.

Cheloufi S, Dos Santos CO, Chong MM, Hannon GJ. 2010. A dicer-independent miRNA biogenesis pathway that requires Ago catalysis. *Nature* **465**: 584-589.

Cifuentes D, Xue H, Taylor DW, Patnode H, Mishima Y, Cheloufi S, Ma E, Mane S, Hannon GJ, Lawson ND et al. 2010. A novel miRNA processing pathway

independent of Dicer requires Argonaute2 catalytic activity. *Science* **328**: 1694-1698.
Cullen BR. 2005. RNAi the natural way. *Nat Genet* **37**: 1163-1165.
Elbashir SM, Lendeckel W, Tuschl T. 2001. RNA interference is mediated by 21- and 22-nucleotide RNAs. *Genes Dev* **15**: 188-200.
Han J, Lee Y, Yeom KH, Nam JW, Heo I, Rhee JK, Sohn SY, Cho Y, Zhang BT, Kim VN. 2006. Molecular basis for the recognition of primary microRNAs by the Drosha-DGCR8 complex. *Cell* **125**: 887-901.
Hutvagner G, Zamore PD. 2002. A microRNA in a multiple-turnover RNAi enzyme complex. *Science* **297**: 2056-2060.
Khoshnaw SM, Rakha EA, Abdel-Fatah TM, Nolan CC, Hodi Z, Macmillan DR, Ellis IO, Green AR. 2012. Loss of Dicer expression is associated with breast cancer progression and recurrence. *Breast Cancer Res Treat* **135**: 403-413.
Lee Y, Ahn C, Han J, Choi H, Kim J, Yim J, Lee J, Provost P, Radmark O, Kim S et al. 2003. The nuclear RNase III Drosha initiates microRNA processing. *Nature* **425**: 415-419.
Mourelatos Z, Dostie J, Paushkin S, Sharma A, Charroux B, Abel L, Rappsilber J, Mann M, Dreyfuss G. 2002. miRNPs: a novel class of ribonucleoproteins containing numerous microRNAs. *Genes Dev* **16**: 720-728.
Nagy A, Gertsenstein M, Vintersten K, Behringer R. 2003. Manipulating the Mouse Embryo: A Laboratory Manual, Third Edition. CSHL press.
Paddison PJ, Caudy AA, Bernstein E, Hannon GJ, Conklin DS. 2002. Short hairpin RNAs (shRNAs) induce sequence-specific silencing in mammalian cells. *Genes Dev* **16**: 948-958.
Park JE, Heo I, Tian Y, Simanshu DK, Chang H, Jee D, Patel DJ, Kim VN. 2011. Dicer recognizes the 5' end of RNA for efficient and accurate processing. *Nature* **475**: 201-205.
Ravi A, Gurtan AM, Kumar MS, Bhutkar A, Chin C, Lu V, Lees JA, Jacks T, Sharp PA. 2012. Proliferation and tumorigenesis of a murine sarcoma cell line in the absence of DICER1. *Cancer Cell* **21**: 848-855.
Silva JM, Li MZ, Chang K, Ge W, Golding MC, Rickles RJ, Siolas D, Hu G, Paddison PJ, Schlabach MR et al. 2005. Second-generation shRNA libraries covering the mouse and human genomes. *Nat Genet* **37**: 1281-1288.
Siolas D, Lerner C, Burchard J, Ge W, Linsley PS, Paddison PJ, Hannon GJ, Cleary MA. 2005. Synthetic shRNAs as potent RNAi triggers. *Nat Biotechnol* **23**: 227-231.
Stegmeier F, Hu G, Rickles RJ, Hannon GJ, Elledge SJ. 2005. A lentiviral microRNA-based system for single-copy polymerase II-regulated RNA interference in mammalian cells. *Proc Natl Acad Sci U S A* **102**: 13212-13217.
Unwalla HJ, Li MJ, Kim JD, Li HT, Ehsani A, Alluin J, Rossi JJ. 2004. Negative feedback inhibition of HIV-1 by TAT-inducible expression of siRNA. *Nat Biotechnol* **22**: 1573-1578.
Yi R, Qin Y, Macara IG, Cullen BR. 2003. Exportin-5 mediates the nuclear export of pre-microRNAs and short hairpin RNAs. *Genes Dev* **17**: 3011-3016.

Zeng Y, Wagner EJ, Cullen BR. 2002. Both natural and designed micro RNAs can inhibit the expression of cognate mRNAs when expressed in human cells. *Mol Cell* **9**: 1327-1333.

Appendix B
FACS and deep sequencing-based assays aiming for measurements of shRNA potency on a large scale

1.1 Abstract

Short-hairpin RNA (shRNA) has been a powerful tool for reversible and stable targeted gene silencing in mammalian cells. While it revolutionized reverse genetics, the application of shRNAs still faces several challenges, one of which is the identification of potent guide sequences. Although a sensor assay is available for this purpose with high accuracy, it is time-consuming and lacks quantitative measurements. Therefore, we aim at developing a fast and quantitative method in order to identify not only the potent shRNAs but also shRNAs with different levels of strength in a high throughput manner. We take advantage of a Venus reporter harboring target site in the 3' UTR and measure either the cleavage efficiency of Venus mRNA or the fluorescence intensity decrease – as markers for silencing efficiency - using FACS and deep sequencing. In the proof-of-principle experiment with a pool of 19 sentinel hairpins, our measurements from both methods well correlated the known efficiencies of the hairpins. An application to a larger scale with technical refinements will not only help identify potent shRNAs, but also provide insights in what determine shRNA potency.

1.2 Introduction

Short hairpin RNA (shRNA) has accelerated reverse genetics in the last decade. It is the product of reprogramming the endogenous miRNA pathway, specifically miR-30 biogenesis. The mature small RNA duplex sequence, embedded in the primary miRNA, can be replaced with sequences of interest and properly processed for silencing (Zeng et al. 2002). Therefore, shRNA is given the maximum versatility to knockdown any mRNA of interest by simply implanting a guide sequence that is complementary to the target. Compared to other gene silencing tools, such as small interfering RNA (siRNA), shRNA has shown several advantages. First, it mimics the nature process of miRNA biogenesis thus is less likely to saturate the RNAi machinery or trigger cellular immune

response. Second, shRNA enables stable expression of RNAi by genomic integration that is unfeasible with siRNA (Silva et al. 2005; Stegmeier et al. 2005). Third, shRNA expression, like an endogenous miRNA, is tightly regulated thus can be controlled using regulating elements (Unwalla et al. 2004). For instance, Tet-On expression system is used for reversible shRNA expression to switch on and off gene expression (Aagaard et al. 2007). However, despite all the power of shRNA, a few challenges have limited its applications, among which the biggest concerns are the off-target effects (Jackson and Linsley 2010) and difficulty in finding the potent guide sequences. Although in theory any 22nt sequence along an mRNA of interest can be targeted for silencing, in practice the silencing efficiency can vary dramatically from one target site to another. Among them, few sites yield satisfactory knockdown (>80%). And predictions have been elusive due to lack of understanding of biogenesis and effector step. To achieve higher knockdown, higher dose of shRNA is often needed. However, that could worsen the off-target effect and make shRNA less specific. Choosing a highly potent shRNA guide sequence is the key to effective and specific gene silencing.

In order to experimentally identify potent shRNAs, a sensor assay was developed using a Venus sensor system (Fellmann et al. 2011). The Venus mRNA harbors a target site in the 3' UTR and the corresponding inducible shRNA is expressed on the same vector. After integrating in the host genome with a single copy, the Venus intensity serves as an indicator of silencing potency of each hairpin sequence. Potent hairpins are enriched by repeated cell sorting cycles and identified using deep sequencing. Despite being an unbiased assay, this method is time-consuming due to multiple sorting cycles and only provides qualitative information about potent hairpins. To overcome the limitations, we aim to develop an alternative method that allows rapid and quantitative measurement of hairpins of all strengths on a large scale. We took advantage of the preexisting sensor system and measured either the cleavage efficiency of the target mRNA or the change of Venus intensity using flow cytometry and deep sequencing. In the proof-of-principle experiments using both methods, our measurements successfully recapitulated the potencies of reference hairpins. For these methods avoid repeated cell sorting, they are much faster while providing quantitative measurement of hairpin potencies.

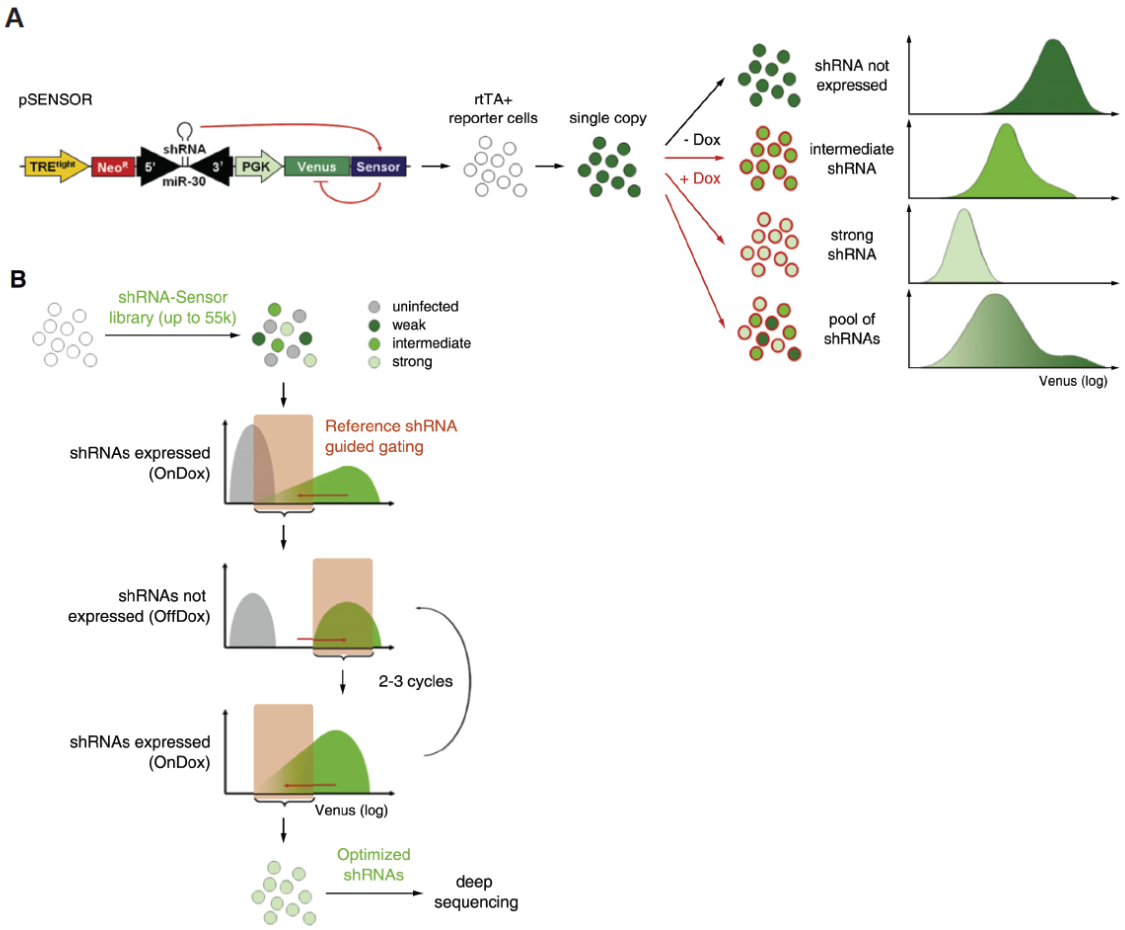

Figure 4.1 Sensor assay for the identification of potent shRNAs. (A) Schematic of the principle. The pSENSOR contains the tested shRNA and a Venus harboring the corresponding target site in the 3' UTR. The sensor construct is introduced into the rtTA+ reporter cells by single-copy retroviral infection. When the shRNA is switched on, Venus intensity is shifted due to silencing. And this change of Venus expression directly reflects silencing efficiency. (B) The schematic of ping-pong sorting strategy. When the shRNAs are switched on, the lower fraction enriched for potent shRNAs is isolated and allowed to recover with no hairpin expression before high Venus fraction is isolated to remove cells with insufficient Venus expression. This cycle is repeated for 2-3 times and final cell fractions are processed for deep sequencing in order to identify the shRNAs. Adapted from (Fellmann et al. 2011).

1.3 Results

Short-hairpin RNAs (shRNAs) are designed perfectly complementary to their targets, in which scenario, RNAi is believed to take place mainly through direct target cleavage. Therefore, we chose two measurements as indicators of hairpin potency – the cleavage efficiency of target mRNAs and depletion of target protein expression. Two parallel methods were developed in order to capture the two parameters: the molecular sensor assay for mRNA cleavage measurements and the binned sensor assay for measurements of Venus sensor expression shifts.

1.3.1 Molecular sensor assay – quantifying the shRNA-mediated target mRNA cleavage

The molecular sensor assay aims at measuring the shRNA-induced direct cleavage of target mRNAs and takes advantage of the pre-existing sensor system (Figure 4.2). In the Venus sensor system, when the shRNA expression is switched on, the cleavage takes place at the sensor site harbored in the 3' UTR of Venus mRNA. In order to measure the target destruction efficacy, this method in fact measures the depletion of intact mRNAs before and after the shRNA is expressed by RT-PCR amplification across the sensor site, where cleavage is supposed to occur. The identity and quantity of each shRNA are then identified using deep sequencing of the corresponding sensor site. Due to the extremely low quantity of Venus mRNAs introduced by single-copy integration, binding sites for MS2 protein are inserted in the 3' UTR of Venus downstream from the sensor site, in order to enrich the Venus mRNAs prior to RT-PCR.

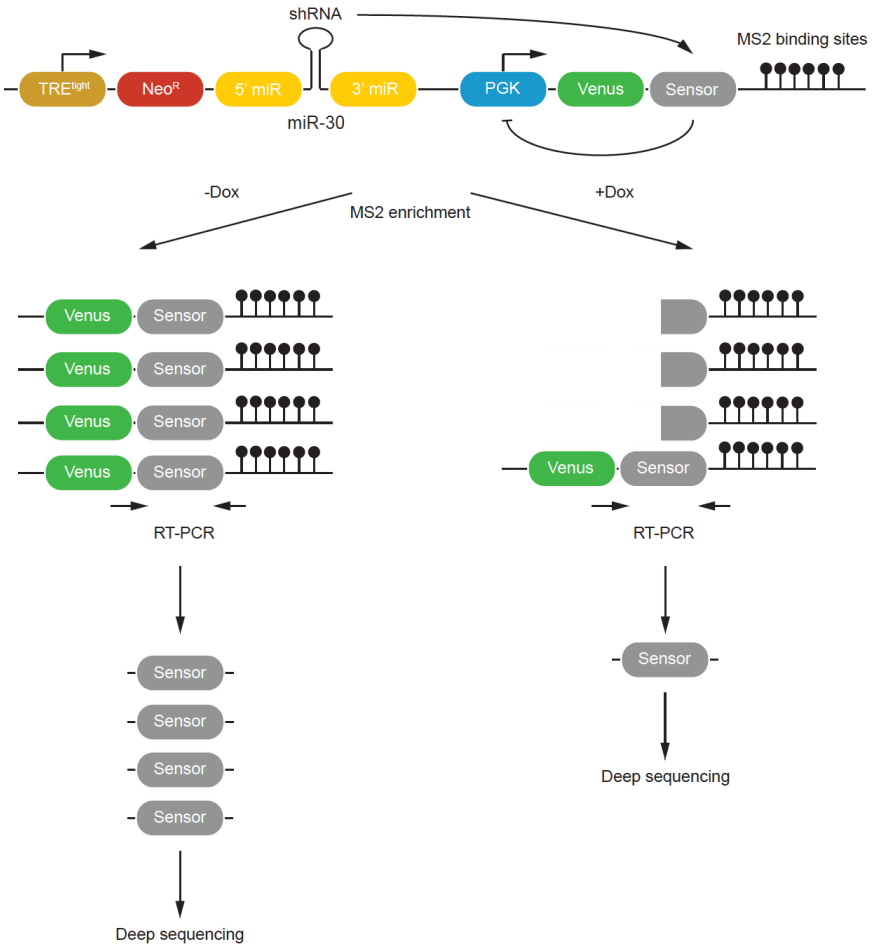

Figure 4.2 Schematic of molecular sensor assay. The sensor construct containing an shRNA and a Venus harboring corresponding target site and MS protein binding sites is introduced into rtTA+ reporter cells by single-copy retroviral infection. The same pool of cells is split and treated with and without Dox in parallel. The Venus mRNAs are enriched by MS2 protein and the intact sensor target sites are amplified using RT-PCR with primers across the entire sensor site. Each sensor sequence is identified and quantified by deep sequencing.

We first conducted a proof-of-principle experiment using 19 reference shRNAs with different degrees of efficiencies and 4 negative controls (true zero) containing scrambled target sites. The true zero controls served as the true baseline for no silencing. To quantify the shRNA-mediated depletion of Venus mRNAs, we calculated the ratio of each shRNAs between hairpin-on (+Dox) and hairpin-off (-Dox) conditions. We observed an overall negative correlation between hairpin potency and this ratio (Figure 4.3A), corroborating that direct target cleavage is the leading contribution to shRNA-mediated silencing. Compared to the overall trend, this correlation, while still present, was less evident among individual shRNAs (Figure 4.3B), suggesting the contributions of other silencing mechanisms.

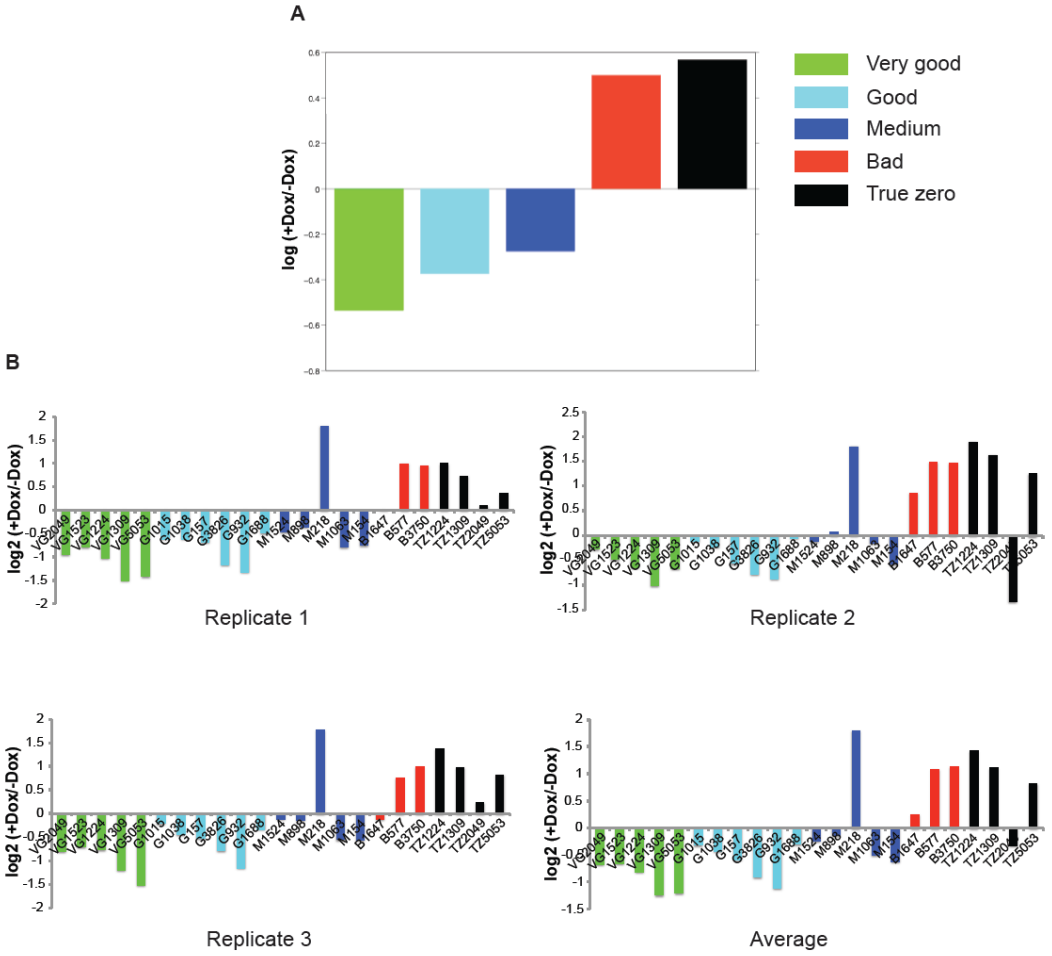

Figure 4.3 Quantification of proof-of-principle experiment using molecular sensor assay. This experiment measured a pool of 19 reference shRNAs with different silencing potencies categorized as very good, good, medium, and bad as well as 4 negative controls (true zero). (A) The average ratio of each category is strongly negatively correlated with the ratio between +Dox and –Dox conditions. (B) The same ratio of individual shRNA and true zero control. VG: very good; G: good; M: medium; B: bad; TZ: true zero.

Despite the consistent correlation, the dynamic range obtained in this experiment seemed narrower than anticipation. Examining the original experimental design, we discovered two caveats. First, measurements were taken from total RNA as starting material, whereas shRNA-mediated target cleavage takes place in the cytoplasm. Pre-

mRNA in the nucleus is detected as intact mRNA that should have been excluded in the first place. Second, transcripts produced by TRE-tight encompassed Venus and sensor site (data not shown). As a result, under the +Dox condition, Venus transcripts have a higher baseline expression than that under the –Dox condition. This bias potentially attenuated the difference between good and bad shRNAs. To resolve the issues, we isolated cytoplasmic RNA as starting material and added internal hairpinless controls, which contain Venus harboring corresponding sensor sites with 1nt variations but lack shRNA expression. Therefore, these hairpinless controls provide accurate baseline Venus mRNA level under the +Dox condition. These improvements were first validated among individual shRNAs tested by quantitative RT-PCR across the cleavage sites (Figure 4.4). Cytoplasmic RNA yielded wider dynamic range than total RNA. Silencing observed with nuclear RNA was likely due to remnant of cytoplasmic RNA. With either total or cytoplasmic RNA, the dynamic range was improved compared to the previous pilot experiment (Figure 4.3).

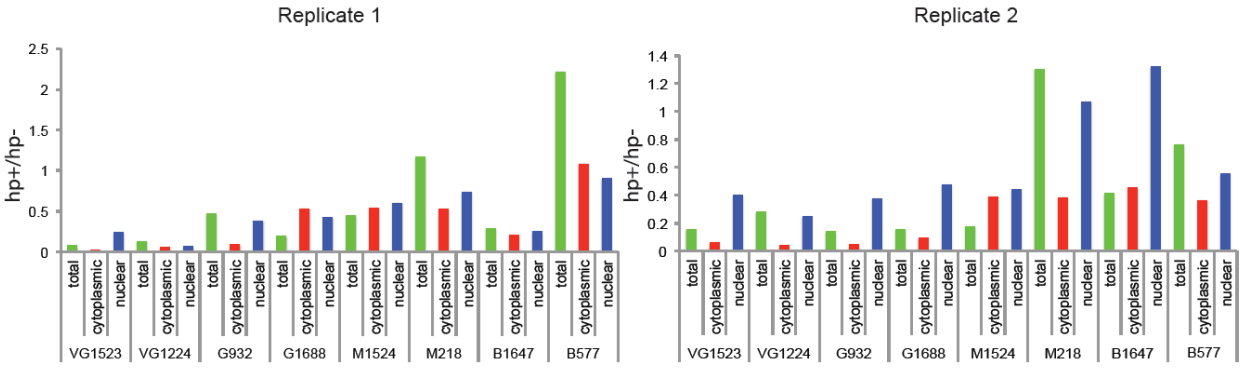

Figure 4.4 Validation of improvements using quantitative RT-PCR across sensor sites. Two biological replicates were performed and measurements were taken from total, cytoplasmic or nuclear RNAs. Ratios between each shRNA and the corresponding hairpinless control (hp+/hp-) are plotted.

Following the individual validations, we applied the same improvements to pooled assay using 8 reference shRNAs. 8 hairpinless controls containing corresponding sensor sites were incorporated for baseline Venus expression level in the presence of Dox. In parallel, the –Dox condition was still obtained for comparison to the original method. Compared to the previous calculation of ratios between +Dox and –Dox, the application of hairpinless controls significantly pulled the good shRNAs further away from the bad ones (Figure 4.5).

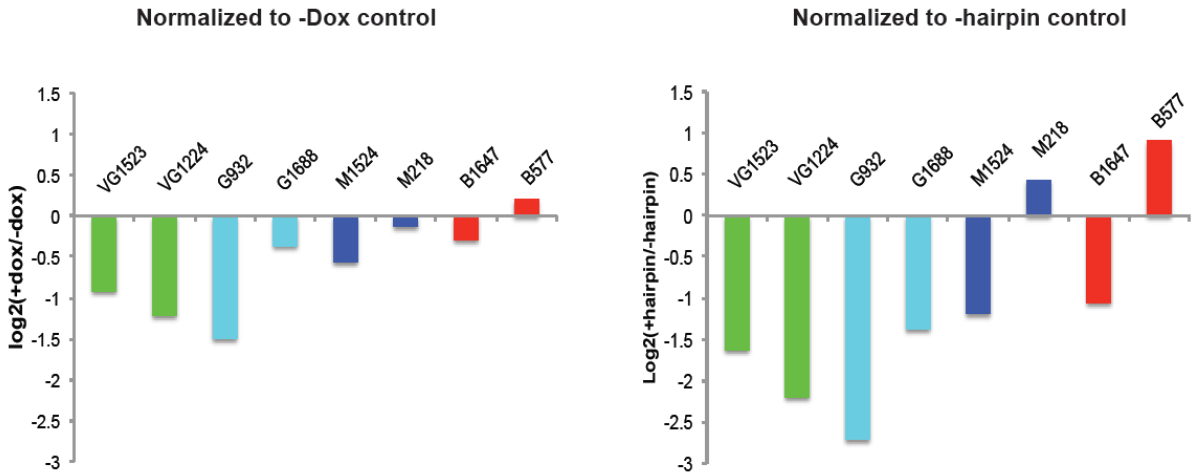

Figure 4.5 Revisions of molecular sensor assay improved dynamic range significantly. VG: very good; G: good; M: medium; B: bad.

1.3.2 Binned sensor assay: quantifying knockdown at protein level

Apart from the molecular sensor assay, we aimed to develop an assay that directly measures the final outcome of silencing – depletion of the target at protein level. Again, this method is based on the Venus sensor system. Instead of the Venus mRNA cleavage, our goal was to quantify the shRNA-induced depletion of Venus protein. The new assay took advantage of the fluorescence of Venus and measured the intensity reduction caused by shRNAs using FACS (Figure 4.6). Briefly, each cell carrying a sensor construct was labeled with a barcode and its intensities before and after the shRNA was switched on were recorded to measure the silencing efficiency. In order to achieve this goal, the pool of sensor-carrying reporter cells were separated based on Venus intensity into a series of intervals (bins), before and after the shRNAs were switched on. Deep sequencing from each bin for the shRNA and barcode sequences retrieved the intensities associated to each sensor clone with and without shRNA expression. The overall efficiency of each shRNA was evaluated based on the performance of all clones of this particular shRNA.

We performed a proof-of-principle experiment using a pool of 18 reference shRNAs with different potencies. In order to identify each individual clone, each shRNA was cloned into barcoded sensor vector. And the pool of 19 was introduced into reporter cells by single-copy integration. The pool of sensor-carrying cells was sorted into 13 bins based on Venus fluorescence intensity with or without shRNA expression (Figure 4.7). Following genomic DNA extraction from all bins, the shRNAs and barcodes were sequenced in order to identify and locate each sensor clone before and after the shRNA was expressed. First, we examined the read counts of each shRNA across all bins under –Dox and +Dox conditions without considering barcodes. Of all shRNA categories (very good, good, medium and bad) the counts shifted towards lower Venus intensity after the shRNA expression was switched on. This shift was well correlated with shRNA potencies. Greatest shift was observed in the “very good” shRNAs while the “bad” shRNAs only showed a subtle shift (Figure 4.8). In order to eliminate variations among different clones of the same shRNA and to enable modeling, we next examined the

distribution of each shRNAs taking into consideration the barcodes. Unexpectedly, the distribution appeared bimodal with two peaks, despite the expected shRNA-induced shift remained and was indicative of silencing potency (Figure 4.9). The bimodal pattern suggested multiple factors determining the distribution of Venus expression instead of silencing efficiency alone.

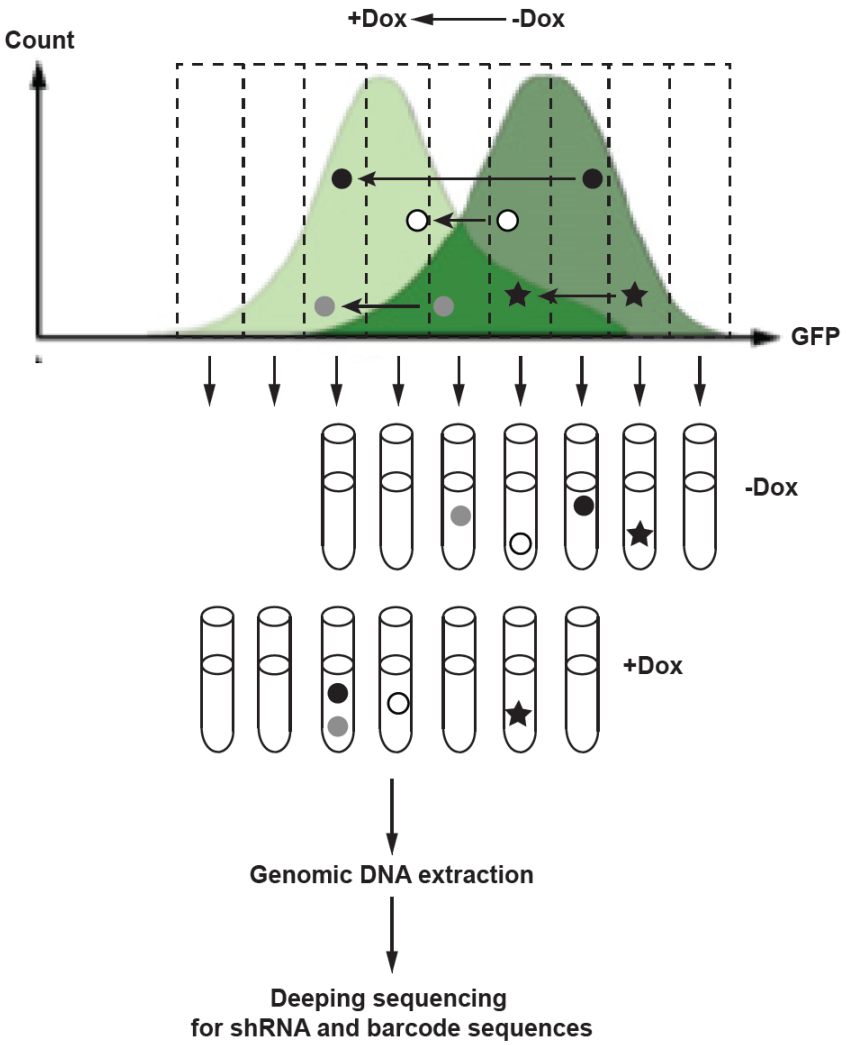

Figure 4.6 Schematic of binned sensor assay. The pool of infected reporter cells, each of which carries a copy of barcoded sensor construct, is maintained on or off Dox. Cells in each condition are then sorted based on Venus intensity into pre-defined bins. The shRNAs are identified using deep sequencing for the shRNA and barcode sequences. Finally the shift of Venus intensity mediated by each shRNA can be retrieved as a measurement of silencing potency.

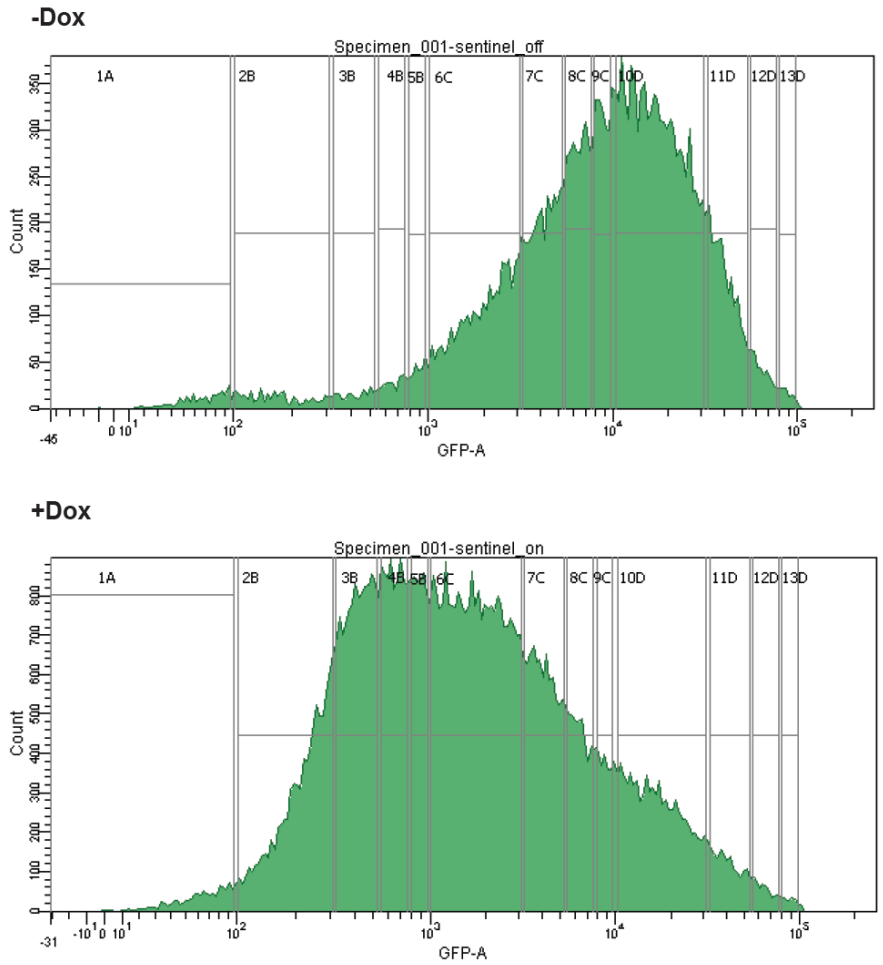

Figure 4.7 Gating strategy of proof-of-principle experiment using binned sensor assay. Reporter cells carrying single copies of sensor constructs are sorted into the 13 pre-defined bins based on Venus intensity under off dox (top panel) or on dox (bottom panel) conditions.

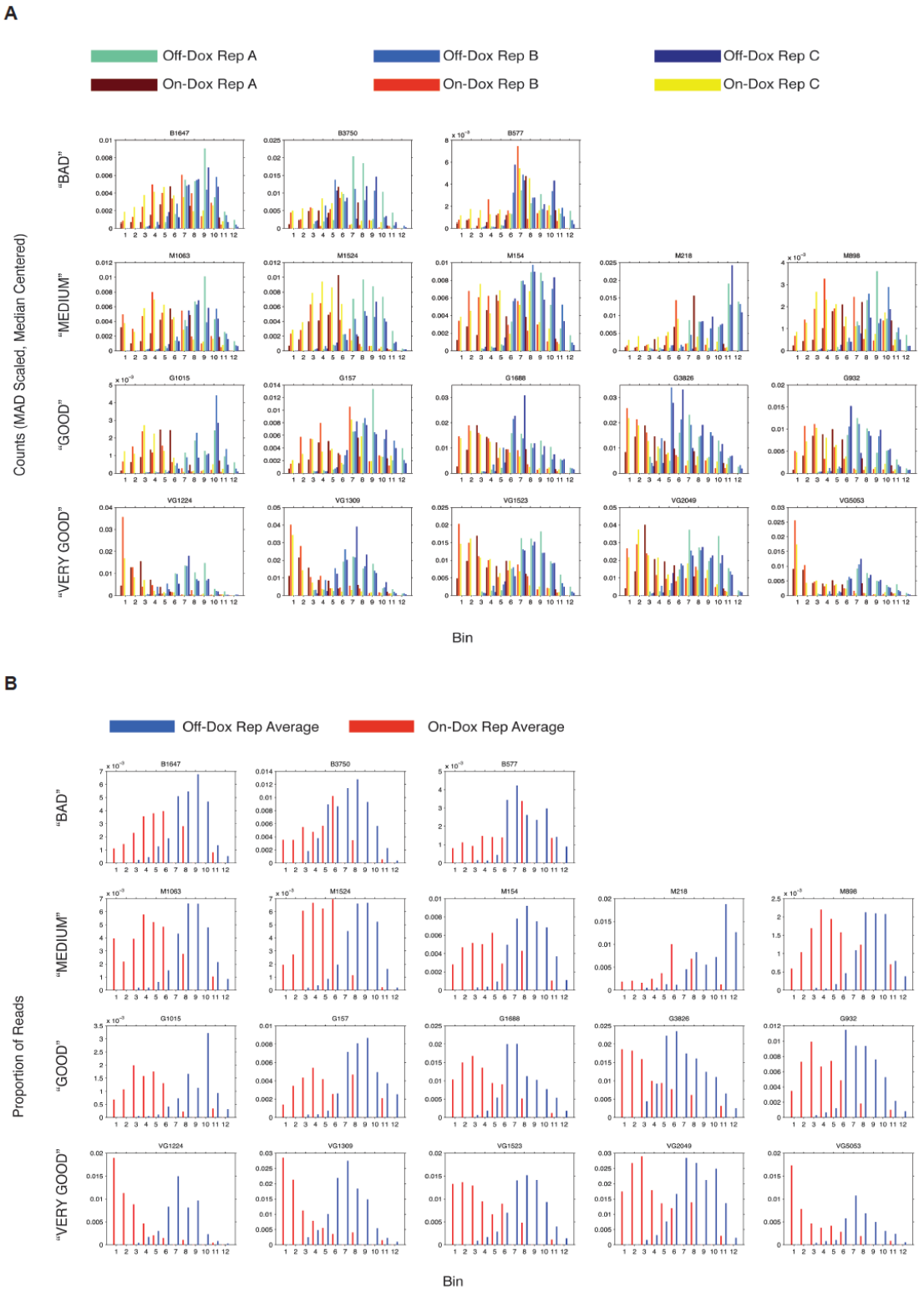

Figure 4.8 Distribution of read counts across all bins with or without shRNA expression ignoring barcodes. Three biological replicates (Rep A, B and C) are shown separately (A) or in average (B) under –Dox (without shRNA expression) and +Dox (with shRNA expression) conditions. The MAD scaled median centered read counts (A) or proportion of reads out of total reads (B) is plotted across all bins. Each plot represents an shRNA.

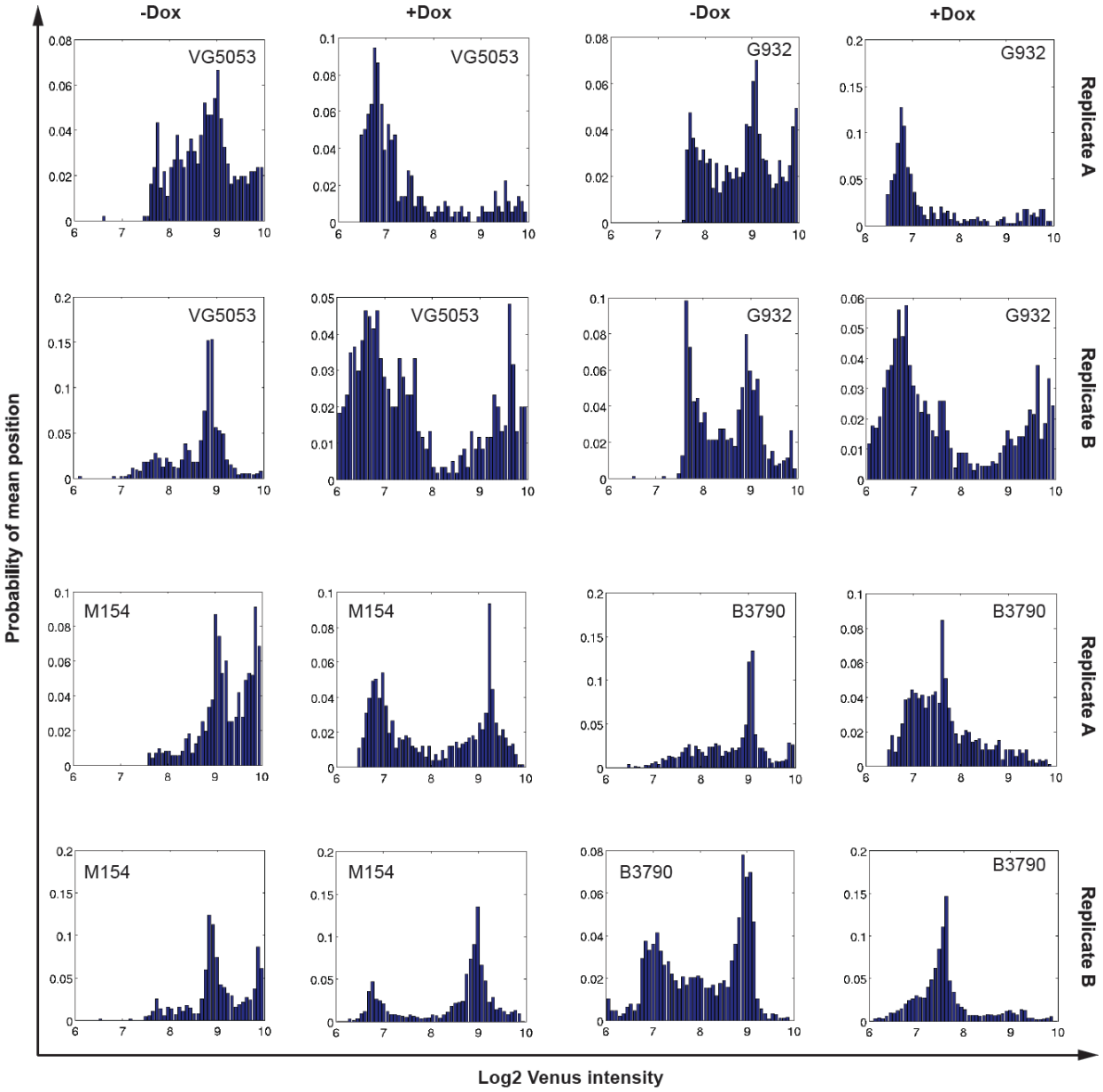

Figure 4.9 Distribution of shRNA considering individual clones labeled by barcodes. The probability of clones is plotted across all bin positions for each shRNA. One shRNA of each category is shown with two biological replicates. VG: very good; G: good; M: medium; B: bad.

1.4 Contribution

This work was a joint effort with Simon Knott and Swagatam Mukhopadhyay. I performed all the experiments while Simon and Swagatam conducted computational analysis of deep sequencing data.

1.5 Discussion

Here we designed two assays for the parallel measurements of shRNA potency from a pool. The two assays – molecular sensor assay and binned sensor assay – in proof-of-principle experiments both showed potential for high throughput application, measuring different parameters of gene knockdown. However, a few caveats were revealed during the pilot experiments of both assays, potentially compromising the performance on larger scale.

During the molecular sensor pilot experiment, two consistencies became evident. First, the relative quantification of mRNA cleavage was not always in line with relative knockdown potency, despite the strong overall correlation between the two properties. For example, the “good” shRNA G932 performed even better than the “very good” shRNA VG2049. This discrepancy is likely to stem from the disconnect between mRNA cleavage and the protein reduction. The most obvious biological explanation is the involvement of silencing mechanisms other than direct mRNA destruction, such as translation repression or mRNA deadenylation, which were not taken into account by our assay. Second, the dynamic range achieved in the pilot experiment seemed considerably narrower than that by quantitative RT-PCR. It was especially the good shRNAs that gave poorer performance, hence narrowing the separation between good and bad shRNAs. And the hairpinless internal controls only partly remedied this discrepancy. We next examined each step of the molecular sensor assay, aiming at the source of biases. We examined the concentration dependency of reverse transcription and PCR steps. PCR amplification seemed to have a rather wide linear range and was unlikely to introduce biases. However, surprisingly, the reserve transcription showed some random variations independent of concentration. Better reverse transcriptase and optimized protocol might be helpful.

Unlike the molecular sensor assay, binned sensor assay directly measure the silencing at protein level, a more reliable measurement of shRNA potency. However, this method faces technical and mathematical challenges when applied on large scale. The intensity of Venus expression is recorded as bin position, which is an interval of Venus intensity. In theory the measurements can become quite precise with a large number of narrow bins, which is nevertheless technically impractical. With a limited number of bins, it remains unknown what the upper limit will be in terms of the shRNA pool size. If a fairly large number of bins were required for an shRNA sensor pool of 22,000, the technical challenge would defeat the purpose. Another challenge originates from the mathematical modeling. When calculating the distribution of shRNA clones, we observed a bimodal pattern, suggesting a complex multi-factor model system involving at least one player other than just shRNA potency. Each factor would need to be identified and modeled separately in order to model the shRNA potency itself. These participating factors remain unknown, one of which might be the RISC concentration.

1.6 Materials and methods

1.6.1 Cloning of vector and sensor constructs

20nt random barcodes and 6 MS2 binding sites were inserted in the 3' UTR of Venus downstream the sensor site insertion site on the sensor recipient vector using restriction digestion and ligation. The shRNAs and corresponding sensor sites were cloned using a 2-step cloning procedure as previously described (Fellmann et al. 2011). To create hairpinless controls, the fragment between EcoRI and XhoI was deleted and sensor sites with 1nt variation were inserted into the designation site.

1.6.2 Cell culture and viral transduction

The rtTA+ reporter ERC cell line (Fellmann et al. 2011) was maintained in DMEM with 5% FBS and 5mM sodium pyruvate. Ecotropic Phoenix cells were cultured in DMEM with 5% FBS. For retroviral packaging, ecotropic Pheonix cells were transfected with sensor constructs. ERC cells were infected with low MOI to ensure single copy integration. Doxycycline was used at 0.5 µg/ml to induce the shRNA expression and Neomycin resistance. Infected cells were selected with G418.

1.6.3 RNA affinity purification using MS2 protein

The HHM protein (His-tagged MBP-M2 fusion protein) was expressed in BL21 (DE3) plysS competent cells (Life Technologies) according to manufacturer's instruction with kanamycin and chloramphenicol. Induction was carried out with 1mM IPTG for 2.5 hours when OD600 reached 0.5-0.7. HHM protein was purified according to previously published method using Ni-NTA resin (New England Biolabs) (Batey and Kieft 2007). RNA affinitiy purification was performed according to previous method with adjustments (Batey and Kieft 2007). 10ug of HHM protein is mixed with 10ug of RNA at 4 °C for 4 hours. Two additional high salt washes with 300mM NaCl were applied in order to remove residual unbound nucleic acids. All elution fractions were combined for downstream applications.

1.6.4 Flow cytometry and genomic DNA extraction

Sensor-infected ERC cells were sorted after G418 selection based on Venus expression to remove residual uninfected cells, and returned to culture. The sorted cells were split and maintained either with or without Doxycycline for 9 days. The two pools of cells then sorted into 13 bins representing intervals of Venus intensity. Cells of each bin were pelleted and genomic DNA was extracted using blood and cell culture DNA midi kit (Qiagen) according to manufacturer's instruction.

1.6.5 Reverse transcription, PCR and deep sequencing

Reverse transcription was performed using SuperScript III reverse transcriptase with 5ug of total, cytoplasmic or nuclear RNA following manufacturer's protocol. Quantitative PCR was performed using SYBR-Green PCR master mix (Life Technologies) on Eppendorf Reaplex thermocycler. For deep sequencing, the entire sensor site was amplified from flanking constant region. Illumina sequencing primer

binding sites, index and p5/p7 adaptors were added by nested PCR. The resulting amplicons were sequenced on Illumina HiSeq 2000.

1.6.6 Cytoplamic/nuclear RNA isolation

Cells were collected by scraping and washed twice in ice-cold PBS. Cell pellet was resuspended and incubated in hypotonic buffer (20 mM Tris-HCl, pH 7.4, 10 mM NaCl, 3 mM $MgCl_2$) on ice for 15min before homogenized using Dounce homogenizer for 10 times. The homogenate was then centrifuged at 3,000 ×*g* for 10 min at 4 °C. The supernatant was collected as cytoplasmic fraction. The pellet was washed in PBS twice and collected as nuclear fraction. RNA was extracted from each fraction using TRIzol according to manufacturer's instruction.

1.6.7 Deep sequencing data analysis

Read counts were normalized to total number of reads. For molecular sensor assay, the +Dox to –Dox ratio or +shRNA to –shRNA ratio was calculated based on normalized read counts of each shRNA. For binned sensor assay, the read counts were scaled by median absolute deviation (MAD) and centered on median. The distribution across all the bins was calculated for each shRNA or clones of each shRNA with or without shRNA expression.

References

Aagaard L, Amarzguioui M, Sun G, Santos LC, Ehsani A, Prydz H, Rossi JJ. 2007. A facile lentiviral vector system for expression of doxycycline-inducible shRNAs: knockdown of the pre-miRNA processing enzyme Drosha. *Mol Ther* **15**: 938-945.

Batey RT, Kieft JS. 2007. Improved native affinity purification of RNA. *Rna* **13**: 1384-1389.

Fellmann C, Zuber J, McJunkin K, Chang K, Malone CD, Dickins RA, Xu Q, Hengartner MO, Elledge SJ, Hannon GJ et al. 2011. Functional identification of optimized RNAi triggers using a massively parallel sensor assay. *Mol Cell* **41**: 733-746.

Jackson AL, Linsley PS. 2010. Recognizing and avoiding siRNA off-target effects for target identification and therapeutic application. *Nat Rev Drug Discov* **9**: 57-67.

Silva JM, Li MZ, Chang K, Ge W, Golding MC, Rickles RJ, Siolas D, Hu G, Paddison PJ, Schlabach MR et al. 2005. Second-generation shRNA libraries covering the mouse and human genomes. *Nat Genet* **37**: 1281-1288.

Stegmeier F, Hu G, Rickles RJ, Hannon GJ, Elledge SJ. 2005. A lentiviral microRNA-based system for single-copy polymerase II-regulated RNA interference in mammalian cells. *Proc Natl Acad Sci U S A* **102**: 13212-13217.

Unwalla HJ, Li MJ, Kim JD, Li HT, Ehsani A, Alluin J, Rossi JJ. 2004. Negative feedback inhibition of HIV-1 by TAT-inducible expression of siRNA. *Nat Biotechnol* **22**: 1573-1578.

Zeng Y, Wagner EJ, Cullen BR. 2002. Both natural and designed micro RNAs can inhibit the expression of cognate mRNAs when expressed in human cells. *Mol Cell* **9**: 1327-1333.

Appendix C
Investigating the roles of Argonaute protein in the bacterial thermophile *Thermus thermophilus*

1.1 Abstract

Argonaute proteins are present in all life domains ranging from bacteria to mammals. Extensive studies have demonstrated the complex and essential roles of eukaryotic Argonaute in many aspects of gene regulation. In contrast, the knowledge of prokaryotic Argonaute proteins remains elusive despite their ubiquitous presence. In this study, we aim at revealing the potential roles of Argonaute in a bacterial thermophile, *Thermus thermophilus.* Our data suggested a protective role of *T.thermophilus* Ago against mobile genetic elements, such as exogenous plasmid DNA. Deletion and overexpression of Ago led to increase and decrease of exogenous plasmid DNA integration respectively. Ago immunoprecipitation during transformation and further analysis of small RNA-protein complexes pinpointed a small RNA population about 20nt long that had 5' monophosphate group and decreased in the absence of Ago. Among this population, small RNAs from exogenous elements including plasmid DNA and CRISPR were highly enriched, further indicating the link between Ago and defense against foreign genetic elements.

1.2 Introduction

Argonaute family proteins are highly conserved and ubiquitous in both prokaryotes and eukaryotes. The roles of Argonaute have been thoroughly studied in plants and animals for more than a decade. This family serves as the central component of various RNA interference pathways, such as microRNA, piRNA and endo-siRNA pathways. Argonaute proteins not only participate the biogenesis of small RNAs, but also mediate the silencing of the targets together with small RNAs as the key factor of RNA induced silencing complex (RISC) (Hammond et al. 2000; Hutvagner and Zamore 2002; Mourelatos et al. 2002). Besides the endogenous gene regulation, one of the most conserved roles of Argonaute is to protect the genomic integrity from mobile genetic elements, such as viruses and transposable elements (TEs) (Zambon et al. 2006; Chung et al. 2008; Czech et al. 2008; Ghildiyal et al. 2008; Xie et al. 2013). The

most famous example is the silencing of TEs during aminal germline development (Sarot et al. 2004; Aravin et al. 2007; Kuramochi-Miyagawa et al. 2008; Xu et al. 2008; Malone et al. 2009). The piRNA and endo-siRNA pathways keep the TEs in check in order to maintain the genomic stability. Disruption of these pathways often leads to DNA damage and developmental defects. Similar defense mechanisms have been discovered in a wide range of organisms. Therefore, Argonaute proteins and the small RNA pathways are regarded as an innate immune system on the cellular level.

In contrast to the extensive knowledge of eukaryotic Argonaute, very little has been known about these proteins in prokaryotes, although the first Argonaute crystal structures were in fact from bacteria and archaea (Song et al. 2004; Wang et al. 2008a; Wang et al. 2008b). Based on the evolution and biochemistry of Argonaute, Argonaute has been predicted to act as the innate defense mechanism in prokaryotes against foreign nucleic acids, such as plasmid DNA and bacteriophages, in a small RNA/DNA-dependent manner (Makarova et al. 2009). A recent study on *Rhodobacter sphaeroides* Argonaute (RsAgo) (Olovnikov et al. 2013) revealed its association with small RNA from all transcripts and DNA enriched in exogenous origins complementary to the small RNAs. The RsAgo was capable of inducing plasmid DNA degradation when expressed in *E. coli*. And deletion of RsAgo led to elevation of some plasmid-encoded genes, indicating its potential involvement in foreign gene regulation. Although the results suggest a RNA-mediated exogenous DNA degradation, how the cleavage takes place remains elusive since RsAgo is catalytically inactive.

In this study, we aim at demonstration of the roles of Argonaute in a bacterial thermophile, *Thermus thermophilus*. The crystal structure of a DNA guide-containing *T. thermophilus* Argonaute (TthAgo) has been described with and without a DNA or RNA target (Wang et al. 2008a; Wang et al. 2008b; Sheng et al. 2014). TthAgo is capable of cleaving RNA target using small DNA guide *in vitro* and when expressed in *E. coli* (Wang et al. 2008b; Swarts et al. 2014), supporting its potential as a defender against foreign genetic elements. In deed, our results as well supported this prediction. Loss of TthAgo led to increased plasmid DNA transformation efficiency in *T. thermophilus* and *vice versa*. On the contrary to previous *in vitro* assay, immunoprecipitation of TthAgo detected small RNAs about 20nt long, originated from all transcripts but enriched in exogenous origins, such as plasmid DNA and CRISPR. Analysis of all small RNA-protein complexes in wild type and TthAgo knockout cells also detected a small RNA population of about 20nt, highly dependent on the presence of TthAgo. Among this population, small RNAs of exogenous origins, including plasmid DNA and CRISPR, were highly enriched. Interestingly, the CRISPR-originated small RNAs seemed to be the products of further processing of crRNAs from CRISPR pathways. Our results collectively indicate the involvement of TthAgo in defense against exogenous genetic invasions and a possible crosstalk with CRISPR pathways.

1.3 Results

1.3.1 *T. thermophilus* Argonaute prevents the genomic integration of foreign DNA

T. thermophilus is naturally competent at all phases during growth (Koyama et al. 1986), making it susceptible to exogenous mobile elements. Bacterial Argonaute has been predicted to protect the genomic integrity against mobile genetic elements. In order to confirm this prediction, we altered the TthAgo expression level by deleting the endogenous TthAgo or overexpressing an inducible His-tagged TthAgo in the cells (Figure 5.1). Additionally, an insertional *TthAgo* mutant was created with the insertion of a thermostable kanamycin resistant gene in the TthAgo ORF. A plasmid DNA pS18a with no *T. thermophilus* origin of replication was used to test the efficiency of integration. We observed a negative correlation between integration efficiency and TthAgo expression level (Figure 5.2 A, B and C). This result demonstrated the protective role of TthAgo against exogenous genetic invasion. To determine whether the interference occurred before or after DNA integration, *TthAgo* knockout and wild type cells were transformed with radiolabeled pS18a plasmid. The uptake of radioactivity was monitored during the first hour. DNase I was used to degrade plasmid that did not enter the cells. TthAgo knockout seemed more amenable to plasmid DNA and displayed an accumulation of radioactivity that was not observed in wild type (Figure 5.2 D). Thus, TthAgo was likely to act as early as foreign DNA entered cells before integration occurred or to even indirectly inhibit the entry of plasmid DNA. Additionally, high expression level of TthAgo caused unusual total RNA profile due to cleavage of ribosomal RNA (Figure 5.3 and data not shown), which was likely to be a direct effect of the excess of Ago.

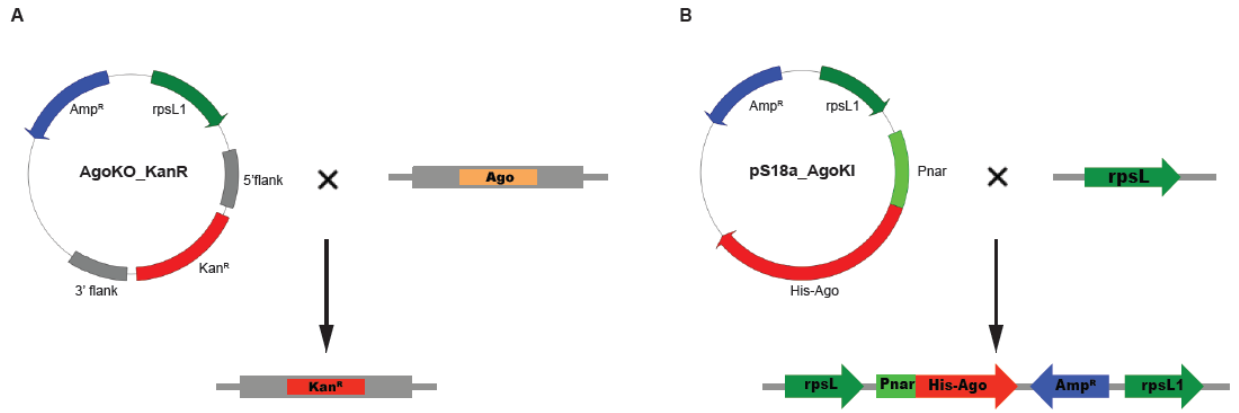

Figure 5.1 Strategy of TthAgo knockdown and knockin. The ampicillin resistant gene (Amp^R) is used for selection in *E. coli*. The thermostable kanamycin resistant gene (Kan^R) and *rpsL1* gene are used for selection in *T. thermophilus*. The *rpsL1* gene creates streptomycin-dependency. To facilitate 2-step homologous recombination for gene knockout, Kan^R (A) is flanked by sequences surrounding the TthAgo ORF from the *T. thermophilus* genome. *Pnar* (B) is a promoter inducible by the combination of nitrate and anoxia.

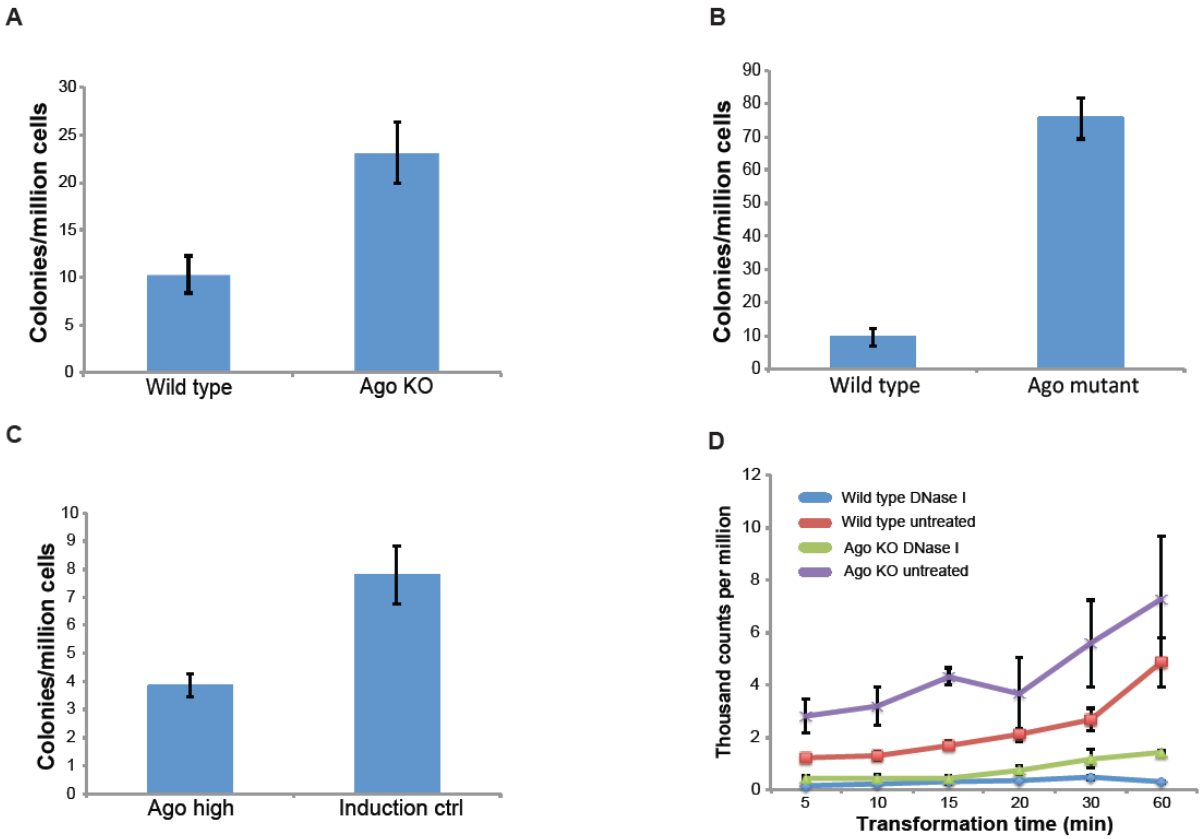

Figure 5.2 Argonaute participates in the prevention of foreign DNA integration in *T. thermophilus*. Colony numbers of *TthAgo* knockout (Ago KO) (A) and insertional mutant (Ago mutant) (B) are plotted in comparison to that of wild type post-transformation. (C) Colony numbers of induced Ago-overexpressing (Ago high) cells and induced cells containing empty vector post-transformation. (D) Counts per minute of radiolabeled pS18a plasmid taken up by *TthAgo* knockout and wild type cells during a time course.

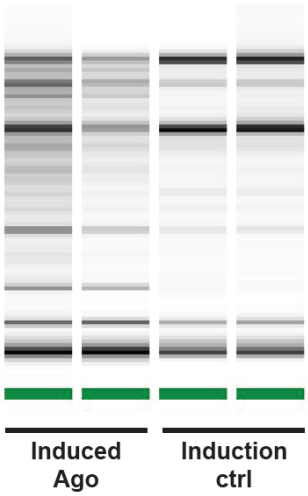

Figure 5.3 Total RNA profiles from TthAgo-overexpressing cells. Cells containing empty vector is treated under the same induction condition as control.

1.3.2 TthAgo is linked to small RNAs enriched for foreign origins

Argonaute proteins function in association with small nucleic acids. To understand the role of TthAgo on the molecular level, we overexpressed and pulled down His-tagged TthAgo in *T. thermophilus.* Three small nucleic acid populations were detected – a ~150nt population, a ~80nt population and ~20nt population (Figure 5.4A), all of which were proved to be RNA (data not shown). Based on the biochemistry of Argonaute, the ~20nt small RNA population was most likely the binding partner. This population had a fairly wide range of sizes (Figure 5.4B and C), majority of which originated from non-coding RNA including ribosomal RNA and transfer RNA (Figure 5.4D). Notably, small RNAs of foreign origins, such as exogenous plasmid and CRISPR loci, were enriched in comparison to their extremely small proportions across the whole genome (Figure 5.4D), although this population did not contain any phage-derived small RNA during bacteriophage TMA infection. The flood of rRNA and tRNA was likely a consequence of degradation related to overexpression of TthAgo, as suggested by the aforementioned total RNA profile (Figure 5.3).

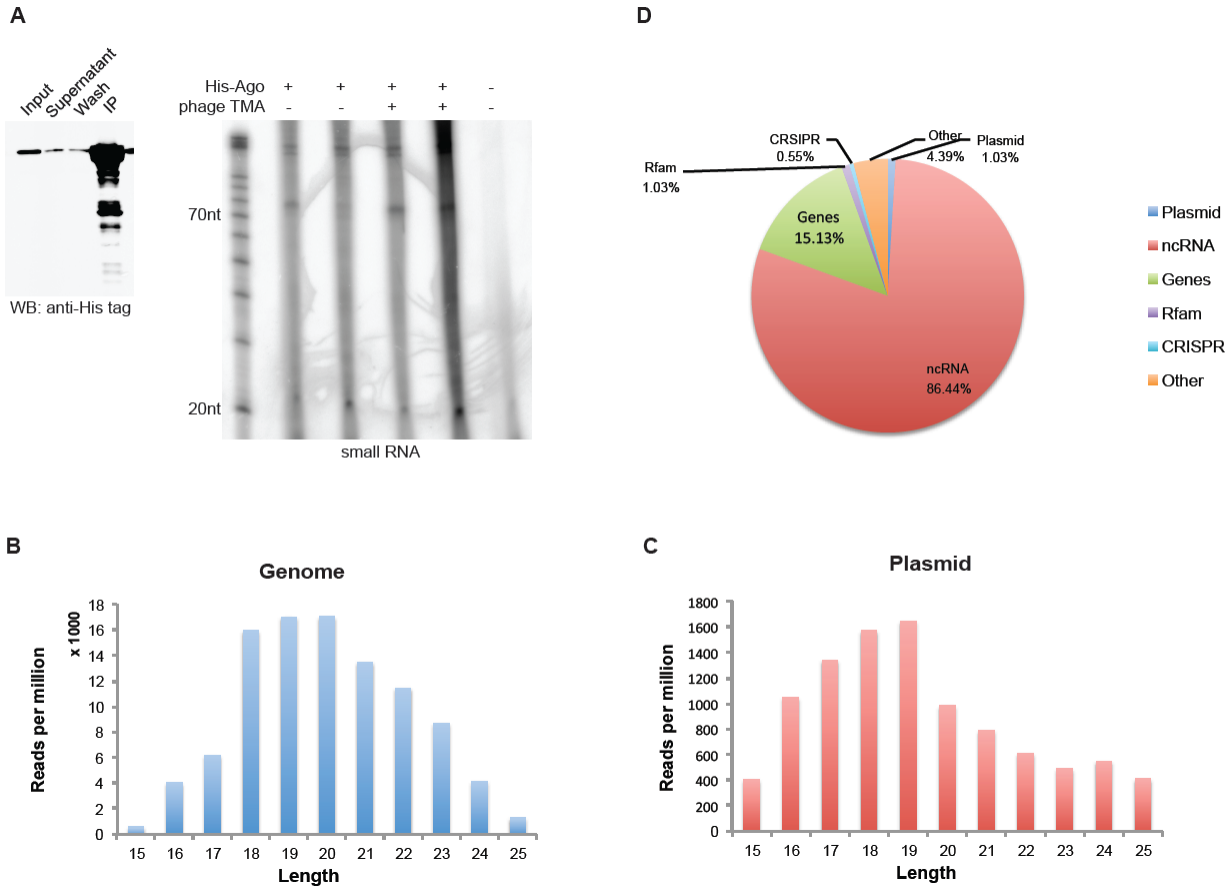

Figure 5.4 TthAgo is associated with small RNAs. (A) Western blot (left) of His-tagged TthAgo immunoprecipitation and end labeling (right) of associated small RNAs. Length distributions of small RNAs mapping to the *T. Thermophilus* genome (B) and to the pS18a exogenous plasmid (C) were plotted. (D) Origins of TthAgo-associated small RNAs from the genome and exogenous plasmid DNA. ncRNA: non-coding RNA including rRNA and tRNA. Rfam: functional non-coding RNAs in Rfam database, such as riboswitch.

To circumvent the caveat of Ago overexpression, we therefore attempted to express the His-tagged TthAgo under physiological condition. However, the expression level was undetectable and immunoprecipitation was technically difficult. We next adopted an indirect approach, isolating all small nucleic acid-bound protein complexes using fast protein liquid chromatography (FPLC). Comparison between wild type and *TthAgo* knockout background was supposed to identify the associated small RNA population. Using anion exchange, we isolated and confirmed the type I and type III CRISPR complexes. At higher NaCl concentration, two 20-30nt nucleic acid fractions, F1 and F2 were eluted (Figure 5.5A). Both fractions were confirmed to be RNA instead of DNA (Figure 5.5B). We next performed 5' end labeling using polynucleotide kinase (PNK) with or without prior phosphate removal by CIP. CIP treatment significantly enhanced PNK labeling of F1 fraction, whereas it did not affect that of F2 fraction (Figure 5.5C). This data suggested that the F1 fraction, but not the F2, had phosphate at the 5' end. 5' monophosphate has been shown required for proper interaction between small RNA and Argonaute. This property posed F1 small RNAs as the strongest candidate as TthAgo-associated small RNAs among all isolated small nucleic acid. We next compared the quantities of 5' phosphorylated F1 small RNAs between wild type and *TthAgo* knockout. Eight *D. melanogaster* miRNAs were spiked into the input protein lysates for normalization. The F1 fractions and total 19-30nt small RNAs were cloned using a method that specifically detects small RNAs with 5' monophosphate and 3' hydroxyl group. Compared to total small RNAs, F1 fraction from both wild type and *TthAgo* knockout was enriched for rRNA/tRNA as well as foreign origins, including exogenous plasmid and CRISPR loci (Figure 5.6A). Moreover, The F1 small RNAs from both endogenous and exgonegous origins were considerably decreased in the absence of TthAgo (Figure 5.6B). On the contrary, among total small RNAs, only those from CRISPR loci showed TthAgo dependency (Figure 5.6B). Interestingly, the CRISPR-derived small RNAs shared the same 5' ends with mature crRNAs, which is 8nt upstream each spacer (Figure 5.7), suggesting these small RNAs were likely to originate from CRISPR biogenesis pathway. Considered as a whole, our data indicate a strong correlation between the F1 small RNA population and TthAgo. However, direct evidence remains absent to reveal the identity of TthAgo-associated small nucleic acids.

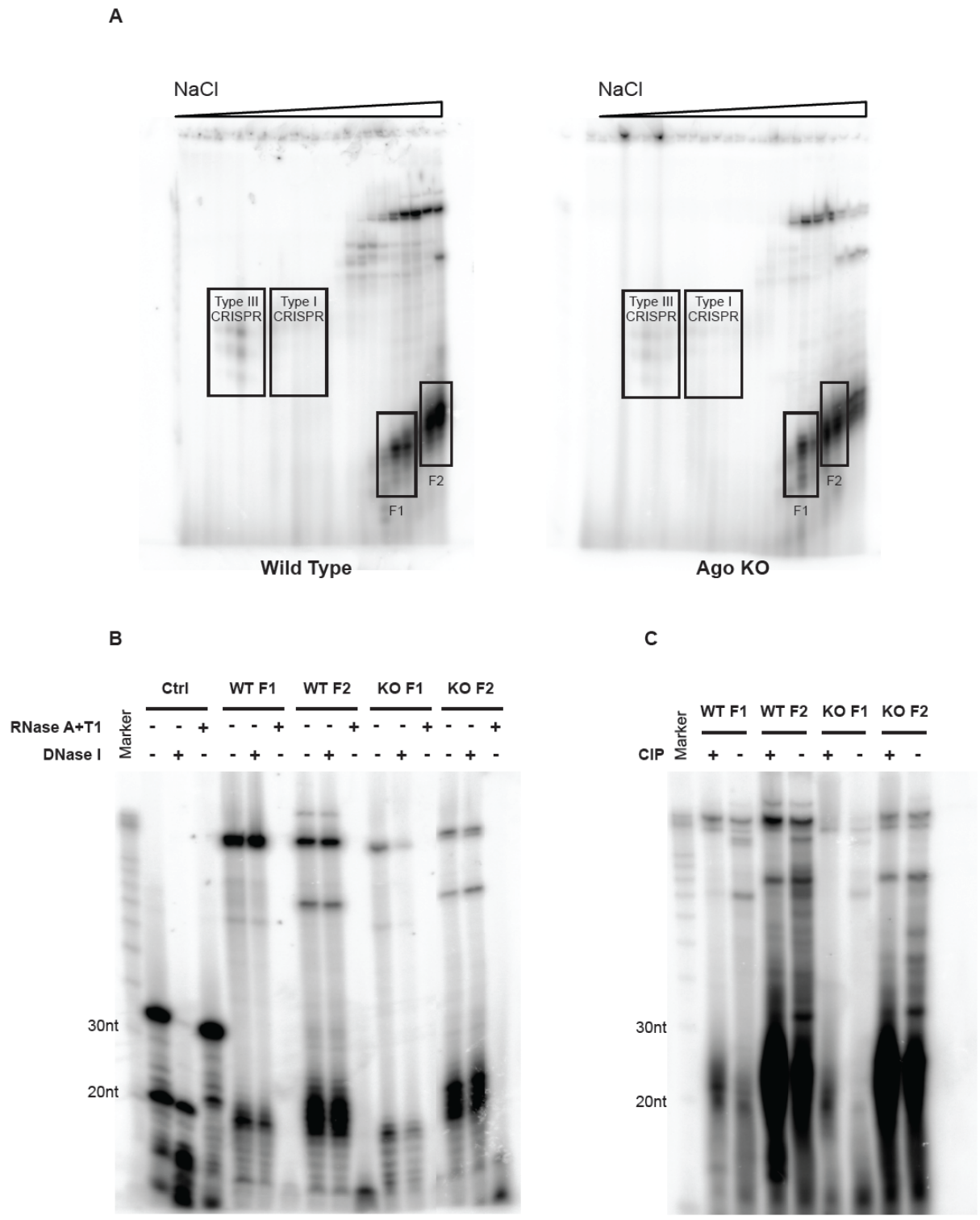

Figure 5.5 Protein-bound small nucleic acids from *T. thermophilus*. (A) End labeling of protein-bound small nucleic acids isolated by anion exchange FPLC. (B) Small nucleic acid profile from the F1 and F2 fractions after treated by RNase or DNase. Ctrl: a mix of 20nt RNA and 30nt DNA as control; WT: wild type; KO: *TthAgo* knockout. (C) End labeling of small nucleic acids from F1 and F2 fractions with or without a pretreatment by CIP.

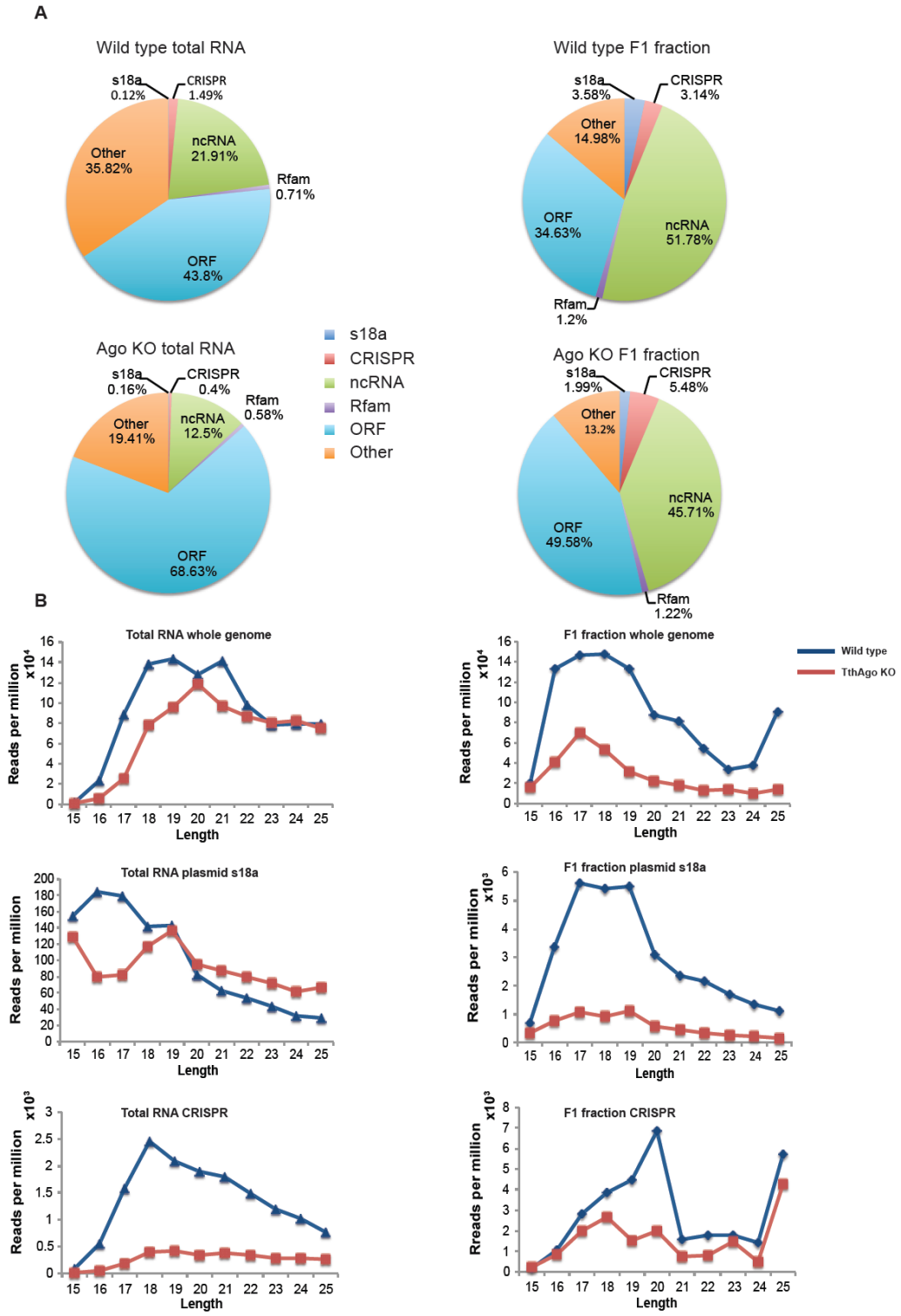

Figure 5.6 Small RNA profile of the F1 fraction from wild type and *TthAgo* knockout. (A) Origins of small RNAs from total RNA or F1 fraction. (B) Read counts of small RNAs of different origins from total RNA or F1 faction normalized to spike-in controls.

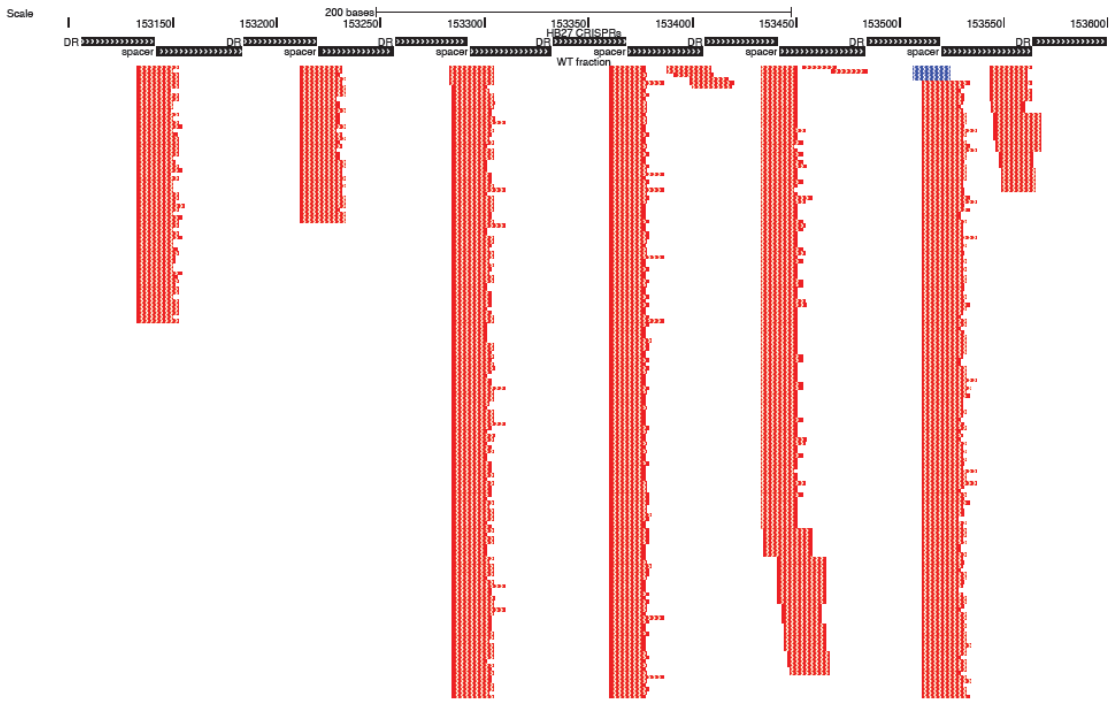

Figure 5.7 Coverage of CRISPR-derived small RNAs of about 20nt in size from the F1 fraction of wild type. Red denotes sense orientation and blue antisense. DR: direct repeat.

1.3.3 Expression levels of CRISPR loci and associated genes are affected by TthAgo expression

In order to investigate whether TthAgo regulates mRNA expression, we performed mRNA sequencing on cells with no TthAgo, endogenous TthAgo and TthAgo overexpression. Interestingly, in response to both *TthAgo* knockout and overexpression, the majority of CRISPR loci underwent elevated expression (Table 5.1 and 5.2). Moreover, upon TthAgo overexpression, some Cas genes were significantly upregulated, most of which are involved in the adaption of new CRISPR loci (Table 5.2). Our results on the mRNA level further supported the potential connection between TthAgo and CRISPR pathway.

Synonym	Product	Expression WT	Expression KO	qValue	Fold change
CR_p_6	CRISPR8	220	77	7.62E-182	0.35
CR_p_5	CRISPR7	36	94	1.47E-45	2.61
CR_Chr_2	CRISPR2	57	153	3.97E-57	2.68
CR_p_2	CRISPR4	46	126	4.72E-89	2.74
CR_p_4	CRISPR6	64	207	1.14E-116	3.23
CR_p_8	CRISPR10	22	83	3.90E-127	3.77
CR_Chr_1	CRISPR1	25	101	1.49E-73	4.04

Table 5.1 Differential expressions of CRISPR loci in TthAgo knockout cells. WT: wild type; KO: TthAgo knockout.

Synonym	Product	Expression Control	Expression KI	qValue	Fold change
CR_Chr_1	CRISPR1	44	92	4.32E-19	2.09
TT_P0204	Cas6	9	20	5.02E-20	2.22
TT_P0133	Cas5d	31	77	1.57E-33	2.48
TT_P0026	Argonaute	5	13	3.24E-39	2.6
CR_p_4	CRISPR6	154	442	2.21E-40	2.87
TT_P0101	Cas2b	7	23	3.62E-17	3.29
TT_P0132	Cas3	7	28	1.32E-121	4
TT_P0195	Cas2a	4	17	1.19E-21	4.25
CR_p_2	CRISPR4	36	192	1.63E-140	5.33
CR_p_1	CRISPR3	4	23	2.97E-72	5.75
CR_p_5	CRISPR7	131	776	2.42E-204	5.92
TT_P0196	Cas1	3	18	3.41E-122	6
CR_p_8	CRISPR10	16	103	0	6.44
TTC1170	Cas1	4	26	6.03E-76	6.5
CR_Chr_2	CRISPR2	49	335	0	6.84
TT_P0197	Cas4	3	26	7.51E-151	8.67
CR_p_7	CRISPR9	3	30	2.16E-303	10
CR_p_6	CRISPR8	53	728	0	13.74
TT_P0215	Cas1	0	6	1.20E-152	NA

Table 5.2 Differential expressions of CRISPR loci and associated genes upon TthAgo overexpression. Control: empty vector for induction control; KI: inducible TthAgo knockin.

1.4 Contribution

All experiments are designed and conducted by myself.

1.5 Discussion

Our findings demonstrated the role of Argonaute protein in the bacteria *Thermus Thermophilus* as a defense against foreign plasmid DNA invasion. A small RNA population about 20nt long has been linked to TthAgo and posed as the potential binding partner. This population presented some hints of mobile genetic element silencing. Furthermore, gene expression profiles indicate a connection between TthAgo and CRISPR systems, particularly the adaption genes. This finding is in line with

another recent study, in which TthAgo stimulated expressions from CRIPSR loci and some genes involved in adaptation when exogenous plasmid was present (Swarts et al. 2015b). It is plausible that TthAgo signals CRISPR system to prepare for the acquisition of new loci from the invader. However, direct evidence from physiological condition is yet to be established, in order to elucidate the precise roles of TthAgo in *T. thermophilus*.

The greatest challenge of this study stems from the undetectable TthAgo expression level under physiological condition. Despite the distinct *TthAgo* knockout phenotype, the endogenous expression level of TthAgo was so low that we failed to detect it by western blot or immunoprecipitation even with a large amount of starting material. Therefore we turned to an inducible overexpression system to scale up TthAgo to a detectable level. However, multiple observations suggested cellular toxicity. With higher TthAgo expression, total RNA was partially degraded during the mere 4 hours of induction. Besides, cells tended to lose TthAgo expression over time, indicating that even the leaky expression was sufficient to induce negative selection force. The most sensible explanation is that excess of TthAgo induces uncontrolled cleavage of essential DNA or RNA, a cellular effect equivalent to autoimmune response. Therefore, TthAgo expression level has to be kept at a fine balance, in order to sufficiently block non-self without harm to self. Facing the same challenge, another independent study addressed the silencing mechanism by ectopic expression in *E. coli* and in vitro biochemical assays (Swarts et al. 2014). Their data supported a small DNA-guided DNA cleavage model. However, it remains an open question whether ectopic expression and in vitro data reflect the biological process in *T. thermophilus*. Another notable factor in this organism is the temperature. While all the data was obtained at 37°C, it is unclear whether the same biochemical properties persist at 55-80°C. Using identical approaches, the same group also demonstrated the DNA-guided DNA cleavage activities by the Argonaute from hyperthermophile *Pyrococcus furiosus* (Swarts et al. 2015a). While the *in vitro* data exhibit some aspects of these prokaryotic Argonautes, it is premature to draw conclusions regarding their endogenous functions. In addition to the low expression level of TthAgo, another challenge is the potential transient interaction between invading DNA and TthAgo. Our data suggest that the interference takes place as early as the first hour of transformation. It might be difficult to capture the right moment when TthAgo acts on the targets. In conclusion, more conclusive evidence is necessary to address the questions regarding the silencing mechanism, such as what are the TthAgo-bound small nucleic acids and whether the catalytic activity of TthAgo is required for silencing.

1.6 Materials and methods

1.6.1 T. thermophilus culture, phage, vectors and gene targeting

Thermus thermophilus HB27 was cultured in a rich medium (0.8% (w/v) polypepton, 0.4% (w/v) yeast extract, 0.2% (w/v) NaCl, 0.35 mM $CaCl_2$ and 0.4 mM $MgCl_2$) at 70°C with agitation. For colony selection, cells were grown on plates with 1% Gelzan CM (Sigma Aldrich) in a humid chamber at 65-70°C. Bacteriophage ϕTMA was

propagated in HB27 culture and stored in MSG buffer (100mM NaCl, 10mM MgSO4, 50mM Tris-HCl, pH 7.5, 0.01% gelatin). The gene targeting vectors were constructed based on the previously described pS18a containing rpsL1 streptomycin dependence gene (Blas-Galindo et al. 2007). To make *TthAgo* knockout vector, a thermostable kanamycin resistance gene was first inserted in multiple cloning sites flanked by sequences surrounding TthAgo coding region (500bp each side). An inducible Pnar promoter-driven His-tagged TthAgo gene was inserted into multiple cloning sites on pS18a in order to make TthAgo knockin vector. For gene targeting, knockin or knockout vector was mixed with the naturally competent HB27 culture when OD600 reached 0.4 and incubated for 4h before plating with the appropriate antibiotics. Colonies were picked for further analysis.

1.6.2 Liquid scintillation counting of radioactive plasmid DNA

Wild type or TthAgo knockout HB27 was cultured with radiolabeled pS18a plasmid for 1h. During the transformation, cells were collected at several time points and treated with DNase I at 37°C for 30min to remove plasmid DNA on the cell surface. Liquid scintillation counting was performed using Ecoscint Ultra cocktail (National Diagnostics) in order to measure the amount of radioactivity within the cells.

1.6.3 TthAgo immunoprecipitation and western blot

His-tagged TthAgo knockin cells were induced for TthAgo overexpression. Cells were lysed in lysis buffer (50mM Tris pH 8.0, 10% glycerol, 0.1% Triton X-100, 100ug/ml lysozyme, 2mM MgCl and bacterial protease inhibitor cocktail (Sigma Aldrich)). His-tagged TthAgo was pulled down using Anti-6X His tag antibody (HIS. H8) (Abcam) and protein A agarose beads (Roche). Precipitates were resuspended in laemmli buffer for western blot or treated with proteinase K at 65°C for 1h following phenol/chloroform purification for RNA extraction. Western blot for His-tagged TthAgo was performed using the aforementioned anti-His tag antibody and IRDye 700 anti-mouse secondary antibody (LI-COR). Images were scanned on Odyssey CLx imager.

1.6.4 Fast protein liquid chromatography

Cell lysate was loaded onto MonoQ 5/50 GL column (GE Healthcare) for binding and washed with buffer A (25mM HEPES, 0.1mM EDTA, 0.5mM NaCl, pH7.6) for 4-5 column volumes. Buffer B (25mM HEPES, 0.1mM EDTA, 1M NaCl, pH7.6) was used to create salt gradient. Proteins were eluted with a NaCl gradient up to 1M. Fractions were collected for further analysis.

1.6.5 RNA extraction, small RNA end labeling and small RNA cloning

Total RNA was isolated using RNAsnap method for Gram-negative bacteria (Stead et al. 2012). For visualization of small RNAs, small RNA samples were treated with calf intestinal alkaline phosphatase (New England Biolabs) at 37°C for 30min, followed by polynucleotide kinase (New England Biolabs) with [γ-^{32}P] ATP (Perkin Elmer) at 37°C

for 1h. Samples were run on 12% PAGE and radioactivity was visualized on phosphorimager. Small RNA was cloned using an established method.

1.6.6 Deep sequencing and data analysis

Small RNA libraries were sequenced on Illumina HiSeq 2000. Small RNA reads were aligned to the *T. thermophilus* HB27 genome as well as pS18a plasmid sequence using bowtie, allowing 2 mismatches. Numbers of reads were normalized to total reads. The alignments were visualized on UCSC microbial genome browser. For mRNA sequencing, differential expression was analyzed using Rockhopper (McClure et al. 2013). Only genes with q value less than 0.05 and fold change more than 2 or less than 0.5 were considered differentially expressed.

References

Aravin AA, Sachidanandam R, Girard A, Fejes-Toth K, Hannon GJ. 2007. Developmentally regulated piRNA clusters implicate MILI in transposon control. *Science* **316**: 744-747.

Blas-Galindo E, Cava F, Lopez-Vinas E, Mendieta J, Berenguer J. 2007. Use of a dominant rpsL allele conferring streptomycin dependence for positive and negative selection in Thermus thermophilus. *Appl Environ Microbiol* **73**: 5138-5145.

Chung WJ, Okamura K, Martin R, Lai EC. 2008. Endogenous RNA interference provides a somatic defense against Drosophila transposons. *Curr Biol* **18**: 795-802.

Czech B, Malone CD, Zhou R, Stark A, Schlingeheyde C, Dus M, Perrimon N, Kellis M, Wohlschlegel JA, Sachidanandam R et al. 2008. An endogenous small interfering RNA pathway in Drosophila. *Nature* **453**: 798-802.

Ghildiyal M, Seitz H, Horwich MD, Li C, Du T, Lee S, Xu J, Kittler EL, Zapp ML, Weng Z et al. 2008. Endogenous siRNAs derived from transposons and mRNAs in Drosophila somatic cells. *Science* **320**: 1077-1081.

Hammond SM, Bernstein E, Beach D, Hannon GJ. 2000. An RNA-directed nuclease mediates post-transcriptional gene silencing in Drosophila cells. *Nature* **404**: 293-296.

Hutvagner G, Zamore PD. 2002. A microRNA in a multiple-turnover RNAi enzyme complex. *Science* **297**: 2056-2060.

Koyama Y, Hoshino T, Tomizuka N, Furukawa K. 1986. Genetic transformation of the extreme thermophile Thermus thermophilus and of other Thermus spp. *J Bacteriol* **166**: 338-340.

Kuramochi-Miyagawa S, Watanabe T, Gotoh K, Totoki Y, Toyoda A, Ikawa M, Asada N, Kojima K, Yamaguchi Y, Ijiri TW et al. 2008. DNA methylation of retrotransposon genes is regulated by Piwi family members MILI and MIWI2 in murine fetal testes. *Genes Dev* **22**: 908-917.

Makarova KS, Wolf YI, van der Oost J, Koonin EV. 2009. Prokaryotic homologs of Argonaute proteins are predicted to function as key components of a novel system of defense against mobile genetic elements. *Biol Direct* **4**: 29.

Malone CD, Brennecke J, Dus M, Stark A, McCombie WR, Sachidanandam R, Hannon GJ. 2009. Specialized piRNA pathways act in germline and somatic tissues of the Drosophila ovary. *Cell* **137**: 522-535.

McClure R, Balasubramanian D, Sun Y, Bobrovskyy M, Sumby P, Genco CA, Vanderpool CK, Tjaden B. 2013. Computational analysis of bacterial RNA-Seq data. *Nucleic Acids Res* **41**: e140.

Mourelatos Z, Dostie J, Paushkin S, Sharma A, Charroux B, Abel L, Rappsilber J, Mann M, Dreyfuss G. 2002. miRNPs: a novel class of ribonucleoproteins containing numerous microRNAs. *Genes Dev* **16**: 720-728.

Olovnikov I, Chan K, Sachidanandam R, Newman DK, Aravin AA. 2013. Bacterial argonaute samples the transcriptome to identify foreign DNA. *Mol Cell* **51**: 594-605.

Sarot E, Payen-Groschene G, Bucheton A, Pelisson A. 2004. Evidence for a piwi-dependent RNA silencing of the gypsy endogenous retrovirus by the Drosophila melanogaster flamenco gene. *Genetics* **166**: 1313-1321.

Sheng G, Zhao H, Wang J, Rao Y, Tian W, Swarts DC, van der Oost J, Patel DJ, Wang Y. 2014. Structure-based cleavage mechanism of Thermus thermophilus Argonaute DNA guide strand-mediated DNA target cleavage. *Proc Natl Acad Sci U S A* **111**: 652-657.

Song JJ, Smith SK, Hannon GJ, Joshua-Tor L. 2004. Crystal structure of Argonaute and its implications for RISC slicer activity. *Science* **305**: 1434-1437.

Stead MB, Agrawal A, Bowden KE, Nasir R, Mohanty BK, Meagher RB, Kushner SR. 2012. RNAsnap: a rapid, quantitative and inexpensive, method for isolating total RNA from bacteria. *Nucleic Acids Res* **40**: e156.

Swarts DC, Jore MM, Westra ER, Zhu Y, Janssen JH, Shnijders AP, Wang Y, Patel DJ, Berenguer J, Brouns SJ et al. 2014. DNA-guided DNA interference by a prokaryotic Argonaute. *Nature* **507**: 258-261.

Swarts DC, Hegge JW, Hinojo I, Shiimori M, Ellis MA, Dumrongkulraksa J, Terns RM, Terns MP, van der Oost J. 2015a. Argonaute of the archaeon Pyrococcus furiosus is a DNA-guided nuclease that targets cognate DNA. *Nucleic Acids Res* **43**: 5120-5129.

Swarts DC, Koehorst JJ, Westra ER, Schaap PJ, van der Oost J. 2015b. Effects of Argonaute on Gene Expression in Thermus thermophilus. *Plos One* **10**: e0124800.

Wang Y, Juranek S, Li H, Sheng G, Tuschl T, Patel DJ. 2008a. Structure of an argonaute silencing complex with a seed-containing guide DNA and target RNA duplex. *Nature* **456**: 921-926.

Wang Y, Sheng G, Juranek S, Tuschl T, Patel DJ. 2008b. Structure of the guide-strand-containing argonaute silencing complex. *Nature* **456**: 209-213.

Xie W, Donohue RC, Birchler JA. 2013. Quantitatively increased somatic transposition of transposable elements in Drosophila strains compromised for RNAi. *PLoS One* **8**: e72163.

Xu M, You Y, Hunsicker P, Hori T, Small C, Griswold MD, Hecht NB. 2008. Mice deficient for a small cluster of Piwi-interacting RNAs implicate Piwi-interacting RNAs in transposon control. *Biol Reprod* **79**: 51-57.

Zambon RA, Vakharia VN, Wu LP. 2006. RNAi is an antiviral immune response against a dsRNA virus in Drosophila melanogaster. *Cell Microbiol* **8**: 880-889.